

δ

$N L L I I$

(linear) evolution of CNOP (the corresponding LSV); $v_{\delta N}$ (v_{LL}): nonlinear (linear) evolution of T (negative anomaly of SST) of local CNOP (the corresponding LSV), indicating the amplitude of La Nina events (from Duan et al. (2004)).

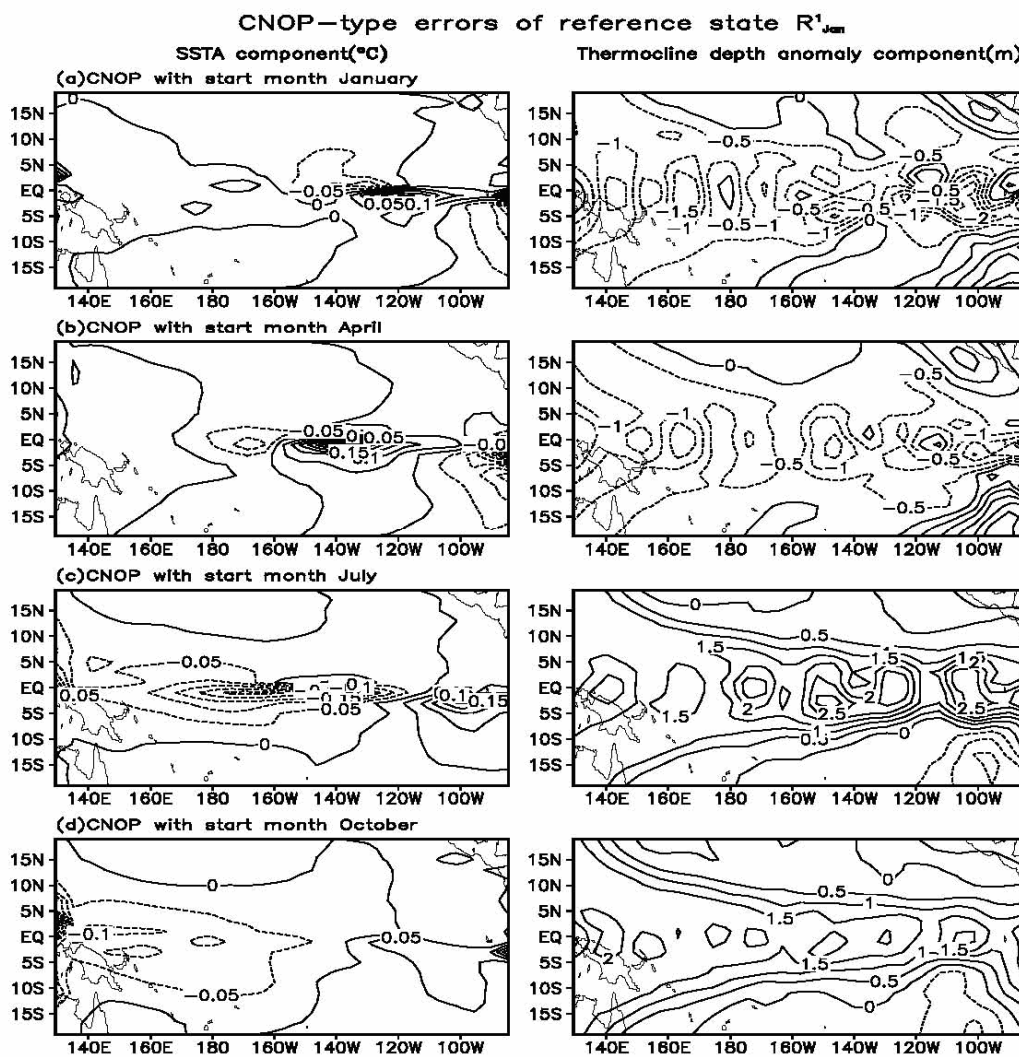


Fig.6

Fig.6. The patterns of CNOP-type error for a given basic-state El Nino. In the left (right) column are SSTA (thermocline depth anomaly) components for the start month being (a) January, (b) April, (c) July, and (d) October (from Mu et al. (2007)).

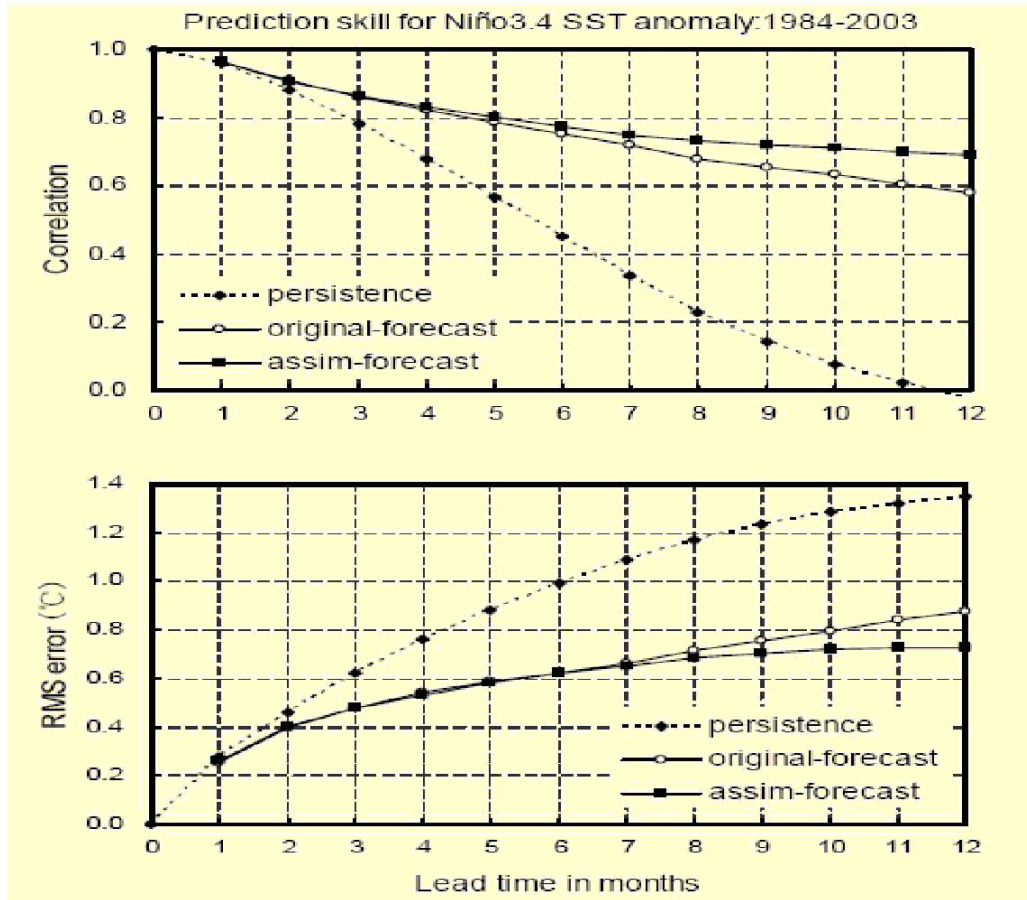


Fig.7

Fig.7. Anomaly correlations and RMS error for the Niño-3.4 SST anomalies that were respectively forecasted by the intermediate coupled model (ICM) with original initialization (solid line with circles; Zhang et al., 2003), by the model with the new initialization (solid line with squares), and by persistence prediction (dot line with squares). All the results are for the period 1984-2003 (from Zheng et al.(2006)).

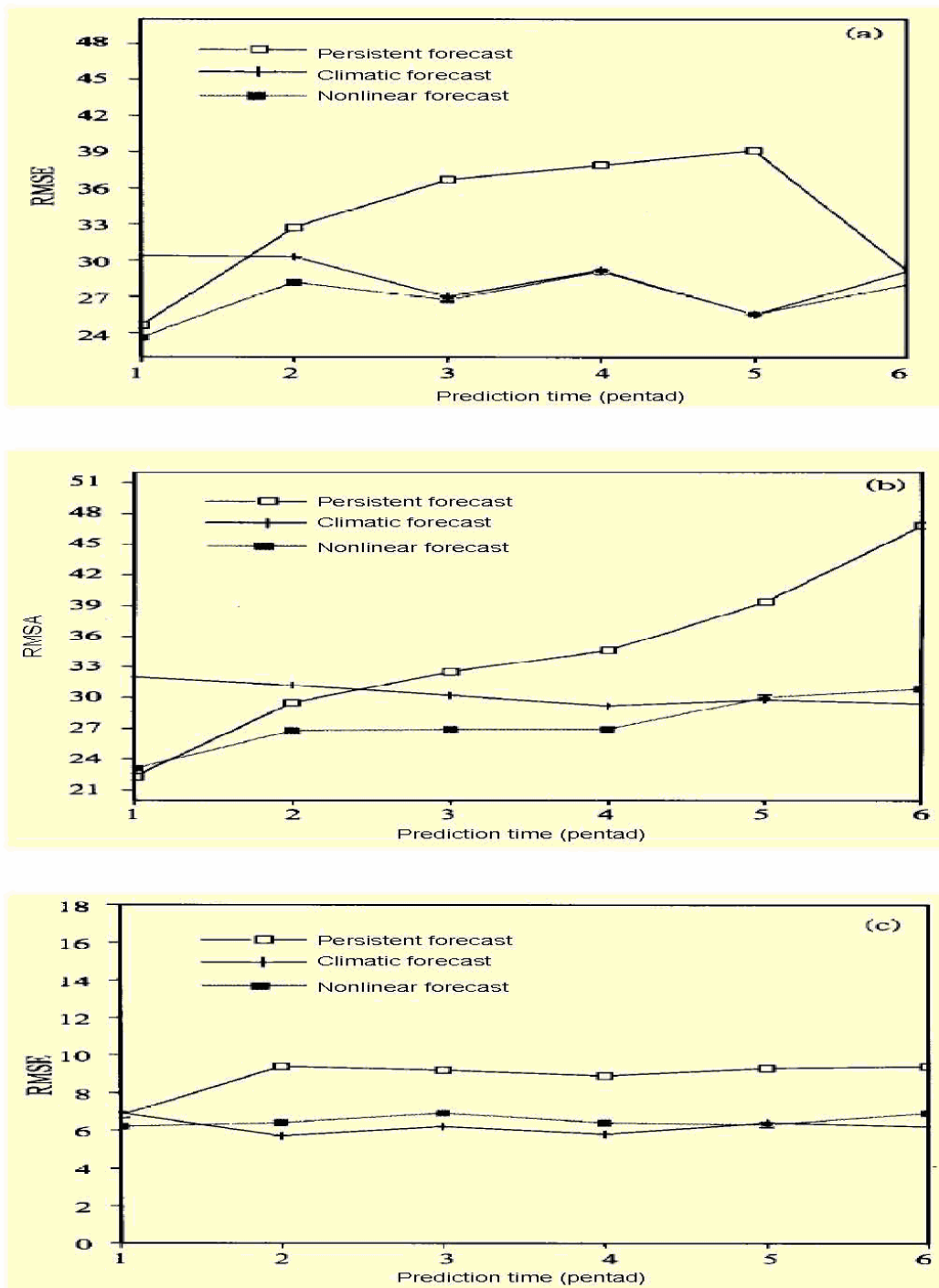


Fig.8

Fig.8. The RMSE of the pentad zonal-mean height of the persistence, climatic and nonlinear forecasts over (a) the Northern Hemisphere, (b) the Southern Hemisphere and (c) the tropical (the average of 12 cases in 1996) (from Chen et al.(2004)).

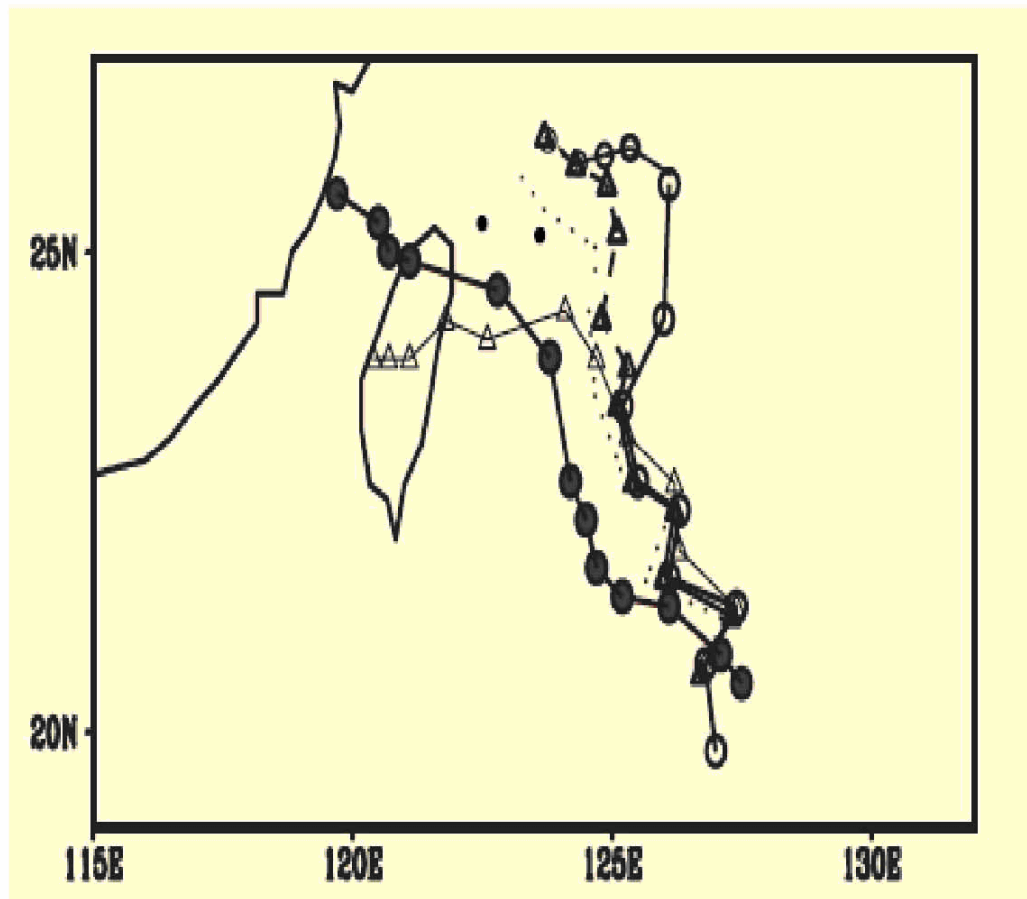


Fig.9

Fig.9. Ensemble tracks (thin lines) of Yancy (Y1700) using the LAF (solid line with triangles), BGM (dot line) and BGMV (dashed line with triangles) techniques. The best track is shown with black dots, the control run with open circles. Positions are plotted every 6 h (from Zhou and Chen (2006)).

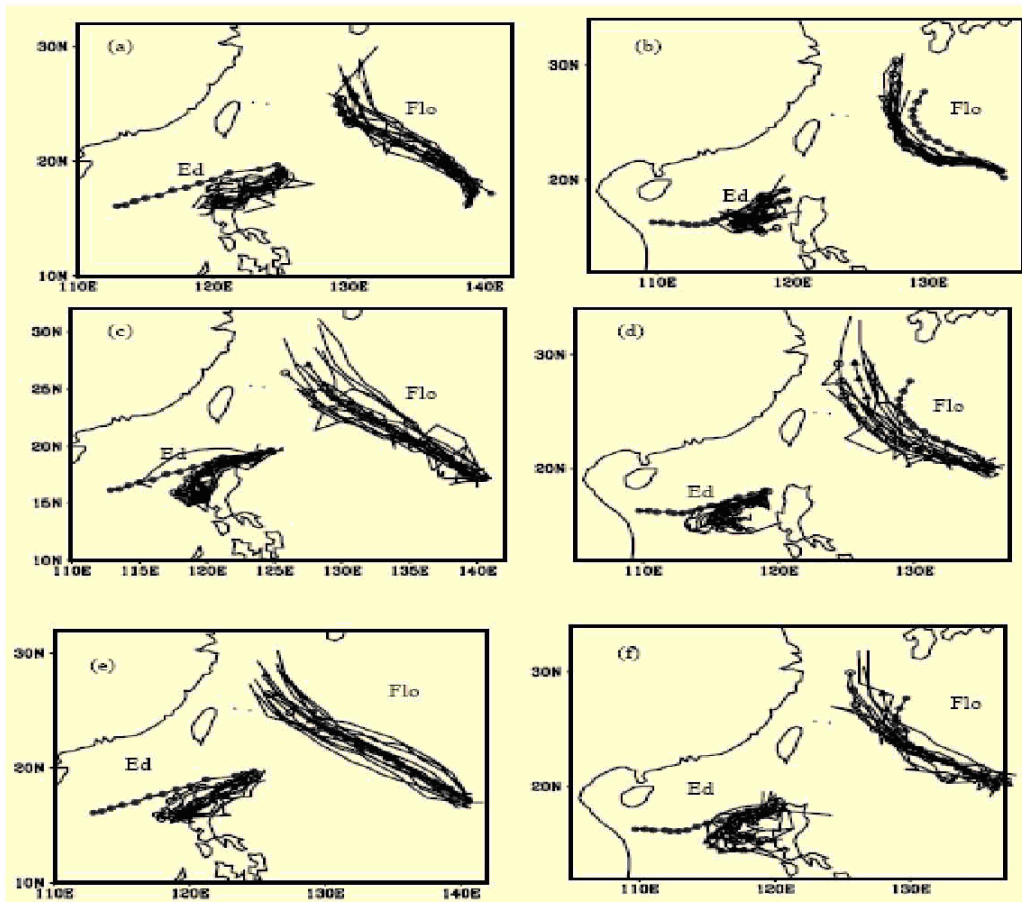


Fig.10 Fig.10. Ensemble tracks (thin lines) of Ed and FLo from (a) 0000 UTC 14 September (E1400, F1400) in LAF and (b) 0000 UTC 15 September (E1500, F1500) in LAF, (c) E1400 and F1400 in BGME, (d) E1500 and F1500 in BGME, (e) E1400 and F1400 in BGMV, (f) E1500 and F1500 in BGMV. The best track is plotted with closed circles, the ensemble mean with triangles, the control with open circles. Positions are plotted every 6 h (from Zhou and Chen (2006)).

A REVIEW OF RECENT ADVANCES IN RESEARCH ON ASIAN MONSOON IN CHINA

*He Jinhai¹ Ju Jianhua^{*2} Wen Zhiping³ LÜ Junmei⁴ Jin Qihua^{1,4}*

¹School of Atmospheric Sciences, Nanjing University of Information Science & Technology, Nanjing, 210044

²China Meteorological Administration Training Centre, Beijing, 100081

³Department of Atmospheric Science, Sun Yat-Sen University, Guangzhou, 510275

⁴Chinese Academy of Meteorological Sciences, Beijing, 100081

Abstract

This paper reviews briefly the advances of recent researches on monsoon by Chinese scholars, including primarily: 1. establishment of various monsoon indices. In particular, the standardized dynamic seasonal variability index of the monsoon can delimit the geographical distribution of the global monsoon systems and determine the date of the abrupt change of the circulation quantitatively. 2. provision of three driving forces for the generation of monsoon. 3. revelation of the heating-pump action of the Tibetan Plateau which strengthens the southerly in the southern and southeastern periphery of the plateau and results in the strong rainfall center from the North Bay of Bengal (BOB) to the plateau. 4. clarification of the initial onset of the Asian summer monsoon (ASM) in the BOB east of 90°E, Indochina peninsula and South China Sea, of which the rapid northward progression of the tropical convection in Sumatra and the rapid westward movement of the South Asia high to Indochina peninsula are the earliest signs. 5. provision of the integrated mechanism of the onset of the East Asian summer monsoon (EASM) which emphasizes the integrated impact of the sensible heat over Indian peninsula, the warm advection of the plateau and the sensible heat and latent heat over Indochina peninsula on one hand, and the seasonal phase-lock effect of the northward propagation of low frequency oscillation on the other hand. 6. revelation of the “planetary-scale moisture transport large-value band” from the Southern Hemisphere through the Asian monsoon region into the North Pacific, which is converged by several large-scale moisture transport belts in the Asian-Australian monsoon regions and whose variation influences directly the temporal and spatial distribution of summer rainfall in China. 7.

* Correspondence should be addressed to Ju Jianhua (E-mail: jujh@cma.gov.cn)

presenting the features of the seasonal advance of the EASM, the propagation of intraseasonal oscillation, and their relationship with rainfall in China; indicating that the intraseasonal oscillation of the EASM propagates in the form of wave-train along the coast and behaves as monsoon surge propagating northward. 8. describing the interannual and interdecadal variation of Asian monsoon, revealing the affecting factors and possible mechanisms of the variation of Asian monsoon. An elementary outlook on the existing problems and future direction of the monsoon research is given in the end.

Key words: recent researches on monsoon in China, review and advances, existing problems and prospects

中国近年来季风研究的回顾和进展

何金海¹ 琚建华² 温之平³ 吕俊梅⁴ 金啟华^{1,4}

1 南京信息工程大学气象学院, 南京 210044;

2 中国气象局培训中心, 北京 100081

3 中山大学大气科学系, 广州 510275;

4 中国气象科学研究院, 北京 100081

摘要: 本文简要回顾了中国学者近年来在季风研究方面的进展, 主要包括: 1. 构建了各种季风指数, 其中动态标准化季节变率季风指数还能划分全球季风系统的地理分布和定量确定环流突变日期。2. 提出了季风形成的三大推动力。3. 揭示青藏高原的热力抽吸作用增强了高原南侧和东南侧的偏南气流并导致孟加拉湾北部至高原的强降水中心。4. 阐明了亚洲夏季风首先在 90°E 以东的孟加拉湾, 中南半岛和南海地区爆发的过程特征, 而该过程以苏门答腊地区热带对流的迅速北进和南亚高压迅速西移至中南半岛为最先征兆。5. 提出了东亚夏季风爆发的综合机制, 强调印度半岛的感热作用, 高原的暖平流, 中南半岛的感热和潜热作用的综合影响以及低频振荡向北传播的季节锁相作用。6. 揭示了亚澳季风区各支大尺度水汽输送最终汇成一支源自南半球经过亚洲季风区进入北太平洋的行星大尺度水汽输送大值带, 其变化直接影响我国夏季降水的时空分布。7. 给出了东亚夏季风的季节推进和季节内振荡的传播特征与我国降水或旱涝的关系, 指出东亚夏季风的季节内振荡在东亚沿海呈波列形式传播, 并表现为随时间向北传播的季风涌。8. 讨论了亚洲季风的年际和年代际变化及其影响因子和可

能机制。文章最后对季风研究中存在的科学问题，未来的研究动向进行了初步展望。

关键词：近年来中国季风研究，回顾和进展，问题和展望

Monsoon is a most important member in the global climate system, whose variation plays a critical role in weather and climate in the monsoon regions. China is located in the East Asian monsoon region, therefore, research on monsoon has always been in the highlight by Chinese meteorologists. The research on monsoon in China has a history of nearly eighty years since 1930s, and many achievements are made by Chinese meteorologists in the research of East Asian monsoon, producing significant influences in China and abroad. In as early as 1930s, Zhu (1934) studied the advancement and withdrawal of summer monsoon and its relationship with the rainfall in China. After then, Tu et al. (1944) explored the advancement and withdrawal of East Asian monsoon and its impact on the intraseasonal variation of climate in China. Ye et al. (1959) investigated the seasonal transition of the atmospheric circulation over the Northern Hemisphere. Later, Chen et al. (1991) and Ding et al. (1994) proposed the structure and seasonal variation of the EASM. Recently, Chinese meteorologists have made important progress in researches on the forming mechanisms, the onset characteristics, and the multi-scale variability of Asian monsoon. We will comment on briefly the recent advances in the related researches.

1. Description of monsoon and monsoon indices

Monsoon index is a critical parameter in quantitatively describing and studying monsoon. In order to reflect the essence of monsoon, investigators put forward various monsoon indices.

In order to define the East Asian winter monsoon (EAWM) index, some factors, for example, differential heating between land and sea, meridional wind regionally averaged over East Asia, and zonal horizontal wind shear, were considered in previous researches (Wu and Wang, 2002; Chen et al., 2000; Yang et al., 2002; Jhun and Lee, 2004). It is well known that the meridional wind is a crucial aspect of the EAWM. However, the zonal wind also plays an important role, as strong zonal winds over mid and high latitudes can obstruct cold air outbreaks southward. Considering two-dimensional wind vectors, two distinct modes of the EAWM had been identified (Wu et al., 2006), resulting in a complete understanding of the EAWM.

Based on the contrary trend between the intensity of the tropical monsoon trough and that of the Meiyu front and the variation of their wind anomaly, Zhang et al. (2003) defined an EASM index

as the difference of the zonal wind anomaly at 850 hPa between the tropical area (10° - 20° N, 100° - 150° E) and the subtropical area (25° - 35° N, 100° - 150° E) in East Asia, which had synoptic meaning, easy to calculate, and reflected well the interannual variation of the wind and rainfall in East Asia. Utilizing the method of combining the dynamic factors and thermodynamic factors, Ju et al. (2005a) dealt with the southwesterly and OLR in the East Asian monsoon region synthetically to build an EASM index which could reflect not only the interannual variation of the East Asian subtropical monsoon appropriately, but also the essence of monsoon system. He et al. (2003) set up a new monsoon index by combining the zonal wind shear between the upper and lower levels with the geopotential height at 850 hPa. They investigated the relationship between the temperature in the troposphere and the ASM, and found that the reverse of the meridional temperature gradient in the upper level is generally earlier than or synchronous with the onset of summer monsoon in whether East Asian monsoon region or Indian monsoon region.

Li and Zeng (2005) presented a standardized dynamic seasonal variability index which can not only describe the seasonal variation and interannual variation in various monsoon regions as well as their relationship with the precipitation, but also line out the distribution of the global monsoon system (Fig1). Therefore, this index was named as the unified monsoon index (Li and Zeng, 2003a,b), and it is a significant progress in the study of monsoon index.

Zeng et al. (2005) and Zhang et al. (2005) adopted the “normalized finite temporal variation” to determine quantitatively the critical day of the abrupt transition in the atmospheric circulation, which is just 2-4 days earlier than the so-called “onset date” of monsoon, i.e. the “presage date” of monsoon onset. Whether in the tropical monsoon region or in the subtropical monsoon region, the seasonal adjustment and transition of atmospheric circulation have already been finished in the stratosphere before summer monsoon breaks out in the lower level, then extend suddenly downward to the troposphere to trigger the onset of monsoon in the lower level, which indicates that the seasonal transition of the atmospheric circulation from winter to summer commences initially in the Southern Hemisphere and in the stratosphere.

There are three aspects in the research of monsoon indices so far: (1) the intensity of monsoon is described by the wind (zonal or meridional), divergence, vorticity or moisture transport averaged over an area, which derives directly from the monsoon circulation itself; (2) the strength of monsoon is depicted by the combination of circulation and rainfall or convective parameters

(e.g. OLR) averaged over an area; (3) the EASM index is defined using the meridional land-sea thermal contrast, zonal land-sea thermal contrast or both of them. Whichever index is employed, it is appropriate as long as it distinguishes floods from droughts and relates significantly to the circulation or parameters of the circulation systems (e.g. the position and area of the subtropical high), and the relation could maintain as the observations database is prolonged. If such an index can reflect the date of the abrupt seasonal transition of the circulation as well, it can be used to determine the onset date of monsoon. Monsoon indices are generalized in a booklet by the research group of the South China Sea Monsoon Experiment (SCSMEX) (He et al., 2001).

2. Mechanisms in forming monsoon

The fundamental mechanism of the formation of monsoon is generally considered as the land-sea thermal contrast. In the meantime, the formation of monsoon is associated with the seasonal difference of the solar radiation between the Northern and Southern Hemispheres. However, if the surface is covered entirely by oceans, monsoon maybe still exists. In such an ocean model, the sea surface temperature (SST) may play an important role in the onset and existence of monsoon. When the forcing of the seasonal variation of SST was introduced, the numerical experiment simulated not only the vivid monsoon circulation, but also the abrupt outbreak and the active-break features (Yano and McBride, 1998). Monsoon is probably the outcome of the seasonal movement of ITCZ (Chao, 2000; Chao and Chen, 2001). The land-sea thermal contrast, like the difference of SST, determines the meridional position of ITCZ band, but orographic change has more influences on monsoon than the land-sea thermal contrast.

The formation of monsoon is resulted from the cooperation of various driving forces. Zeng and Li (2002) suggested two driving forces for the monsoon generation: the first driving force is the planetary thermal convective circulation (induced by the seasonal difference of the solar radiation between the Northern and Southern Hemispheres), and the second driving force is the quasi-stationary planetary wave induced by the difference of the surface characteristics (including land-sea thermal contrast, orographic height, etc.). He et al. (2004a, b) considered moist process as the third driving force of monsoon. The phase-change of moisture in the air and its transporting process can store and redistribute the solar energy in the tropics and subtropics, release the energy selectively, and determine the intensity and location of monsoon circulation and rainfall.

The research on the role of Tibetan Plateau in the ASM has achieved new progress recently. Numerical experiments showed that in “no-orography experiment” (Fig2), monsoon appears in Africa, South Asia and East Asia, and the rough distribution of monsoon regions is similar to the actual situation, indicating that the distribution of land and sea is primary in the formation of Asian monsoon. After introducing the ideal plateau in the experiment, northerly occurs round the west side of the plateau in the lower troposphere, and monsoon on the southwest side of the plateau withdraws southward, thus the monsoon rainfall in Africa to the west of the plateau is separated from that in Asia. The heating-pump action of the plateau strengthens the southerly in the southern and southeastern periphery and results in the strong rainfall center from the North BOB to the south of the plateau. Seen from the difference of two experiments, the low-level cyclonic circulation triggered by the plateau in summer strengthens significantly the southwesterly in the southeast of the Eurasian continent and brings the EASM to Northeast China at 50°N which greatly strengthens the East Asian monsoon (Wu et al., 2004; Wu et al., 2005).

The thermal contrast between the African continent or Indian subcontinent and the surrounding areas (including the Indian Ocean, the Arabian Sea and BOB) might be the main mechanism maintaining the Indian monsoon circulation, in particular, the former has more influences. However, the thermal contrasts between the Indochina peninsula and South China Sea, Australia and West Pacific play a crucial role in forming the tropical monsoon of the EASM, which indicated the reasonability to divide Asian monsoon system into East Asian monsoon and South Asian monsoon (Jin et al., 2006).

3. Onset of the ASM and its mechanisms

3.1 Onset time and characteristics

Each year the ASM in the 10°-20°N latitudinal band breaks out initially in the BOB east of 90°E, Indochina peninsula and South China Sea (SCS), then expands westward and northward, and the EASM and Indian summer monsoon establish one after the other. The Indian summer monsoon breaks out later than the EASM (Tao and Chen, 1987; Mooley and Shukla, 1987). The rapid northward progression of the tropical convection in Sumatra in late April and early May is the first sign of such process (He et al., 1996; Qian et al., 2004; Ding et al., 2004; Liu and Ding, 2005c; LÜ et al., 2006).

The Asian tropical summer monsoon is established initially in the equatorial East Indian Ocean

and Sumatra in late April (Pentad 24) and then in the east of BOB and Indochina peninsula in the 2nd pentad of May (Pentad 26), signifying the outbreaks of summer monsoon in these region. The tropical summer monsoon proceeds northeastward to the central SCS in the 4th pentad of May (Pentad 28), signifying the outbreak of the South China Sea monsoon (SCSM); it advances northwestward in late May and early June, with its front arriving at southern Indian peninsula. Two tropical summer monsoons from the west coast of India and BOB converge in the central Indian peninsula in the 1st and 2nd pentad of June (Pentad 31-32), which signifies the outbreak of Indian monsoon; they arrive at the northwest of India in early July, signifying the establishment of tropical summer monsoon in the whole India.

The process of summer monsoon onset in East Asia seems complex. It is well known that tropical summer monsoon has proceeded to the Yangtze River and its southern areas in the 1st and 2nd pentad of June after it breaks out in SCS initially. However, Zhao et al. (2006) pointed out that the persistent low-level southwesterly wind occurs earliest over southeastern China and gradually advance northward, resulting in the onset of the large-scale southwesterly wind over eastern China. Moreover, the southerly wind extends southward to the SCS. It suggests the EASM breaks out earliest over southeastern China.

Accompanied with the northward march of the EASM, summer monsoon rainfall occurs in South China in the First Flood Period in mid and late May, moves northward rapidly in early June, and brings Meiyu in the Yangtze River valley and Baiu in Japan in mid-June. Meiyu front lasts in the Yangtze River valley and then proceeds rapidly northward to North China in early July when the North China rainy season begins. In mid-July, the front of summer monsoon arrives at Northeast China which is the northern-most position of the ASM. The entire process is represented as three still phases and two abrupt jumps, which is closely associated with the activities of the western Pacific subtropical high (WPSH) (Ding, 2004). Jiang et al. (2006) distinguished Meiyu in the Huai-River and in the south of Yangtze River, and pointed out that the rain belt has three jumps northward.

It can be seen from the difference of 500-200 hPa thickness between 20°N and 5°N that the difference turns from negative to positive in early May first in the longitude of 100°E, i.e. Indochina peninsula, and expands eastward to SCS on the 4th pentad of May (Pentad 28) and westward to Indian subcontinent on the 1st and 2nd of June (Pentad 31-32), which corresponds to

the onset of summer monsoon in these regions. In addition, the axis of the maximal thermal contrast tilts obviously to the west with time, indicating the maximal thermal gradient moves regularly westward. Therefore, the reverse of the meridional thermal gradient and the westward propagation of the maximal gradient are the manifestation of Asian monsoon advancing from east to west after breaking out in the tropical east Indian Ocean and Indochina peninsula.

Through summarization of the SCSMEX, Ding et al. (2004) revealed a series of important phenomena accompanying the outbreak of monsoon as follows: cross-equatorial flow develops in the equatorial East Indian Ocean and Somali; the heat sources in Indochina peninsula, South China, Tibetan plateau and surrounding areas strengthen rapidly in seasonal transition; the lower-level westerly accelerates in the equatorial East Indian Ocean; the subtropical high belt splits in the BOB and monsoon low or cyclonic circulation forms; the tropical southwesterly expands eastward from the tropical East Indian Ocean; rainy season comes in the BOB and Indochina peninsula; under the influence of mid-latitude systems, southwesterly expands further to SCS; the main body of the subtropical high weakens significantly and withdraws eastward; convective cloud, rainfall, low-level southwesterly and upper-level northeasterly develop abruptly in SCS, etc. These achievements provide favorable references for the research of Asian monsoon and East Asian monsoon.

3.2 Onset mechanisms

3.2.1 Impact of the Tibetan Plateau on the onset position and intensity of the ASM

The “heating pulley” action of the plateau strengthens the southerly, increases rainfall, and strengthens the latent heat over the land to the southeast of the plateau; meanwhile, it produces the northerly, decreases rainfall, and strengthens the sensible heat over the land surface to the southwest of the plateau. The plateau anchors the location of the ASM onset. In the background of the tropical land-sea distribution, the ASM breaks out initially on the east side of the ocean and west side of the continent to the southeast of the plateau, thus the monsoon rainfall in Asia is redistributed. The initial outbreak of the ASM in the east of BOB is associated with the obvious heating in the south side of the plateau in spring. It is proved after analyzing the evolution of the common boundary of the easterly and westerly that in the lower troposphere in the Asian monsoon region, the transition from easterly prevalent in winter to southwesterly in summer occurs firstly in the east of BOB due to the heating of the plateau in spring, accompanied with drastic convective

rainfall in its east. Therefore, the east of BOB-the west of Indochina peninsula may be the region where Asian monsoon initially breaks out (Wu et al., 2004; Wu et al, 2005; Liang et al., 2005).

3.2.2 Impact of the onset of BOB monsoon on the onset of the SCSM

The introduction of the convective latent heating over the BOB results in vigorous ascending motion and the BOB monsoon onset, as well as the development of westerly and vertical ascent over the northern SCS due to an asymmetric Rossby-wave response. Together with the low-level moisture advection, convection is induced over the northern SCS. It is the condensation heating over the northern SCS that causes the overturning of the meridional gradient of temperature. Consequently the vertical slope of the ridge of the subtropical high over the SCS turns from the winter-pattern to summer-pattern according to the relation of the thermal wind, i.e. the subtropical high in the low-level weakens and moves southward. Eventually, as convection develops over the entire SCS domain, the subtropical high moves out of the region and the SCSM breaks out (Liu et al., 2003a, 2003b).

3.2.3 The antecedent effect of the “Asian-Australian land bridge” on the onset of the ASM

Within the South Asian region (10-20°N), convection flares up initially in Indochina peninsula (ICP), then in the BOB and SCS, and last in India. The activity of convection in ICP is related to the sensible heating of its earth surface, but more importantly, it is the result of the northward progression of the tropical convection in Sumatra and the arrival of South Asia high at this place. The latent heating in ICP is favorable for triggering a cyclonic circulation on its west side, while the sensible heating in Indian peninsula favors triggering a cyclonic circulation or trough on its east side. The effective match of these two, along with the aroundflow and thermodynamic effects of the plateau and the thermodynamic effect in middle and high latitudes in East Asia, helps the subtropical high belt in South Asia to split first in the BOB. Accompanied by the formation and strengthening of the BOB trough, eastern BOB is controlled by tropical southwesterly in front of the trough, then large quantities of moisture is transported to SCS and converges with the flow from the west side of the subtropical high. Therefore, the atmosphere is destabilized; convection perks up; and summer monsoon is established. In the meantime, the convective latent heating in the BOB triggers two-dimensional asymmetric Rossby-waves, which generates the diversion of the meridional gradient of temperature in SCS and favors the onset of the SCSM. The rapid eastward retreat of the eastern subtropical high after the belt splits results directly in the onset of

the SCSM and its explosive characteristics. As India is controlled by northwesterly in front of the ridge (i.e. behind the BOB trough) after the high belt breaks, it is unfavorable for the onset of summer monsoon in India. Therefore, summer monsoon is established last in India. As a matter of fact, the break of subtropical high belt, the occurrence of the BOB trough, the eastward retreat of subtropical high and the onset of the SCSM are completed rapidly and accompanied by the seasonal abrupt change of large-scale circulation and moisture transport in Asia. However, in terms of the source of the onset of summer monsoon, the rapid northward progression of the tropical convection in Sumatra in late April and early May is the earliest sign of the onset of the ASM (Xu et al., 2001, 2002; He et al., 2002; Zhang and Qian, 2002; Liu et al., 2003a; Luo and li, 2004; Qian et al., 2004; He et al., 2004a; Wen et al., 2004; Wang et al., 2004; Wen and Zhang, 2005; Zhang et al., 2004; Liang et al., 2005; Zhou et al., 2005; He et al., 2006). This process can be represented in Fig3.

3.2.4 Impact of the thermal anomalies of the oceans on the onset of the SCSM

A series of studies have been carried out on the impact of the anomalous SST in the tropics on the onset of the SCSM. Many researchers suggested that the preceding SST anomalies (SSTAs) in the tropical Indian Ocean and Pacific Ocean have a good relation with the onset of the SCSM. Wen et al. (2006b) indicated that the sign of the SSTAs in the tropical Indian Ocean and Pacific Ocean are opposite in some years, so their impacts on the early or late onset of the SCSM are different. The negative (positive) SSTA in the tropical Indian Ocean is favorable (unfavorable) to the early establishment of the anti-Walker circulation over South Asia; while the negative (positive) SSTAs in the tropical Pacific Ocean favor (disfavor) the early strengthening of the Walker circulation over the Pacific. The SSTAs in the tropical Indian Ocean and Pacific Ocean have an impact on the early or late onset of the SCSM through influencing the Walker circulation.

Warm SST in the SCS in winter and spring is favorable for the formation of monsoon circulation throughout all levels of the atmosphere over the sea, which hastens the onset of the SCSM. The effect of cold SST is generally the opposite. The local land-sea thermal contrasts in the SCS are one of the possible reasons for the SCSM onset (Ren and Qian, 2003).

3.2.5 Impacts of the anomalous atmospheric circulation in different latitudes on the onset of the SCSM

The SCSM onset is influenced by the low-latitude circulation and the anomalous atmospheric

circulation in the mid and high latitudes as well. Through studying the impacts of the mid- and high- latitude atmospheric circulation anomalies and of the activities of 30-60d low-frequency convection over low latitude areas on the onset of the SCSM, Wen et al. (2006a) discovered that when there exists an anomalous wave train with negative anomalies of geopotential height field (low-frequency cyclone) over the Ural Mountains and its western region and along the seacoast of eastern China, and with the positive anomalies (low-frequency anticyclone) over mid-latitude continent and the Sea of Okhotsk during May 1-15, the ridge of subtropical high will withdraw earlier from the SCS. At the same time, the low-frequency convection over the eastern part of the BOB is active and moves eastward, that around the Philippines develops and moves westward, that over South China is active and moves southward and that over Kalimantan is also active and moves northward. In this case, the establishment of the SCSM is earlier.

3.3 Integrated mechanism of the onset of the EASM

As shown in Fig. 4, due to the existence of the Indian peninsula and its corresponding surface sensible heating, the BOB trough strengthens, the convection and precipitation strengthen initially in this area, and the subtropical high weakens and breaks first here in the seasonal progression of the atmospheric circulation. The ascending motion is evidently set up in the tropical eastern Indian Ocean-Indochina peninsula and SCS region subsequently under the effect of the positive vortex advection (PVA) in front of the BOB trough, while the northwesterly behind the trough is unfavorable for the establishment of the southerly in India and the development of the ascending motion (there is descent behind the trough). On the other hand, the cooperation of the warm westerly advection over the eastern plateau and the sensible heat and latent heat over the Indochina peninsula reverses the temperature gradient in the area, builds the upper-level easterly, and forces the subtropical high to withdraw eastward. The weakening and withdrawal of the subtropical high conduce to the further development and strengthening of convection and precipitation, and then the tropical eastern Indian Ocean-Indochina peninsula summer monsoon breaks out. Correspondingly, the upper-level westerly weakens and is entirely substituted by the tropical easterly; the low-level westerly strengthens and advances eastward to the SCS area. In the meantime, the 30-60d and 10-20d low-frequency oscillations from the east and west in the tropics propagating to the north are phase-locked in the SCS and its surrounding areas around mid-May, which triggers the rapid onset of the SCSM (Liu and Ding, 2005c). The cold air from the north

also can trigger the onset of summer monsoon in some years (Ding et al., 2005; Zhang et al., 2005).

4. Moisture transport of Asian monsoon

The activities of the ASM are closely associated with moisture transport. Based on the vertically integrated moisture transport, Fasullo and Webster (2003) employed the Hydrologic Onset and Withdrawal Index (HOWI) to investigate the interannual variation of the onset date of Indian summer monsoon. The results showed that there is intimate relationship between moisture transport and the onset of summer monsoon.

A planetary-scale water vapor transport band of high values is formed through the converging of large-scale water vapor transport bands in the Asian-Australian regions in summer; and it starts from the Southern Hemisphere, crosses the Asian monsoon region, and then flows to the North Pacific. The north border of moisture transfer by the southerly is near 50°N in Northeast China, and the west border of moisture transfer by the southeasterly from the south side of the WPSH is near 100°E in the southeast of Gansu province (Zhou et al., 2005). The relations of the moisture transport from Indian monsoon region with that over East Asia and their influences on summer rainfall in China are investigated. It is found that the distribution and transport of moisture in the East Asian monsoon region differed greatly from those in the Indian monsoon region (Huang et al, 1998). That is to say, the former that has larger meridional transport and the moisture convergence and divergence is resulted primarily from moisture advection, while the latter that has more zonal transport and the moisture convergence and divergence is resulted primarily from the convergence and divergence of the wind field. Moreover, the moisture transport from Indian monsoon region is inverse to that over East Asia, i.e. more Indian monsoon moisture transport corresponds to less moisture transport over East Asian and less rainfall in the middle and lower reaches of the Yangtze River valley(Zhang, 2001).

Further researches showed that there are four moisture corridors influencing summer rainfall in China which are the southwest corridor, SCS corridor, southeast corridor from the low latitude and the weak northwest corridor from the high latitude, representing the impacts of the South Asian monsoon, the SCSM, subtropical monsoon and mid-latitude westerly on summer rainfall in China, respectively; while the region affected by the EASM is located to the east of 100°E . The southwest corridor is the moisture source of the central South China, Southwest China and Northwest China;

the SCS corridor influences rainfall in South China directly; the southeast corridor transfers moisture to the Yangtze River valley; the northwest corridor transports moisture to the mid and upper reaches of Yellow River and the eastern North China (Tian et al., 2004; Wang et al., 2004).

There are bifurcations on the primary corridor of the moisture transport to the Yangtze River valley. For instance, Xu et al. (2003) considered that the moisture transport of Meiyu belt has the structure of multi-sources, with the BOB, SCS and the tropical western Pacific the primary sources. There is also a moisture corridor in the mid- and high- latitudes in the western Pacific which converges with the former in the Yangtze River valley. The moisture flows from the SCS and the Indian Ocean converges in the BOB, then transfers northward, and turns eastward by the dynamic forcing of the Qinghai-Tibetan plateau to the Yangtze River valley, which forms the principal moisture corridor of the Meiyu rain belt in the Yangtze River valley.

The water vapor transport in the SCS is closely related to the strong rainfall in China. The moisture over SCS is mainly from West Pacific before the monsoon onset, while it is from the tropical eastern Indian Ocean and BOB on the onset pentad. After the SCSM onset, moisture from the west side through Indochina peninsula to SCS increases significantly, which becomes the primary water vapor source, and forms an obvious moisture source region in the SCS where large quantities of moisture is accumulated and transferred northward to South China and the Yangtze River valley, providing necessary moisture conditions for strong precipitation (Ding and Hu, 2003; Liu et al., 2005c; Ding and Chan, 2005).

5. Variability of monsoon and its relationship with other circulation systems

5.1 Intraseasonal oscillation of East Asian monsoon

There is an intimate relationship between the onset of summer monsoon and intraseasonal oscillation (ISO). The low-frequency zonal westerly appears 2d earlier than the SCSM onset; the strong development of the atmospheric ISO to the east of Philippine and its westward extension play an important role in the ISO of the atmosphere in the SCS and the onset of summer monsoon (Li, 2004a). The intraseasonal oscillation of the EASM is arranged in a pattern of wave train along the seacoast of East Asia, and is represented by the northward propagation of monsoon surge with the time. The monsoon surge consists of several ISO wet phases, and summer monsoon breaks out when ISO wet phase is introduced or developed (Qian et al., 2000; Ju et al., 2005a). The quasi-biweekly oscillation of the tropical atmosphere has a critical role in the establishing process

of summer monsoon. Investigations found that the coherent adjustments of the convective disturbance and the wind fields associated with the atmospheric Rossby waves response may be an important maintaining mechanism of the tropical quasi-biweekly oscillation (Wen and Zhang, 2005).

Intraseasonal oscillation is one of the factors affecting the early or late onset of summer monsoon. Using the 30-60d filtered data of OLR averaged over SCS for 1981-1996, Wen et al. (2004) defined an index to describe the “low-frequency convection outbreak” of SCS and analyzed ten “low-frequency convection outbreak” years synthetically. They pointed out that the dry phase of ISO in the low latitude inhibits the development of southwesterly and cyclonic circulation in the SCS before the outbreak of low-frequency convection; together with the northeastward propagation of ISO in the tropical Indian Ocean areas, there appears anomalous low-frequency cyclonic circulation in the SCS, and the low-frequency southwesterly and convection strengthen rapidly, then the SCSM breaks out.

Two preferential modes (30-60d and 10-20d) may play a significant part in the adjustment of the EASM. Analysis on the data of 1998 indicates that activities of the SCS are mainly controlled by 30-60d oscillation, but adjusted by 10-20d mode. The low-frequency oscillation waves propagating northward in the form of wave train and monsoon surge along the East Asia coast connect activities in the tropics and subtropics, which results in contrary phases in these two regions. Quasi-30-60d oscillation is obvious in strong monsoon surge years, producing more rainfall in the mid and lower reaches of Yangtze River; while it weakens in weak monsoon surge years when 10-20d oscillation is the primary period, producing drought in the mid and lower reaches of Yangtze River (Ding, 2004; Ju et al., 2005a, c). Analysis showed no matter whether the EASM is strong or weak, the westward propagation of the atmospheric ISO in the Pacific is stronger in every flood summer for several regions of East Asia, while it is weaker in every drought summer, indicating that strong or weak westward propagation of the ISO in the Pacific is the necessary condition for the precipitation amount in the EASM region (Han et al., 2006).

ISO has also two significant modes in the western North Pacific (WNP) monsoon region, in which 30-60d mode is predominant (Wang et al., 2005). The synthetic analysis on different phases pointed out that the low-frequency convection and westerly in WNP propagate to the west and to the north. The monsoon rainfall, convection and active-break cycle in WNP are adjusted by

30-60d and 10-20d low frequency oscillation to a great extent. But 30-60d oscillation in the SCS and tropical WNP in summer is also influenced by ENSO in the preceding winter (Lu and Ren, 2005).

The strongest center of kinetic energy in the tropical ASM region is located over 75° - 95° E, with the secondary over Somali jet channel around 50° E. The disturbances of both kinetic energy and meridional wind are observed east of 90° E, mainly coming from the western Pacific and propagating westward to the BOB through SCS. But the propagation directions of both kinetic energy and meridional wind are rather disorderly between the BOB and the Somali jet channel. Therefore, the EASM and the Indian summer monsoon are different in the propagation features of the disturbances of kinetic energy and meridional wind. Above facts indicate that East Asian monsoon system exists undoubtedly even at the equatorial region, and quite distinct from the Indian monsoon system, it is mainly affected by the disturbances coming from the tropical western Pacific rather than from the Indian monsoon region. The boundary of the two monsoon systems is around 95° - 100° E, which is more westward than the counterpart as proposed in earlier studies by 5° - 10° E degrees in longitude (Chen et al., 2004; Gao et al., 2005).

5.2 The affecting factors of the interannual variation of East Asian monsoon and its possible mechanisms

Huang et al. (2003a,b) summarized that the reasons for the interannual variation of East Asian monsoon are complicated and affected by many factors. The interannual variation of East Asian monsoon is jointly influenced by the Indian monsoon, the WPSH, disturbances in mid-latitude, ENSO cycle, warm pool in the tropical western Pacific, the thermal conditions of the tropical Indian Ocean, the land surface process, snow cover in Eurasia, the dynamic and thermal effects of the Tibetan Plateau, the sea-ice of the Arctic Ocean, and so on.

5.2.1 Warm pool in the western Pacific and its convective activities and the interannual variation of the EASM

Huang et al. (2005) perfected and developed the viewpoints on the characteristics of the interannual variations of onset and advance of the EASM and their associations with thermal states of the tropical western Pacific. Fig. 5 shows that when the tropical western Pacific is in a warming (cooling) state in spring and summer, convective activities are intensified (weakened)

around the Philippines. In this case, there is an anomalous cyclonic (anticyclonic) circulation in the lower troposphere over the SCS, and the WPSH shifts eastward (westward), thus, the early (later) onset of the SCSM can be caused. Moreover, since the WPSH shifts northward abruptly in mid-June and early July, respectively, when the tropical western Pacific is warm, the abrupt northward shift of the EASM rain band from South China to the Yangtze River and the Huaihe River valleys is obvious in mid-June and this monsoon rain band again jumps northward to the Yellow River valley, North China and Northeast China in early July. As a result, summer monsoon rainfall is below normal and drought may occur in the Yangtze River and the Huaihe River valleys, but summer rainfall is normal or above normal in the Yellow River valley, North China and Northeast China. On the other hand, when the tropical western Pacific is in a cooling state in spring and summer, the EASM rain band can be maintained in the Yangtze River and Huaihe River valleys. That is to say, the summer monsoon rainfall is above normal and flood may occur in these two valleys, but summer rainfall is below normal and drought may occur in North China.

5.2.2 El Niño

Observational analyses and numerical experiments found that El Niño has certain impact on the early or late onset of southwesterly monsoon in SCS, which is less significant than the anomalous SST in western Pacific dose. In the preceding periods of the strong (weak) SCSM years, the tropical SST is distributed as La Niña (El Niño) pattern, in which the distribution of SST in December relates most with the intensity of the coming SCSM (Liang and Wu, 2002, 2003; Zhang et al., 2004).

Zhang and Sumi (2002) investigated features of the moisture circulation over East Asia during different El Niño episodes. It is found that in the El Niño mature phase, the anomalies of precipitation in China, water vapor transport and moisture divergence over East Asia differ from those in the rest of the phases, and the impact of El Niño on the East Asian climate is significant. The physical process through which El Niño affects the climate in East Asia was also discussed.

5.2.3 SST in the Indian Ocean

The Indian Ocean Dipole (IOD) has significant impacts on the weather and climate in East Asian monsoon region, especially in summer and in El Niño period. In the positive phase of the IOD, southwesterly monsoon in East Asia breaks out later, with its intensity strengthening and rainfall increasing in China; while in the negative phase of the IOD, southwesterly monsoon in

East Asia breaks out earlier, with its intensity weakening and plentiful rainfall in Southeast China (Yan and Zhang, 2004a). Furthermore, the SSTA in the equatorial east Pacific and the IOD exert cooperative influences on climate variation over East Asian monsoon region. The possible processes, through which the Indian Ocean SSTA impacts on the onset of the SCSM, are also different when the ENSO signal is included or removed. (Yan and Zhang, 2004b; Wen et al., 2006). Lu et al. (2006) pointed out that SST in the Atlantic also has important impacts on the EASM and rainfall.

5.2.4 Snow state over the Tibetan Plateau

Numerical simulation shows that the increase of both snow cover and snow depth over the Tibetan Plateau can delay the onset and weaken the intensity of summer monsoon obviously, resulting in the decrease of precipitation in South China and North China while the increase in the Yangtze and Huaihe River basins. The influence of the winter snow depth is more substantial than that of both the winter snow cover and the spring snow depth. The snow anomalies over the Tibetan Plateau change the soil moisture and the surface temperature through melting process of snow firstly, in the meantime heat, moisture and radiation fluxes from the surface to the atmosphere are altered. Abnormal circulation conditions induced by changes of surface fluxes may affect the underlying surface properties in turn. Such a long time interaction between the wetland and the atmosphere is the key process resulting in later climate changes (Qian et al., 2003).

5.2.5 Somali jet

Somali jet, the predominant cross-equatorial flow, plays a key role in the water vapor transport between the two hemispheres. It transports water vapor through the equator from the southern hemisphere to the northern hemisphere during boreal summer time, and from the northern hemisphere to the southern hemisphere during boreal winter time. The interannual variation of Somali jet is found to be linked with the many changes around the globe, including the wave pattern along East Asia coast, the South Asian high, dipole pattern to the southeast of Australia, and SSTA in the northern Indian Ocean in spring. The results also reveal that interannual variation of Somali jet at boreal spring has significant influences on the East Asian summer rainfall and atmospheric circulation (Wang and Xue, 2003).

5.2.6 Circulations in the Southern Hemisphere

Studies on the interannual variation of Mascarene High and Australian High indicated that the

former is controlled by Antarctic Oscillation (AAO), while the latter is related to both ENSO and AAO. In spring and summer, especially in spring, the intensity of Mascarene High and Australian High is closely associated with summer rainfall in East Asia. When Mascarene High strengthens in spring and summer, there is more rainfall from Yangtze River valley to Japan and less rainfall from South China to western Pacific east of Taiwan and mid-latitude in East Asia. The influence of Australian High on summer rainfall in East Asia is restricted in specific area. When Australian High strengthens, rainfall is less in South China. The influence of Australian High on East Asia monsoon is weaker than that of Mascarene High that plays a crucial role in the interactions between the atmospheric circulations of the two hemispheres. Studies proves that AAO is another strong interannual signal influencing summer rainfall in East Asia (Xue et al., 2003a,b).

Nan and Li (2005) found that there are a significantly positive correlation between the boreal spring southern hemisphere annular mode (SAM) and the following summer precipitation in the mid and lower reaches of Yangtze River valley. While there is strong SAM in spring, a pair of anomalous anticyclones exists in the Mongolia Plateau and Tianshan Mountains, respectively. Meanwhile the anomalous northerly prevails from Northeast China to the mid-latitude of South China. These anomalous circulations may persist till the following summer and weaken the EASM; the west ridge of the WPSH strengthens and extends westward in summer following the spring of strong SAM. These circulation anomalies are related to more precipitation in the mid and lower reaches of Yangtze River valley.

5.2.7 The activities of stationary planetary waves and East Asian winter monsoon

Chen et al. (2005) investigated the relationship between the activities of stationary planetary waves and East Asian winter monsoon and suggested that in winter when the stationary planetary waves act frequently, the upward propagations of the waves from troposphere to stratosphere weaken, along with small polar vortex disturbance, which results in chilling and strengthening of the polar vortex. In the meantime, westerly jet in East Asia, East Asian trough, the Siberian high and Aleutian low become weakening significantly, which weakens the northeasterly over East Asia and warms this area. Further studies pointed out that the planetary waves of zonal two-wave pattern play a leading role in the variability of East Asia winter monsoon.

5.3 Interdecadal variation of the Asian monsoon

There exists interdecadal variation in Asian monsoon circulation (Fong et al., 2005; Li and Zeng,

2005; Jiang and Wang, 2005; Wu, 2005; Zhao and Zhou, 2005; Zhao and Zhang, 2006). The EASM has been weakening since 1960s on a decadal scale, and appears two interdecadal abrupt changes in the mid-1960s and in late 1970s, but there is still disputes over whether such decadal weakening is related to global warming induced by human activities or not. The position and intensity of the WPSH also occurred obvious interdecadal variation in the mid-1970s. As a result, the summer southwesterly influences directly the areas from lower reaches of Yangtze River to Korea after the mid-1970s when rainfall is less in North China and more in Yangtze River to Korea; while before the mid-1970s, summer southwesterly can reach North China, then rainfall is more in North China and less in Yangtze River (Dai et al., 2003; LÜ et al., 2004; Qian, 2005). The East Asian winter monsoon has obvious interdecadal variation as well. The temperature in the north of East Asia has been rising significantly since the mid-1970s, which is directly influenced by the interdecadal variation of East Asian winter monsoon (Ju et al., 2004).

The interdecadal variation of Asian monsoon may be associated with temperature decrease in the troposphere and the interdecadal variation of the sea thermal states. Wu (2005) found that in the two weakening processes of Indian summer monsoon in mid-1960s and in late 1970s, the thermal contrast in the troposphere decreases between East Asia and the tropical regions from east Indian Ocean to tropical western Pacific, which weakens the Indian summer monsoon circulation. In recent 20 years, the impact of El Niño on East Asian summer circulation is increasing, and the warm phase of Pacific Decadal Oscillation (PDO) synchronizes basically with the interdecadal variation of the atmospheric circulation in East Asia (Wang and Kiyotoshi, 2005). Yang et al. (2005) pointed out the interdecadal anomaly of rainfall in North China is significantly correlated with the anomalous sea thermal states in the upper layer in the Pacific, and further revealed the related mechanism.

Another affecting factor is possibly Arctic Oscillation (AO) (Ju et al., 2005). In recent 20 years, the Asian continent in winter and spring warms in mid and high latitudes and cools in the low latitude, along with the trend in the AO toward its high-index polarity after the late 1970's. In the meantime, rainfall increases in Tibetan plateau and South China, which increases the soil moisture. Due to the memory of soil moisture, the cooling of southern continent is maintained to summer and the warming of Asian continent in summer slows down. Moreover, the Pacific to the east and the Indian Ocean to the south of Asia are warming from winter to summer, therefore, the land-sea

thermal contrast decreases in summer, which results in weakening of the EASM circulation.

5.4 Relationship between the ASM and other circulation systems

5.4.1 Relationship between the summer rainfall in East Asia and the West Pacific subtropical high

The northward progression of summer monsoon in East Asia is closely associated with the variation of the subtropical high. The seasonal northward advancement of the subtropical high in March-July is represented mainly by three abrupt changes, corresponding temporally to the onset of the SCSM, the occurrence of the Meiyu and the end of the Meiyu, respectively (Shu and Luo,).

When the ridge-line of the WPSH shifts more southward than the normal, or the ridge-point shifts to more west than the normal, the EASM circulation is weaker. Correspondingly, there is an anti-cyclonic circulation in the anomalous wind field at 850 hPa over the tropical area in East Asia, and there is a cyclonic circulation over the subtropical area. The anomalous ascending motion at 500 hPa weakens over the tropical area in East Asia, while the ascending motion over the Meiyu frontal area strengthens. Meantime, at 500 hPa there is the blocking situation over the Sea of Okhotsk which is located in the high latitude in East Asia. The cold air from the high latitude reaches mid-latitude and strengthens the disturbance of the Meiyu front. As a result, the rainfall in the Yangtze River Valley is above normal. On the contrary, when the ridge-line of subtropical anticyclone over the western Pacific shifts more northward than normal, or the ridge-point shifts to more east than normal, the EASM circulation is stronger. The activities of the circulation systems appear opposite anomaly pattern, and the rainfall in the Yangtze River Valley is below normal (Zhang and Tao, 2003). Studies also showed that the WPSH has two ridge lines sometimes, influencing the distribution of rainfall in eastern China and the genesis and lysis of Meiyu (Zhan et al., 2005; Qi et al., 2006).

In the seasonal scale, the intensity of the WPSH, the position of its western boundary, and the intensity of the South Asia high are closely associated with the strength of the EASM, while the meridional position of the northern boundary of the WPSH and the blocking situation over the Ural area are related to the rainfall amount in East Asia (Liu et al., 2004).

Lu (2001) pointed out that the monsoon rainfall in East Asia is influenced by not only the meridional but also the east-west movement of the subtropical high. He also showed that the anomalous atmospheric convection over the Philippines impacts the east-west movement of

subtropical high through Rossby wave, which modifies Gill's theory and makes a new progress.

5.4.2 Multi-scale conditions of strong summer monsoon rainfall

The east-west movement and meridional shift of subtropical high determine the position of the EASM rainbelt; the SCSM surge transports large warm and wet air from sea to land, ensuring abundant provision of moisture for continuous rainfall; cold air in mid and high latitudes increases the moisture contrast of the air in the north and south, maintains and strengthens Meiyu front; the meso- α scale convective systems in the plateau propagate eastward to Yangtze River valley, promote the formation and development of the meso- α scale systems in Meiyu front. Such interactions among different scales systems provide the circulation conditions for the occurrence of continuous strong rainfall in the mid and lower reaches of Yangtze River valley. When the above systems are best combined (locked), i.e. they are all in an active phase, it is prone to obtain large-scale and long-time rainstorms which may cause severe floods (Zhang et al., 2002). Gao et al. (2002) and Zhou (2004) found "double fronts" (dew-point front and Meiyu front) structure of the summer monsoon rainfall in East Asia, and further suggested the conception of Meiyu front system, which sheds light on the structure of the summer monsoon rainfall.

5.4.3 Relationship between monsoon circulation and meso-scale systems

There is a kind of positive feedback mechanism between large-scale circulations and meso-scale convective systems. At the early stage of the monsoon onset, the wide range background provides favorable synoptic and dynamic conditions for the summer monsoon onset and the formation of meso-scale convective activities; whereas after the summer monsoon onset, occurrence of persistent and large-scale meso-scale convective activities produces obvious feedback effect on large-scale circulation. Because of the release of latent heating driven by enhanced convective activities, the intense atmospheric heating appears over the northern SCS, which results in the meridional temperature gradient over the SCS reversing from upper-level to low-level, and then the large-scale circulations are changed seasonally. Correspondingly, the surface pressure over the northern SCS deepens continually and forms broad monsoon trough and obvious pressure-reducing areas, thus making the subtropical high moving out of the SCS eventually. With the development of the low pressure circulations in the mid and lower troposphere, the meso-scale convective systems further enhance and extend southward, which is favorable to the SCSM onset and maintaining over the central and southern SCS. The deepening

of monsoon trough promotes strengthening of the monsoon flow and moisture transport on the southern side of it, consequently the monsoon onset reaching prevalence (Liu et al., 2005a,b).

5.4.4 Relationship between monsoon and westerly Jet

Liao et al. (2004) analyzed the activities of the subtropical westerly jet in boreal summer and the association with the distribution of anomalous SST in the equatorial central Pacific-subtropical North Pacific-extratropical central North Pacific which exert influences on the intensity of South Asia high at 200 hPa, the anomaly of the EASM and the anomaly of rainfall in East China.

The upper westerly jet jumps northward twice during the transition process from winter to summer and they are intimately related to the EASM activities. Li et al. (2004) emphasized that the northward jump of the upper westerly jet in East Asia for the first time occurs about on 8 May averagely, and it is about 7 days earlier than the onset date of the SCSM (mean date is 15 May). The northward jump of upper westerly jet over East Asia for the second time occurs about on 7 June averagely, and it is about 10 days earlier than the beginning date of the Meiyu rainfall in the Yangtze River and Huaihe River basins (mean date is 18 June) and can be the forewarning of Meiyu rainfall beginning. These two-time northward jumps of the upper westerly jet are related to two-time reverses of meridional temperature gradient in the upper-middle troposphere (500-200 hPa), respectively. During the seasonal transition, the continent is heated quickly, so that the meridional temperature gradient in the upper-middle troposphere will be reversed in 5°-25°N in South Asia. Then through the geostrophic adjustment, the flow field adjusts to the pressure field (temperature field) and it will lead to the northward jumps of the upper westerly jet location. The analyses also show that sometimes the enhancement and northward moving of the upper westerly jet in the southern hemispheric subtropics can also influence the first northward jump of the upper westerly jet in East Asia.

5.4.5 Correlation with the anomalous circulation in the western Pacific

There is key relation between the tropical western Pacific circulation anomaly in winter and the following the ASM. The winter time anti-cyclonic (cyclonic) circulation anomaly in the tropical western Pacific moves gradually northeastward and expands westward, and the anomalous easterly (westerly) to the south of the anti-cyclonic (cyclonic) circulation extends westward to Indian peninsula, leading to the weakening (strengthening) of South Asian summer monsoon (Huang et al., 2003a,b; Wu et al., 2003).

Li and his research group (Li et al., 2005; Pu et al., 2006) paid special attention to the impact of the East Asian winter monsoon on the anomalous circulation in the western Pacific, and pointed out that a anomalous pattern of pressure exists in a long period in the western Pacific and Southeast Asia (Fig.6). The different pressure gradients in the equatorial western Pacific region induced by strong (weak) East Asian winter monsoon play an important role in the formation of anomalous westerly (easterly) in the equatorial western Pacific; meanwhile, the anomalous westerly (easterly) formed in the equatorial western Pacific and the anomalous easterly (westerly) triggered in around 20°N cooperate with the anomalous northerly (southerly) along the East Asian coast, favoring the anomalous cyclonic (anti-cyclonic) circulation to the east of Philippine which is a key factor influencing monsoon weather and climate and provides critical signal for prediction of weather and climate in China.

6 Problems and outlook

(1) How to describe quantitatively the intensity of the East Asian monsoon and its interannual variability is still a basic scientific problem in the study of monsoon. Obviously, we expect using a simple and effective index to represent the intensity and variability of monsoon. The Southern Oscillation index is a best instance employing one parameter to describe a complex phenomenon. An appropriate monsoon index is favorable to the quest of correlation among monsoon variability, other circulation systems and climate variability, to the establishment of association among monsoon variability and the inner and outer forcing factors, and to the objective evaluation of numerical models' potential to reproduce monsoon variability. Various monsoon indices so far have certain effects, but they are not conformable to all wishes. The key problem lies in that the East Asian monsoon contains both the SCS-western Pacific tropical monsoon and China mainland-Japan subtropical monsoon. It covers a distance of 40-50 latitudes and is significantly influenced by mid and high latitudes. Therefore, the choice of East Asian monsoon index is much more difficult than the choice of Indian monsoon index. The circulation intensity and rainfall amount in the East Asian monsoon region have the characteristic of "distribution" rather than "unanimity", so indices defined by different sub-areas and different parameters have no "comparability", and even get contrary conclusions. We believe a "common area" and a "common parameter" should be chosen to define East Asian monsoon index that can reflect both the wind and rain, thus scholars can discuss it on a "common language". Hence, further exploration is

needed to obtain an accepted monsoon index.

(2) The essence of East Asian subtropical monsoon and its interaction with the tropical monsoon is a scientific problem that is not paid much attention to. As is said earlier, East Asian monsoon contains both the tropical monsoon and subtropical monsoon which are interacted and influence directly large-scale flood and drought in China. But what on earth is subtropical monsoon? Or what is the essence of subtropical monsoon? There are generally two misunderstandings: one is based on regions, i.e. monsoon prevalent in the subtropical areas in East Asia is called “East Asian subtropical monsoon”; the other consider the northward extension of tropical monsoon in East Asia as subtropical monsoon. Both neglect the reason why subtropical monsoon exists. We believe that the meridional land-sea thermal contrast in East Asia is the key driving force of tropical monsoon, while the seasonal cycle formed by the thermal contrast between Asian continent (including the plateau) and western Pacific may be an independent driving force of subtropical monsoon. Obviously if there was no land-sea contrast between Asian continent and western Pacific, the subtropical high belt would not break, and the East Asian tropical monsoon could not extend to Northeast China around 50°N. We may imagine that the northward progression of East Asian monsoon is the result of coordination and interaction between the East Asian tropical monsoon and the East Asian subtropical monsoon. Therefore, we have to study thoroughly the essence of East Asian subtropical monsoon and its interaction with tropical monsoon, which will improve the prediction of flood and drought in China.

(3) If the East Asian subtropical monsoon is an independent system from tropical monsoon, what members are involved in East Asian subtropical monsoon system? What about the seasonal cycle? When is the East Asian subtropical monsoon established and ended? It is directly related to the seasonal cycle in East China, so it is a scientific problem worthy of studying.

(4) The thermal effect of Tibetan Plateau strengthens the meridional land-sea (Asian continent and Indian Ocean) thermal contrast and the zonal land-sea thermal contrast (Asian continent and the Pacific). Especially, as an uplifted heat source (or cold source), the plateau makes the seasonal transition of thermal contrast more sensitively and more ahead. That is to say, the plateau is the key and sensitive area to monitor and predict monsoon. So studies on the plateau are very important.

(5) The East Asian subtropical summer monsoon rainbelt locates on the forward side of summer

monsoon, so rainbelt moves northward as the summer monsoon marches northward. Rainfall is relatively less in the controlling region of summer monsoon, i.e. the activity on the forward side of summer monsoon is directly related to the progression of rainbelt. Hereby the research on monsoon edge is also a meaningful problem.

(6) Asian monsoon is the outcome of interactions among the earth, ocean, atmosphere, hydrosphere, biosphere and cryosphere, and the evolving rule and variability of monsoon influence greatly the plantation, bio-earth, chemistry, economy and society in the entire Asian monsoon region. Therefore, it is necessary to place monsoon in the coupled system of land-sea-atmosphere and to know its characteristics and mechanisms through studying the interactions among different spheres, layers, systems and scales.

(7) The seasonal prediction of monsoon activities is critical to national economy and social development, but the predicting ability of the present coupled model of land-sea-atmosphere has many difficulties. The proper description of Tibetan plateau in the model, the correct introduction of land-atmosphere process, and the reasonable parameterization of physical processes are critical to upgrade the ability to predict the East Asian monsoon. Thus, the progress in the study of models are highly expected.

(8) The change of the coverage on land and the atmospheric components in both regional and global scales induced by human activities may influence the future of Asian monsoon to a great extent. Researches on this aspect help to regulate human activities, realize the harmony between human and nature, and protect living environment of human beings.

To sum up, the mechanisms of variation of East Asian monsoon, the mechanisms of East Asian monsoon influencing weather and climate in China especially flood and drought, and the theories and methods of predicting East Asian monsoon are still the primary aims in the study of monsoon in future.

Acknowledgments. The authors would like to thank all the authors of the references for their research achievements. We also wish to thank Chen hua, Wei Jin and Zhu Xiaying for their kind assistance. This work was jointly supported by the National Natural Science Foundation of China (Granted No. 40633018; 40675056) and the key project A of the State Ministry of Science and Technology of China “South China Sea Monsoon Experiment (SCSMEX)”.

References

- Chao, Winston C., 2000: Multiple quasi equilibria of the ITCZ and the origin of monsoon onset. *J. Atmos. Sci.*, **57**, 641–651.
- Chao, Winston C., and Baode Chen, 2001: Multiple quasi equilibria of the ITCZ and the origin of monsoon onset. Part II: rotational ITCZ attractors, *J. Atmos. Sci.*, **58**, 2820–2831.
- Chen, Longxun, Qiagen Zhu, Huibang Luo, Jinhai He, Min Dong, and Zhiqiang Feng, 1991: *East Asian Monsoon*. China Meteorological Press, Beijing, 362pp. (in Chinese)
- Chen, Longxun, Hui Gao, Jinhai He, Shiyan Tao, and Zuhui Jin, 2004: Zonal propagation of kinetic energy and convection in the South China Sea and Indian monsoon regions in boreal summer. *Science in China (Series D)*, **34**(2), 171–179. (in Chinese)
- Chen, Wen, H.-F. Graf, and Ronghui Huang., 2000: The interannual variability of East Asian winter monsoon and its relation to the summer monsoon. *Adv. Atmos. Sci.*, **17**, 48–60.
- Chen, Wen, S. Yang, and Ronghui Huang, 2005: Relationship between stationary planetary wave activity and the East Asian winter monsoon. *J. Geophys. Res.*, **110**, D14110, doi: 10.1029/2004JD005669.
- Dai, Xingang, Ping Wang, and Jifan Chou, 2003: Multiscale characteristics of the rainy season rainfall and interdecadal decaying of summer monsoon in North China. *Chinese Science Bulletin*, **38**(23), 2483–2487. (in Chinese)
- Ding, Yihui, 1994: *Monsoons over China*. Dordrecht Boston London: Kluwer Academic Publisher, 419 pp.
- Ding, Yihui, and Guoquan Hu, 2003: A study on water vapor budget over China during the 1998 severe flood periods. *Acta Meteorologica Sinica*, **61**(2), 129–145. (in Chinese)
- Ding, Yihui, Chongyin Li, Jinhai He, and Longxun Chen, 2004: South China Sea monsoon experiment (SCSMEX) and the East-Asian monsoon. *Acta Meteorologica Sinica*, **62**(5), 561–586. (in Chinese)
- Ding, Yihui, 2004: Seasonal march of the East-Asia summer monsoon. *East Asian Monsoon*, C. P. Chang, Eds, World Scientific Publishing, Singapore, 562 pp.
- Ding, Yihui, and Johnny C. L. Chan, 2005: The East Asian summer monsoon: an overview. *Meteorol. Atmos. Phys.*, **89**, 117–142.
- Fasullo, J., and P. J. Webster, 2003: A hydrological definition of indian monsoon onset and withdrawal. *J. Climate*, **16**, 3200–3211.
- Fong, Soikun, Anyu Wang, Tinggai Tong, Guoli Li, Kinhang Lam, Jianyin Liang, Chisheng Wu, and Qi Fan, 2005:

- Climatological characteristics of the maintaining period of South China Sea summer monsoon II Interdecadal Variation. *Journal of Tropical Meteorology*, **21**(2), 123–130. (in Chinese)
- Gao, Hui, Longxun Chen, Jinhai He, Shiyao Tao, and Zuhui Jin, 2005: Characteristics of zonal propagation of atmospheric kinetic energy at equatorial region in Asia. *Acta Meteorologica Sinica*, **63**(1), 21–29. (in Chinese)
- Gao, Shouting, Yushu Zhou, and Ting Lei, 2002: Structural features of the Meiyu front system. *Acta Meteorologica Sinica*, **16**(2), 195–204. (in Chinese)
- Han, Rongqing, Weijing Li, and Min Dong, 2006: The impact of 30 - 60 day oscillations over the subtropical Pacific on the East Asian summer rainfall. *Acta Meteorologica Sinica*, **64**(2), 149–163. (in Chinese)
- He, Haiyan, Chung-Hsiung Sui, Maoqi Jian, Zhiping Wen, and Guangdong Lan, 2003: The evolution of tropospheric temperature field and its relationship with the onset of Asian summer monsoon. *J. Meteorol. Soc. Japan*, **81**(5), 1201–1223.
- He, Jinhai, Qiangen Zhu, M. Murakami, 1996: T_{BB} data-revealed features of Asian-Australian monsoon seasonal transition and Asian summer monsoon establishment, *J. Trop. Meteor.* (in Chinese), **12**(1), 34-42.
- He, Jinhai, Yihui Ding, Hui Gao, Haimin Xu, 2001: The definition of onset date of South China Sea summer monsoon and the monsoon indices. China Meteorological Press, Beijing, 123 pp. (in Chinese)
- He, Jinhai, Min Wen, Xiaohui Shi, and Qiaohua Zhao, 2002: Splitting and eastward withdrawal of the subtropical high belt during the onset of the South China Sea summer monsoon and their possible mechanism. *Journal of Nanjing University (Natural Sciences)*, **38**(3), 318–330. (in Chinese)
- He, Jinhai, Lijuan Wang, Haiming Xu, and Bing Zhou, 2004a: Climatic features of SCS summer monsoon onset and its possible mechanism. *Bimonthly of Xinjiang Meteorology*, **27**(1), 1–7. (in Chinese)
- He, Jinhai, Jingjing Yu, Xinyong Shen, and Hui Gao, 2004b: Research on mechanism and variability of East Asian monsoon. *Journal of Tropical Meteorology*, **20**(5), 449–459. (in Chinese)
- He, Jinhai, Min Wen, Lijuan Wang, and Haiming Xu, 2006: Characteristics of the onset of the Asian Summer Monsoon and the importance of Asian-Australian “land bridge”. *Adv. Atmos. Sci.*, **23**(6), 951-963.
- Huang, Ronghui, Zhenzhou Zhang, Gang Huang, and Baohua Ren, 1998: Characteristics of the water vapor transport in East Asian monsoon region and its difference from that in South Asian monsoon region in summer. *Scientia Atmospherica Sinica*, **22**(4), 460–469. (in Chinese)
- Huang, Ronghui, Wen Chen, Yihui Ding, and Chongyin Li, 2003a: Studies on the monsoon dynamics and the interaction between monsoon and ENSO cycle. *Chinese Journal of Atmosphere Sciences*, **27**(4), 484–502. (in

Chinese)

Huang, Ronghui, Liantong Zhou, and Wen Chen, 2003b: The progress of recent studies on the variability of the East Asian monsoon and their causes. *Advan. Atmos. Sci.*, **20**(1), 55–69.

Huang, Ronghui, Lei Gu, Yuhong Xu, Qilong Zhang, Shangsens Wu, and Jie Cao, 2005: Characteristics of the interannual variations of onset and advance of the East Asian summer monsoon and their associations with thermal states of the tropical western Pacific. *Chinese Journal of Atmosphere Sciences*, **29**(1), 20–36. (in Chinese)

Huang, Ronghui, Jilong Chen, Gang Huang, and Qilong Zhang, 2006: The quasi-biennial oscillation of summer monsoon rainfall in China and its cause. *Chinese Journal of Atmosphere Sciences*, **30**(4), 545–560. (in Chinese)

Jhun, J.-G., and E.-J. Lee, 2004: A new East Asian winter monsoon index and associated characteristics of the winter monsoon. *J. Climat*, **17**, 711–726.

Jiang, Dabang, and Huijun Wang, 2005: Natural interdecadal weakening of East Asian summer monsoon in the late 20th century. *Chinese Science Bulletin*, **50**(20), 2256–2262. (in Chinese)

Jiang, Zhihong, Jinhai He, Jianping Li, Jinhua Yang, and Ji Wang, 2006: Northerly advancement characteristics of the East Asian summer monsoon with its interdecadal variations. *Acta Geographica Sinica*, **61**(7), 675–686. (in Chinese)

Jin, Qihua, Jinhai He, Longxun Chen, and Congwen Zhu, 2006: Impact of ocean-continent distribution over southern Asian on the formation of summer monsoon. *Acta Meteorologica Sinica*, **20**(1), 95–108.

Ju, Jianhua, Juzhang Ren, Junmei LÜ, 2004: Effect of interdecadal variation of Arctic Oscillation on temperature increasing in North of East Asian Winter. *Plateau Meteorology*, **23**(4), 429–434. (in Chinese)

Ju, Jianhua, Cheng Qian, and Jie Cao, 2005a: The intraseasonal oscillation of East Asian summer monsoon. *Chinese Journal of Atmosphere Sciences*, **29**(2), 187–194. (in Chinese)

Ju, Jianhua, Junmei LÜ, Jie Cao, and Juzhang Ren, 2005b: Possible impacts of the Arctic Oscillation on the interdecadal variation of summer monsoon rainfall in East Asia. *Adv. Atmos. Sci.*, **22**(1), 39–48.

Ju, Jianhua, and Erxu Zhao, 2005c: Impacts of the low frequency oscillation in East Asian summer monsoon on the drought and flooding in the middle and lower valley of the Yangtze River. *Journal of Tropical Meteorology*, **21**(2), 163–173. (in Chinese)

Li, Chongyin, 2004: Recent progress in atmospheric intraseasonal oscillation research. *Progress in Natural Science*, **14**(7), 734–741. (in Chinese)

- Li, Chongyin, Zuotai Wang, Shizhe Lin, and Hanru Gao, 2004: The relationship between East Asian summer monsoon activity and northward jump of the upper westerly jet location. *Chinese Journal of Atmosphere Sciences*, **28**(5), 641–658. (in Chinese)
- Li, Chongyin, Shunqiang Pei, and Ye Pu, 2005: Dynamical influence of anomalous East Asian winter monsoon on zonal wind over the equatorial western Pacific. *Chinese Science Bulletin*, **50**(11), 1136–1141. (in Chinese)
- Li, Jianping, and Qingcun Zeng, 2003a: A new monsoon index and the geographical distribution of the global monsoons. *Adv. Atmos. Sci.*, **20**(2), 299–302.
- Li, Jianping, and Qingcun Zeng, 2003b: A unified monsoon index. *Geophys. Res. Lett.*, **29**(8), 1151–1154.
- Li, Jianping, and Qingcun Zeng, 2005: A new monsoon index, its interannual variability and relation with monsoon precipitation. *Climatic and Environmental Research*, **10**(3), 351–365. (in Chinese)
- Liang, Jianyin, and Shangsen Wu, 2002: A study of southwest monsoon onset date over the South China Sea and its impact factors. *Chinese Journal of Atmosphere Sciences*, **26**(6): 829–841. (in Chinese)
- Liang, Jianyin, and Shangsen Wu, 2003: The study on the mechanism of SSTA in the Pacific Ocean affecting the onset of summer monsoon in the South China Sea-Numerical experiments. *Acta Oceanologica Sinica*, **25**(1), 28–41. (in Chinese)
- Liang, Xiaoyun, Yimin Liu, and Guoxiong Wu, 2005: Effect of Tibetan Plateau on the site of onset and intensity of the Asian summer monsoon. *Acta Meteorologica Sinica*, **63**(5), 799–805. (in Chinese)
- Liao, Qinghai, Shouting Gao, Huijun Wang, and Shiyan Tao, 2004: Anomalies of the extratropical westerly jet in the North Hemisphere and their impacts on East Asian summer monsoon climate anomalies. *Chinese Journal of Geophysics*, **47**(1), 10–18. (in Chinese)
- Liu, Changzheng, Huijun Wang, and Dabang Jiang, 2004: The Configurable Relationships between Summer Monsoon and Precipitation over East Asia, *Chinese Journal of Atmosphere Sciences*, **28**(5), 700–712. (in Chinese)
- Liu, Yanju, Yihui Ding, and Nan Zhao, 2005a: A study on the meso-scale convective systems during summer monsoon onset over the South China Sea in 1998: I analysis of large-scale fields for occurrence and development of meso-scale convective systems. *Acta Meteorologica Sinica*, **63**(4): 431–442. (in Chinese)
- Liu, Yanju, and Yihui Ding, 2005b: A study on the meso-scale convective systems during summer monsoon onset over the South China Sea in 1998: II effect of the meso-scale convective systems on large-scale fields. *Acta Meteorologica Sinica*, **63**(4), 443–454. (in Chinese)
- Liu, Yanju, (Supervised by Ding Yihui) , 2005c: Study of the South China Sea summer monsoon onset and its

- predictability. Dissertation for Ph.D., Institute of Atmospheric Physics, Chinese Academy of Sciences. (in Chinese)
- Liu, Yimin, Zhongliang Chen, Jiangyu Mao, Guoxiong Wu, 2003a: Impacts of the onset of the Bay of Bengal monsoon on the onset of the South China Sea monsoon. Part I : a case study. *Acta Meteorologica Sinica*, **61**(1), 1–10. (in Chinese)
- Liu, Yimin, Zhongliang Chen, and Guoxiong Wu, 2003b: Impacts of the onset of the Bay of Bengal monsoon on the onset of the South China Sea monsoon. Part II: numerical experiments. *Acta Meteorologica Sinica*, **61**(1), 11–19. (in Chinese)
- Lu, Riyu and Buwen Dong, 2001: Westward extension of North Pacific subtropical high in summer. *J. Meteorol. Soc. Japan*, **79**, 1229–1241.
- Lu, R., and B. Ren, 2005: The influence of ENSO on the seasonal convection evolution and the phase of 30-60-day oscillations during boreal summer. *J. Meteor. Soc. Japan*, **83**, 1025–1040.
- Lu, R., B. Dong, and H. Ding, 2006: Impact of the Atlantic Multidecadal Oscillation on the Asian summer monsoon. *Geophys. Res. Lett.*, in press.
- LÜ, Junmei, Juzhang Ren, and Jianhua Ju, 2004: The interdecadal variability of East Asian Monsoon and its effect on the rainfall over China. *Journal of Tropical Meteorology*, **20**(1), 74–80. (in Chinese)
- LÜ, Junmei, Qingyun Zhang, Shiyan Tao, and Jianhua Ju, 2006: The onset and advance of the Asian summer monsoon. *Chinese Science Bulletin*, **51**(1), 80–88.
- Luo, Meixia, and Chongyin Li, 2004: A study of the onset of the summer monsoon over the South China Sea. *Climatic and Environmental Research*, **9**(3), 495–509. (in Chinese)
- Mooley, D. A., and J. Shukla, 1987: Variability and forecasting of the summer monsoon rainfall over India. *Monsoon Meteorology*, C.-P. Chang and T. N. Krishnamurti, Eds, Oxford University Press, Oxford, 26–59.
- Nan, Sulan, and Jianping Li, 2005: The relationship between the summer precipitation in the Yangtze River Valley and the boreal spring Southern Hemisphere annular mode: I basic facts, *Acta Meteorologica Sinica*, **63**(6), 837–846. (in Chinese)
- Pan, Jing, and ChongYin Li, 2006: Comparison of climate characteristics between two summer monsoon troughs over the South China Sea and India. *Chinese Journal of Atmospheric Sciences*, **30**(3), 377–390. (in Chinese)
- Pu, Ye, Shunqiang Pei, Chongyin Li, and Yuejuan Chen, 2006: Influence of anomalous East Asian winter monsoon on zonal wind anomalies over the equatorial western Pacific. *Chinese Journal of Atmospheric Sciences*, **30**(1), 69–79. (in Chinese)

- Qi, Li, Jinhai He, Ruifen Zhan, and Zuqiang Zhang, 2006: Characteristics of the western Pacific subtropical high double ridges process in 1962. *Chinese Journal of Atmospheric Sciences*, **30**(4), 682–692. (in Chinese)
- Qian, W H, H S Kang, and D K Lee, 2000: Seasonal march of Asian summer monsoon. *Int J Climat*, **20**(11), 1371–1378.
- Qian, Weihong, 2005: Review of variations of the summer monsoon from seasonal to interannual and interdecadal scales. *Journal of Tropical Meteorology*, **21**(2), 199–206.
- Qian, Yongfu, Yan Zhang, and Yiqun Zheng, 2003: Impacts of the Tibetan Plateau snow anomaly in winter and spring on precipitation in China in spring and summer. *Arid Meteorology*, **21**(3), 1–7. (in Chinese)
- Qian, Yongfu, Jing Jiang, Yan Zhang, Yonghong Yao, and Zhongfeng Xu, 2004: The earliest onset area of the tropical Asian Summer monsoon and its mechanism. *Acta Meteorologica Sinica*, **42**(2), 129–139. (in Chinese)
- Ren, Xuejuan, and Yongfu Qian, 2003: Numerical simulation experiments of the impacts of local land-sea thermodynamic contrasts on the SCS summer monsoon onset. *Journal of Tropical Meteorology*, **9**(1), 1–8.
- Shu, Tingfei and Huibang Luo, 2003: Abrupt change of the west Pacific subtropical high and its interannual variation during the later spring and early summer. *Journal of Tropical Meteorology*, **19**(1), 17-26. (in Chinese)
- Tao, Shiyan, and Longxun Chen, 1987: A review of recent research on the East Asian summer monsoon in China. *Monsoon Meteorology*. C.-P. Chang and T. N. Krishnamurti, Eds, Oxford University Press, Oxford, 60–92.
- Tian, Hong, Pingwen Guo, and Weisong Lu, 2004: Characteristics of vapor inflow corridors related to summer rainfall in China and impact factors. *Journal of Tropical Meteorology*, **20**(4), 401–408. (in Chinese)
- Tu, Changwang, Shisong Huang, and Youxi Gao, 1944: The advance and retreat of the summer monsoon, *Meteor. Mag.*, **18**, 1-20.
- Wang, Baojian, Yuxia Huang, Jinhai He, and Lijuan Wang, 2004: Relation between vapour transportation in the period of East Asian summer monsoon and drought in Northwest China. *Plateau Meteorology*, **23**(6), 912-918. (in Chinese)
- Wang, Huijun, Feng Xue, 2003: Interannual variability of Somali jet and its influences on the inter-hemispheric water vapor transport and on the East Asian summer rainfall. *Chinese Journal of Geophysics*, **46**(1), 18–25. (in Chinese)
- Wang, Lijuan, Jinhai He, and Zhaoyong Guan, 2004: Characteristics of convection activities over Sumatra area and its relationship with SCS summer monsoon onset. *Journal of Nanjing Institute of Meteorology*, **27**(4), 451–460. (in Chinese)

- Wang, Hui, Yihui Ding, and Jinhai He, 2005: The climate research of summer monsoon over the western North Pacific. *Acta Meteorologica Sinica*, **63**(4), 418–430. (in Chinese)
- Wang, Yafei, and Takahashi Kiyotoshi, 2005: Decadal climate variability of rainfall around the middle and lower reaches of Yangtze River and atmospheric circulation. *Journal of Tropical Meteorology*, **21**(4), 351–358. (in Chinese)
- Wen, Min, Jinhai He, and Ziniu Xiao, 2004: Impact of the convection over the Indo-China Peninsula on the onset of SCS summer monsoon. *Chinese Journal of Atmospheric Sciences*, **28**(6), 864–875. (in Chinese)
- Wen, Min, and Renhe Zhang, 2005: Possible maintaining mechanism of climatological atmospheric quasi-biweekly oscillation around Sumatra. *Chinese Science Bulletin*, **50**(10), 1054–1056.
- Wen, Zhiping, Ronghui Huang, Haiyan He, and Guangdong Lan, 2006a: The influences of anomalous atmospheric circulation over mid-high latitudes and the activities of 30-60d low frequency convection over low latitudes on the onset of the South China Sea summer monsoon. *Chinese Journal of Atmospheric Sciences*, **30**(5), 952–964. (in Chinese)
- Wen, Zhiping, Zhaoning Liang, and Liji Wu, 2006b: The relationship between the Indian Ocean sea surface temperature anomaly and the onset of South China Sea summer monsoon II. mechanism analysis. *Chinese Journal of Atmospheric Sciences*, **30**(6), 1138–1146. (in Chinese)
- Wen, Zhiping, Haiyan He and Ronghui Huang, 2004: The influences of 30-60 d oscillation on the development of the South China Sea summer monsoon. *Acta Oceanologica Sinica*, **23**(4), 568–579.
- Wu, Binyi, and Jia wang, 2002: Winter Arctic Oscillation, Siberian high and East Asian winter monsoon. *Geophys. Res. Lett.*, **29**, 1897, doi:10.1029/2002GL015373.
- Wu, Bingyi, 2005: Weakening of Indian summer monsoon in recent decades. *Advan. Atmos. Sci.*, **22**(1), 21–29.
- Wu, Bingyi, Dongxiao Wang, and Ronghui Huang, 2003: Relationship between sea level pressures of the winter tropical western Pacific and the subsequent Asian summer monsoon. *Advan. Atmos. Sci.*, **20**(4), 496–510.
- Wu, Bingyi, Renhe Zhang and Rosnaae D'Arrigo, 2006: Distinct modes of the East Asian winter monsoon. *Mon. Wea. Rev.*, **134**, 2165-2179.
- Wu, Guoxiong, and Yongsheng Zhang, 1998: Thermal and mechanical forcing of the Tibetan Plateau and the Asian monsoon onset. Part I: situating of the onset. *Chinese Journal of Atmospheric Sciences*, **22**(6), 825–838. (in Chinese)
- Wu, Guoxiong, Jiangyu Mao, Anmin Duan, and Qiong Zhang, 2004: Recent progress in the study on the impacts of Tibetan Plateau on Asian summer climate. *Acta Meteorologica Sinica*, **62**(5), 528–540. (in Chinese)
- Wu, Guoxiong, Yimin Liu, Xin Liu, Anmin Duan, and Xiaoyun Liang, 2005: How the heating over the Tibetan Plateau affects the Asian climate in summer. *Chinese Journal of Atmospheric Sciences*, **29**(1), 47–56. (in Chinese)

Chinese)

- Wu, Shangsen, Jianyin Liang, and Chunhui Li, 2003: Relationship between the intensity of South China Sea summer monsoon and the precipitation in raining seasons in China. *Journal of Tropical Meteorology*, **19**(Supp), 25–36. (in Chinese)
- Xu, Haiming, Jinhai He, and Min Dong, 2001: Numerical study of the effect of Indian peninsula on South Asian summer monsoon process. *Journal of Tropical Meteorology*, **17**(2), 117–124. (in Chinese)
- Xu, Haiming, Jinhai He, Min Wen, and Min Dong, 2002: A numerical study of effects of the Indo-China Peninsula on the establishment and maintenance of the South China Sea summer monsoon. *Chinese Journal of Atmospheric Sciences*, **26**(3), 330–342. (in Chinese)
- Xu, Xiangde, Lianshou Chen, Xiurong Wang, Qiuju Miao, and Shiyan Tao, 2003: Moisture sink and source for the Meiyu rain band in the Yangtze River valley. *Chinese Science Bulletin*, **48**(21), 2288–2294. (in Chinese)
- Xue, Feng, Dabang Jiang, Xianmei Lan, and Huijun Wang, 2003a: Influence of the Mascarene high and Australian high on the summer monsoon in east Asia: ensemble simulation. *Advan. Atmos. Sci.*, **20**(5), 799–809.
- Xue, Feng, Huijun Wang, and Jinhai He, 2003b: Interannual variability of Mascarene high and Australian high and their influences on summer rainfall over East Asia. *Chinese Science Bulletin*, **48**(3), 287–291. (in Chinese)
- Yan, Xiaoyong, and Ming Zhang, 2004a: A Study of the Indian Ocean dipole influence on climate variations over East Asian monsoon region. *Climatic and Environmental Research*, **9**(3), 427–436. (in Chinese)
- Yan, Xiaoyong, and Ming Zhang, 2004b: Numerical simulation of the Indian Ocean dipole influence on climate variations over East Asian monsoon region during equator east Pacific SSTA. *Journal of Tropical Meteorology*, **20**(4), 376–382. (in Chinese)
- Yang, Song, K.-M. Lau, and K. M. Kim, 2002: Variations of the East Asian jet stream and Asian-Pacific-American winter climate anomalies. *J. Climate*, **15**, 306–325.
- Yang, XiuQun, Qian Xie, YiMin Zhu, XuGuang Sun, and YanJuan Guo, 2005: Decadal-to-interdecadal variability of precipitation in North China and associated atmospheric and oceanic anomaly patterns. *Chinese Journal of Geophysics*, **48**(4), 789–797. (in Chinese)
- Yano, Jun-Ichi, and Jonh L. McBride, 1998: An Aquaplanet Monsoon. *J. Atmos Sci*, **55**, 1373–1399.
- Ye, Duzheng, Shiyan tao, and Maicun Li, 1959: The abrupt change of circulation over the Northern Hemisphere during June and October, *The Atmosphere and the Sea in Motion*, Rockefeller Institute, New York, 249-267.
- Zeng, Qingcun, and Jianping Li, 2002: Interactions between the Northern and Southern Hemispheric atmospheres and the essence of monsoon. *Chinese Journal of Atmospheric Sciences*, **26**(4), 433–448. (in Chinese)

- Zeng, QingCun, DongLing Zhang, Ming Zhang, et al., 2005: The abrupt seasonal transitions in the atmospheric general circulation and the onset of monsoons part I : basic theoretical method and its application to the analysis of climatological mean observations. *Climatic and Environmental Research*, **10**(3), 285–302. (in Chinese)
- Zhan, Ruifen, Jianping Li, and Jinhai He, 2005: Statistical characteristics of the double ridges of subtropical high in the Northern Hemisphere. *Chinese Science Bulletin*, **50**(20), 2336–2341.
- Zhang, Ming, DongLing Zhang, Ruiting Zuo, Juanxiong He, and Qingcun Zeng, 2005: The abrupt seasonal transitions in the atmospheric general circulation and the onset of monsoons part II: the onset of summer monsoon in South China Sea region. *Climatic and Environmental Research*, **10**(3), 303–314. (in Chinese)
- Zhang, Ming, Min Zhu, and Lifeng Zhang, 2006: Instability of barotropic atmosphere on sphere and dynamical mechanism of Indian Summer monsoon onset. *Chinese Journal of Atmospheric Sciences*, **30**(2), 193–201. (in Chinese)
- Zhang, Qingyun, Shiyan Tao, and Lieting Chen, 2003: The interannual variability of East Asian summer monsoon indices and its association with the pattern of general circulation over East Asia. *Acta Meteor Sinica*, **61**(4), 559–568. (in Chinese)
- Zhang, Renhe, 2001: Relations of water vapor transports from Indian monsoon with those over East Asia and the summer rainfall in China. *Adv. Atmos. Sci.*, **18**, 1005-1017.
- Zhang, Renhe and A. Sumi, 2002: Moisture circulation over East Asia during El Niño episode in northern winter, spring and autumn. *J. Meteor. Soc. Japan*, **80**, 213-227.
- Zhang, Shunli, Shiyan Tao, Qingyun Zhang, and Jie Wei, 2002: Multi-scale conditions of torrential rain causing floods in the mid- and lower reaches of the Yangtze River. *Chinese Science Bulletin*, **47**(6), 467–473. (in Chinese)
- Zhang, Yaocun, and Yongfu Qian, 2002; Mechanism of thermal features over the Indo-China Peninsula and possible effects on the onset of the South China Sea monsoon. *Adv. Atmos. Sci.*, **19** (5), 885–900.
- Zhang, Yong, An Xie, and Nianjun Dai, 2004: Preceding features associated with the anomalous summer monsoon over the South China Sea. *Journal of Tropical Meteorology*, **20**(5), 460–471. (in Chinese)
- Zhang, Zuqiang, Johnny C. L. Chan, and Yihui Ding, 2004: Characteristics, evolution and mechanisms of the summer monsoon onset over Southeast Asia. *Int. J. Climatol.*, **24**, 1461–1482.
- Zhao, Ping, and Zijiang Zhou, 2005: East Asian subtropical summer monsoon index and its relationships to rainfall. *Acta Meteorologica Sinica*, **63**(6), 933–941. (in Chinese)

- Zhao, Ping , and Renhe Zhang, 2006: Relationship of interannual variation between an Eastern Asia- Pacific dipole pressure pattern and East Asian monsoon. *Chinese Journal of Atmospheric Sciences*, **30**(2), 307–316. (in Chinese)
- Zhao, Ping, Renhe Zhang, Jiping Liu, Xiuji Zhou, and Jinhai He, 2006: Onset of Southwesterly Wind over Eastern China and Associated Atmospheric Circulation and Rainfall. *Climate Dynamics*, DOI 10.1007/s00382-006-0212-y.
- Zhou, Changyan, Jinhai He, Wei Li, and Longxun Chen, 2005: Climatological characteristics of water vapor transfer over East Asia in summer. *Journal of Nanjing Institute of Meteorology*, **28**(1), 18–27.
- Zhou, Wen, Zhongliang Chen, Chongyin Li, 2005: South China Sea summer monsoon onset in relation to the off-equatorial ITCZ. *Adv. Atmos. Sci.*, **22**(5), 665–676.
- Zhou, Y S, S T Gao, and S Shen, 2004: A diagnostic study of formation and structures of the Meiyu front system over East Asia. *J. Meteorol. Soc. Japan*, **82**(6), 1565–1576.
- Zhu, Kezhen, 1934: Southeast monsoons and rainfall in China. *J. Chin. Geogr. Soc.*, **1**, 1-27.

Captions:

Fig. 1. Distribution of global surface monsoon. Red, green and blue areas represent the tropical monsoon region, subtropical monsoon region, and extratropical monsoon region, respectively. The red and blue bold solid lines show the positions of ITCZ in summer and winter respectively (Li and Zeng, 2005).

Fig. 2. Distribution of the surface wind vectors (unit: m/s) and rainfall (unit: mm/d) in July in ideal experiments. (a) no-orography experiment; (b) orography experiment; (c) difference of (b)-(a). The bold dashed line is the land boundary, the curve covers the region where wind diverges more than 120° in January and July, and the ellipse is the contour line of the 1500m plateau (Wu et al., 2005).

Fig. 3. Diagrams of the relationship among the northwestward movement of convection in Sumatra along “land bridge”, the onset of convection in Indochina peninsula, the break of the subtropical high belt, the formation of the BOB trough and the onset of South China Sea summer monsoon (He et al., 2006).

Fig. 4. The sketch map of the onset mechanism of the ASM based on the outcome of South China Sea Monsoon

Experiment (SCSMEX) (Liu and Ding 2005).

Fig. 5. The sketch map of the relationship among the thermal states of the tropical western Pacific (warm pool), the convective activities around Philippine, the early or late onset of the SCSM, the western Pacific subtropical high, and the distribution of drought and flood in the Yangtze River and Huaihe River valleys: (a) warm pool in a warm state; (b) warm pool in a cold state (Huang et al., 2005).

Fig. 6. Distribution of the sea surface pressure anomaly in December in the tropical western Pacific region in strong (a) and weak East Asian winter monsoon (b) (Li et al., 2005).

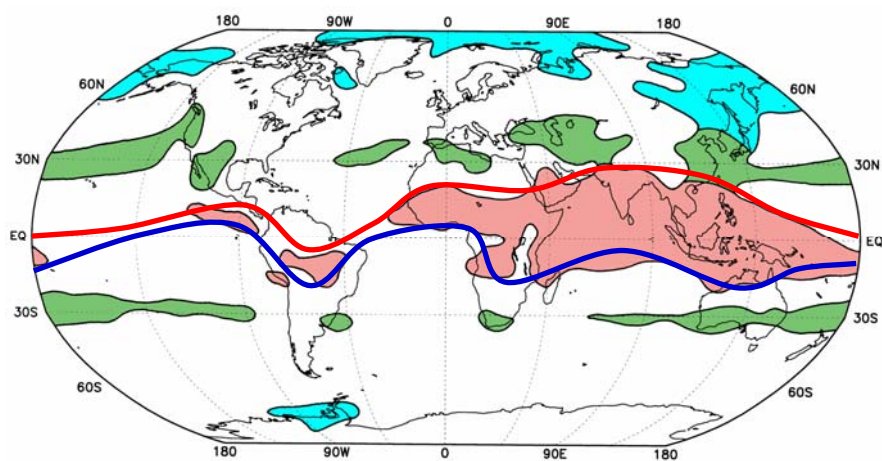


Fig. 1. Distribution of global surface monsoon. Red, green and blue areas represent the tropical monsoon region, subtropical monsoon region, and extratropical monsoon region, respectively. The red and blue bold solid lines show the positions of ITCZ in summer and winter respectively (Li and Zeng, 2005).

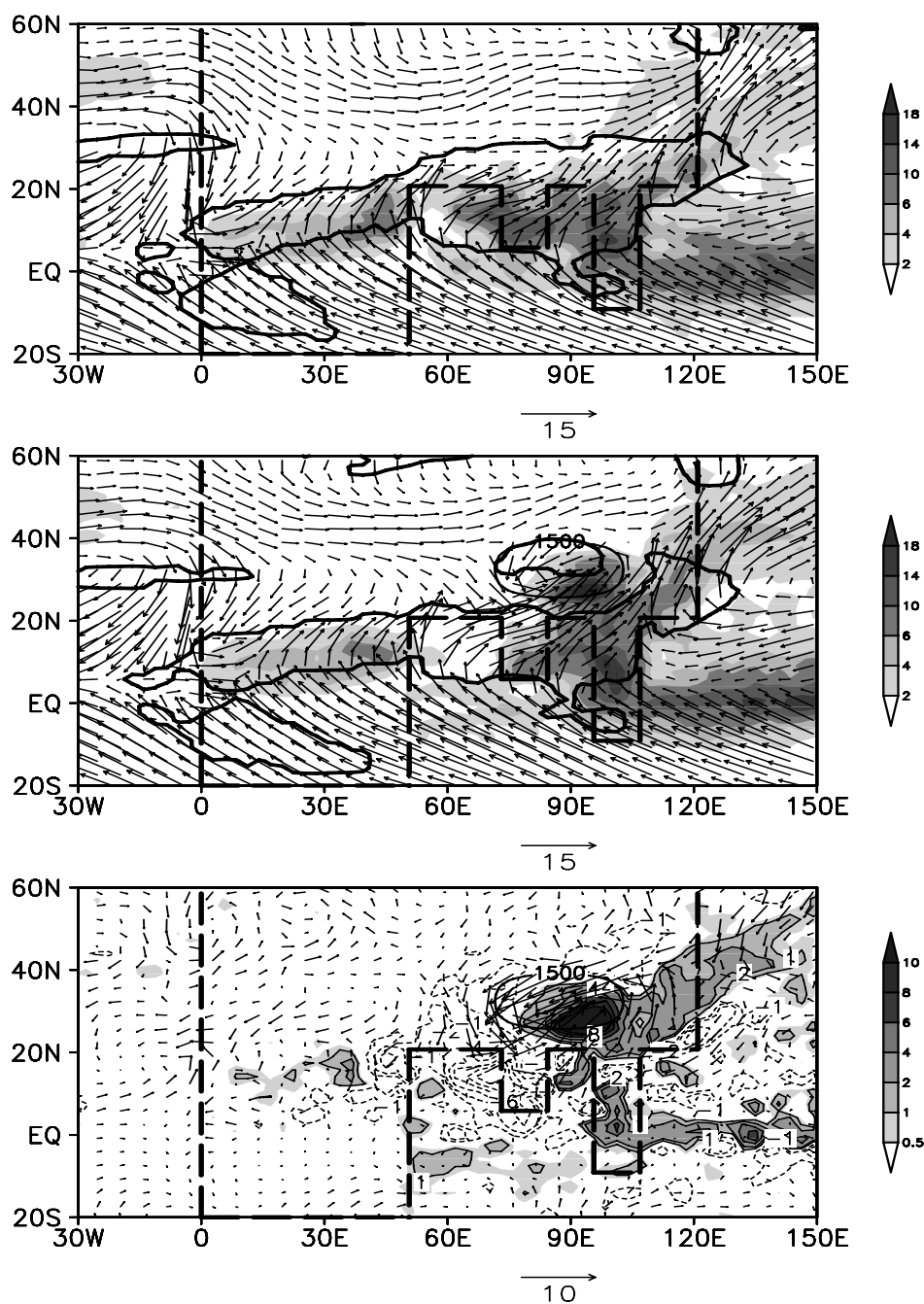


Fig. 2. Distribution of the surface wind vectors (unit: m/s) and rainfall (unit: mm/d) in July in ideal experiments. (a) no-orography experiment; (b) orography experiment; (c) difference of (b)-(a). The bold dashed line is the land boundary, the curve covers the region where wind diverges more than 120° in January and July, and the ellipse is the contour line of the 1500m plateau (Wu et al., 2005).

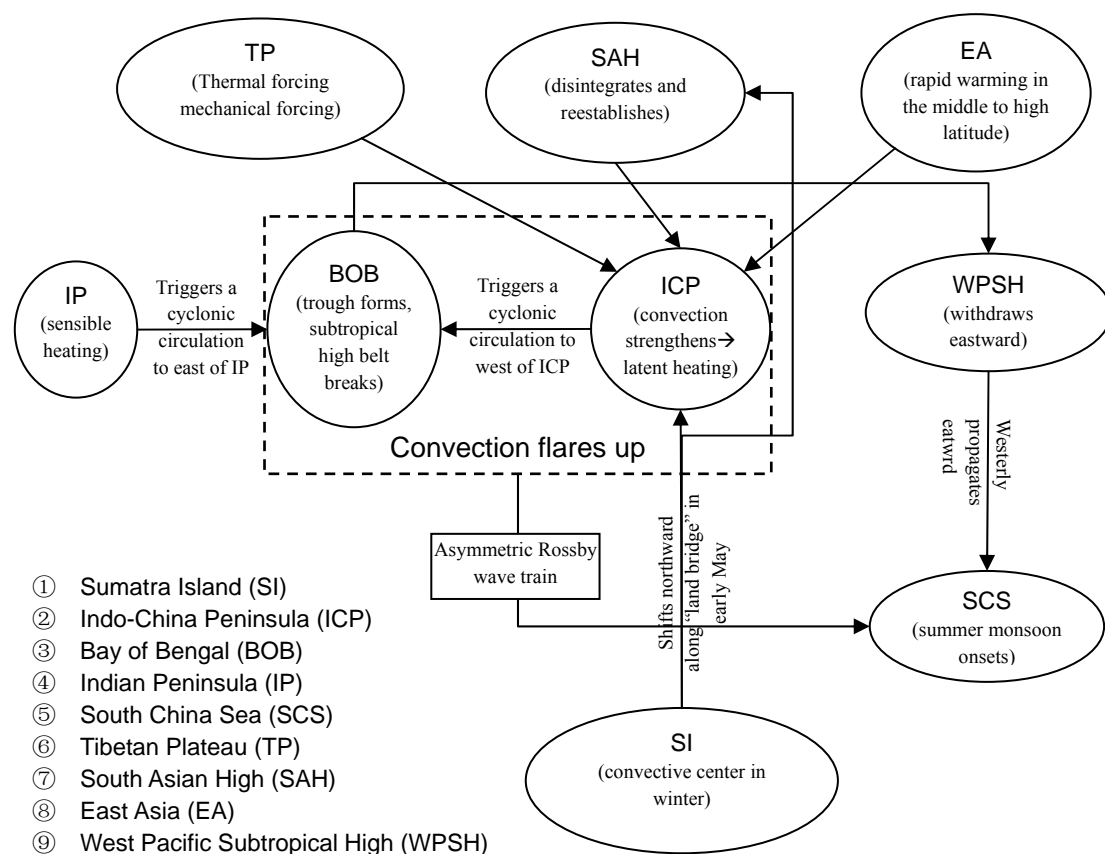


Fig. 3. Diagrams of the relationship among the northwestward movement of convection in Sumatra along “land bridge”, the onset of convection in Indochina peninsula, the break of the subtropical high belt, the formation of the BOB trough and the onset of South China Sea summer monsoon (He et al., 2006).

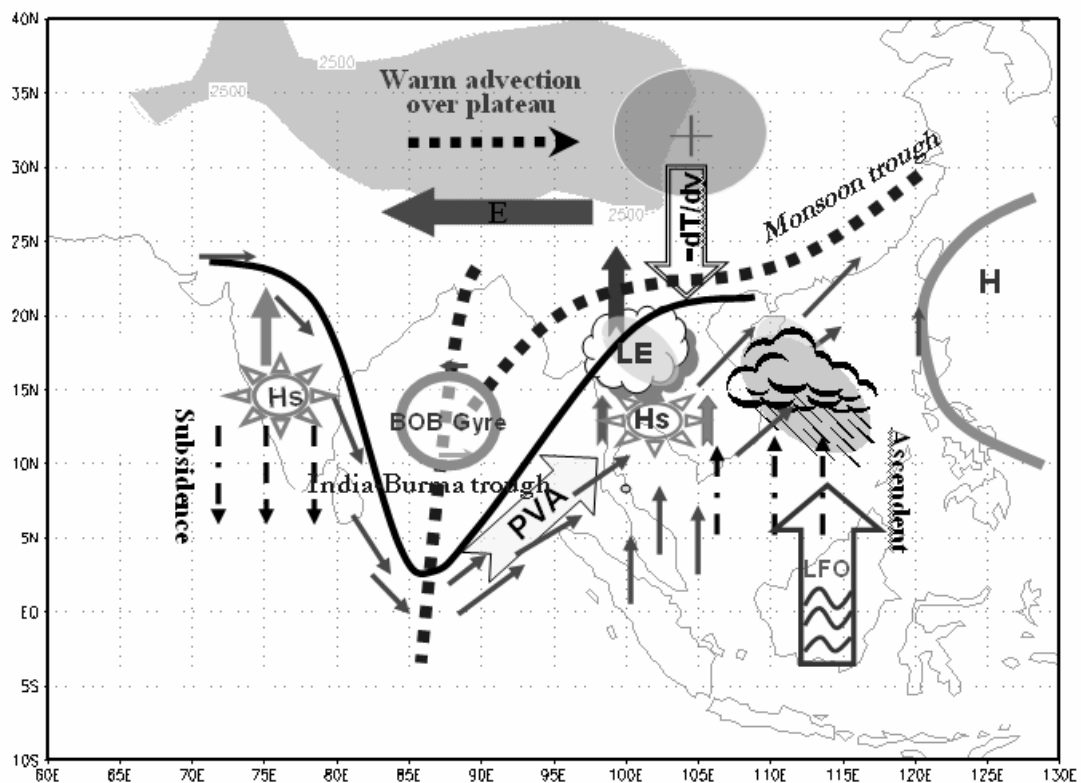


Fig. 4. The sketch map of the onset mechanism of the Asian summer monsoon based on the outcome of South China Sea Monsoon Experiment (SCSMEX) (Liu and Ding 2005).

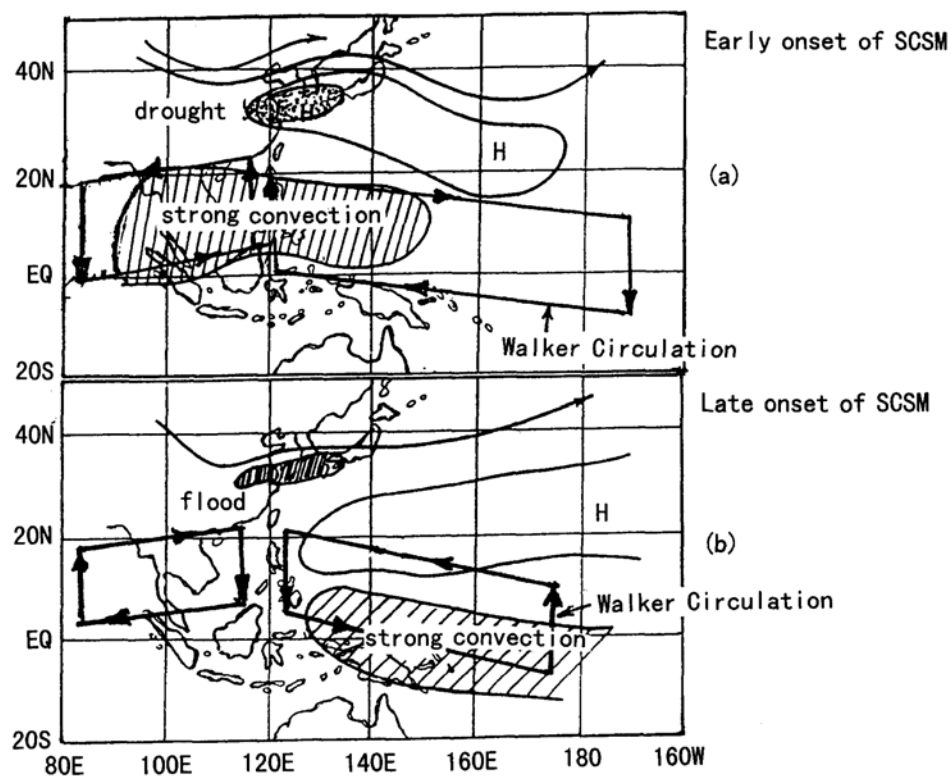


Fig. 5. The sketch map of the relationship among the thermal states of the tropical western Pacific (warm pool), the convective activities around Philippine, the early or late onset of South China Sea monsoon, the western Pacific subtropical high, and the distribution of drought and flood in the Yangtze River and Huaihe River valleys: (a) warm pool in a warm state; (b) warm pool in a cold state (Huang et al., 2005).

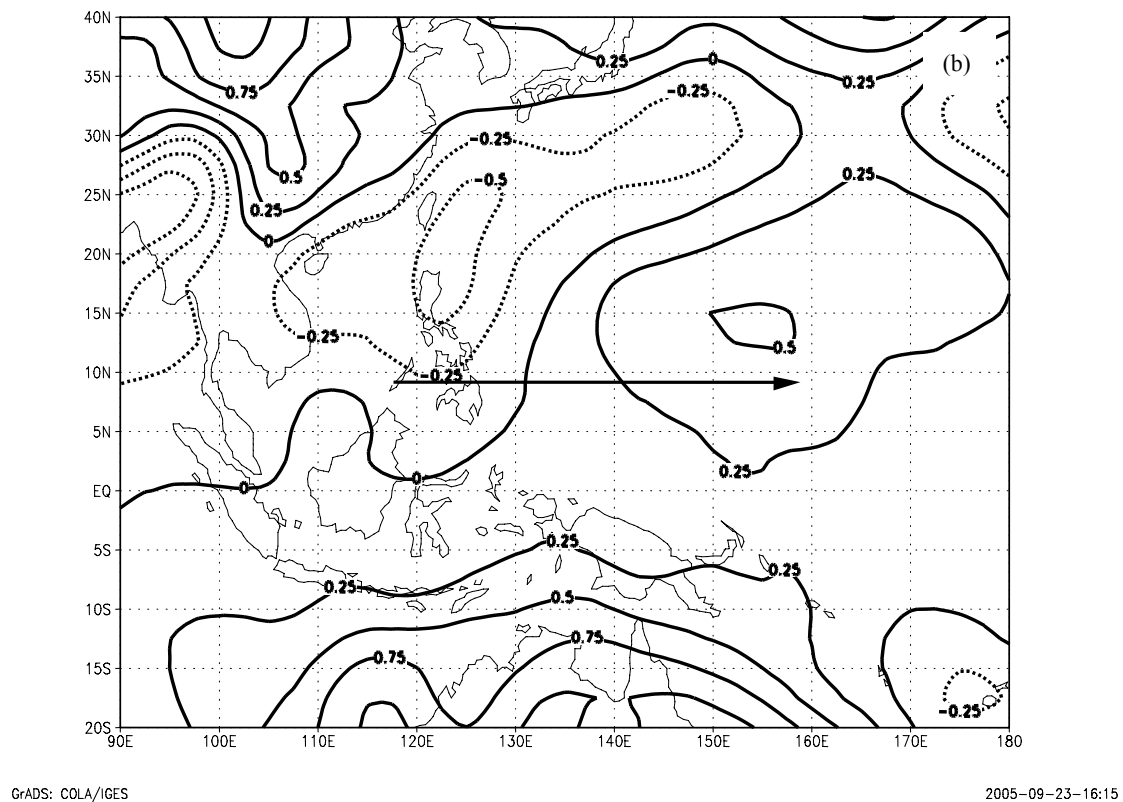
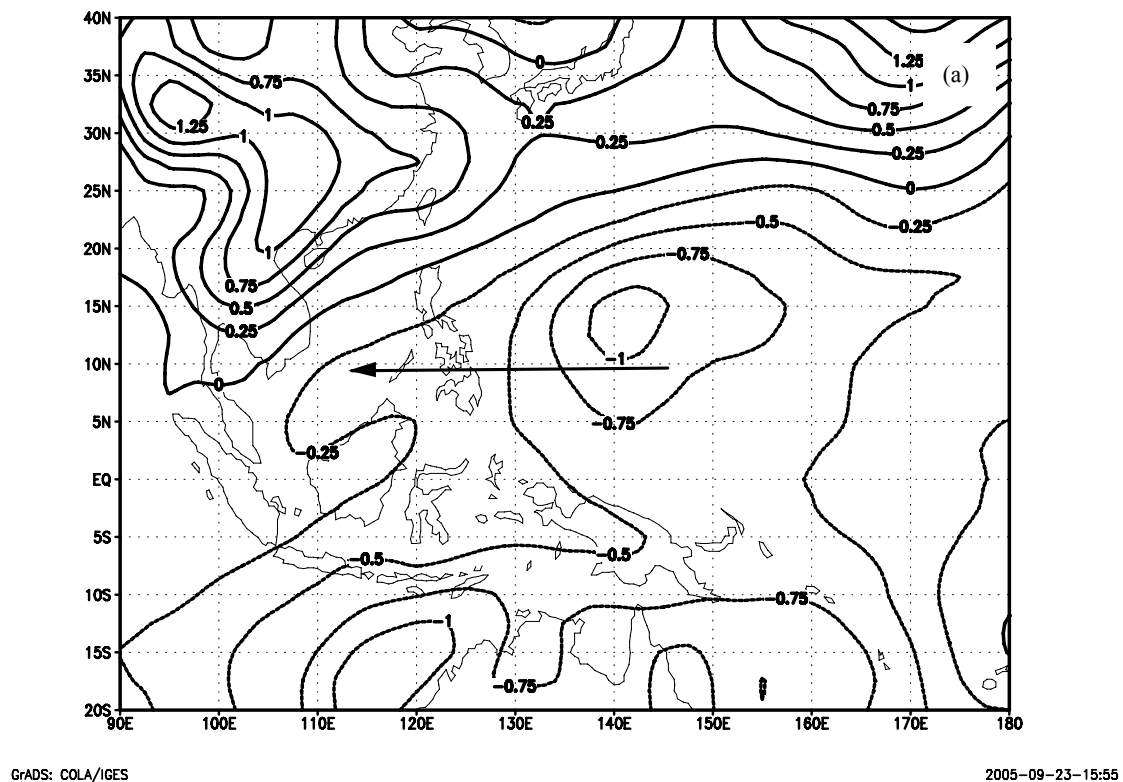


Fig. 6. Distribution of the sea surface pressure anomaly in December in the tropical western Pacific region in (a)strong and (b)weak East Asian winter monsoon. The arrow represents latitudinal pressure gradient (Li et al., 2005).

CHARACTERISTIC AND VARIABILITY OF THE EAST ASIAN MONSOON CLIMATE SYSTEM AND ITS IMPACTS ON SEVERE CLIMATIC DISASTERS IN CHINA

HUANG Ronghui (黄荣辉), CHEN Jilong(陈际龙), HUANG Gang(黄刚)

Center for Monsoon System Research, Institute of Atmospheric Physics, Chinese Academy of Sciences,

Beijing 100080

Abstract Recent advances in studies on the characteristics of structure and temporal-spatial variations of the East Asian monsoon(EAM)system and the impacts of the system on severe climatic disasters in China are reviewed in this paper. Through recent studies, some significant advancements in understanding the basic characteristics of horizontal and vertical structures and their annual cycle of the EAM system and the water vapour transports in the EAM region have been achieved. It is shown from these studies that the EAM system is a relatively independent subsystem of the Asian-Australian monsoon system. And many studies showed that there is an obvious quasi-biennial oscillation, i.e., the TBO, with a meridional tripole pattern distribution in the interannual variations of EAM system. Moreover, due to the further understandings of the basic physical processes including the internal and external processes that influence the variabilities of EAM system, a new concept of the East Asian monsoon climate system including atmosphere, ocean and land surface process etc. has been put forward. This shows that the EAM subsystem is not only a circulation system, but also an air-sea-land coupling climate system. Furthermore, it is also discussed in this paper that the interaction and relationship among various components of this system may be through the EAP pattern teleconnection and the teleconnection pattern of meridional wind anomalies along the westerly jet stream in the upper troposphere over East Asia. Based on these understandings, the occurring cause of severe floods in the Yangtze River and the Huaihe River valleys and the climate background of the occurrence of the prolonged droughts in North China have been revealed from the interannual and interdecade variabilities and anomalies of East Asian monsoon climate system, respectively. Besides, the scientific problems on the East Asian monsoon climate system and its impact on severe climatic disasters in China, which should be studied further in the near future, are also suggested in this paper.

Key words: East Asian monsoon climate system, climatic disaster, persistent drought, severe flood, EAP pattern teleconnection

1. Introduction

China is located in the East Asian monsoon region, thus, climate in China is mainly influenced by the East Asian monsoon (EAM) (e.g., Zhu, 1934; Tu and Huang, 1944). Since the interannual and interdecadal variabilities of EAM are significant, climatic disasters such as droughts and floods frequently occur in China (e.g., Huang and Zhou, 2002; Huang et al., 2006). Especially, since the 1980s, severe climatic disasters over large areas have caused huge damage to agricultural and industrial production in China. Each year, the economic losses due to droughts and floods can reach over 200 billion yuan (i.e., about US\$24 billion), accounting for 3%~6% of China's GDP in the early 1990s (e.g., Huang et al., 1999; Huang and Zhou, 2002). In the summer of 1998, for example, the particularly severe floods occurred in the Yangtze River basin and the Songhua and Nen River valleys caused the losses as high as 260 billion yuan (i.e., about US\$ 31 billion)(e.g., Huang et al, 1998). In addition, the severe persistent droughts in North China from the late 1970s to now not only brought huge losses to agriculture and industry, but also seriously affected the water resources and ecological environment in this region, which caused a great increase of the occurring frequency of sand-dust storms there. To reduce the losses due to severe climatic disasters, it is, therefore, urgently necessary to undertake research on the formation and prediction of severe climatic disasters in China. Thus, this research was one among the first batch of projects supported by the National Key Program for Developing Basic Sciences (e.g., Huang et al., 1999; Huang, 2001, 2004), and it was also a major project supported by the National Natural Science Foundation of China.

The occurrence of severe climatic disasters such as droughts and floods in China, especially the severe flooding disaster occurred in the Yangtze River basin in the summer of 1998 and the persistent droughts occurred in North China from the late 1970s to now, is closely associated the EAM system. Because the climate variabilities and anomalies of EAM system are effected not only by the internal dynamical and thermodynamical processes in the atmosphere, but also by the interactions among various spheres of the climate system including atmosphere, ocean, ice and snow, and land surface process and so on. This can show that the EAM is not only a circulation

system, but also a climate system, which is also called as the East Asian monsoon climate system. To study the occurring regularity and cause of severe climatic disasters in China, the variabilities of various components of the East Asian monsoon climate system including the EAM, the western Pacific subtropical high, and disturbances in mid-and high latitudes in the atmosphere, thermal states of the West Pacific warm pool and convective activity around the Philippines, and ENSO cycle in the tropical Pacific, the dynamical and thermal effects over the Tibetan Plateau, and the land surface process in the arid and semi-arid areas of Northwest China, and the snow cover on the Tibetan Plateau were analyzed in detail for recent years (e.g., Huang et al., 1998; Huang et al 2001; Huang et al., 2004). And the internal and external physical processes that influence these variabilities were also discussed, recently.

This paper attempts to summarize the advances in recent studies on characteristic, variability of the East Asian monsoon climate system and its impacts on severe climatic disasters in China. Because the authors's knowledge about the studies of the East Asian monsoon climate system variability and its impact on severe climatic disasters in China is finite, and hence limited, this review mainly emphasize the results made by Chinese meteorologists, especially the studies known by authors.

2. Characteristic of the East Asian monsoon circulation system

The Asian-Australian monsoon system is an important circulation system in the global climate system. Many studies have shown that the Asian and Australian monsoons play an important role in the global climate variability (e.g., Tao and Chen, 1987; Ding, 1994; Huang, et al., 1996; Webster, et al. 1998; Huang et al., 2003; Huang et al., 2004). Since there is a close association among the South Asian monsoon (SAM), the East Asian monsoon(EAM) and the North Australian monsoon (NAM), some scholars considered them as three subsystems of the Asian-Australian monsoon system (e.g., Webster et al., 1998). However, there are some differences among these monsoon subsystems. For example, the East Asian summer monsoon (EASM) is not only a part of tropical monsoon, but also has a property of subtropical monsoon because it is influenced by the western Pacific subtropical high and the disturbances in middle latitudes (e.g. Tao and Chen, 1987). But the South Asian summer monsoon (SASM) and the North Australian summer monsoon (NASM) are only tropical monsoon. Therefore, the EASM is different from the SASM and the NASM in many aspects.

2.1 A relatively independent component of the Asian-Australian monsoon system in the horizontal and vertical structures of wind field

According to Krishnamurti's (1982) study, the principal components of the SASM include: the Mascarene high, the Somali cross-equatorial low-level flow and the monsoon trough over North Indian in the lower troposphere, and the South Asian high and the cross-equatorial flow, which flows from north to south, in the upper troposphere. However, Tao's investigation (e.g., Tao and Chen, 1985) showed the main components of EASM monsoon include: the Indian SW monsoon flow, the Australian cold anticyclone, the cross-equatorial flow along the east to 100°E, the monsoon trough (or ITCZ) over the South China Sea (SCS) and the tropical western Pacific, the western Pacific subtropical high and the tropical easterly flow, the Meiyu (or Baiu in Japan, or Changma in Korea) frontal zones, and the disturbances in mid-latitudes. Therefore, the EASM is a relatively independent monsoon circulation subsystem.



Figure 1. Altitude-time cross section of zonal wind averaged for 1979~2003 over (a) South Asia (0~25°N, 60°~100°E), (b) East Asia (0~45°N, 100°~140°E) and (c) North Australia (0~15°N, 110°~150°E). Unit: m/s. The solid and dashed lines in Figs.1a~c indicate the westerly and easterly winds, respectively. The NCEP/NCAR reanalysis data (e.g., Kalnay et al. 1996) is used in the study.

Recently, Chen and Huang (2006) analyzed the climatological characteristics of wind structure and seasonal evolution of these subsystems of the Asian-Australian monsoon system, i.e., the SASM over the area (0°-25°N, 60°E-100°E) and the EASM over the area (0°-45°N, 100°E-140°E) in boreal summer, and the NASM over the area (0°-15°S, 110°E-150°E) in the Southern Hemisphere summer, respectively. The result shows that, as shown in Fig. 1, both the SASM and the NASM purely belong to the tropical summer monsoons with strong zonal flow and vertical easterly shear, i.e., low-level westerlies and high-level easterlies, and vertical easterly shear in the SASM region is stronger than that in the NASM region. However, the vertical structure of zonal flow in the EASM region is complex. It includes the vertical easterly shear in the region to the south of 25°N, such as the South China Sea (SCS) and the tropical western Pacific, and the vertical westerly shear in the subtropical monsoon region to the north of 25°N, such as the mainland of China, Korea and Japan. Thus, the EASM is composed of the tropical and subtropical summer monsoons with a significant meridional flow and vertical northerly shear, i.e., low-level southerlies and high-level northerlies, as shown in Fig. 2. Moreover, compared to the meridional component of wind field in the SASM and NASM regions, the low-level southerlies in the EASM region are stronger than those in the SASM and NASM regions.



Figure 2. As in Fig.1 except for the meridional wind

2.2 Annual cycle between summer and winter monsoons in the EAM region and its difference from that in the SAM and NAM regions.

It may be clearly seen from either precipitation and wind system near the ground surface or circulation and air temperature in the troposphere that the SAM and the NAM are a phenomenon with a annual cycle (e.g., Li and Yanai, 1996; Tomas and Webster, 1997; Goswami et al., 2006). This annual cycle is more obvious in the EAM region.

Tao and Chen (1987) pointed out that the earliest onset of the ASM is found over the SCS, and, then, it moves northward to South China, the Yangtze River and Huaihe River valleys, Korea and Japan, and reaches North China and Northeast China in early or mid-July. The annual cycle of the EAM may be well seen from the seasonal variations of monsoon rainband over East Asia (e.g., Huang et al., 2003). Fig. 3 is the latitude-time cross section of 5 day precipitation along 115°E(110°~120°E) averaged over the last 40 years from 1961 to 2000. Fig. 3 clearly shows that the monsoon rainband is located over South China in spring, then moves northward to the south of the Yangtze River during the period from May to the first 10 days of June, and then it abruptly moves northward to the Yangtze River and Huaihe River valley of China, Japan and South Korea. This is the beginning of the Meiyu season in the Yangtze River and Huaihe River valley and the Baiu in Japan. Moreover, it may be also seen from Fig. 3 that the monsoon rainband again moves northward to North China and North Korea in early July. Due to this northward movement of the rainband, the Meiyu season ends in the Yangtze River and Huaihe River valley (i.e., Jianghuai valley in Chinese) and the rainy season begins in North China and Northeast China. This northward movements of summer monsoon rainband over East Asia are in good agreement with the onset of EAM in various regions of East Asia proposed by Tao and Chen (1987).

The northward movement of the rainband is closely associated with the northward shift of the western Pacific subtropical high (e.g., Huang and Sun; 1992; Ding 1992; Huang et al., 2003; Huang et al, 2005). Yeh et al. (1959) first discovered the abrupt change of the circulation over East Asia during early and mid-June. This abrupt change of planetary-scale circulation brings the onset of EASM. Later, Krishnamurti and Ramanathan (1982), and McBride (1987) further pointed out the abrupt change of the SASM and the NASM circulations. These abrupt changes of

planetary-scale circulations also show the onset of the SASM and NASM. However, the study by Huang and Sun (1992) has shown that the abrupt change of circulation over East Asia during early or mid-June is closely associated with convective activity around the Philippines.



Figure 3. Latitude-time cross section of 5-day precipitation along 115°E (average for 110°~120°E) averaged for the period of 1961~2000. Units: mm.

The southward retreat of the EASM is very rapid. Generally, the EASM will move fastly southward to South China during two weeks after mid-August, and, then, the EAWM will begin and the strong northerly wind will prevail over East Asia. In October, this strong northeasterly wind will reach the area over the SCS, and it become into the easterly wind over the Indo-China Peninsula. Therefore, the annual cycle between the EASM and EAWM is mainly shown in the meridional direction, which is different from those in the SAM and NAM regions. In the SAM and NAM regions, the annual cycle between winter and summer monsoons in the zonal direction is dominant.

The differences of annual cycle of wind field among these three monsoon subsystems can be also seen from the altitude-time cross sections of zonal and winds averaged for East Asia, South Asia and North Australia, as shown in Figs. 1 and 2. From Figs. 1a and 1c, it may be seen that the strong westerly wind prevails in the lower troposphere below 500hPa and the strong easterly wind is found in the upper troposphere above 500hPa from early June over South Asia. However, from early October, the westerly wind becomes into the easterly wind in the lower troposphere below 700hPa, while the easterly wind becomes into the westerly wind in the upper troposphere above 500hPa over this region. Therefore, in the SAM region, the annual cycle between summer and winter monsoons is obvious in zonal wind field. The same phenomenon also appears in the NAM region, but the reverse of zonal wind in this region occurs in early November, when just is summer season in the Southern Hemisphere. However, compared Fig. 1b with Figs. 1a and 1c, the seasonal reverse of zonal wind in the troposphere over East Asia is not significant, but as shown in Fig. 2b, the seasonal reverse of meridional wind obviously occurs in both the lower troposphere and the

upper troposphere over East Asia in early June and mid-September, respectively.

From the above-mentioned analysis, it may be seen that the annual cycle between summer and winter monsoons is significant in the meridional direction and mainly appears in the meridional component of wind field in the EAM region. This is different from the annual cycle of wind field in the SAM and NAM regions.

2.3 The characteristics of water vapour transports in the EASM region and its difference from those in the SASM and NASA regions

The result investigated by Huang et al. (1998) showed that the characteristic of water vapour transports in the EAM region are greatly different from that over the SASM. In the SASM region, the zonal transport of water vapour is dominant and the meridional transport is smaller, but the meridional transport of water vapour is very large in the EASM region. Moreover, the convergences of water vapour, which are closely associated with monsoon rainfall, are mainly caused by the moisture advection and convergences of wind field over the EASM region, however, over the SASM region, they are mainly caused by the convergences of wind field.

Recently, Chen and Huang (2006) again analyzed the characteristic of water vapour transports over the EASM, the SASM and NASM regions using the ERA-40 reanalysis data for 1979~2002. The results analyzed by Chen and Huang (2006) are in good agreement with those by Huang et al.(1998). The convergences of water vapour transports over the SASM region are mainly due to the convergences of wind field in the lower troposphere over this region because there is a large vertical velocity caused by large vertical shear of zonal wind shown in Fig.1a. And the similar result can be found over the NASM region in the Southern Hemisphere summer (figure is omitted). However, over the EASM region, those are not only due to the divergences of wind field, but also due to the moisture advection caused by the southerly monsoon flow in the lower troposphere over this region because there is a smaller vertical velocity caused by smaller vertical wind shear shown in Fig.1b than that in the SAM region.

From the above-mentioned results, it may be well explained that the EAM subsystem is a relatively independent component of the Asian-Australian monsoon system although the EASM is also influenced by the SASM.

3. Characteristics of temporal and spatial variabilities of the EAM subsystem and their impact on droughts and floods in China

Since the EASM is influenced by not only the SASM, but also the western Pacific subtropical high (e.g., Tao and Chen, 1987; Huang and Sun, 1992), the interannual and interdecadal variations of EASM are significant but very complex. Compared to summertime surface air temperature, the interannual and interdecadal variabilities of summer monsoon rainfall are more obvious in East Asia and have a large impact on climatic disasters in China (e.g., Huang et al., 1999; Huang et al., 2002). Therefore, the interannual and interdecadal variabilities of summer monsoon rainfall and water vapour transports in East Asia are emphasized in this Section.

3.1 Interannual variations of onset and northward advance of the EASM and their impact on droughts and floods in China

The interannual variability of summer monsoon rainfall in East Asia is influenced by not only the EASM strength, but also its onset date. According to the studies by Tao and Chen (1987), and He et al. (1987), the earliest onset of the ASM is found over the SCS and the Indo-China Peninsula, as shown in Fig.4. Recently, Ding and He (2006) proposed that the earliest onset of the ASM is over the tropical eastern Indian Ocean. Since the onset of the SCSM has a direct impact on the northward advance of the ASM over East Asia, the study on the SCSM onset is emphasized in the review. The appearance of strong convective activity and the southwesterly flow over the SCS signals the onset of the ASM. Generally, the summer monsoon over the SCS is called as the South China Sea summer monsoon (SCSM) in China. In order to investigate the interannual variability of onset date and process of the SCSM, it is necessary to define an index for measuring the SCSM onset. However, there are many definitions of the SCSM onset (e.g., Wang et al, 2004). Compared with other definitions of the SCSM onset, the definition proposed by Lian and Wu (2002) appears to be more reasonable and was used in many studies (e.g., Huang et al., 2005; Huang et al., 2006).



Figure 4. Climatological-mean onset dates of the EASM (from Tao and Chen, 1987)

Huang et al. (2005), and Huang et al. (2006) analyzed the characteristics of interannual variations of the SCSM onset and process. Their results showed that the interannual variability of SCSM onset date is very large and it closely associated with the thermal states of the tropical

western Pacific in spring. When the tropical western Pacific is in a warming state in spring, since the western Pacific subtropical high shifts eastward, the twin anomalous cyclones are early caused over the Bay of Bengal and Sumatra before the SCSM onset. In this case, the cyclonic circulation located over the Bay of Bengal can be early intensified and becomes into a strong trough. Thus, the westerly flow and convective activities can be intensified over Sumatra, the Indo-China Peninsula and the SCS in mid-May. This leads to early onset of the SCSM, as shown in Fig. 5a. On the other hand, when the tropical western Pacific is in a cooling state in spring, since the western Pacific subtropical high anomalously shifts westward, the twin anomalous anticyclones are located over the equatorial eastern Indian Ocean and Sumatra from late April to mid-May. Thus, the westerly flow and convective activities cannot be early intensified over the Indo-China Peninsula and the SCS. Only when the western Pacific subtropical high moves eastward, and then the weak trough located over the Bay of Bengal can be intensified and becomes into a strong trough. As a result, the strong southwesterly wind and convective activities can be intensified over the Indo-China Peninsula and the SCS in late May, generally. This leads to late onset of the SCSM, as shown in Fig. 5b.

Following the SCSM onset, the monsoon will move northward over East Asia. Huang and Sun (1992), Huang et al (2004), and Huang et al. (2005) also investigated the interannual variations of the northward advance of the EASM. Their results showed the northward advances of the EASM after the onset over the SCS are greatly influenced by the thermal states of the tropical western Pacific in summer. They pointed out that there are close relationships among the thermal states of the tropical western Pacific, the convective activity around the Philippines, the western Pacific subtropical high, and the summer monsoon rainfall in East Asia. As shown in Fig. 5a, when the SST in the tropical western Pacific is above normal, i.e., the warm sea water is accumulated in the West Pacific warm pool, and the cold tongue extends westward from the Peruvian coast along the equatorial Pacific in summer, convective activity is intensified from the Indo-China Peninsula to the east of the Philippines, and the western Pacific subtropical high shifts unusually northward. In this case, the summer monsoon rainfall may be below normal in East Asia, especially in the Yangtze and Huaihe River basins of China, South Korea, and Japan. On the other hand, as shown in Fig.1b, when the SST in the tropical western Pacific is below normal, i.e., the warm sea water extends eastward from the West Pacific warm pool along the equatorial western Pacific in summer,

the convective activity is weak around the Philippines, and the western Pacific subtropical high may shift southward. In this case, the summer monsoon rainfall may be above normal in the Yangtze and Huaihe River valleys of China, South Korea, and Southwest Japan. Therefore, following a spring with late onset of the SCSM, severe floods may occur in the Yangtze River and Huaihe River valley, but droughts will be caused in North China in summer.



Figure 5. Schematic map of the relationships among the thermal states of the tropical western Pacific (TWP)(i.e., Eq.~14°N, 130°~150°E) in spring, the convective activity around the Philippines, the western Pacific subtropical high, the onset of SCSM and the summer monsoon rainfall in East Asia. (a) in the warming state of the TWP; (b) in the cooling state of the TWP.

Therefore, the thermal state of the tropical western Pacific, especially the NINO. west (i.e., Eq.~14°N, 130°~150°E), in spring (March-May) can be considered as a physical factor affecting the SCSM onset and summertime droughts and floods in the Yangtze River and Huaihe River valleys, South Korea and Japan.

3.2 The EAP index and the interannual variability of EASM strength

The monsoon index is a criterion measuring the strength of monsoon, and it is necessary for the study of the interannual variability of ASM. So far, two kinds of definitions of the Asian monsoon index are used to measure the monsoon strength. One is defined from the thermodynamic elements such as precipitation or OLR (e.g., Tao and Chen, 1987; Murakami and Matsumoto, 1994). The other is defined from the dynamic elements, such as the difference of zonal wind between lower and upper troposphere (e.g., Webster and Yang, 1992; Zeng et al., 1994), or the difference of sea level pressure between the Eurasian continent and North Pacific (e.g., Guo, 1983). The former is easily influenced by local thermodynamic conditions, but the latter is only suitable for the SAM and the NAM regions because there is a large difference of zonal wind between lower and upper troposphere over the SASM and NASM regions, as described in Section 2. However, since the difference of zonal wind is small in the EASM region,

the definition of monsoon index proposed by Webster and Yang (1992) seems to be not suitable for the EASM region. The study by G. Huang (2004) showed that the interannual variability of EASM can be well described using the EAP index, which is defined with the 500 hPa height anomalies in summer according to the EAP (East Asia/Pacific) teleconnection pattern of the summer circulation anomalies suggested by Nitta (1987) and Huang and Li (1987,1988).



Figure 6. Distributions of the correlation coefficients between summer rainfall anomalies in East Asia with (a) the EAP index, (b) the WY index, and (c) the SM index, respectively. The areas of confidence level over 95% are shaded in the Figs. 6a~c, and the Xie-Arkin precipitation data for 1979~1998 (e.g., Xie and Arkin, 1997) is used in the correlation analyses.

The Figs.6a~c show the correlations between the EAP index suggested by G. Huang (2004), the Webster-Yang index (WY index) proposed by Webster and Yang (1992), and the SM index suggested by Gao (1983) and summer rainfall in East Asia, respectively. Compared Fig.6a with Figs. 6b and 6c, it can be clearly shown that the EAP index can well describe the summer rainfall in East Asia than the WY index and the SM index because there are large correlations between the EAP index and summer monsoon rainfall in East Asia, as shown in Fig. 6a. And from Fig.6a, it can be seen that if the EAP index is negative (positive), summer monsoon rainfall may be above (below) normal in the Yangtze River and Huaihe River valleys, for example, in the summers of 1954, 1957, 1980, 1987, 1993 and 1998, the EAP indexes were largely negative values, the severe floods occurred in these regions. Moreover, Fig.6a also exhibits a meridional tripole pattern in the distribution of correlation coefficients in East Asia and Northeast Asia, which can explain that the interannual variations of summer monsoon rainfall generally appear the meridional tripole pattern distribution in East Asia.

3.3 The quasi-biennial oscillation and the tripole pattern distribution of the EASM anomalies over East Asia and their impacts on droughts and floods in China

The quasi-biennial oscillation of circulation in the tropical troposphere, i.e., the TBO, is a

foundamental characteristic of the interannual variations of air-sea coupling system in the SAM and NAM regions (e.g., Mooley and Parthasarathy, 1984; Yasunari and Suppiah, 1988). And Miao and Lau (1990), Yin et al.(1996), and Chang et al. (2000) proposed that the TBO can be found in the interannual variations of summer monsoon rainfall in East Asia. Recently, the result analyzed by Huang et al. (2006) showed that there is also an obvious oscillation with a period of two~three years, i.e., the TBO, in the corresponding time-coefficient series of the EOF1 of summer rainfall in China shown in Fig. 7b, especially from the mid-1970s to the late 1990s. And as shown in Fig. 7a, a strong negative signal is in the Yangtze River and Huaihe River valleys. Moreover, it is also shown that this oscillation is closely associated with the quasi-biennial oscillation in the interannual variations of water vapor transport fluxes by summer monsoon flow over East Asia shown in Fig. 8b. Moreover, as the same as the spatial distribution of the EOF1 of summer rainfall in China shown in Fig.7a, the spatial distribution of the EOF1 of water vapour transports over East Asia and Northeast Asia similarly exhibits a meridional tripole pattern, as shown in Fig.8a.



Figure 7. (a) The spatial distribution and (b) the corresponding time coefficient series of the first component of EOF analysis (EOF1) of summer (JJA) rainfall in China from 1958 to 2000. The EOF1 explains 15.6% of the variance.



Figure 8. (a) The spatial distribution and (b) the corresponding time coefficient series of the first component of zonal water vapour transports in summer. The NCEP/NCAR reanalysis dataset of moisture and wind fields from 1951 to 1999 was used in the study (e.g., Kalnay, and Co-authors, 1996). The EOF1 explains 24.3% of the variance.

This meridional tripole pattern distribution can be clearly shown in the circulation anomalies at 500hPa or 700hPa. Figs. 9a and 9b are the composed anomaly distributions of the height anomaly field at 500hPa over East Asia for the summers with high EAP index and with low EAP

index, respectively. It may be seen from Figs. 9a and 9b that either in the summer with high EAP index, corresponding to a drought summer, or in the summer with low EAP index, corresponding to a flood summer in the Yangtze River and Huaihe River valleys, the summer monsoon circulation anomalies also exhibit the meridional tripole pattern distribution over East Asia and Northeast Asia.



Figure 9. Composite anomaly distributions of the 500hPa height anomalies over East Asia and the tropical western Pacific (a) for the summers with high EAP index and (b) for the summers with low EAP index. Units: gpm. The areas of confidence level over 95% are shaded in Figs.9a and 9b, and the NCEP/NCAR reanalysis data of height field is used in the composite analyses.

The above-mentioned results showed that the interannual variability of EASM clearly exhibits a quasi-biennial oscillation with a meridional tripole pattern distribution over East Asia and the tropical western Pacific. This may be a significant characteristic of the interannual variability of EASM. Therefore, the occurring frequency of drought and flood disasters also exhibits a quasi-biennial oscillation in the Yangtze River and the Huaihe River valleys, and the spatial distributions of these disasters often appear a meridional tripole pattern in East Asia.

3.4 Interannual variability of the East Asian winter monsoon (EAWM) and its relation to the EASM

East Asia is also a region of strong winter monsoon. The East Asian winter monsoon (EAWM) features strong northwesterlies over North China, Northeast China, Korea and Japan and strong northeasterlies along the coast of East China (e.g., Academia Sinica, 1957; Chen et al., 1991; Ding, 1994). The strong winter monsoon not only can bring disasters such as low temperature and severe snow storms in Northwest China and Northeast China, North Korea, and North Japan in winter and severe dust-storms in North China and Northwest China in spring etc., but also can cause strong convective activities over the maritime continent of Borneo and Indonesia. (e.g., Chang et al. 1979; Lau and Chang, 1987). Besides, strong and frequent activities of cold waves caused by

the strong EAWM also can trigger the occurrence of El Niño (e.g., Li, 1988).

Chen and Graf (1998), and Chen et al. (2000) systematically investigated the interannual variability of EAWM and its relation to the EASM with a new definition of the EAWM index. This index is defined by using the normalized meridional wind anomalies at 10 m over the East China Sea (25°~40°E, 120°~140°E) and the South China Sea (10°~25°N, 110°~130°E), averaged from November to March of the next year. Their result showed that there is significant variability in the interannual variations of EAWM. If the index is negative (positive), corresponding to the strong (weak) northerly winds along the coast of East Asia, then a cold (warm) winter appears in East Asian continent and its surrounding seas, and the high pressure in the lower troposphere is strong (weak) over the East Asian continent, and the East Asian trough at 500 hPa is also strong (weak) over Northeast China.

The EAWM intensity can influence the subsequent EASM intensity. The study by Chen et al. (2000) also showed that following a strong (weak) EAWM, a drought (flood) summer may occur in the Yangtze River and the Huaihe River valleys. For example, in the summer of 1998, the severe flood occurred in the Yangtze River valley following the weak EAWM in the winter of 1997 shown in Fig.10.

3.5 Interdecadal variability of the EASM

(1) An dipole pattern distribution in the interdecadal variability of EASM over East Asia

Huang et al. (1999), and Huang (2001) analyzed the interdecadal variations of summer monsoon rainfall in East Asia. Their results showed that the interdecadal fluctuations of summer (June-August) monsoon rainfall is more obvious than surface air temperature in East Asia. And they pointed out that the summer monsoon rainfall began to decrease in North China from the mid-1960s, and it obviously decreased from the late 1970s to now, thus, the prolonged severe droughts occurred in this region, as shown in Fig. 18 in Section 5. However, a opposite phenomenon appeared in the Yangtze River and Huaihe River valleys and Northwest China. In these regions, summer rainfall obviously increased from the late 1970s. This interdecadal oscillation may be also presented in the corresponding time-coefficient series of the EOF2 of summer rainfall in China shown in Fig.10b, and the oscillation exhibits an dipole pattern in spatial distribution in China, as shown in Fig.10a. Besides, this interdecadal variability of summer

monsoon rainfall also appeared in the occurring frequency of heavy rainfall. As pointed by Bao and Huang (2006), more heavy rainfall occurred in the 1980s than the 1970s and followed by a increase in the 1990s in the middle and lower reaches of the Yangtze River and the Huaihe River valley. However, the decrease of heavy rainfall has occurred in the eastern part of North China since the late 1970s to now.



Figure 10. As in Fig.7 except for the EOF2 of summer rainfall in China from 1958 to 2000, The EOF2 explains 12.7% of the variance.

(2) Possible impact of the African summer monsoon on the EASM on interdecadal time-scale

The decrease of summer monsoon rainfall in North China from 1965, especially from the late 1970s, is closely association the weakening of EASM. As pointed out by G. Huang and Zhou (2004), and Huang et al (2004), the southerly wind over North China was obviously weakened. Recently, Huang et al. (2006) analyzed the interdecadal variations of drought and flood disasters in China and their association with the EAM subsystem. As shown in Fig. 11, influenced by the interdecadal El Niño-like SST anomaly pattern appeared in the tropical central and eastern Pacific from the late 1970s to now, an interdecadal meridional tripole circulation anomaly distribution, which is like to the EAP pattern teleconnection, appeared over the West Pacific. And compared Fig. 11b with Fig. 11a, the anticyclonic anomaly distribution of circulation located over the Mongolian Plateau during 1961~1976 obviously shifted southward to North China, and cyclonic anomaly distribution of circulation appeared over the Yangtze River and Huaihe River valleys from the late 1970s. Thus, the circulation anomalies exhibited a meridional dipole pattern distribution over East Asia during this period. This has led to the weakening of EASM in North China and the southward and westward shifts of the western Pacific subtropical high to the south of the Yangtze River. On the other hand, their results also showed that the interdecadal variability of the Walker circulation from the late 1970s to now caused the intensification of descending flow in North Africa, which led to the intensification of the anticyclonic anomaly circulation over the Sahelian region and the east of North Africa shown in Fig.11b. Due to the propagation of

quasi-stationary planetary waves, the intensification of anticyclonic anomaly circulation over the Sahelian region caused the appearance of an anticyclonic anomaly circulation over South China and the Indo-China Peninsula from the late 1970s. Besides, as shown in Figs. 11a and 11b, an interdecadal anomaly distributions of circulations in the lower troposphere over mid- and high latitudes also appeared the Eurasian (EU) pattern-like teleconnection. And an anticyclonic circulation anomaly distribution over North China was caused after 1976. These led to the weakening of the southerly monsoon flow in North China and the convergence of water vapor transports in the Yangtze River valley and the Huaihe River valleys. As a result, the interdecadal variation of droughts and floods in China was caused from the late 1970s.



Figure 11 Interdecadal variations of the summer (JJA) circulation anomalies at 700hPa over East Asia and tropical western Pacific: (a) 1966~1976; (b) 1977~2000. The climatological mean of monthly circulation for 1961~1990 is taken as the normal, and the data of wind field are from the ERA-40 reanalysis data (e.g., Uppala et al., 2005)

(3) Interdecadal variability of the EAWM

Similarly, the EAWM also has a significant interdecadal variability. As shown in Fig.10, the EAWM as stronger from the mid-1970s to the late 1980s, but it tended to be weaker from the late 1980s to 2003, which has caused continuously warm winters in China and increase of spring rainfall in North China during this period (e.g., Huang et al, 2006; Kang et al, 2006)

The interdecadal variations of the EASM and EAWM have a significant impact on not only drought and flood disasters in China, but also on the marine environment in the offshore area of China including the Baohai Sea, the Yellow Sea, the East China Sea and the South China Sea, and its adjacent ocean. According to the study by Cai et al. (2006), since the winter and summer monsoon flows became weak over the offshore area of China and its adjacent ocean from 1976 to now, the winter and summer sea surface wind stresses, especially the meridional sea surface wind stresses, have been weakened, and the obvious increase of SST also has occurred in the areas. These can provide a favorable marine environment for the frequent occurrence of red tide in the

offshore area of China.

4. Variability of the East Asian monsoon climate system

The interannual and interdecadal variabilities of EASM and EAWM are influenced by many circulation system such as the SAM, the western Pacific subtropical high, the disturbances in mid-and high latitudes in the atmosphere, but also other factors such as thermal states of the West Pacific warm pool and convective activity around the Philippines, ENSO cycle in the tropical Pacific, the dynamical and thermal effects over the Tibetan Plateau, and the land surface process in the arid and semi-arid areas of Northwest China, and the snow cover on the Tibetan Plateau and so on. As shown in Fig. 12, these factors affecting the EAM is an air-sea-land coupling climate system, thus, Huang et al. (2004) called this system as the East Asian monsoon climate system.



Figure 12 Schematic map of various components of the East Asian monsoon climate system

Since there are complex interactions among these components and physical processes in the East Asian monsoon system variability. In the following, the impacts of air-sea and air-land coupling components of this system on the interannual and interdecadal variabilities of EAM subsystem are simply discussed.

4.1 Thermal effect of the tropical western Pacific on the EAM variability

Ocean has a significant thermal-effect on Asian monsoon. Yang and Lau (1998) studied the influences of SST and ground wetness (GM) on Asian monsoon using a GCM and pointed out that SST anomalies with ocean basin-scale have a stronger impact on the interannual variability of Asian monsoon compared to GW anomalies.

Studies by many scholars (e.g., Nitta, 1987; Huang and Li 1987; Kurihara, 1989; Huang and Sun, 1992) showed that the thermal states of tropical western Pacific and convective activity around the Philippines play important roles in the interannual variability of EASM, as shown in Fig.5. Nitta (1987), Huang and Li(1987), and Huang and Sun (1992, 1994) made systematic

investigations of the thermal influence of the tropical western Pacific and the convective activity around the Philippines on the interannual variability of EAM circulation from observed data and dynamic theory, and they proposed the P-J oscillation or the EAP pattern teleconnection of summer circulation anomalies over the Northern Hemisphere. As described in Section 3, their results showed that the thermal states of tropical western Pacific and convective activity around the Philippines have a obvious effect on the meridional shifts of the western Pacific subtropical high in summer. And Lu (2001), and Lu and Dong (2001) also showed convective activity over the tropical western Pacific has a significant impact on the zonal shifts of the western Pacific subtropical high. Moreover, Huang et al. (2005) pointed out that the onset date of the SCSM is closely associated with the thermal states of the tropical western Pacific and convective activity around the Philippines in spring.

Recently, Huang et al. (2005), and Huang et al. (2006) investigated the interannual variability of thermal state in the subsurface of the tropical western Pacific. It can be found from Fig.13 that there is also a significant quasi-biennial oscillation in the interannual variations of thermal state of the tropical western Pacific. As studied by Huang et al. (2005), the oscillation has a great impact on the interannual variability of the northward advance of EASM and the water vapor transports driven by the monsoon flow. As shown in Fig. 14a, the anomaly distribution of water vapour transport anomalies in a warming state of tropical western Pacific is opposite to that in a cooling state shown in Fig.14b. And the anomaly distributions of water vapour transports shown in Figs. 14a and 14b also exhibit a meridional tripole pattern. Thus, through the influence of the thermal states of tropical western Pacific on water vapour transports over East Asia, the TBO mechanism of summer monsoon rainfall in China or East Asia can be well explained (e.g., Huang et al. 2006).



Figure 13 Time-depth cross section of sea temperature in the surface and subsurface of the tropical western Pacific averaged over 5°N~10°N along 137°E. Units: °C. The data used in this study is taken from the dataset observed by the Oceanographic Research Vessel “Ryofu-Marui”, JMA.



Figure 14 Composite distributions of water vaport transport anomalies over East Asia and Northeast Asia for the summers with (a) warming state and (b) with cooling state of the tropical western Pacific in summer. Units: $10^3\text{g}\cdot\text{s}^{-1}\cdot\text{cm}^{-1}$. The moisture and wind fields data are taken from the ERA-40 reanalysis dataset. (e.g. Uppala et al., 2005)

4.2 ENSO cycle and its impact on the EAM variability and annual cycle

It is well known that ENSO cycle is one of the most striking phenomena in the tropical Pacific and has a great influence on the Asian-Australian monsoon system. The weak SASM tends to occur in a El Niño year. Huang and Wu's study (1989) first showed that summer monsoon rainfall anomaly in East Asia depends on the stage of ENSO cycle. Recently, Huang and Zhou (2002) pointed out from the composite analyses of summer monsoon rainfall anomalies for different stages of ENSO cycles during the period of 1951~2000 that droughts in North China tend to occur in the developing stage of El Niño events, as shown in Fig. 15a. On the other hand, during the decaying stage of El Niño events, floods tend to occur in the Yangtze River valley of China, especially in the regions to the south of the Yangtze River, as shown in Fig.15b. Zhang et al. (1996), and Zhang (2001) also pointed out that southerly wind anomalies can appear in the lower troposphere over the southeastern coast of China during the mature phase of ENSO events, and the intensified southerly winds will be favourable for the transport of water vapor from the Bay of Bengal and the tropical western Pacific to South China. Thus, during the mature phase of El Niño events, rainfall generally is stronger in South China.



Figure 15 Composite distributions of summer (June-August) rainfall anomalies (in percentage) (a) for the summers in the developing stage and (b) for the summers in the decaying stage of El Niño events occurred in the period from 1951 to 2000. The solid and dashed contours indicate positive and negative rainfall anomalies, respectively, and positive rainfall

anomalies are shaded in the figures.

ENSO cycle also has a significant influence on the annual cycle between the EAWM and the EASM. Chen (2002), and Huang et al. (2004) proposed that the interannual variations of the EAWM are closely associated with ENSO cycle. Chen(2002) analyzed the composite distribution of the meridional wind anomalies at 850hPa for the winters preceding the occurrence of El Niño events, and he pointed out that there are anomalous northerly winds from the coastal area of China to the SCS, thus, the EAWM is strong. And he also pointed out that there is an anomalous cyclonic circulation over the West Pacific, and anomalous northeasterly winds are located over the Yangtze River and the Huaihe River valleys and the southeastern coast of China, which indicates a weak western Pacific subtropical high and a weak EASM in a summer when an El Niño event is in its developing state. Moreover, following the developing stage, an El Niño event generally can reach its mature phase, anomalous southerly winds will prevail in the southeastern coast of China and the SCS. This shows that a weak EAWM may appear in a winter when an El Niño event is in its mature phase. In the following summer, the El Niño event may be in decay, there is an anomalous anticyclonic circulation over the West Pacific, which represents the strong western Pacific subtropical high. In this case, anomalous southwesterly winds distribute over the region from South China to the Yangtze River valley. This can show that a strong EASM may appear in a summer when an El Niño event is in its decaying phase.

4.3 Dynamic effect of circulation and zonal wind anomalies over the tropical western Pacific on ENSO cycles

Since El Niño events can cause severe climate anomalies in many regions of the world, especially in the Asian-Australian monsoon region (e.g., Webster et al., 1998), many meteorologists and oceanographers put much effort into studies on the regularity and physical mechanism of ENSO cycle. For example, Bjerknes (1969) first proposed a hypothesis that El Niño cycle may be a result of air-sea interaction over the equatorial eastern Pacific. However, after the implementation of the TOGA experiment, scientists have gradually realized that ENSO cycle may originate from the tropical western Pacific, thus, the physical mechanism of ENSO cycle has been studied further from the propagation of the equatorial oceanic waves (e.g., McCreay, 1983; McCreay and Anderson, 1984), and from the tropical oceanic coupling waves and the instable

air-sea interaction (e.g., Philander, 1981; Yamagata, 1985; Schopf and Suarez, 1988; Chao and Zhang, 1988). In particular, the theory of delayed oscillator in the air-sea coupled system over the tropical Pacific was proposed by some scholars (e.g., Anderson and McCreay, 1985; Cane and Zebiak, 1985; Schopf and Suarez, 1988; McCreay and Anderson, 1991).

Because of the interaction between the Asian-Australian monsoon system and ENSO cycles, the physical processes of ENSO cycles are very complex. The tropical western Pacific not only provides the necessary thermal condition for ENSO cycle (e.g. Huang and Wu, 1992; Li and Mu, 1999; Li and Mu, 2002; Chao et al., 2002, 2003), but also the atmospheric circulation and zonal wind anomalies over this region can provide the necessary dynamic condition for ENSO cycles. Li (1988, 1990) pointed out the triggering effect of the anomalous EAWM on El Niño events. Huang and Fu (1996), Huang et al. (1998), Huang et al. (2001) analyzed the atmospheric circulation and zonal wind anomalies in the lower troposphere over the tropical western Pacific and their roles in the developing and decaying processes of the El Niño events occurred in the 1980s and the 1990s. Figs. 16a-d show the distributions of the seasonal-mean circulation anomaly field at 850 hPa over the tropical western Pacific before the developing stage of the El Niño events, From these figures, it can be seen that before the developing stage of the El Niño events, there were cyclonic circulation anomalies in the lower troposphere over the tropical western Pacific, which caused the westerly wind anomalies over the tropical western Pacific around Indonesia. The westerly wind anomalies were favorable for the formation of the eastward-propagating warm Kelvin wave along the equatorial Pacific and caused the occurrence of these El Niño events. On the other hand, Huang et al. (2001) also analyzed the distributions of the seasonal mean circulation anomaly field at 850 hPa over the tropical western Pacific during the mature phase of these El Niño events(figures are omitted). The result also showed that in the mature phase of these El Niño events, there were obvious anticyclonic circulation anomalies in the lower troposphere over the tropical western Pacific, which caused the easterly wind anomalies over the region from Papua-New Guinea to Sumatra Island along Indonesia. The easterly wind anomalies caused the eastward-propagating cold Kelvin wave along the equatorial Pacific, thus, the El Niño events decayed and vanished.



Figure 16 Distributions of the circulation anomaly field at 850hPa over the tropical western Pacific before the developing stage of the El Niño events occurred in the period of 1980~1998. Units: ms^{-1} . (a) spring of 1980, (b) winter the 1985, (c) spring of 1991, (d) winter of 1996.

Huang et al. (2001), and Huang et al., (2004) further discussed theoretically the dynamic effect of the westerly wind anomalies over the tropical Pacific on the development and decay of the 1997/98 El Niño event with a simple tropical air-sea coupled model and the observed anomalous wind stress near the sea surface of the tropical Pacific during 1997 and 1998. The theoretical result identified the triggering effect of zonal wind anomalies over the tropical western Pacific on the equatorial oceanic Kelvin wave and Rossby waves in the tropical Pacific.

From the studies, it may be seen that the tropical western Pacific plays not only a reflecting effect on the equatorial oceanic Rossby waves by its western coast, as shown in the theory of the delayed oscillator proposed by Cane and Zebiak (1985), and Schopf and Suarez (1988), etc., but also important thermal and dynamic effects on ENSO cycles.

4.4 Dynamic and thermal effects of the Tibetan Plateau on the EASM

The Tibetan Plateau has an important thermal and dynamic effects on the interannual variability of EASM. Ye and Gao (1979) first pointed out the thermal effect of the Tibetan Plateau on the ASM. Later, many investigators also emphasized the thermal effect of the Tibetan Plateau on the ASM and pointed out that the heating anomaly over the Tibetan Plateau has a large impact on the ASM anomalies (e.g., Nitta 1983; Luo and Yanai, 1984; Huang, 1984, 1985). Wu and Zhang (1997) explained that the heating over the Tibetan Plateau is an air pump for the ASM onset and plays a triggering role in the ASM onset. Recently, Zhang et al. (2002) pointed out that the heating over the Tibetan Plateau has an important effect on the east-west oscillation of the South Asian high, which has a significant influence on the EASM. Wei and Luo (1996) pointed out that the snow cover seriously influences the heating over the Tibetan Plateau, and there is a largely positive correlation between snow cover in the Tibetan Plateau and summer monsoon rainfall in the upper and middle reaches of the Yangtze River.

Recently, Wei et al. (2002, 2003) analyzed the interannual and interdecadal variations of the

days and depth of snow cover in the Tibetan Plateau using the observed data of daily snow cover at 72 observational stations located in the Tibetan Plateau during 1960~1999. They discovered that there are obvious variations of the days and depth of snow cover in the Tibetan Plateau on the interannual and interdecadal time scales. The analyzed result showed that there are large positive correlations in the middle and upper reaches of the Yangtze River and negative correlations in South China and Northeast China between the depth of snow cover in winter and spring and the following summer rainfall. This may explain that if the snowfall in the Tibetan Plateau is heavy in previous winter and spring of a year, then the following summer rainfall will be strong in the upper and middle reaches of the Yangtze River. For example, in the winter of 1997 and the spring of 1998, the particularly heavy snowfall occurred in the Tibetan Plateau, then the severe flood disaster was caused in the Yangtze River valley in the summer of 1998. Moreover, compared the days and depth of snow cover in the Tibetan Plateau during the period from the late 1970s to the late 1990s with those during the period from the early 1960s to the mid-1970s, it is clearly seen that the time of snow cover has become longer and the snow depth has become deeper from the late 1970s. The interdecadal variation of snow cover in the Tibetan Plateau have an important impact on the summer monsoon rainfall in the middle and upper reaches of the Yangtze River (e.g., Wei et al. 2002, 2003; Huang et al., 2004).

Besides, G. Huang and Zhou (2004) investigated the variability of the northerly wind branch circulating the west side of the Tibetan Plateau and its impact on the EASM circulation. Their result also showed that after 1965, especially from 1977, since the northerly wind branch circulating the west side of the Tibetan Plateau has become weak, the southerly component of the EASM has been weakened, and the water vapor transported into North China was also weakened greatly. This caused the decrease of summer rainfall and the severe droughts in North China.

4.5 Thermal effect of the difference between surface temperature and surface air temperature and sensible heating in the arid and semi-arid regions of Northwest China on the EASM

Since monsoon results from the land-sea thermal contrast, thus, the variability of EAM is influenced by not only the thermal states of the tropical western Pacific, but also by the thermal states of the Eurasian continent, especially the thermal states in the arid and semi-arid of Northeast China. Zhou and Huang (2003, 2006) analyzed the interannual and interdecadal variations of the difference between surface temperature and the surface air temperature, i.e, $T_s - T_a$, in spring in the

arid and semi-arid regions of Northwest China and their impact on summer monsoon rainfall in China. The result shows that the Ts-Ta has obvious interannual and interdecadal variabilities in the arid and semi-arid regions of Northwest China. Before the late 1970s, the Ts-Ta anomalies were negative, but its anomalies became largely positive from the late 1970s, the largest positive anomaly appeared in the western part of Xinjiang Province. Moreover, from the correlation analyses, it is shown that when Ts-Ta appears a positive anomaly in the arid and semi-arid regions of Northwest China in a spring, then, rainfall may be strong in the lower reach of the Yangtze River, but it may be weak in North China in following summer. Therefore, the interdecadal variation of the spring Ts-Ta in the arid and semi-arid regions of Northwest China may be one of the causes of interdecadal variability of the EASM occurred in the late 1970.

5. Climate background of the occurrence of severe climatic disasters in China associated with the variability and anomaly of the East Asian monsoon climate system

5.1 Climate background of the severe floods in the Yangtze River and Huaihe River valleys

The occurring causes of severe floods in the Yangtze River valley, especially the particularly severe flood in the summer of 1998, as shown in Fig.17, have been systematically studied from the interannual variability and anomaly of the East Asian monsoon climate system including atmosphere, ocean and land surface shown in Fig. 12 (e.g., Huang et al., 1998; e.g., Huang and Zhou, 2002; Huang et al. 2003). Furthermore, the influence of the East Asian monsoon climate system variability and anomaly on severe flooding disasters in China was analyzed further by combing with the actual process of severe flood occurred in the Yangtze River valley in the summer of 1998 (e.g., Huang et al., 2003, 2004). Thus, a disposition of various component anomalies of the East Asian monsoon climate system caused the severe floods in the Yangtze River and Huaihe River valleys was proposed. As shown in Fig. 17, when the tropical western Pacific is in a cooling state, then convective activity is weak around the Philippines, and the western Pacific subtropical high unusually shifts westward and southward, which are favorable for the maintenance of summer monsoon rainbelt over the Yangtze River valley for longer time. And if the time of snow cover is long and the its depth is deeper in previous winter and spring, which are also favorable for the maintenance of summer monsoon rainbelt in the upper and middle reaches of the Yangtze River, then the following summer rainfall is strong in these regions. In

addition, when a low trough in the westerly zone is located over Inner-Mongolia and Northeast China, thus, weak cold air can be continuously transported from the low trough to the Yangtze River valley, which is necessary for the maintenance of the Meiyu front over the Yangtze River and Huaihe River valleys. Besides, the strong northeastward propagating 30~60 days oscillation from the Bay of Bengal to the Yangtze River valley is also an important factor for severe floods in the Yangtze River and Huaihe River valleys because it can bring large amount of water vapour from the Bay of Bengal and the SCS into the Yangtze River valley. In the summer of 1998, as shown in Fig.17, various components of the East Asian monsoon climate system all appeared large anomalies, thus, the particularly severe flood occurred in these regions and brought huge economic losses to China.



Figure. 17 Schematic diagram of various component anomalies of the East Asian monsoon climate system associated with the occurrence of severe floods in the Yangtze River and Huaihe River valleys. The distribution of precipitation anomaly percentages shown in the figure is those in the summer of 1998 and the precipitation anomaly percentages over 80% are shaded.

5.2 Climate background of the persistent droughts in North China

Similarly, the occurring causes of the persistent droughts in North China from the late 1970s have been also systematically investigated from the interdecadal variability and anomaly of various components of the East Asian monsoon climate system (e.g., Huang et al. 1999; Huang, 2001; Huang and Zhou, 2002; Huang et al, 2006). Their results clearly showed that influenced by the interdecadal variability of the tropical Pacific SSTs, the interdecadal anomalies of circulation over the tropical western Pacific are obvious, which have a large impact on the EASM and the summer monsoon rainfall in China, especially in North China. Due to the obvious warming of the tropical eastern and central Pacific from the late 1970s, the Walker circulation became weak over the tropical Pacific, which caused the weakening of the trade winds over the tropical western Pacific and the EASM. The weakening of the EASM led to the occurrence of the persistent

droughts in North China from the late 1970s.

The warming of the tropical eastern and central Pacific from the late 1970s also caused the Walker circulation anomaly over the tropical Atlantic and North Africa (e.g., Huang et al. 2006). An anomaly ascending and an anomaly descending were obviously located over the tropical eastern Pacific and North Africa, respectively. The intensification of the anomalous descending over the Sahelian region of North Africa led to a strong anticyclonic distribution of anomaly circulation over this region from the late 1970s. Moreover, their result also showed that there seems to be a teleconnection pattern of circulation anomalies from the Sahelian region of North Africa to South China by the Arabian Peninsula through the propagation of the Rossby wave-train and the circulation anomalies over South China can influence those over North China through the EAP pattern teleconnection. Because this anticyclonic distribution of circulation anomalies over North China was not helpful for the northward progress of the southerly wind to North China, this led to the weak monsoon rainfall in this region. As shown by Rodwell and Hoskins (1996), diabatic descending flow by the Asian summer monsoon can play a significant effect on the desertification of the Sahelian region through the propagation of Rossby wave-train. However, as shown by Huang et al. (2006), the intensification of the anticyclonic circulation anomalies over the Sahelian region also can influence the EASM over North China through the propagation of the Rossby wave-train. Therefore, it is also possible that the desertification of the Sahelian region may have an influence on the ASM on interdecadal time-scale.

In addition, the interdecadal variation of land surface process also have an impact on the ASM variability on interdecadal time scale. The results analyzed by Wei et al. (2002, 2003) have indicated that the days and thickness of winter and spring snow cover in the Tibetan Plateau were increased from the late 1970s. And the difference between ground surface temperature and surface air-temperature in spring became large in the arid and semi-arid areas of Northwest China from the late 1970s (e.g., Zhou and Huang, 2003, 2006). These are also helpful to the increase of summer monsoon rainfall in the Yangtze River and the Huaihe Rivers valley and the decrease of summer rainfall in North China.

From the above-mentioned studies, the climate background of the persistent droughts in North China, i.e., the interdecadal variations of various components of the East Asia monsoon climate system, may be summarized in Fig. 18.

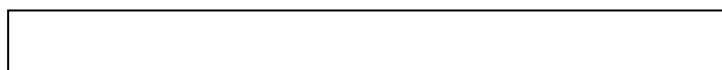


Figure 18 Schemataic diagram of the climate background of the persistent droughts in North China. In the figure, the summer precipitation anomaly percentages in China are the difference between summer rainfall anomalies averaged for 1977~2000 and those for 1966~1976 at 160 observational stations of China, and the areas of positive values are shaded.

6. Dynamic processes in the East Asian monsoon climate system associated with the occurrence of severe climatic disasters in China

The variability and anomaly of the East Asian monsoon climate system associated with the occurrence of severe climate disasters in China are closely associated with not only the variability and anomaly of ocean and land, as described in Section 4, but also the internal dynamic processes in atmosphere. Just because of the dynamic processes in this system, there are close relationships among the variabilities of various components of this system.

6.1 The East Asia/Pacific (EAP) pattern teleconnection

As described in Sections 2 and 3, there is an obvious tripole pattern either in the distributions of summer monsoon rainfall anomalies in China and the summer water vapour transports over East Asia or in the distributions of summer monsoon circulation anomalies over East Asia. As a result, the distributions of droughts and floods in China are closely associated with this meridional tripole pattern. Huang et al (2004), and Huang et al. (2006) used the EAP pattern teleconnection proposed by Nitta (1987), and Huang and Li (1987, 1988) to interpret the physical mechanism of the above-mentioned meridional tripole pattern. From the analyses of observed data, dynamic theory and simulation, they pointed out that the distribution of atmospheric circulation anomalies with the meridional tripole pattern over East Asia and the West Pacific can be caused by the thermal anomaly of tropical western Pacific or convective activity anomaly around the Philippines. Of course, as shown in Fig.19, this meridional tripole pattern of circulation anomalies is also associated with the EU pattern teleconnection proposed by Wallace and Gutzler (1981).



Figure 19 Distribution of the 500hPa height anomalies regressed by the EOF1. The solid and dashed lines indicate positive and negative height anomalies, respectively, and the areas of confidence level over 95% are shaded

Lu and Huang (1996a, b, 1998) investigated the variability of blocking high over Northeast Asia and its impact on summer monsoon rainfall in the Yangtze River and the Huaihe River valleys. They pointed out that there is a good relationship between the variations of the blocking high over Northeast Asia, especially over the Sea of Okhotsk, and summer monsoon rainfall variability in the Yangtze River and Huaihe River valleys. And they proposed that this relationship is due to the EAP teleconnection of circulation anomalies over the Northern Hemisphere summer suggested by Nitta (1987), and Huang and Li (1987,1988). When the tropical western Pacific is in a cooling state in a summer, then convective activity is weakened around the Philippines and the western Pacific subtropical high will shift southward and westward in the summer. Due to the Rossby wave-train propagation, i.e., the EAP pattern teleconnection, an anticyclonic distribution of anomalous circulation will appear over Northeast Asia, thus, the blocking high will be maintained over Northeast Asia for long time. Therefore, in this case, the Meiyu front will be also maintained in the Yangtze River and the Huaihe River valleys for longer time, which will cause severe flood in these regions.

6.2 The North Africa/East Asia teleconnection of meridional circulation anomalies in the upper troposphere

Yang et al. (2002) analyzed the association of Asian-Pacific-American winter climate with the East Asian jet stream (EAJS) on interannual timescale. They proposed that the EAJS is coupled to a teleconnection pattern extending from Asian continent to North America with the strongest signals over East Asia and the West Pacific in boreal winter. Moreover, Lu et al. (2002), and Lin and Lu (2005) analyzed the variability of meridional circulation anomalies using the HadAM3 data by Haddley center for the boreal summers of 1986~2000. Their results showed that there is an obvious teleconnection pattern in the meridional circulation anomalies in the upper troposphere over the regions from North Africa to East Asia. And they pointed out that this teleconnection may

be due to the eastward propagation of the Rossby wave-train along the westerly jet stream at 200hPa (e.g., Lu and Kim, 2004). Recently, Tao and Wei (2006) demonstrated further from the analysis of isentropic potential vorticity that the northward advance (southward retreat) of the western Pacific subtropical high may be associated with the propagation of the Rossby wave-train along the Asian jet in the upper troposphere because it may form a high ridge (trough) along the eastern coast of China. Thus, the above-mentioned meridional tripole structure of circulation anomalies over East Asia may be also associated with the teleconnection pattern along the Asian jet in the upper troposphere (e.g., Hsu and Lin, 2006).

6.3 Interannual and interdecadal oscillations of quasi-stationary planetary wave activity in the troposphere and stratosphere and their impacts on the EAWM.

Huang and Gambo (1982, 1983 a, b, 1984) investigated the three-dimensional propagation of quasi-stationary planetary waves responding to forcing by topography and stationary heat sources in the troposphere in boreal winter with a 34-level model in addition to the theoretical analyses with the refractive index square and E-P flux of waves. They pointed out that there are two wave guides in the three-dimensional propagations of quasi-stationary planetary waves, one is the so-called as the polar waveguide, by which the quasi-stationary planetary waves can propagate from the troposphere to the stratosphere over high latitudes, and other is the so-called as the low-latitude waveguide, by which the waves can propagate from the lower troposphere over mid-and low latitudes to the upper troposphere over low latitudes. Based on these studies, recently, Chen et al. (2002, 2003, 2005), Chen and Huang (2005) studied the interannual variations of propagating wave guides from quasi-stationary waves with the wave E-P fluxes using NCEP/NCAR and ERA-40 reanalysis data and AGCM simulation data, respectively. Their results presented that these two wave guides for the quasi-stationary planetary waves evidently have an interannual oscillation. When the polar wave guide is strong (weak) in a winter, then the low latitude wave guide may be weak (strong), oppositely. Moreover, it was also found that due to the wave-flow interaction, the interannual oscillation of these two wave guides for the quasi-stationary planetary wave guides has a significant influence on the Arctic Oscillation (AO) through the Northern Annular Model (NAM) proposed by Thompson and Wallace (1998, 2000). When the equatorward propagation of quasi-stationary planetary waves from the lower troposphere over middle latitudes toward the upper troposphere over low latitudes is strong during a winter, then the upward

propagation of quasi-stationary planetary waves from the troposphere into the stratosphere become weak in the winter. This can lead to the weakening of the East Asian westerly jet stream because of the convergence of the wave activity fluxes for quasi-stationary planetary waves over this region. Thus, the East Asian trough, the Siberian high and the Aleutian low can become weak during the winter, which can decrease the northwesterly wind and cause warming winter over East Asia.

Recently, Huang and Wang (2006) also investigated the interdecadal variation of quasi-stationary planetary waves and its impact on the EAWM. Their result showed that an obvious interdecadal variability of the EAWM has occurred in East Asia from the late 1980s. The weakening of the EAWM may be affected by the AO proposed by Thompson and Wallace (1998). Moreover, Huang and Wang (2006) also pointed out that there was also an obvious interdecadal variation of planetary wave activity in the late 1980s. As shown in Fig.20, the so-called low latitude wave guide for quasi-stationary planetary waves was intensified from 1987, which has caused the intensification of amplitudes of quasi-stationary planetary waves in the upper troposphere over low latitudes. Their result also showed that the intensification of quasi-stationary wave propagation from mid-and high latitudes to low latitudes led to the deceleration of zonal-mean zonal wind over the latitudes around 35°N. This caused the intensification of the AO, the weakening of EAWM and the prolonged warm winter in China from 1987. Therefore, the interdecadal variation of planetary wave activity from the late 1980s has an important impact on the interdecadal variation of EAWM.

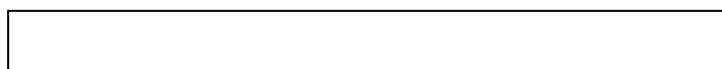


Figure 20 Composite distributions of the E-P flux for the quasi-stationary planetary waves 1~3 averaged for (a) the Northern Hemisphere winters of 1976~1987, and for (b) the winters of 1988~2001, and (c) difference between them.

7. Conclusions and problems for further study

From the review mentioned above, it may be seen that there has been some significant advancements in understanding the basic characteristic, property of the East Asian monsoon

climate system and its spatial and temporal variabilities, which are closely associated the occurrence of severe climatic disasters in China. And the basic physical processes of its variabilities including internal and external processes that influence these variabilities have been studied further. The advancements may be summarized as follows:

(1) The EAM system is a relatively independent monsoon subsystem of the Asian-Australian monsoon system. Either the horizontal and vertical structure of wind field and the water vapour transports or the annual cycle in this subsystem are different from the SAM and the NAM subsystems.

(2) The interannual variability of this subsystem exhibits an obvious quasi-biennial oscillation, i.e., the TBO, with a meridional tripole pattern in spatial distribution, which can cause a tripole pattern in spatial distribution of drought and flood disasters in East Asia .

(3) The EAM subsystem is not only a circulation system, but also an atmosphere-ocean-land surface coupled climate system, which may be called as the East Asian monsoon climate system. Therefore, the East Asian monsoon climate system is a system including various components of atmosphere, ocean and land surface process.

(4) Since the occurrence of severe climatic disasters in China is closely associated with variability and anomaly of various components of the East Asian monsoon climate system, the climate background of the occurrences of the severe floods in the Yangtze River and Huaihe River valleys and the prolonged droughts in North China are also put forward from the interannual and interdecadal variations of the East Asian monsoon climate system, respectively. These have been applied to the seasonal and annual predictions of climate anomalies in China.

(5) The EAP and EU pattern teleconnections of summertime circulation anomalies as well as the teleconnection of meridional wind anomalies along westerly jet stream in the upper troposphere can be used to explain well the physical mechanism of the meridional tripole pattern in spatial distributions of summer monsoon rainfall, water vapour transports and circulation anomalies over East Asia.

However, many problems on the basic physical processes of the East Asian monsoon climate system variability and their impacts on severe climatic disasters in China are still not clear and need to be studied further:

(1) The East Asian monsoon climate system is of relatively independent horizontal and vertical

structures of wind field, which are different from the SAM and NAM subsystems. These differences can seriously influence the annual cycle and action including their onset, active and break of these monsoon subsystems. Thus, the association and difference among onset, active and break, and annual cycle processes of these monsoon subsystems should be studied further.

(2) Many investigations showed that the interdecadal variability of the East Asian monsoon climate system has a significant impact on its interannual variations, which also influence its intraseasonal variations. However, physical processes in the interactions between different time-scale variabilities of this system are not yet clear. Therefore, the physical processes in the interactions among different time-scale variabilities of this system is an important issue for the future study.

(3) There are complex dynamic and thermal processes in the interannual variability of East Asian monsoon climate system. The dynamic process of quasi-biennial oscillation i.e., the TBO, with the meridional tripole pattern distribution and the thermal effect of tropical heating on the TBO are emphasized in recent studies. However, according to the study by Yang et al. (2004), the extratropical process also has an important effect on the ASM. Therefore, the effect of extratropical process on interannual variability of the East Asian monsoon climate system needs to be put attention in the future study.

(4) The East Asian monsoon climate system has a large interdecadal variability. However, the physical processes of this variability, for example, the dipole pattern distribution, are not yet clear, and studies on this problem are not sufficient. This problem should be studied further from the air-land-ocean interactions on interdecadal time-scale.

The above review shows that the East Asian monsoon climate system variabilities on interannual and interdecadal time scales are still important research issues for the future study. If the physical processes of these variabilities cannot be revealed further, the increase of seasonal and annual predictabilities of severe climatic disasters in China may be difficult. Therefore, understanding of the internal and external dynamic processes affecting the interannual and interdecadal variabilities of the Asian monsoon climate system still is a main objective of the future study. We may believe that through the implementation of some National Research Programs, it will be possible to further understand the physical mechanism of the interannual and interdecadal variabilities of the East Asian monsoon climate system.

Acknowledgments. This paper was supported by the “National Key Programme for Developing Basic Sciences” Project G2006CB403601 and the project 40575026, and the Excellent National Key Lab. Founding, National Natural Science Foundation of China, Project 40523001, respectively.

References

- Anderson, D. L. T., and J. P. McCreary, 1985: Slowly propagating disturbances in a coupled ocean-atmosphere model. *J. Atmos. Sci.*, **42**, 615~629.
- Bao Ming, and Huang Ronghui, 2006: Characteristics of the interdecadal variations of heavy rain over China in the last 40 years. *Chinese J. Atmos. Sci.*, **30**, 1057~1067. (in Chinese)
- Bjerknes, J., 1969: Atmospheric teleconnection from the equatorial Pacific. *Mon. Wea. Rev.*, **97**, 163~172.
- Cai Rongsuo, Chen Jilong, and Huang Ronghui, 2006: The response of marine environment in the offshore area of China and its adjacent ocean to recent global climate change. *Chinese J. Atmos. Sci.*, **30**, 1019~1033.
- Cane, M. A., and S. E. Zebiak, 1985: A theory of El Niño and the Southern Oscillation. *Science*, **228**, 1085~1087.
- Chang, C. P., J. Erickson, and L.M. Lau, 1979: Northeasterly cold surges and near-equatorial disturbances over the winter-MONEX area during 1974. Part I: Synoptic aspects. *Mon. wea. Rev.*, **107**, 812~829.
- Chang, C. P., Y. S. Zhang, and T. Li, 2000: Interannual and interdecadal variations of the East Asian summer monsoon and tropical Pacific SSTs. I.II. *J. Climate*, **13**, 4310~4340.
- Chao Jiping, and Zhang Renhe, 1988: The air-sea interaction waves in the tropics and their instability. *Acta Meteor. Sinica*, **2**, 275~287. (in Chinese)
- Chao Jiping, Yuan Shaoyu, Chao Qingchen, and Tian Jiwei, 2002: A data analyses on the evolution of the El Niño / La Niña cycle. *Adv. Atmos. Sci.*, **20**, 837~844.
- Chao Jiping, Yuan Shaoyu, Chao Qingchen, and Tian Jiwei, 2003: The origin of warm sea water in the surface layer of the West Pacific warm pool-The analysis of the 1997/1998 El Niño event. *Chinese J. Atmos. Sci.*, **27**, 145~151.(in Chinese)
- Chen Jilong, and Huang Ronghui, 2006: The comparison of climatological characteristics among Asian and Australian monsoon subsystem, Part I, the wind structure of summer monsoon. *Chinese J. Atmos. Sci.*, **30**, 1091~1102. (in Chinese)
- Chen Jilong, and Huang Ronghui, 2007: The comparison of climatological characteristics among Asian and Australian monsoon subsystems. Part II. Water vapor transport by summer monsoon. *Chinese J. Atmos. Sci.*, **31** (to be published). (in Chinese)
- Chen Longxun, Zhu Qiangen and Luo Huibang, 1991: *East Asian Monsoon*, China Meteorological Press, Beijing, 362pp. (in Chinese)

- Chen Wen, 2002: The impact of El Niño and La Niña events on the East Asian winter and summer monsoon cycle. *Chinese J. Atmos. Sci.*, **26**, 595~610. (in Chinese)
- Chen, W., and Hans-F. Graf, 1998: The interannual variability of East Asian winter monsoon and its relationship to global circulation. *Max-Planck-Institute für Meteorologie, Report No. 250*.
- Chen Wen, Hans-F. Graf, and Huang Roghui, 2000: Interannual variability of East Asian winter monsoon and its relation to the summer monsoon. *Adv. Atmos. Sci.*, **17**, 48-60.
- Chen, W., Hans-F. Graf, and M. Takahashi, 2002: Observed interannual oscillation of planetary wave forcing in the Northern Hemisphere winter. *Geophys. Res. Letter.* **29**(22), 2073, doi:1029/2002 GL016062.
- Chen, W., M. Takahashi, and Hans-F. Graf, 2003: Interannual variations of stationary planetary wave activity in the Northern winter troposphere and stratosphere and their relations to NAM and SST. *J. Geophys. Res.*, **108** (D24), 4797, doi:10.1029/2003 HD003834.
- Chen, W., S. Yang, and R. H. Huang, 2005: Relationship between stationary planetary wave activity and the East Asian winter monsoon. *J. Geophys. Res.*, **110**, D 14110, doi:10. 1029/2004JD 5669.
- Chen Wen, and Huang Ronghi, 2005: The three-dimensional propagation of quasi-stationary waves in the Northern Hemisphere winter and its interannual variations. *Chinese J. Atmos. Sci.*, **29**, 139~146. (in Chinese)
- Ding, Y. H. 1992: Summer monsoon rainfall in China. *J. Meteor. Soc. Japan*, **70**, 373~396.
- Ding, Y. H., 1994: *Monsoon over China*. Kluwer Academic Publishers, 420 pp.
- Ding Yihui, and He Chun, 2006: The summer monsoon onset over the tropical eastern Indian Ocean: The earliest onset process of the Asian summer monsoon. *Adv. Atmos. Sci.*, **23**, 940~950.
- Goswami, B. N., Wu, G. X., and T. Yasunari, 2006: The annual cycle, intraseasonal oscillations, and roadblock to seasonal predictability of the Asian summer monsoon. *J. Climate*, **19**, 5078~5099.
- Hsu, H. H., and S. M. Lin, 2006: The tripole pattern of East Asian summer rainfall. *Proceedings of the Symposium on Asian monsoon*, Kuala Lumpur, Malaysia, 4~7, April, 2006. 28~29.
- Huang Gang, 2004: An index measuring the interannual variation of the East Asian summer monsoon-The EAP index. *Adv. Atmos. Sci.*, **21**, 41~52.
- Huang Gang, and Zhou Liantong, 2004: The variability of the wind system circulating round the west side of the Tibetan Plateau and its relation to the East Asian summer monsoon and summer rainfall in North China. *Clim. & Envir. Res.*, **9**, 316~330. (in Chinese)
- Huang, R. H., and K. Gambo, 1982: The response of a hemispheric multi-level model atmosphere to forcing by topography and stationary heat sources. Parts I, II. *J. Meteor. Soc. Japan*, **60**, 78~108.
- Huang, R. H., and K. Gambo, 1983a: The response of a hemispheric multi-level model atmosphere to forcing by topograph and stationary heat sources in summer. *J. Meteor. Soc. Japan*, **61**, 495~509.

- Huang, R. H., and K. Gambo, 1983b: On other wave guide in stationary planetary wave propagations in the winter Northern Hemisphere. *Science in China*, **26**, 940~950.
- Huang Ronghui, 1984: The characteristics of the forced planetary wave propagations in the summer Northern Hemisphere. *Adv. Atmos. Sci.*, **1**, 85-94.
- Huang Ronghui, 1985: Numerical simulation of the three-dimensional teleconnections in the summer circulation over the Northern Hemisphere. *Adv. Atmos. Sci.*, **2**, 81-92.
- Huang Ronghui, and Li Weijing, 1987: Influence of the heat source anomaly over the tropical western Pacific on the subtropical high over East Asia. *Proceedings of the International Conference on the General Circulation of East Asia*, Chengdu, April 10-15, 1987, 40-51.
- Huang Ronghui, and Li Weijing, 1988: Influence of the heat source anomaly over the tropical western Pacific on the subtropical high over East Asia and its physical mechanism. *Chinese J. Atmos. Sci.*, **14**, Special Issue, 95~107. (in Chinese)
- Huang Ronghui, and Wu Yifang, 1989: The influence of ENSO on the summer climate change in China and its mechanisms. *Adv. Atmos. Sci.*, **6**, 21-32.
- Huang, R. H. and F. Y. Sun, 1992: Impact of the tropical western Pacific on the East Asian summer monsoon. *J. Meteor. Soc. Japan*, **70**, (1B), 243-256.
- Huang Ronghui, and Wu Yifang, 1992: Research on ENSO cycle dynamics. *Proc. Oceanic Circulation Conferences*, Zeng Qingcun et al., Eds., China Oceanological Press, Beijing, 41~51.
- Huang Ronghui, and Sun Fengying, 1994: Impact of the thermal state and convective activities over the western Pacific warm pool on summer climate anomalies in East Asia. *Chinese J. Atmos. Sci.*, **18**, 262-272. (in Chinese)
- Huang Ronghui, and Fu Yunfei, 1996: The interaction between the East Asian monsoon and ENSO cycle. *Clim. & Envi. Re.*, **1**, 38~54. (in Chinese)
- Huang Ronghui, Zhang Zhenzhou, Huang Gang, and Ren Baohua, 1998: Characteristics of the water vapor transport in East Asian monsoon region and its difference from that in South Asian monsoon region in summer. *Chinese J. Atmos. Sci.*, **22**, 460~469. (in Chinese)
- Huang Ronghui, Xu Yuhong, Wang Penghui, 1998: The features of the particularly severe flood over the Changjiang (Yangtze River) basin during the summer of 1998 and exploration of its cause. *Clim. & Envir. Res.*, **3**, 300~313. (in Chinese)
- Huang Ronghui, Zang Xiaoyan, Zhang Renhe, and Chen Jilong, 1998: The westerly anomalies over the tropical Pacific and their dynamical effect on the ENSO cycles during 1980~1994. *Adv. Atmos. Sci.*, **15**, 135~151.
- Huang Ronghui, Xu Yuhong, and Zhou Liantong, 1999: The interdecadal variation of summer precipitations in China and the drought trend in North China. *Plateau Meteor.*, **18**, 465~476 (in Chinese).
- Huang Ronghui, Zhang Renhe, and Yan Bangliang, 1999: Progresses in the studies on the interannual variability of East Asian climate system and problems to be studied further. *Basic Res. in China*, **2**, 66~73. (in Chinese)
- Huang Ronghui, 2001: Decadal variability of the summer monsoon rainfall in East Asia and its association with the SST anomalies in the tropical Pacific. *CLIVAR Exchange*, **2**, 7-8
- Huang Ronghui, 2001: Progresses in the studies on the formation mechanism and prediction theory of severe

- climatic disasters in China. *Basic Res. in China*, **4**, 4~8. (in Chinese)
- Huang Ronghui, Zhang Renhe, and Yan Bangliang, 2001: Dynamical effect of the zonal wind anomalies over the tropical western Pacific on ENSO cycles. *Science in China (Series D)*, **44**, 1089~1098.
- Huang Ronghui, and Zhou Liantong, 2002: Research on the characteristics, formation mechanism and prediction of severe climate disasters in China. *J. Nature Disasters*, **11**, 1-9 (in Chinese).
- Huang Ronghui, Zhou Liantong, and Chen Wen, 2003: The progress of recent studies on the variabilities of the East Asian monsoon and their causes. *Adv. Atmos. Sci.*, **20**, 55~69.
- Huang Ronghui, Huang Gang, and Wei Zhigang, 2004: Climate variations of the summer monsoon over China. *East Asian Monsoon*, C. P. Chang Ed., World Scientific Publishing CO. Pte. Ltd., 213~270.
- Huang Ronghui, 2004: Review of the studies on the formation mechanism of severe climatic disasters in China. *Basic Res. in China*, **4**, 6~13. (in Chinese)
- Huang, Ronghui, Chen Wen, Yan Bangliang, and Zhang Renhe, 2004: Recent Advances in studies of the interaction between the East Asian winter and summer monsoon and ENSO cycle. *Adv. Atmos. Sci.*, **21**, 407~424.
- Huang Ronghui, Gu Lei, and Xu Yuhong, et al., 2005: Characteristics of the interannual variations of onset and northward advance of the East Asian summer monsoon and their associations with thermal states of the tropical western Pacific. *Chinese J. Atmos. Sci.*, **29**, 20~36.(in Chinese)
- Huang Ronghui, 2006: Progresses in research on the formation mechanism and prediction theory of severe climatic disasters in China. *Adv. in Earth Sci.*, **21**, 564~575. (in Chinese)
- Huang Ronghui, Cai Rongshou, Cheng Jilong, and Zhou Liantong, 2006: Interdecadal variations of droughts and floodings in China and their association with the East Asian climate system. *Chinese J. Atmos. Sci.*, **30**, 730~743. (in Chinese)
- Huang Ronghui, Chen Jilong, Huang Gang, and Zhang Qilong, 2006: The quasi-biennial oscillation of summer monsoon rainfall in China and its cause. *Chinese J. Atmos. Sci.*, **30**, 545~560. (in Chinese)
- Huang Ronghui, Gu Lei, Zhou Liantong, and Wu Shangsen, 2006: Impact of the thermal state of the tropical western Pacific on onset date and process of the South China Sea summer monsoon. *Adv Atmos. Sci.*, **23**, 909~924.
- Huang Ronghui, and Wang Lin, 2006: Interdecadal variations of Asian winter monsoon and its association with the planetary wave activity. *Proceedings of the Symposium on Asian Monsoon*, Kuala Lumpur, Malaysia, 4~7 April, 2006, 126.
- Kalnay, E. M., and Co-authors, 1996: The NCEP/NCAR 40-year reanalysis project. *Bull. Amer. Meteor. Soc.*, **77**, 437~471.
- Kang Lihua, Chen Wen, and Wei Ke, 2006: The interdecadal variation of winter temperature in China and its

- relation to the anomalies in atmospheric general circulation. *Clim. & Envir. Res.*, **11**, 330~339.
- Krishnamurti, T. N., and Y. Ramanathan, 1982: Sensitivity of monsoon onset to differential heating. *J. Atmos. Sci.*, **39**, 1290-1306.
- Kurihara, K., 1989: A climatological study on the relationship between the Japanese summer weather and the subtropical high in the western northern Pacific. *Geophys. Mag.*, **43**, 45-104.
- Lau, K. M. and C.P. Chang, 1987: Planetary scale aspects of the winter monsoon and atmospheric teleconnections. *Monsoon Meteorology*, C. P. Chang and T. W. Krishnamurti, Eds. Oxford Uni. Press, 161-201.
- Li Chongyin, 1988: The frequent actions of the East Asian trough and the occurrences of El Niño, *Science in China (Series B)*, 667-674. (in Chinese)
- Li Chongyin, 1990: Interaction between anomalous winter monsoon in East Asia and El Niño events. *Adv. Atmos. Sci.*, **7**, 36-46.
- Li Chongyin, and Mu Mingquan, 1999: The occurrence of El Niño event and the sea temperature anomalies in the subsurface of the West Pacific warm pool. *Chinese J. Atmos. Sci.*, **23**, 513~521. (in Chinese)
- Li Chongyin, and Mu Mingquan, 2000: ENSO-A cycle of the subsurface sea temperature anomaly in the tropical Pacific driven by the anomalous zonal wind over the equatorial western Pacific. *Adv. in Earth Sci.*, **17**, 631~638. (in Chinese)
- Li, C., and M. Yanai, 1996: The onset and interannual variability of the Asian summer monsoon in relation to land-sea thermal contrast. *J. Climate*, **9**, 358~275.
- Lin Zhongda, and Lu Riyu, 2005: Interannual meridional displacement of the East Asian upper-tropospheric jet stream in summer. *Adv. Atmos. Sci.*, **22**, 199~211.
- Lu, R. Y., Y. S. Chung, and R. H. Huang, 1995: Interannual variations of the precipitation in Korea and the comparison with those in China and Japan. *J. Korean Environ. Sci. Soc.*, **4**, 345-365.
- Lu Riyu, and Huang Ronghui, 1996a: The transformed meridional circulation equation and its application to the diagnostic analysis of the blocking high formation. *Chinese J. Atmos. Sci.*, **20**, 138~148.(in Chinese)
- Lu Riyu, and Huang Ronghui, 1996b: Energetics examination of the blocking episodes in the Northern Hemisphere. *Chinese J. Atmos. Sci.*, **20**, 270~278. (in Chinese)
- Lu Riyu, and Huang Ronghui, 1998: Influence of East Asia/Pacific teleconnection pattern on the interannual variations of the blocking highs over the Northeastern Asia in summer. *Chinese J. Atmos. Sci.*, **22**, 727~735. (in Chinese)
- Lu, R.Y., 2001: Interannual variability of the summertime North Pacific subtropical high and its relation to atmospheric convection over the warm pool. *J. Meteor. Soc. Japan*, **79**, 771~783.
- Lu, R. Y. and B. W. Dong, 2001: Westward extension of North Pacific subtropical high in summer. *J. Meteor. Soc. Japan*, **79**, 1229~1241.
- Lu R,Y., J. H. Oh, and B. J. Kim, 2002: 200hPa mid-latitude Rossby waves as a possible link between the Indian and East Asian summer monsoon. *Tellus*. **54A**, 44~55.
- Lu, R. Y., and B. J. Kim, 2004: The climatological Rossby wave source over the STCZs in the summer Northern

- Hemisphere. *J. Meteor. Soc. Japan*, **82**, 657~669.
- Luo, H. B. and M. Yanai, 1984: The large-scale circulation and heat sources over the Tibetan Plateau and surrounding areas during the early summer of 1979. *Mon. Wea. Rev.*, **108**, 1849-1853.
- McCreary, J. P., and D. L. T. Anderson, 1984: A simple model of El Niño and the Southern Oscillation. *Mon. Wea. Rev.*, **112**, 934~946.
- McCreary, J. L., and D. L. T. Anderson, 1991: An overview of coupled ocean-atmosphere models of El Niño and the Southern Oscillation. *J. Geophys. Res.*, **96**, 3125~3150.
- McBride, J. J., 1987: The Australian summer monsoon. *Monsoon Meteorology*, C. P. Chang and T. N. Krishnamurti, Eds., Oxford University Press, 203-232.
- Miao, J. H., and K. M. Lau, 1990: Interannual variability of the East Asian monsoon rainfall. *Quart. J. Appl. Meteor.*, **1**, 377-382 (in Chinese).
- Mooley, D. A., and B. Parthasarathy, 1984: Fluctuations in all-india summer monsoon rainfall during 1871~1978. *Climate Change*, **6**, 287~301.
- Murakami, T., and J. Matsumoto, 1994: Summer monsoon over the Asian continent and western North Pacific. *J. Meteor. Soc. Japan*, **72**, 745~791.
- Nitta, Ts., 1983: Observational study of heat sources over the eastern Tibetan Plateau during the summer monsoon. *J. Meteor. Soc. Japan*, **61**, 590-605.
- Nitta, Ts., 1987: Convective activities in the tropical western Pacific and their impact on the Northern Hemisphere summer circulation. *J. Meteor. Soc. Japan*, **64**, 373-390.
- Philander, S. G. H., 1981: The response of equatorial ocean to a relaxation of trade winds. *J. Phys. Oceanogr.*, **11**, 176~189.
- Rodwell, M. J., and B. J. Hoskins, 1996: Monsoon and dynamics of deserts. *Quat. J. R. Meteor. Soc.*, **122**, 1385~1404.
- Schopf, P. S., and M. J. Suarez, 1988: Vacillations in a coupled ocean-atmosphere model. *J. Atmos. Sci.* **45**, 549~566.
- Staff members of Academia Sinica, 1957: On the general circulation over Eastern Asia (I). *Tellus*, **9**, 432~446.
- Tao Shiyun, and Chen Longxun, 1985: The East Asian summer monsoon. *Proceedings of International Conference on Monsoon in the Far East*. Tokyo, Nov 5~8. 1985, 1~11.
- Tao S. Y. and Chen L. X., 1987: A review of recent research on the East Asian summer monsoon in China. *Monsoon Meteorology*, C. P. Cheng and T. N. Krishnamurti, Eds., Oxford University Press, 60-92.
- Tao Shiyun, and Wei Jie, 2006: The westward, northward advance of the subtropical high over the West Pacific in summer. *J. of Applied Meteor. Sci.*, **17**, 513~524.
- Thompson, D. W. J., and J. M. Wallace, 1998: The Arctic Oscillation signature in the wintertime geopotential height and temperature fields. *Geophys. Res. Letter*, **25**, 1297~1300.
- Thompson, D. W. J., and J. M. Wallace, 2000: Annual modes in the extratropical circulation. Part 1: Month to-month variability. *J. Climate*, **13** 1000~1016.
- Tomas, R., and P. J. Webster, 1997: On the location of the intertropical convergence zone and near equatorial

- convection-The role of inertial instability. *Quart. J. Roy. Meteor. Soc.*, **123**, 1445~1482.
- Tu, C. W., and S. S. Huang, 1944: The advance and retreat of the summer monsoon. *Meteor. Mag.*, **18**, 1-20.
- Uppala, S. M., Kallberg, P. W., and A. J. Simmons, et al., 2005: The ERA-40 reanalysis. *Quat. J. Roy. Meteor. Soc.*, **131**, 2961~3012.
- Wallace, J. M., and D. S. Gutzler, 1981: Teleconnection in the geopotential height field during the Northern Hemisphere winter. *Mon. Wea. Rev.*, **109**, 748~812.
- Webster, P. J., and S. Yang, 1992: Monsoon and ENSO: Selectively interactive system. *Quart. J. Roy. Meteor. Soc.*, **118**, 877-926.
- Webster, P. J., V. O. Magana, T. B. Palmer, J. Shukla, R. A. Tomas, M. Yanai, and T. Yasunari 1998: Monsoons: processes, predictability, and the prospects for prediction. *J. Geophys. Res.*, **103**, 14451~14510
- Wei Zhigang, and Luo Shiwei, 1996: Impact of the snow cover in western China on the precipitation in China during the rainy season, *Collected Papers of the Project "Disastrous Climate Prediction and Its Impact on Agriculture and Water Resources", II. Processes and Diagnosis of Disatrous Climate*, Huang Ronghui et al., Eds., China Meteorological Press, Beijing, 40-45 (In Chinese).
- Wei Zhigang, Huang Ronghi, and Chen Wen, et al., 2002: Spatial distributions of interdecadal variations of the snow at the Tibetan Plateau. *Chiense J. Atmos. Sci.*, **26**, 496~508.(in Chinese)
- Wei Zhigang, Huang Ronghi, and Dong Wenjie, 2003: Interannual and interdecadal variations of air temperature and precipitation over the Tibetan Plateau. *Chinese J. Atmos. Sci.*, **27**, 157~170. (in Chinese)
- Wu, G. X. and Y. S. Zhang, 1997: Tibetan Plateau forcing and the timing of the monsoon onset over South Asia and the South China Sea. *Mon. Wea. Rev.*, **126**, 917~927.
- Xie P. A., and P. A. Arkin, 1997: Analyses of global monthly precipitation using gauge observations, satellite estimates and numerical model prediction. *J. Climate.*, **9**, 804~858.
- Yang, S., and K. M. Lau, 1998: Influences of sea surface temperature and ground wetness on Asian monsoon. *J. Climate*, **11**, 3230~3246.
- Yang, S., Lau, K. M., and K. M. Kim, 2002: Variations of the East Asian jet stream and Asian-Pacific-American climate anomalies. *J. Climate*, **15**, 306~325.
- Yang, S., K. M. Lau, and S. H. Yoo, et al., 2004: Upstream subtropical signals preceding the Asian summer monsoon circulation. *J. Climate*, **17**, 4213~4229.
- Yamagata, T., and Y. Matsumoto, 1989: A simple ocean-atmosphere coupled model for the origin of a warm El Niño /Southern Oscillation event. *Phil. Trans. R. Soc. London, A* **329**, 225~236.
- Yasunari, T., and R. Suppiah, 1988: Some problems on the interannual variability of Indonesian monsoon rainfall. *Tropical Rainfall measurement*, J. S. Theon and N. Fugono, Eds. Daepok, Hampton, Va., 113~132.
- Ye D. Z., and Gao Y. X., 1979: *Tibetan Plateau Meteorology*, Science Press, Beijing, 279pp (in Chinese).
- Yin Baoyu, Wang Lianying, and Huang Ronghui, 1996: Quasi-biennial oscillation of summer monsoon rainfall in East Asia and its physical mechanism, *Collected papers of the Project "Disastrous Climate Prediction and Its Impact on Agriculture and Water Resources", II. Processes and Diagnosis of Disatrous Climate*, Huang Ronghui et al. Eds., China Meteorological Press, Beijing, 196-205 (in Chinese).
- Zeng, Q. C., B. L. Zhang and Y. L. Liang, 1994: East Asian summer monsoon-a case study. *Proc. Indian Nation. Sci. Acad.*, **60**(1), 81-96.
- Zhang, Q., G. X. Wu, and Y. F. Qian, 2002: The bimodaity of the 100hPa South Asian high and its association on

the climate anomaly over Asia in summer. *J. Meteor. Soc. Japan*, **80**, 733-744.

Zhang, Renhe, 2001: Relations of water vapor transport from Indian monsoon with those over East Asia and the summer rainfall in China. *Adv. Atmos. Sci.*, **18**, 1005-1017.

Zhang R. H., A. Sumi, and M. Kimoto, 1996: Impact of El Niño on the East Asian monsoon: A diagnostic study of the 86/87 and 91/92 events. *J. Meteor. Soc. Japan*, **74**, 49-62.

Zhou Liantong, and Huang Ronghui, 2003: Research on the characteristics of interdecadal variability of summer climate in China and its possible cause.. *Clim & Envir. Res.*, **8**, 274~290. (in Chinese)

Zhou Liantong, and Huang Ronghi, 2006: Characterisitcs of the interdecadal variability of difference between surface temperature and surface air temperature in spring in the arid and semi-arid region of Northwest China and its impact on summer precipitation in North China. *Clim. & Envir. Res.*, **11**, 1~13. (in Chinese)

Zhu, K. E., 1934: Southeast monsoon and rainfall in China. *Chinese J. Geogr. Soc.*, **1**, 1-27. (in Chinese)

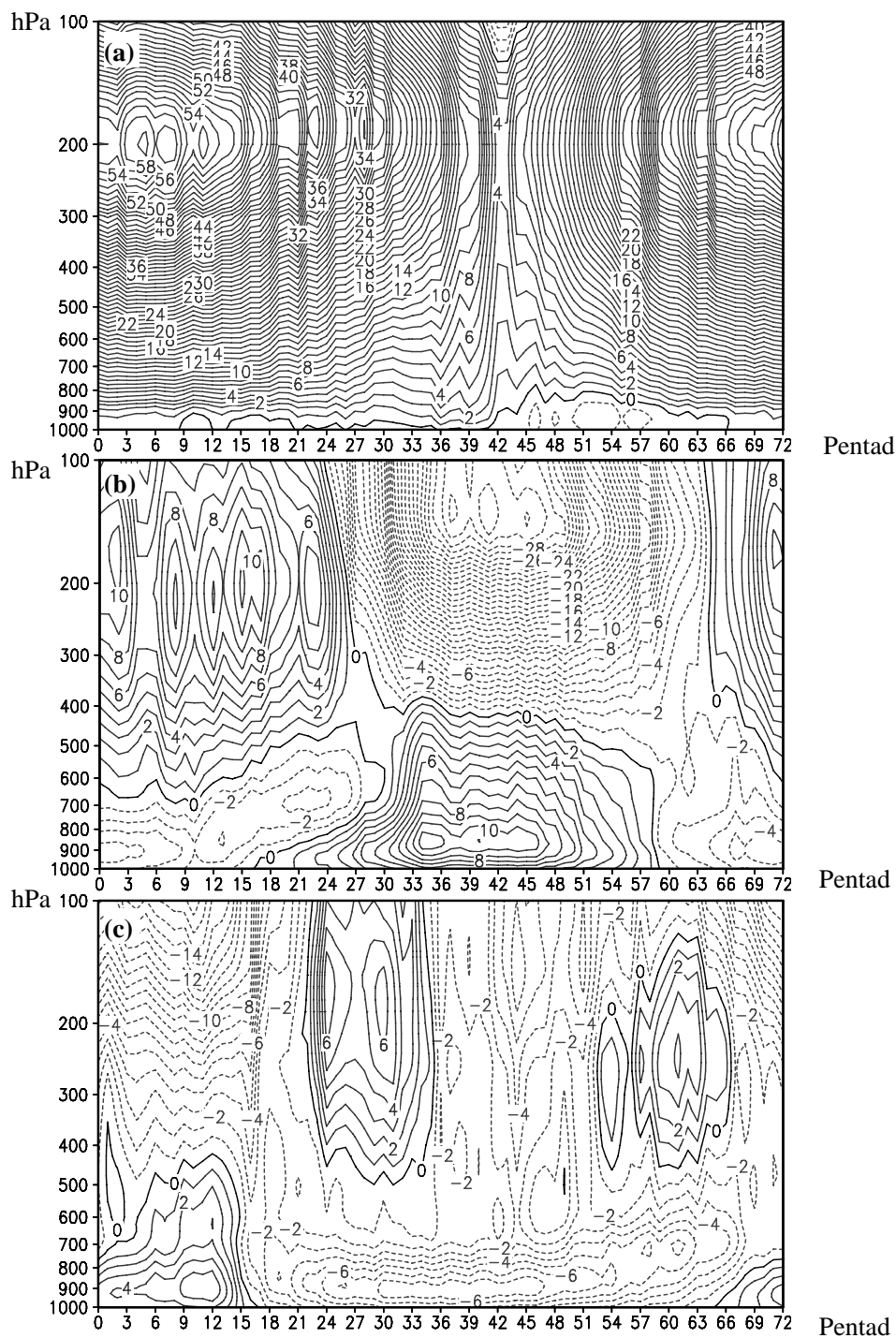


Figure 1

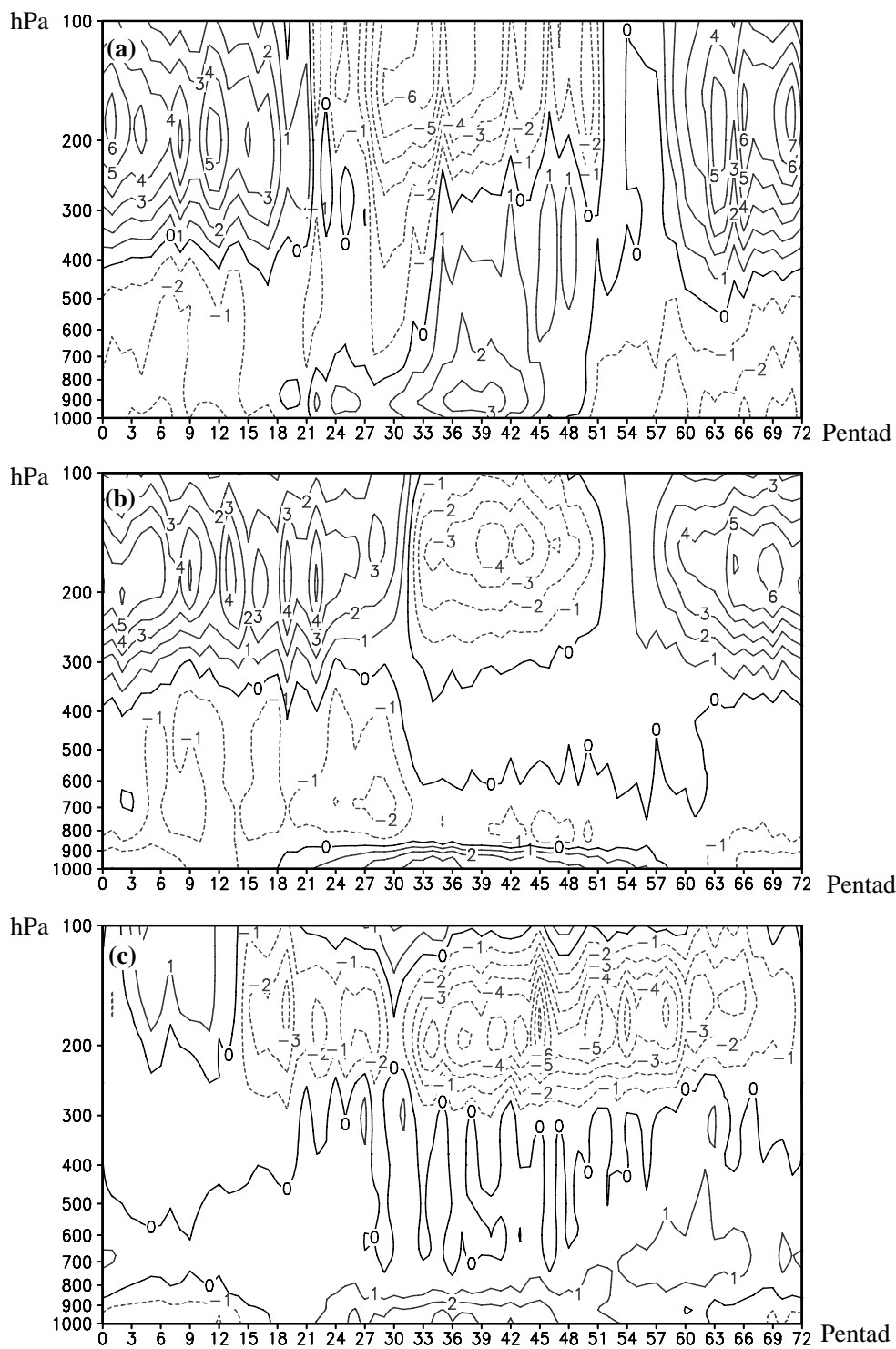


Figure 2

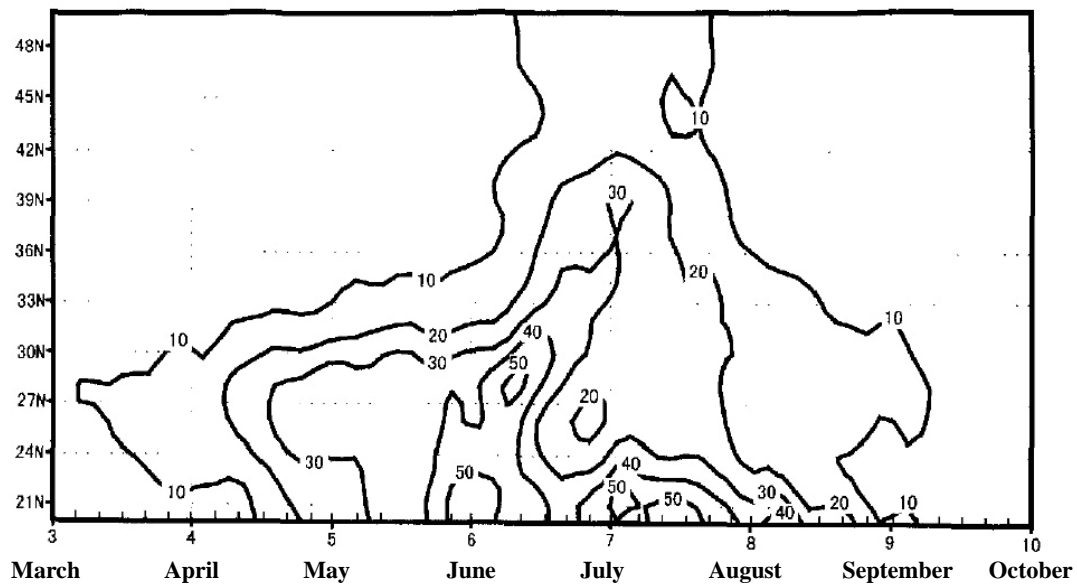


Figure 3

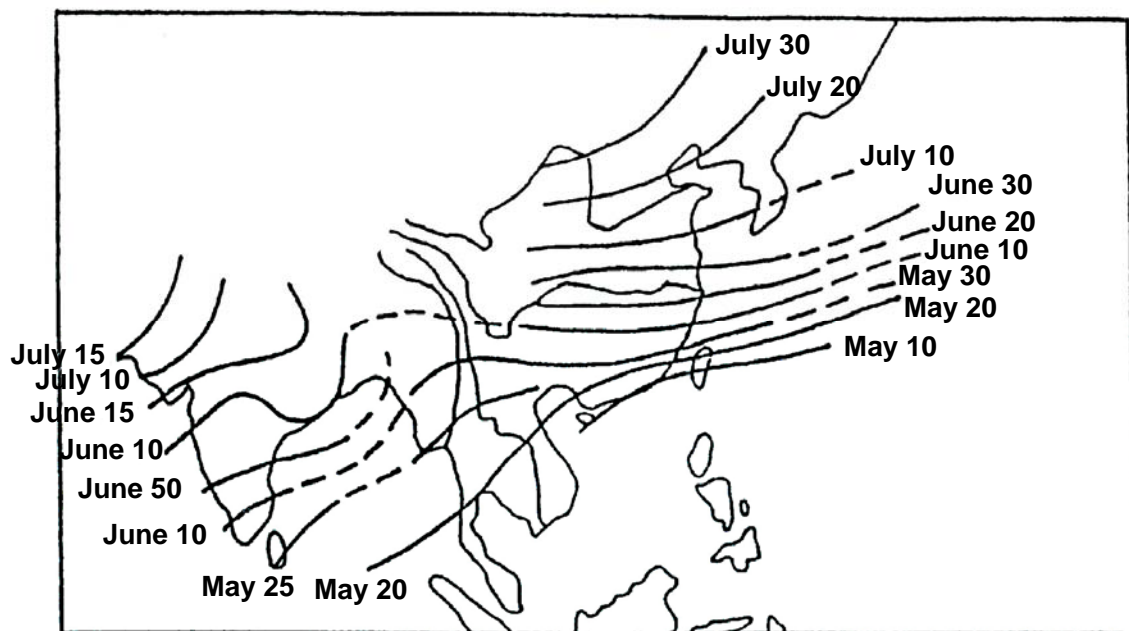


Figure 4

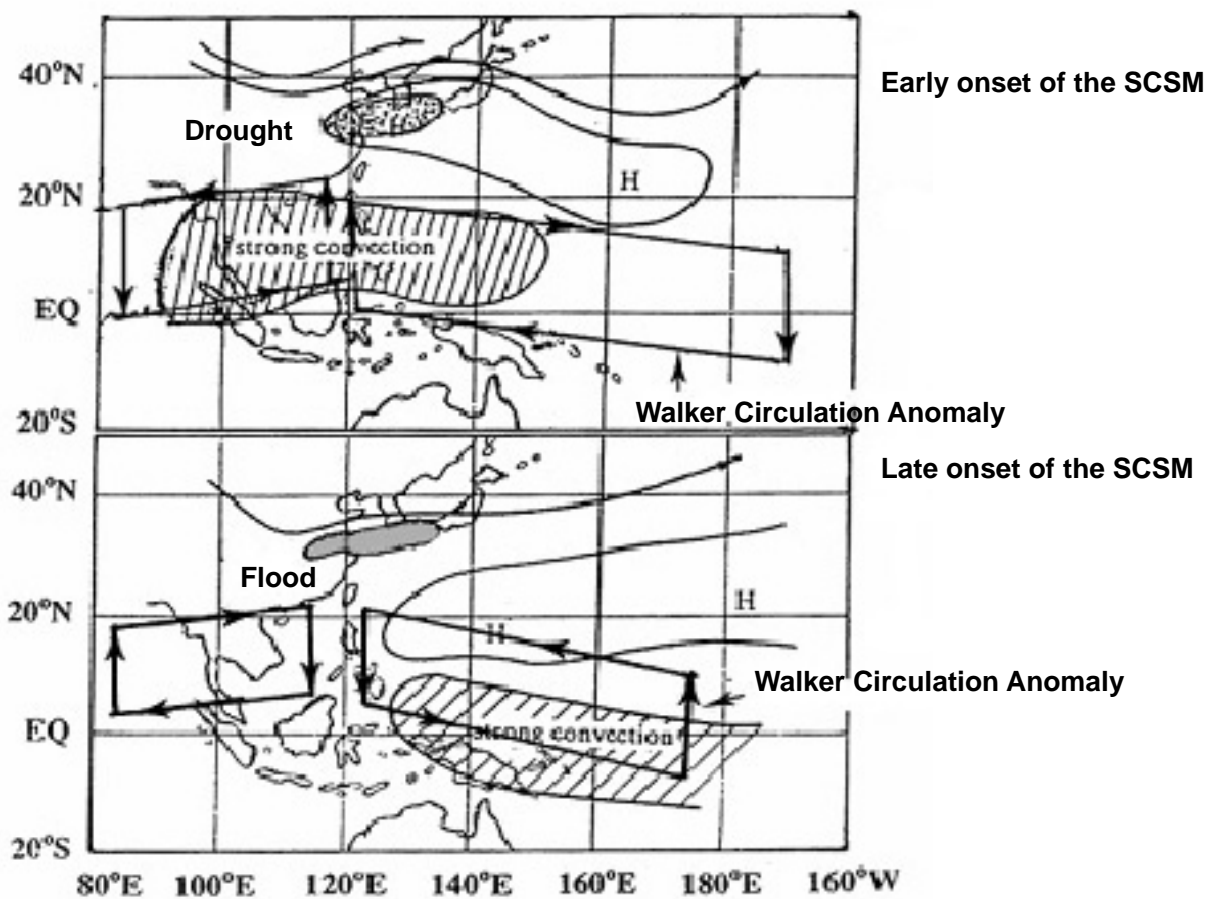


Figure 5

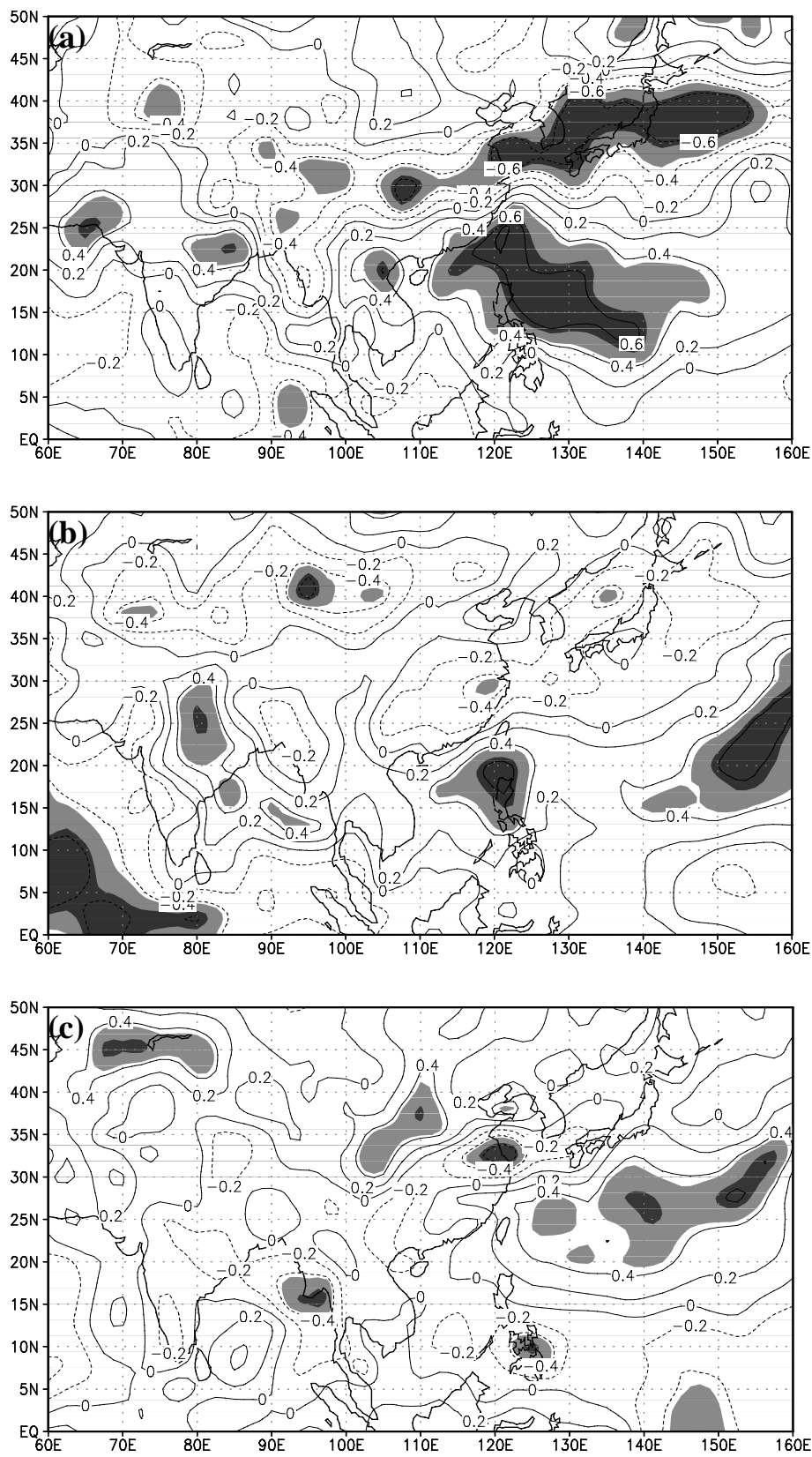


Figure 6

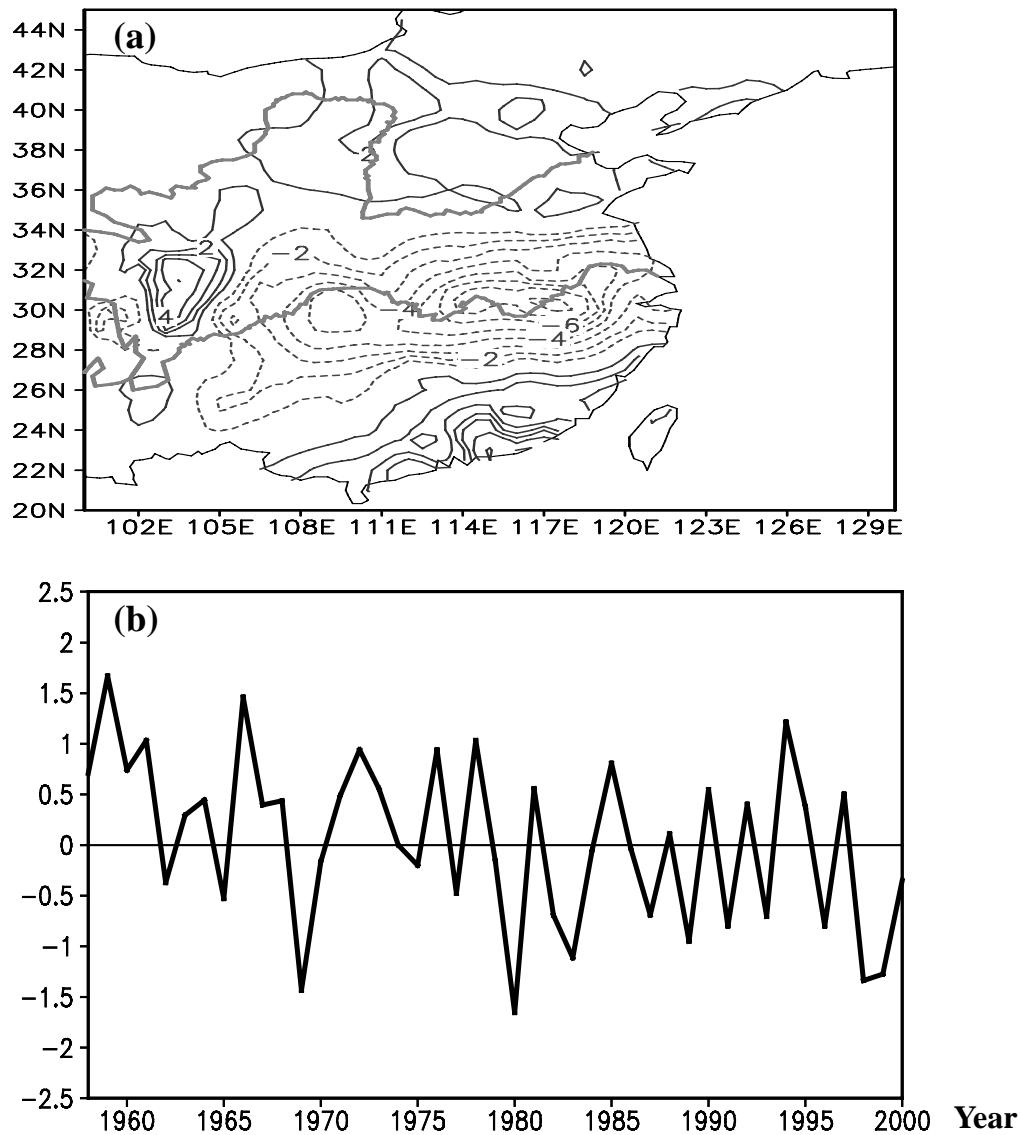


Figure 7

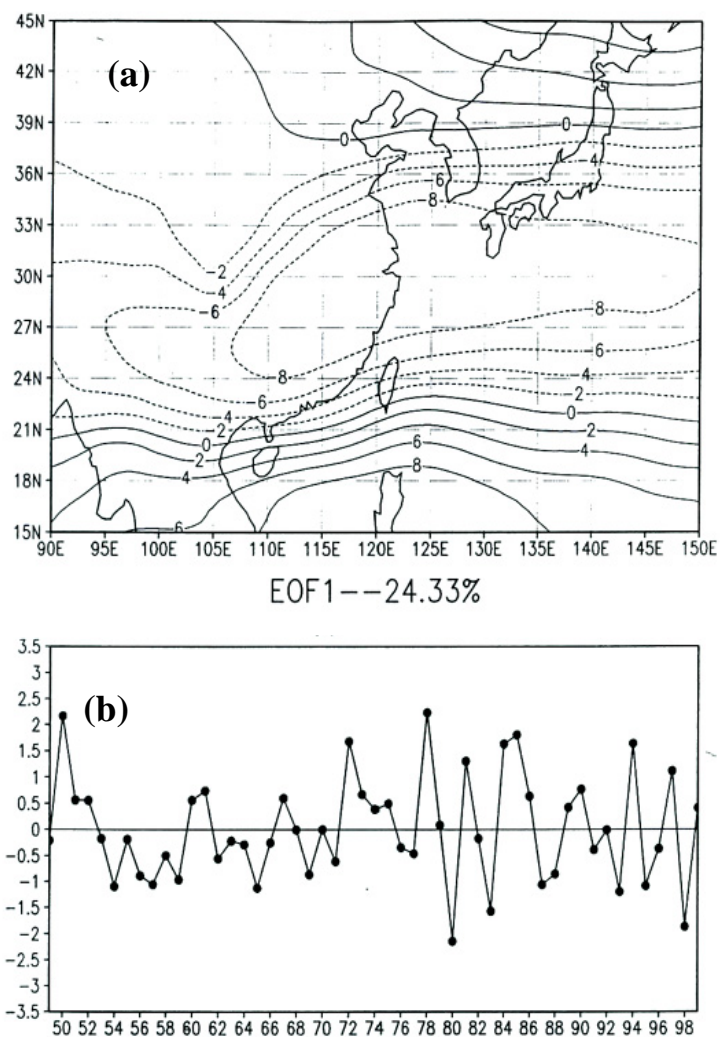


Figure 8

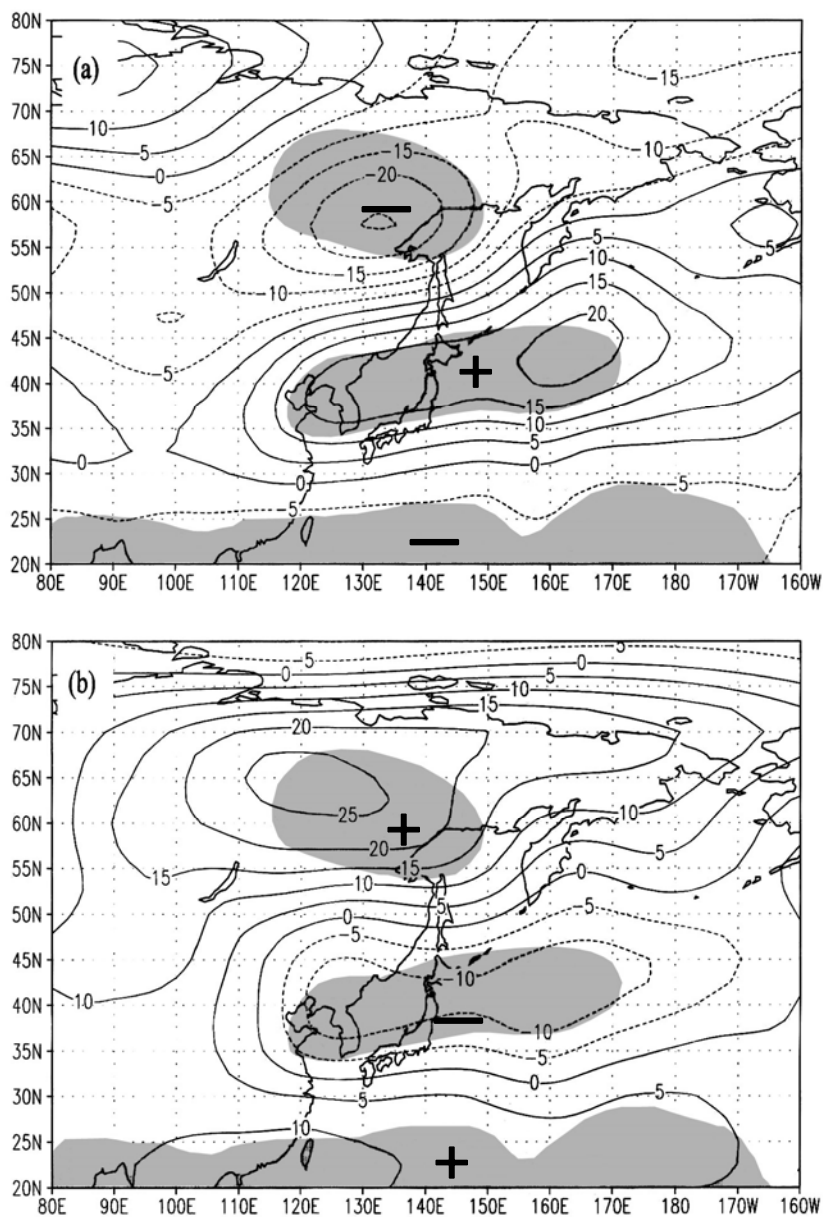


Figure 9

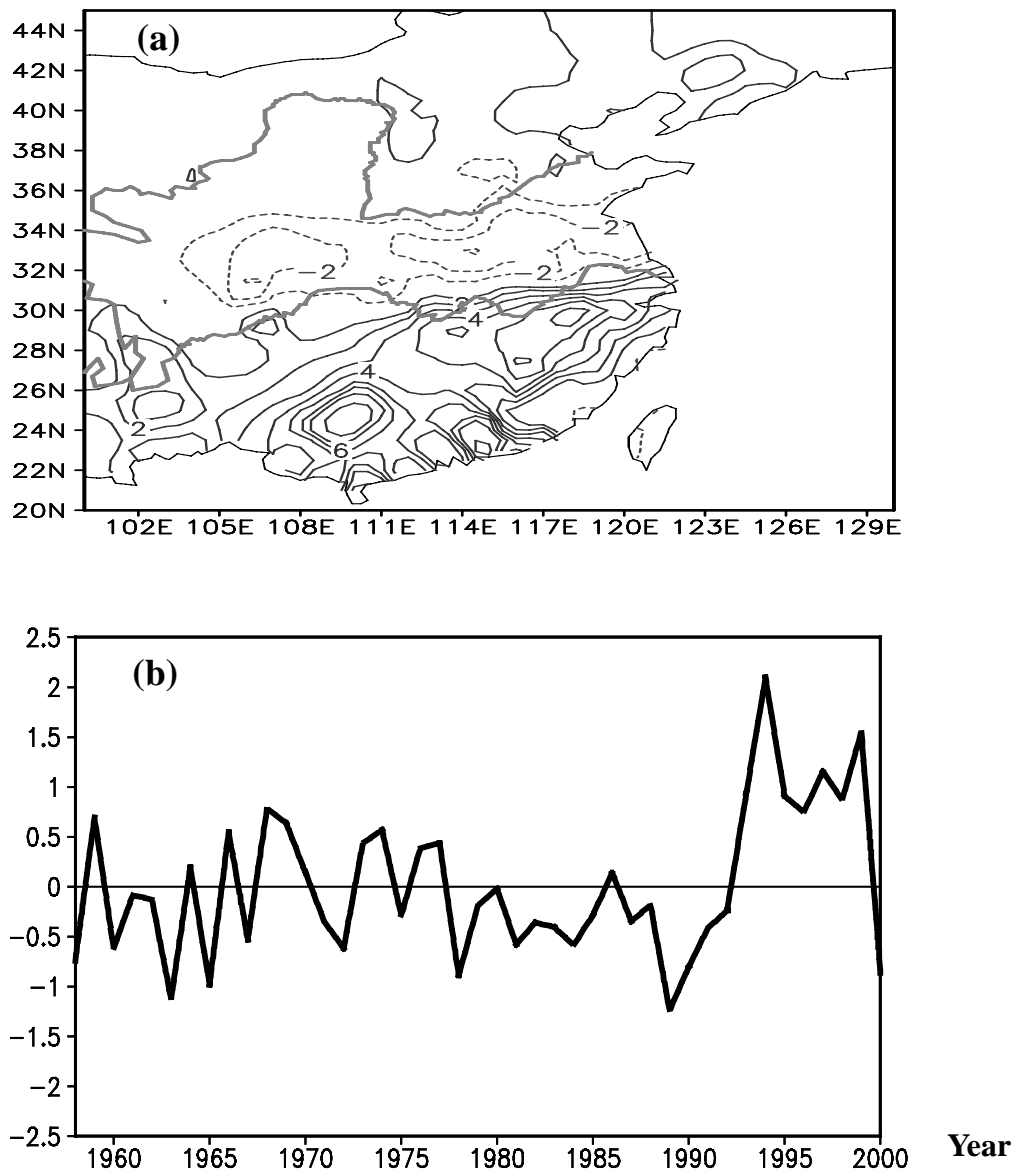


Figure 10

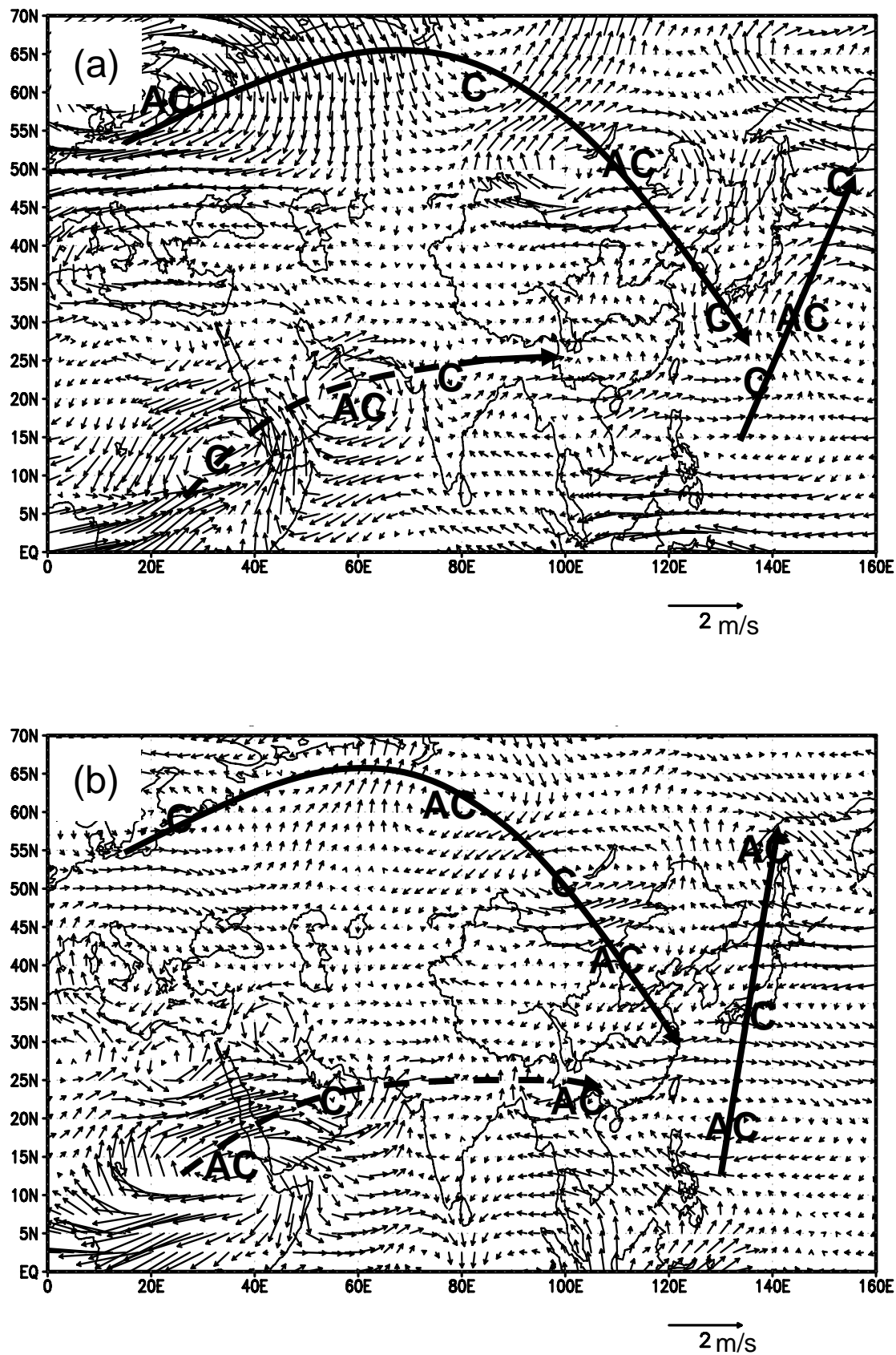


Figure 11

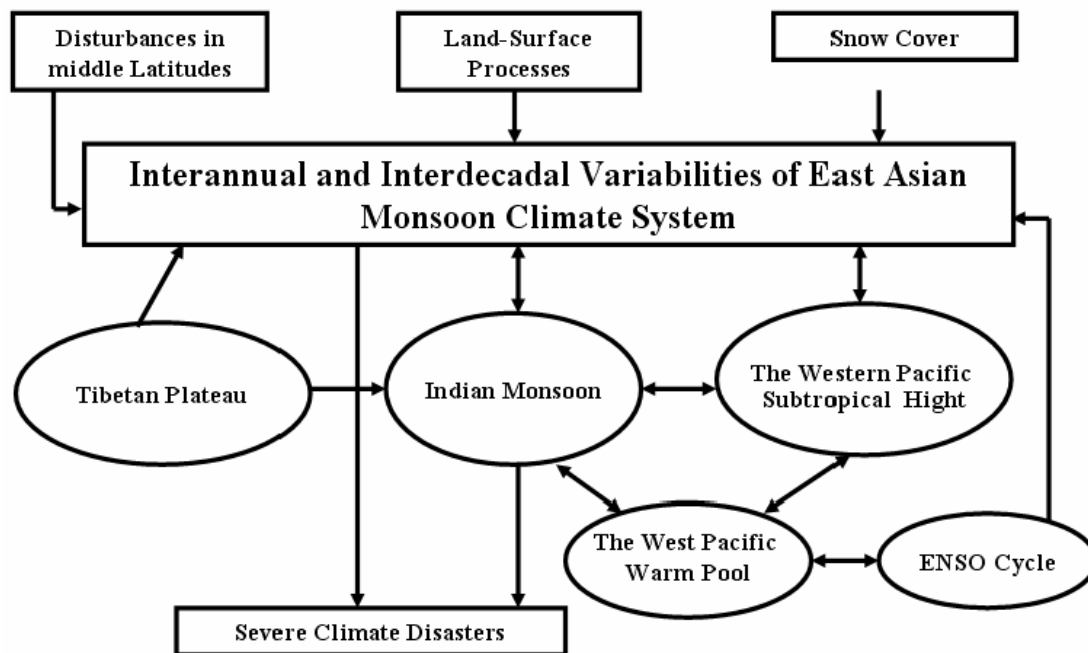


Figure 12

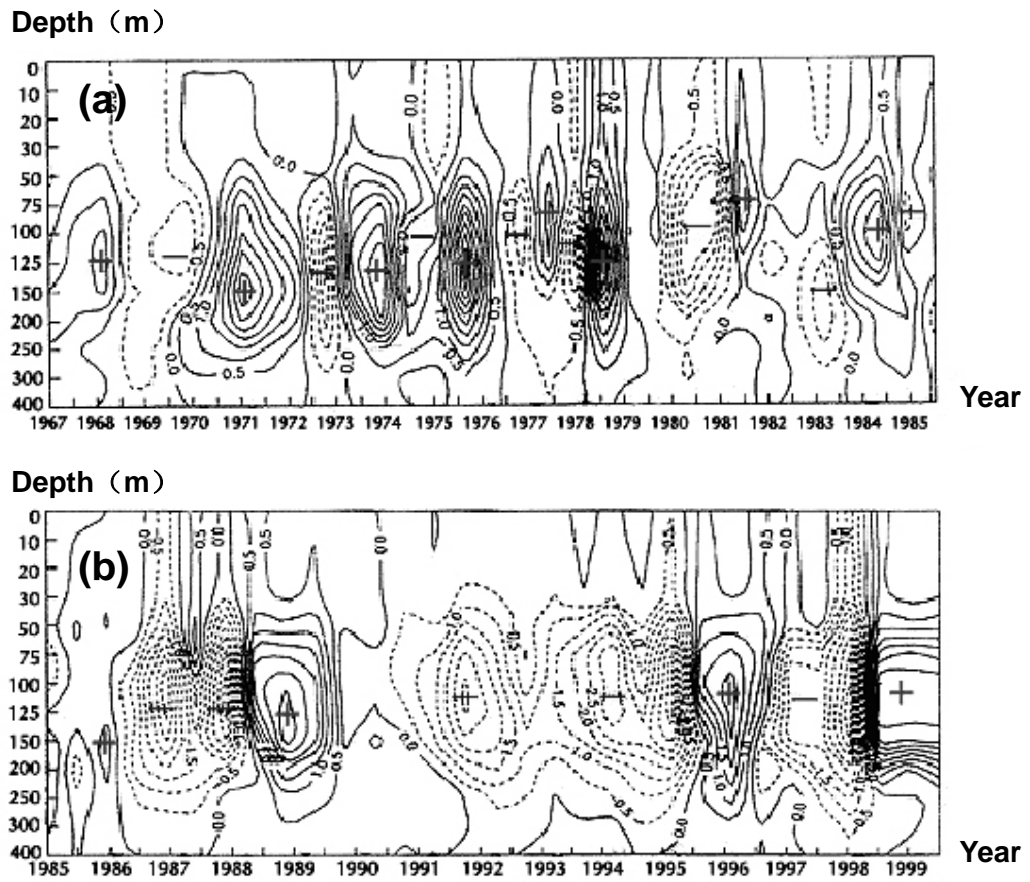


Figure 13

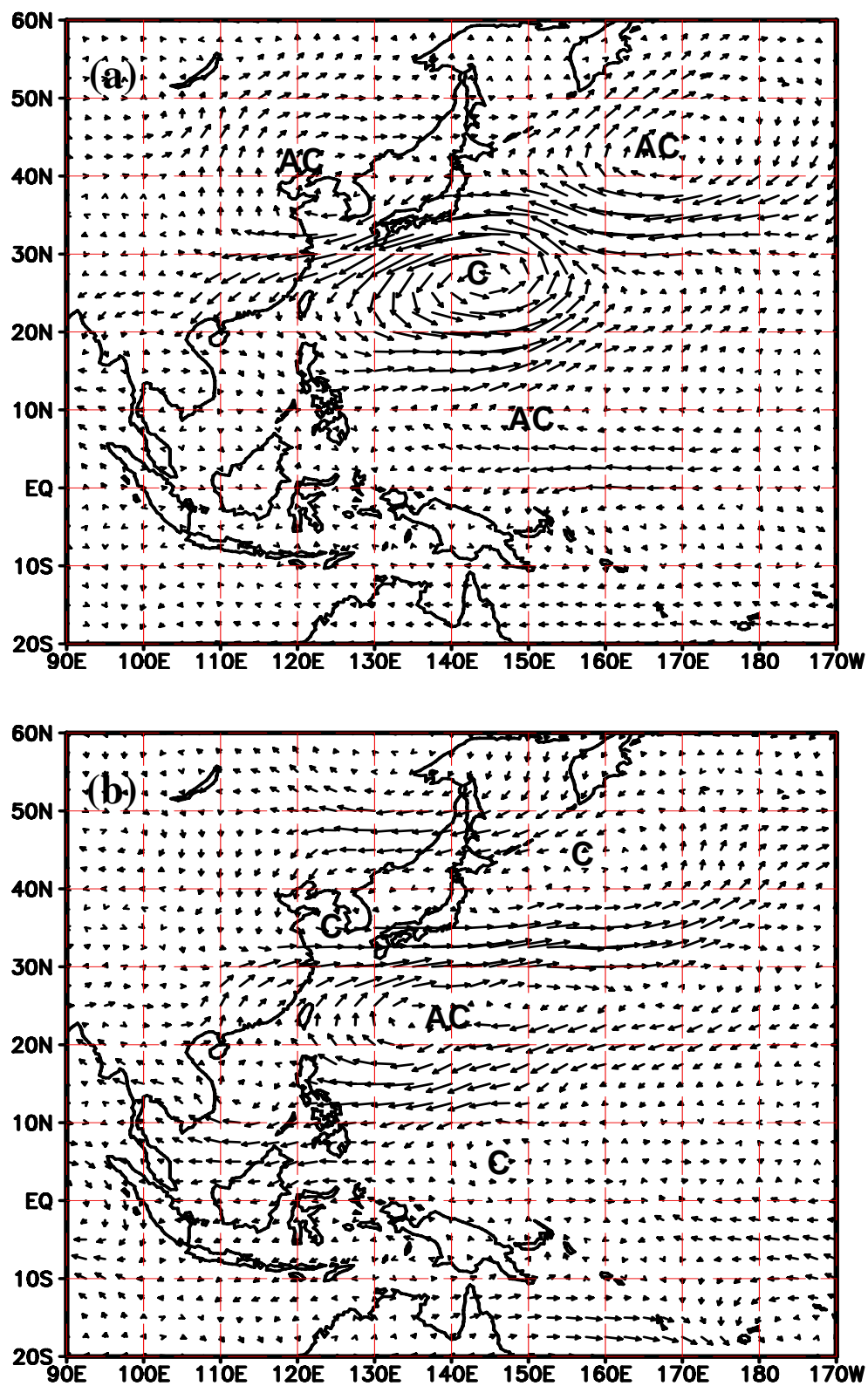


Figure 14

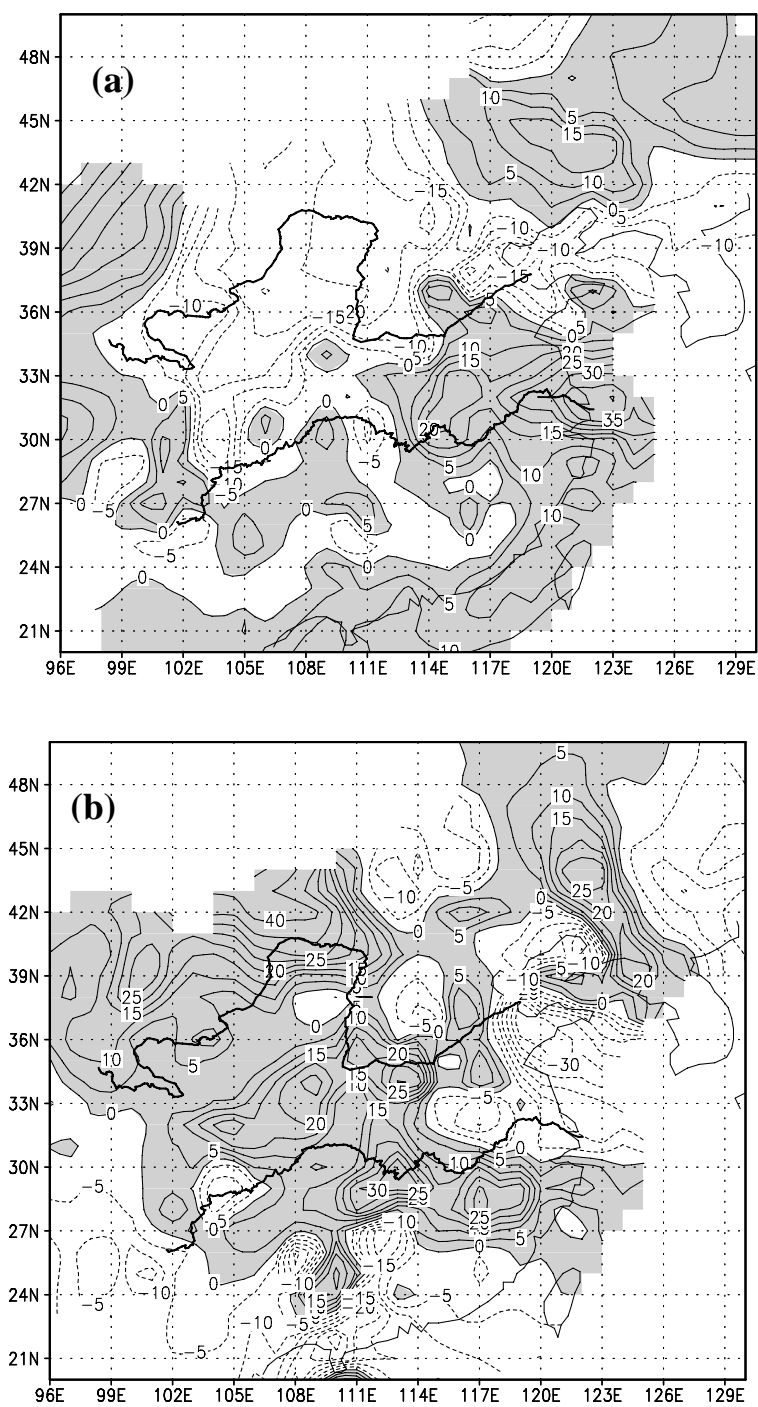


Figure 15

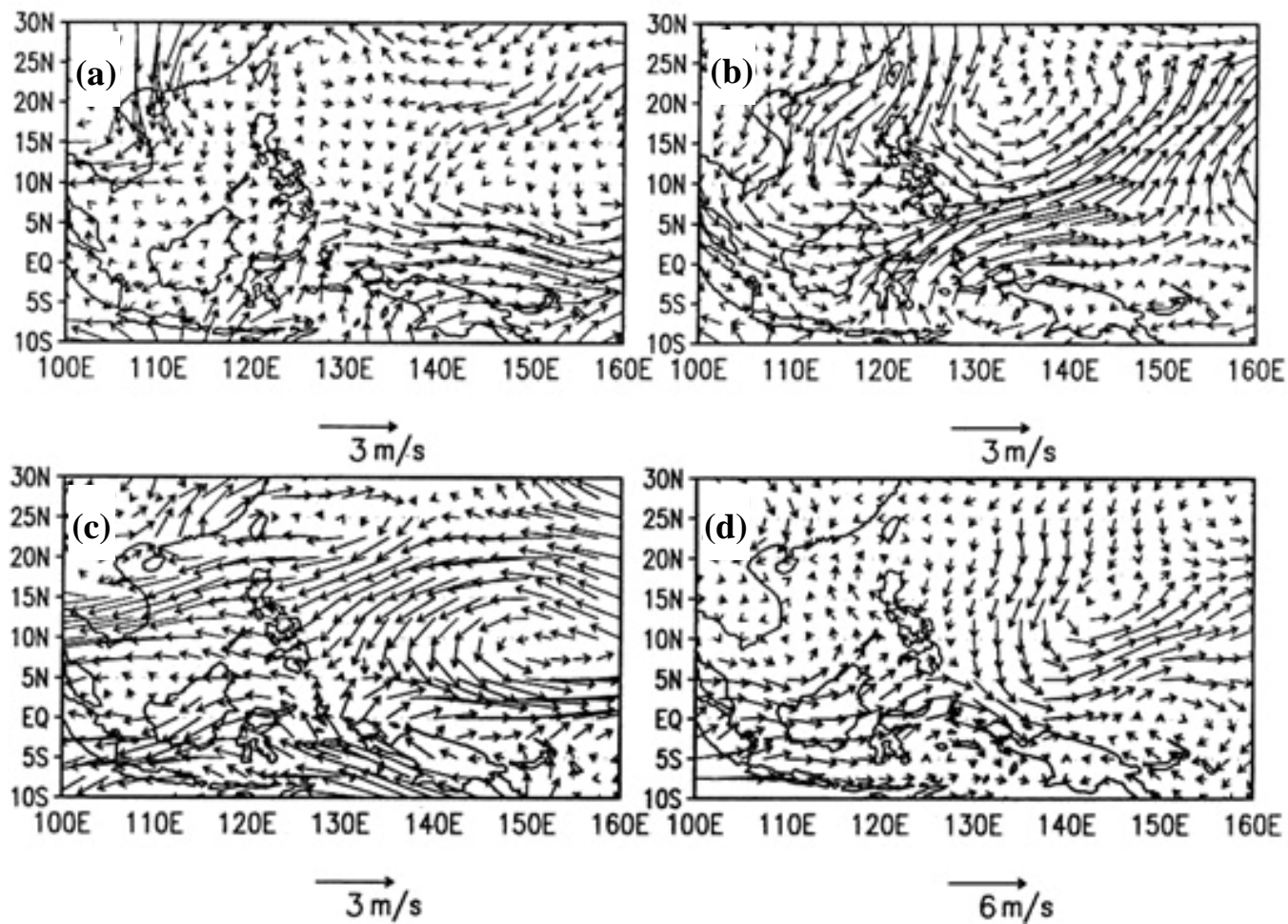


Figure 16

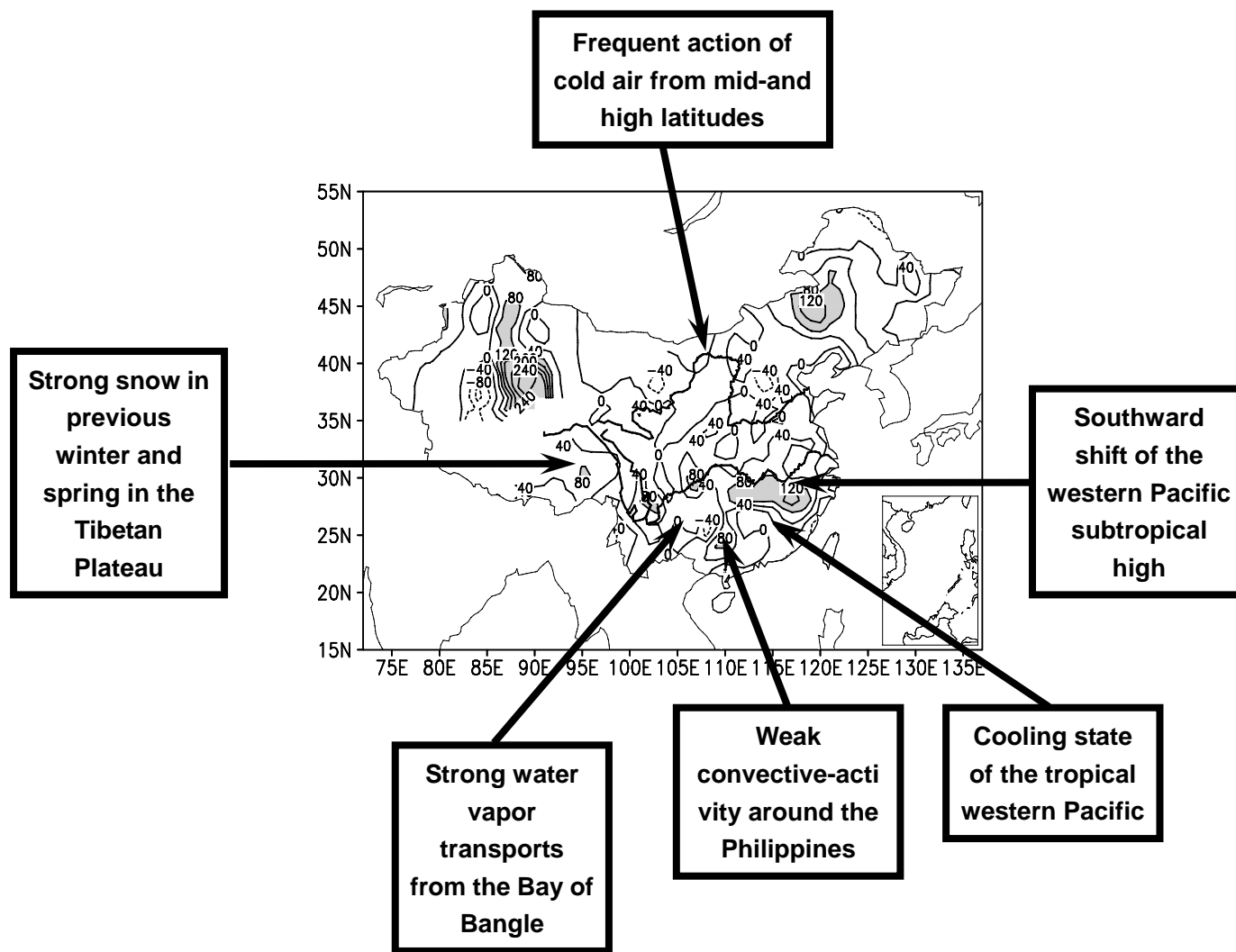


Figure 17

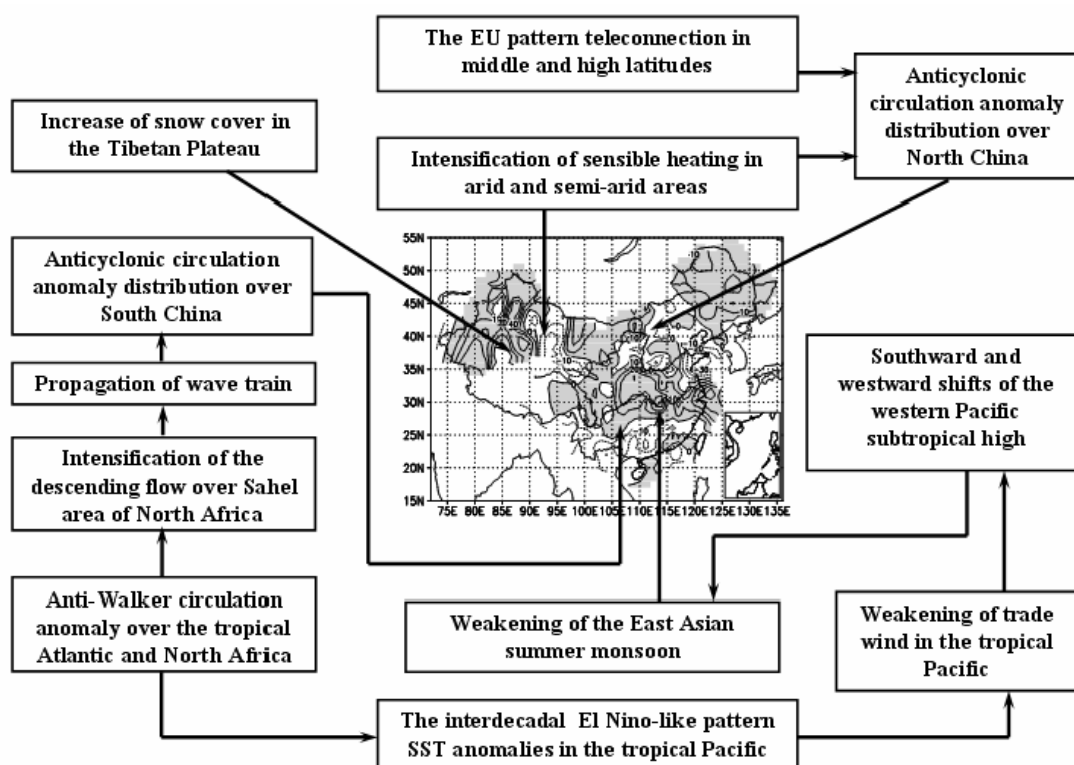


Figure 18

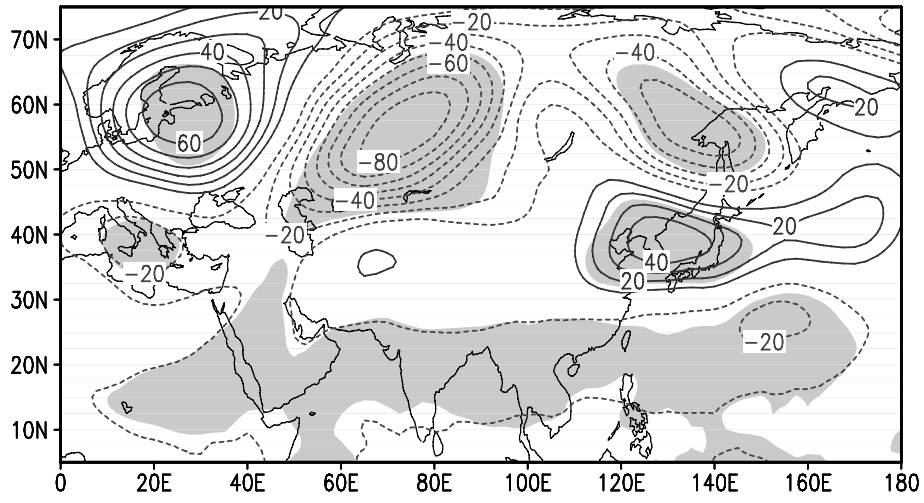


Figure 19

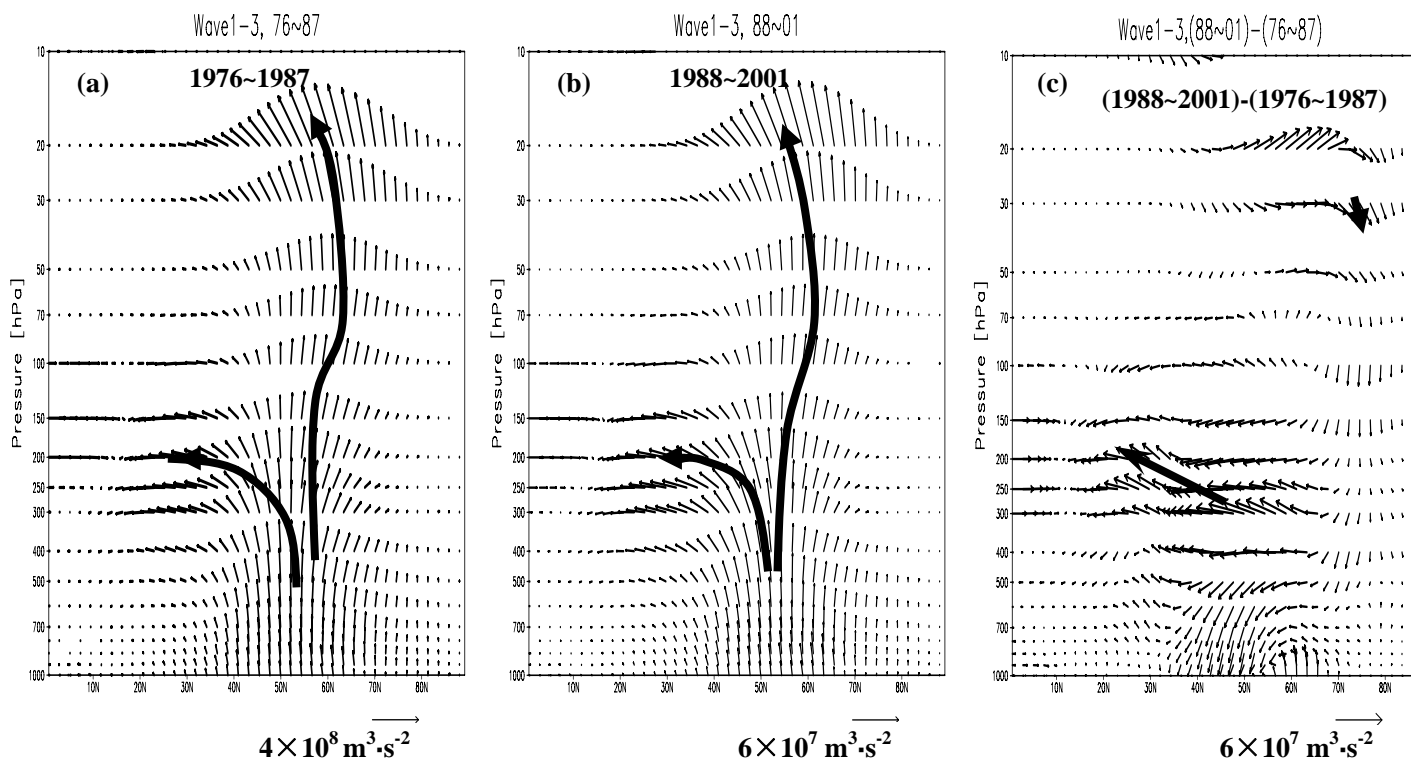


Figure 20

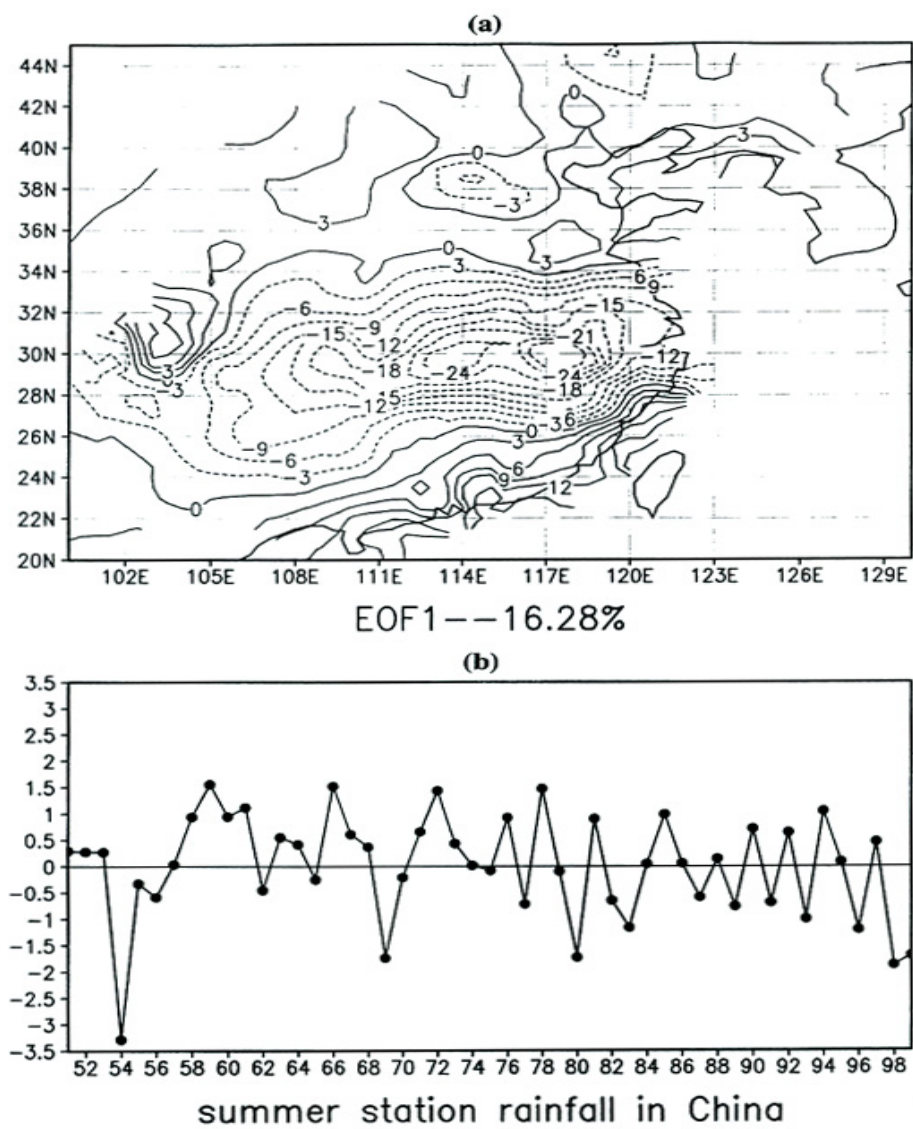


Figure 7

CLIMATE CHANGE DURING THE HOLOCENE IN CHINA

Ge Quansheng¹, Wang Shaowu², Wen Xinyu², and Hao Zhixin¹

1. Institute of Geographical Sciences and Natural Resources Research, Chinese Academy of Sciences,
Beijing 100101, China;

2. Department of Atmospheric Science, School of Physics, Peking University, Beijing, 100871, China

E-mail: haozx@igsnr.ac.cn

Abstract: The climate change characteristics in China were described during the Holocene period, with reviewing published climatic change research references for the recent decades. The main conclusions were as follows: At the Holocene time scale, the climate of the Holocene was unstable, generally warm is the main characteristics, and the Megathermal was the warmest period of the Holocene in China, but a series of cold events occurred in 8.7-8.5 kaBP, 7.3 kaBP, 5.5kaBP and 4.0 kaBP; At the last 2000 years time scale, a warming trend in the 20th century was clearly detected, but from the several reconstructed series, the warming magnitude was less than the maximum level, which occurred in the last 2000 years; the dry/wet spatial pattern has significant regional difference in Eastern China, which not only caused that the dry/wet trend in the Yangze and Huaihe valley was opposite with that in the North China, but also changed the dry/wet difference spatial pattern during the last 2000 years; At the centennial time scale, the modern warm period lasted till now only about twenty years from 1987 to 2006; Bi-decadal oscillation for the precipitation was dominated over China during the 20th Century.

Key words: Proxy data, Climate change, Holocene, China

It is now widely accepted that increasing concentrations of greenhouse gases in the atmosphere are causing higher global atmospheric temperature. However, there is still a great deal of uncertainty about the variability of temperature and precipitation, and what driving the climate change, etc. While, the climate change not only has synchronization phenomenon with global scale, but also has significant regional difference. How does the climate change during the Holocene in China? The Chinese scholars are dedicated to the historical climate research and

progress in the methodology, theory and application of natural proxy data has been rapid over recent decades. The limited space available here is used to review some recent research with more immediate relevance for “unique climate change” in China studies. That is taken to mean work concerned with long series, new ideas and large spatial data sets. This review concentrates on the three stages---Holocene, 2000 years and after 1880 (Meteorological instrumental records), based on the focused time scale in their research papers.

1. Climate of the Holocene

Palaeoclimate records indicated that the Holocene began at 11.5kaBP of calendar years (Cal) over land areas, especially over the Northern Hemisphere, which was corresponding to about 10.0kaBP of ^{14}C years. Palaeoclimate data of China showed similar result, and the beginning of the Holocene can be estimated from the ending of the Younger Dryas (short for “YD”) (Wang et al.,1994; Wang et al.,1996; Yang et al.,1997). The climate of the Holocene in China was generally warm, which was the main characteristics of the climate during the inter-glacial period. Shi et al. (1992) has indicated that, the Megathermal was the warmest period of the Holocene in China, which appeared between 8.5-3.0 ka BP from pollen data and other proxy data. It has been found that temperature in the Megathermal was 1-5°C higher than the present. Temperature difference between the Megathermal and the present was 3-4°C in northern China and 1-2°C in southeastern China. Wang et al. (2001) reconstructed the mean temperature series of China for the last 10ka with 250a time resolution, using area weighted average of 10 regional series. It showed that temperature in 7.5-7.0 kaBP and 6.0 kaBP was 2°C higher than the present. This reconstruction was carried out mainly based on pollen data (Shi et al., 1992), which was also used by Shi et al. (1992). Small temperature difference was found between Wang et al. (2001) and Shi et al. (1992), which was related with the reconstructed technique. Temperature difference averaged for whole China (Wang et al., 2001) should be less than the single regional maximum (Shi et al. 1992), for the timing of occurrence of the maximum temperature at the different regions.

It is worth noting that all of the results by Shi et al. (1992) and Wang et al. (2001) were mainly obtained from pollen data; the chronology of which was constructed using ^{14}C years without correction with tree-ring data. Therefore, the real timing (calendar years) should be shifted to an earlier date than the ^{14}C years, for example, from 0.5 ka to 1.0ka in early Holocene. The

conclusion of the Megathermal by Shi et al. (1992) is generally accepted in China. However, data of ice core indicated that the warmest period in western China may occur before 7.0kaBP (Cal) (Thompson et al. 1997). It manifests the diversity of the timing of the warming in mid-Holocene over China.

Shi et al. (1992) have claimed that climate of the Holocene was in general wet. This conclusion was supported by a series of pollen, lake level, and loess data. Recently, it was challenged by the studies, which provided high-resolution palaeoclimate records. The new series showed reduction of effective wetness over Inner-Mongolian Plateau (Table 1 and Fig.1) in the mid-Holocene.

An (2000) found that maximum increment of precipitation occurred at 9kaBP, 6kaBP, and 3kaBP in North China, Changjiang River Valley and Zhujiang River Valley respectively. An et al. (2000) later detailed the picture of precipitation variations in the mid-Holocene over China, by analyzing proxy data from 45 places, which covered the mainland of the country. It has been indicated that maximum increment of precipitation was found in 10-7 kaBP over North China, and 7-5 kaBP along the Changjiang River Valley. An's study supported the conclusion of reduction of wetness in Central North China, where the precipitation is usually low when the summer monsoon is weak, while the precipitation is often concentrated along the Changjiang River Valley. However, reduction of wetness does not necessarily mean the decreasing of precipitation. Persistent warming significantly increases the evaporation over the arid and semi-arid zones, and then reduces the wetness to a great extent.

Table 1 Evidence of climate aridity in Central North China during mid-Holocene

No	Place	Lat., Long.	Timing	Author
1	Midiwan	38°N, 108°E	7.5-3.5 (Cal)	Zhou et al., 1996
2	Tengger Desert	38°N, 104°E	7.0-5.6 (¹⁴ C)	Guo et al., 2000
3	Guan Zhong	34°N, 108°E	6.8-5.7 (Cal)	Huang et al., 2000
4	Qinghai Lake	37°N, 100°E	8.0-3.0 (¹⁴ C)	An, 2000; An et al., 2000
5	Dali Nor	43°N, 116°E	5.6-4.5 (Cal)	Wang et al., 2001
6	Lake Yanhaizi	40°N 108°E	8.0-4.3 (¹⁴ C)	Chen C.-T. et al., 2003
7	Zhuyeze Lake	39°N, 103°E	7.5-5.0 (Cal)	Chen et al. 2003

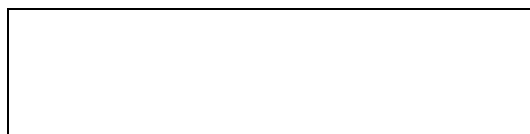


Fig.1. $\delta^{18}\text{O}$ in Guliya (1), simple pollen diversity (2), total pollen concentration (3) and upland pollen concentration (4), in Zhuyeze Lake, after Chen Fahu et al. 2003.

The address of millennial scale of cold events in the Holocene is one of the main results in climate studies of the last 10 years. Bond et al. (1997) constructed a typical chronology of cold events over the North Atlantic according to the percentage of hematite-stained grains, numbering the cold events as 0 to 8. The Little Ice Age was referred as 0 and that at the very beginning of the Holocene as 8 (Table 2). Shi et al. (1992) have indicated that the climate of China in the Holocene was unstable, and a series of cold events occurred in 8.7-8.5 kaBP, 7.3 kaBP, 5.5kaBP and 4.0 kaBP. It was nearly identical to the chronology of 6th –3rd cold events (^{14}C) exhibited by Bond et al. (1997) five years later. The cold events are manifested well in ice core data in China, the chronology (Cal) of which is quite similar to that over the North Atlantic (Table 2). Cold events occurred with a failure of summer monsoon in many places of China. Exception is found in Northeast China, where monsoon rainfall increased when cold events occurred.

Table 2 Cold events over the North Atlantic and monsoon failures in China (ka BP, Cal)

region	climate	0	1	2	3	4	5	6	7	8	Authors
North Atlantic	Cold	0.4	1.4	2.8	4.3	5.9	8.2	9.5	10.3	11.1	Bond et al., 1997
Qinghai-Tibetan Plateau	Cold	0.9	1.7	3.4	4.0	5.5	8.3	9.0	10.1	11.2	Thompson et al., 1997
Qilian Mountain	Cold	0.4	1.5	3.0	4.0	5.2	8.8	9.7			Yao et al., 1992
Inner-Mongolia	Dry	0.4	1.7	3.0	4.2	6.0	8.6	9.3	10.5	11.4	Chen et al., 2003
Zoigê	Dry	0.3	1.5	2.8	4.4	5.9	8.2	9.5	10.2	11.3	Zhou et al., 2002
Hongyuan	Dry	0.3	1.5	2.8	4.1	5.9	8.3	9.5	10.4	11.2	Hong et al., 2005
South China Sea	Dry	0.3	1.2	3.1	4.3	6.0	8.3	9.5			Wang et al., 1999
Northeast China	Wet	0.3	1.5	2.8	4.3	5.9	8.4	9.7	10.4	11.4	Hong et al., 2005

Except for the reconstructed data, an atmospheric general circulation model (AGCM) and an oceanic general circulation model (OGCM) were asynchronously coupled to simulate the climate of the mid-Holocene period. The role of the solar radiation and ocean in the mid-Holocene East Asian monsoon climate was analyzed, and some mechanisms were revealed. At the forcing of changed solar radiation induced by the changed orbital parameters and the changed SST simulated by the OGCM, compared with when there was orbital forcing alone, there was more precipitation and the monsoon was stronger in the summer of East Asia, and the winter temperature increased over China. These agree better with the reconstructed data (Wei and Wang, 2004).

2. Climate change during the last 2000 years

The past 2000 years is a very important timespan for studying the climate change, and within this timespan, the human activities are impacting the earth system, as well the written records and natural archives reflecting the environmental change information are co-existing. More importantly, recognizing the climate change history of the past 2000 years is the basis to estimate the environmental change trend during the next several decades, even up to centuries, and therefore climatic change during the past 2000 years is one of the two highlights for PAGES (Eddy, 1992). The science assessment reports by IPCC (Intergovernmental Panel on Climate Change) are paying more attentions to the period of past 2000 years for objectively understanding the climate change (IPCC, 1990; 1992; 1996; 2001).

2.1 Temperature (Cold/Warm)

Chu (1973) was the first to use a variety of sources to reconstruct temperature variation in China for the past 5000 years. Since then, many studies have been conducted using a variety of data sources and methodologies to reconstruct the temperature change series, with different timespans and resolutions (Zhang, 1980; Wang et al., 1990; 1991; Zheng and Zheng, 1993), but most of them only focused on the past 1000 years. However, the temperature series by the different researchers cannot be compared with one another, because of the different proxy-data, reconstruction methods and different studied regions. After that, Wang et al. (1998a and 2000a) constructed the temperature series in the whole China, Eastern and Western part with the same criteria, calculated by the linear regression and area-weighted average, based on the published homogenous temperature series before. But limited by the available proxy data, these

reconstructed series only can reach up to 1200 years length and 50 years time resolution, which cannot show the detailed temperature change during the last 2000 years completely. Recently, the research on temperature reconstruction has made a noticeable and exciting improvement. Yang et al. (2002) established China-wide temperature composites at 10-years' resolution covering the last 2000 years by combining multiple paleoclimate proxy records obtained from ice cores, tree rings, lake sediments and historical documents; Five periods of temperature variation can be identified: a warm stage in AD 0-240, a cold interval between AD 240 and 800, a return to warm conditions from AD 800-1400, including the Medieval Warm Period between AD 900-1300, the cool Little Ice Age period between 1400-1920, and the present warm stage since 1920. The temperature reconstructions for China and the Northern Hemisphere showed good agreement over the past millennium.

Meanwhile, Tan et al. (2003,2004) reconstructed a 2650-year (BC665-AD1985) warm season (MJJJA: May, June, July, August) temperature series, derived from a correlation between thickness variations in annual layers of a stalagmite from Shihua Cave, Beijing, China and instrumental meteorological records. Their reconstruction revealed that centennial-scale rapid warming was occurred repeatedly following multicentennial cooling trends during the last millennia. The comparison between warm season warm record and long-term yearly-reconstructed total solar irradiance suggested that the sun may directly couple hemispherical climate changes on centennial to millennial scales.

Ge et al. (2002) reconstructed winter half-year (October to April) temperatures, at 10–30 years' resolution, for the past 2000 years in the central region of eastern China, extracting from phenological cold/warm events recorded in Chinese historical documents. Because of the uneven spatial and temporal distribution of the phenological records, the reconstruction of the regional mean temperature involves two steps: reconstruction for individual sites within the region and calculation of the regional mean. For a single site, the reconstruction involves: identifying the difference in dates in phenological events for both historical and modern records; establishing the conversion function between the date difference and temperature change from the modern records; and converting the historical records into temperature variation. The spatial representativeness of the individual sites was studied by examining the correlation between individual sites and regional mean temperature from modern instrumental data. The correlation was then used as the basis for

constructing the regional mean winter half-year temperature for the past 2000 years. From the beginning of the Christian era, climate became cooler at a rate of 0.17°C per century, and around the AD 490s temperature reached about 1°C lower than that of the present (the 1951-80 mean). Then, abruptly, temperature entered a warm epoch from the AD 570s to 1310s with a warming trend of 0.04°C per century; the peak warming was about $0.3\text{-}0.6^{\circ}\text{C}$ higher than present for 30-year periods, while a maximum warming of 0.9°C occurred during the AD 1230s-1250s and 0.7°C occurred during the AD 1260s-1280s. After the AD 1310s, temperature decreased rapidly at a rate of 0.10°C per century; the mean temperatures of the four cold troughs were $0.6\text{-}0.9^{\circ}\text{C}$ lower than the present, with the coldest value 1.1°C lower. Temperature has been rising rapidly during the twentieth century, especially for the period 1981-99, and the mean temperature is now 0.5°C higher than for 1951-80, in the third place, which at least means that the warming at the twentieth century is not the only one during the last 2000 years. Compared with the previous studies, indices with much more definite physical implications have been adopted in the newly reconstructed sequences, and the conversion of information is based on modern statistical relations, which greatly reduce subjectivities and uncertainties, and represent the up-to-date synthesis idea of global change studies.

Ge et al's work synthesized the methods and results on historical temperature changes over the eastern China conducted by many other researchers, but in western China, a comprehensive analysis of proxy records, like ice cores, tree rings and lake sediments, has not to be published until Yang et al. (2003) constructed the relative amplitude of temperature change at 50-year time resolution on the Tibetan Plateau. The results showed that the Tibetan Plateau experienced climatic episodes such as the warm intervals during AD 800-1100 and 1150-1400, the "Little Ice Age" between AD 1400 and 1900, and an earlier cold period between the 4th and 6th centuries.

Figure 2 compared the temperature reconstruction results over the last 2000 years for Beijing, Eastern China, the Tibetan Plateau (covering most of the western China) and the whole China described series above. The correlation at 30-year resolution between b and d series is 0.47, which suggested that the significant climate variations might have been reflected in both of them. For example, at the period of 250s-570s, the temperature is lower than 0°C reference anomaly value, alternated with the increasing and decreasing trend. After this period, the temperature is increasing rapidly, and higher than 0°C . The similar climate change trend and characteristics are presented at

the period of 1100-1300, but the famous Medieval Warm Period (900-1300 AD, Mann et al, 2002) seems not so evident in China as a whole, even the warming peak is lower than the period of 150s-250s, while the warming during 1230s-1280s might have been higher than any decades of the 20th century in eastern China. For the Little Ice Age, the two of series are both marked with coldness during the period of 1400-1900. Also, we compared the temperature change in western China with that in the whole China, and the notable similarities were presented at the two periods of 50-550AD and 1400-2000 AD, the Medieval Warm Period is not shown in western China at 2000a time scale as well. Moreover, it is worth noted that Beijing lies in eastern China, but very few consistent temperature variation is described between the two series of a and b at centennial or 30-year scale, due to the covered small spatial region.



Fig. 2. The reconstructed temperature series during the last 2000 years in China derived from various historical climate proxy data. (a) summer temperature (May-Aug.) in Beijing by Tan et al.(2003), line: annual temperature, bar: temperature change with 30-year resolution; (b) Winter half year temperature in Eastern China at 30-year time resolution by Ge et al.(2003); (c) temperature change at 50-year resolution in whole Tibet Plateau by Yang et al.(2003); (d) Weighted temperature reconstruction over China by Yang et al(2002), line: 10-year resolution, bar: 30-year resolution.

2.2 Precipitation (Dry/Wet)

During the historical times, existing high-resolution proxy data archives, such as tree rings, ice core, speleothems, and historical records have been proven to be useful in determining the intensity and duration of droughts (Zhang, 1988; Cook et al., 1999; Fleitmann et al., 2003). However, tree rings, ice core and speleothems have not been shown to be effective in estimating the spatial coverage of droughts due to their sparse sites, particularly in eastern China, although the former offers some potential in the region with dense tree chronologies, e.g. a drought area index in North America developed by Cook et al. (1997). Chinese historical data, mainly compiled

from county (*Xian*) and district (*Fu* or *Zhou*) gazettes and archives, tends to provide the needed spatial coverage, in addition to the information on intensity and duration, which provided abundant data for studying precipitation change during the last 2000 years. Since 1970s, the Chinese researchers on climate collected government archives and local gazettes, and reconstructed the drought/flood (D/F) index covering 120 stations over the last five centuries, as well as published drought/flood atlas (AMS, 1981). After that, Zhang et al. (1996) made a correction and supplement for D/F index in 1993 and 2003. Followed up on this, the dry/wet series in the six regions of Hebei, Shanxi, Lower of the Yellow River, Henan, Yangze and Huanhe valley, together with Suzhou and Hangzhou were developed, the annual precipitation anomaly pattern gridded $1^{\circ} \times 1^{\circ}$ (latitude \times longitude) was reconstructed as well, covering the eastern china during the last 500 years (Zhang et al, 1997). Based on these series and related records, the drought/flood characteristics and spatial patterns during the last 500-1000 years were studied further (Wang et al, 1993).

Man (Zhang, 1996) reconstructed D/F index in 63 divisions at the period 137BC-1470AD for understanding the precipitation change characteristics during the past 2000 years, then they recalculated the selected 45 stations, where the historical records were relative abundant, by combining with the series of Zhang (1996), and developed the D/F series during the past 2000 years in the eastern China, which covered 45 stations. This combined series was missing a lot of data in the last 1000 years, due to lack of historical documents, but it indeed provides important reference to disclose dry/wet change during the last 2000 years. Based on this series, Zhang and Zheng et al (1994, 1999) analyzed the drought/flood change phases and climate shifts, and the results were presented as: the climate was relative wet before 280s AD, and became drier and drier after 280s AD, until after 1230s AD, the climate lied in a relative dry level. 280s AD and 1230s AD were two important abrupt decades. A more attractive conclusion showed that climate was unstable at the period of 280s-1230s AD, and most of big climate fluctuations and dry/wet transitions were occurred in this time.

Furthermore, the dry/wet spatial pattern has significant regional difference, even in Eastern China (east of 105°E , $25\text{-}40^{\circ}\text{N}$ approximately), which not only caused that the dry/wet trend in the Yangze and Huaihe valley was opposite with that in the North China, but also changed the dry/wet difference spatial pattern during the last 2000 years. On the centennial scale, during the period of

the 2-11th centuries, the spatial pattern of drought/flood in the eastern part of China was characterized by the east (SE,wet)-west (NW, dry) difference demarcated at 115°E, but from the 12th to 15th centuries, the east-west difference coexisted with the south-north difference, and the former was still the dominant pattern; However the dominant spatial pattern changed to the south(wet)-north(dry) difference during 16th-19th centuries demarcated at 35°N(Zheng et al., 2001). Recently, Zheng et al.(2006) reconstructed a proxy precipitation index (Figure 3b) at 1-year high resolution for the period 501-2000 over Eastern China using the same historical documents and definition of dry-wet index, then analyzed the decadal-to-centennial dry/wet variability with focus on three sub-regions, North China Plain (34-40°N approximately), Jiang-Huai Area (31-34°N approximately) and Jiang-Nan Area (25-31°N approximately). On the centennial time scales, the dry/wet variation in eastern China exhibited four dry epochs (500s-870s, 1000s-1230s, 1430s-1530s and 1920s-1990s) and three wet epochs (880s-990s, 1240s-1420s and 1540s-1910s), with multi-decadal dry/wet fluctuations within each epoch. But the variation showed strong regional differences, for example, opposite trends were found in Jiang-Nan Area and Jiang-Huai Area during the 11-13th centuries and in North China Plain and Jiang-Nan Area since the 16th century. The data also showed 16 drought and 18 flood events in Eastern China, with the most severe drought event occurred in 1634-1644. Droughts dominated in 12-14th centuries, but floods overwhelmed since the middle of 17th century. The severity of floods during 20th century was comparable in intensity during historical times, but the droughts were usually less severe.

Moreover, during the recent several years, precipitation amount reconstruction using the detailed snow and rainfall archives, e.g. Qing-Yu-Lu (Clear and Rain Records) and Yu-Xue-Fen-Cun (rainfall infiltration and snowfall depth), made an exciting progress in North China and Mid-Lower Yangtze region, which provided the important evidence for analyzing the precipitation characteristics quantitatively, in despite of only 300 years length. For example, Zhang et al. (2002; 2005) reconstructed annual and seasonal precipitation series in Beijing (1724-1903), Nanjing (1723-1798), Suzhou (1736-1806) and Hangzhou (1723-1773) using Clear and Rain Records, and traced the Meiyu (plum rain) activity for the 18th century in the lower reaches of Yangtze river. It is found that the early Meiyu occurred frequently at the period of 1740s-1770s, characterized by the strong summer monsoon and excessive rainfall. Recently, Ge et al. (2005) conducted a rainfall infiltration experiment at the Luancheng ecosystem experimental

station, following the Yu-Xue-Fen-Cun measurement, and built an empirical relationship between the rainfall and infiltration depth, which is an innovative and reasonable idea to use the historical document. The reconstructed summer and winter precipitations at the period 1736-1911 in Shijiazhuang were generally higher than the 1961-1990 means, with much larger fluctuations in summer. Note that the characteristics of a wetter climate during the Little Ice Age were also demonstrated in the climate model simulations by Liu et al. (2004). During the winter, there existed a decreasing precipitation trend for the period 1825-1875 and an increase afterwards, reaching the pre-1825 level. Shijiazhuang, influenced by the East Asian summer monsoon, showed significantly large fluctuations in the summer precipitation, with a distinctive wet period from 1785-1815 separating a relatively wetter earlier period and a latter period with the precipitation closer to the 1961-1990 means. Furthermore, Zheng et al. (2005) reconstructed precipitation series over the Middle and Lower Reaches of Yellow River and its 4 sub-regions, Hebei, Weihe, Jinnan and Shandong, going back to 1736. Analysis of the time series indicated the abrupt change from high to low was occurred around 1915. During the three periods of 1791~1805, 1816~1830 and 1886~1895, the precipitation was marked higher than the mean of the series. While both the periods of 1916~1945 and 1981~2000 were characterized by less precipitation.

In western China, almost over 20 precipitation (dry/wet) series derived from various proxy records (ice cores, sediments, tree rings and speleothems) during the last 2000 years were conducted in the recent 10 years, which covered Xinjiang, Xizang, Qinghai and Shaanxi regions (Zhang et al., 1992; Xu et al., 2000; Duan et al., 2002; Liu et al., 2004; Yu et al., 2005; Shao et al., 2006). The time resolutions and study methods both are better than the previous studies. In particular Wang et al. (2002a) analyzed precipitation changes in Western China during the last 400 years, using 17-sites series of proxy precipitation data, among which 11 were tree ring series, 4 were historical data series and 1 is ice core series. The first Empirical Orthogonal Function (EOF1) time series of precipitation in western China showed significant dry period in the 17th century, especially in the first half of the century. An increasing of precipitation was found in the second half of the 20 century, especially during the last 30 years. These dry periods and the increasing of precipitation may associate with the Little Ice Age and Modern Warming respectively.

Shao et al. (2004, Figure 3a) analyzed the tree ring width of *Sabina przewalskii* Kom in

Delingha region of Qaidam basin, and found the water was a critical factor to *Sabina przewalskii* *Kom* growth, which was distinct with the previous studies since 1970s, usually focused on the temperature change. The reconstructed annual precipitation series for the last 1000 years showed that the rainy periods were concentrated in 1520-1633 and 1933-2001, while the rainless periods were occurred in 1429-1519 and 1634-1741. Again, the precipitation fluctuation was small with 15mm before 1430, but during the period of 1430-1850, the amplitude fluctuation reached up to 30mm, and since 1990, the precipitation was decreasing in this region, which was opposite to the climate warming. The more excellent work was made by Shao et al. (2006) recently, which extended the length of the reconstructed precipitation back to the past 1437a, and this is the longest precipitation series from tree rings so far.

As one of the most typical monsoon climate countries in the world, with two-third area influenced by monsoon, the western and eastern China has distinct dry/wet climate characteristics. Because of the lack of long precipitation (dry/wet) series, especially for the high resolution, here we compared two precipitation (dry/wet) series, derived from the historical documents and tree rings respectively, to express the climate difference between eastern and western China (Figure 3). No significant consistent increasing or decreasing trend was shown in figure 3 besides the two periods of 1400s-1600s and 1710s-1960s at 30-year time resolution. For the annual resolution, no closely correlated relationship is found. But a noticeable precipitation (dry/wet) trend with increasing in western China and decreasing in eastern China is found after 1970s, and when the precipitation reaches to the maximum value during the last 1000 years, which is agree with the result of Shi et al (2003), the climate change from warm-dry to warm-wet, in the context of the climate warming.



Fig. 3. The reconstructed precipitation (dry/wet) series from the tree ring in western China during the last 1000 years (a, Shao et al., 2004) and historical document in eastern China during the last 1500 years (b, Zheng et al., 2006). The consistent increasing or decreasing change trend is marked with shaded area, the heavy line: 31-year running average smoothing.

3. Climate change since AD 1880

The global warming is undoubtedly the most important issue in studies of climate change during the last century. A homogeneous and consistent series is necessary to estimate accurately the warming rate. National Climate Center (NCC) has issued the climate series of monthly temperatures and precipitations from 1951 to the present. It consisted of a data set at 160 stations, which covered the most land areas of China. However, the length of 50 years is not long enough for examining the warming. Therefore, a lot of authors have worked in construction of the climate series of China for longer time period. Wang et al. (1998b) extended the instrumental observations with the proxy data, reconstructing a temperature series of China since 1880. It was the average of ten regional series with weighting according to area size of the region; Northeast, North, East, South, Taiwan, Central, Southwest, Northwest, Xinjiang and Tibet. The border between the regions was estimated according to the correlation coefficients between temperatures for the period of 1961-1990 at $1^{\circ} \times 1^{\circ}$ (lat \times long) grid points and that at region representative stations, which were called as central stations. Mean temperature series of China was found by averaging ten regional temperatures throughout the period studied, so impact of the bias associated with change of the data coverage or the number of stations used in study was significantly reduced. Ice core, tree-ring and documentary data were applied to fill in the gaps of instrumental observations. In this series, the errors mainly came from the uncertainty of proxy data. By the way, the time resolution is low, only annual series are reconstructed, for the low time resolution of the proxy data.

Recently, Tang and Ren (2005) constructed a seasonal mean temperature series of China using instrumental observations. Mean of maximum and minimum temperatures is used instead of average for three or four time observations per day to avoid the bias with change of daily number of observations. Altogether, observations at 616 stations were used. The number of stations used in study reduced to 231 before 1951. Firstly, temperature anomalies at $5^{\circ} \times 5^{\circ}$ lat \times long grid points were found referred to the normal of 1971-2000. Then, mean temperatures of China were calculated considering the size of the grid using all available grid point data. The shortcoming of this series was the changing of the coverage of data. Only about one third of the mainland area of China was covered by the observations in early of the 20th century.

The series of CRU* is the third one presented in this part. Climate Research Unit (CRU) of East Anglia University, UK issued in 2005 a new monthly temperature and precipitation data set at $0.5^{\circ} \times 0.5^{\circ}$ lat \times long grid points. Temperature anomalies at grid points over land area were found by statistical interpolation using instrumental observations only. Mean temperature series of China were worked out by Wen et al. (2006) based on the data set of CRU. This series provided a complete set of grid point temperature anomalies without any gaps in time series and change of data coverage. Only instrumental observations were applied in construction of the series, so no uncertainty of proxy data was contained. A possible shortcoming of CRU dataset was the obscurity of temperature information in Western China, especially over the Tibetan plateau in first half of the 20th century. Statistical interpolation usually reduced in some extent the extreme value of temperature anomalies. Both these issues were needed to take into consideration in using the series.



Fig.4. Temperature series of China. Red: Wang et al., 1998, blue: Tang and Ren(2005), black: CRU, and average of 1971-2000 as reference value.

Three temperature series of China are shown in Fig.4. Correlation coefficients (CC) between the series are attached in the corner of Fig.4, which are significant at 99.9% confidence level. High CC between the series constructed based on different dataset and different technique infers great reliability of the series. Fig.4 shows that temperatures by the end of the 19th to early of the 20th century kept low, attended a high level in the 1940's, and hereafter lowed to a minimum about 1970. Significant warming began in the middle of 1980's. Therefore, the modern warm period lasted till now only about twenty years from 1987 to 2006.

Spatial scale of precipitation anomalies is usually smaller than that of temperature anomalies, so it is difficult to characterize the precipitation variations over China by using limited number of regional series as done for temperatures. Therefore, a station precipitation data set was reconstructed, which consisted of seasonal precipitation data at 35 stations since 1880 (Wang et al.,

* <http://www.cru.uea.ac.uk/~timm/grid.CRU-TS-2-1.html>

2000b). Then, the series was extended to 71 stations* (referred hereafter as Wang). Red line in Fig.5 shows annual precipitation averaged for the area in the east of 105°E at 1°×1° lat × long grid points, which were found on the bases of station data at 71 stations. Blue line in Fig.5 gives the anomalies calculated using CRU data Set (Wen et al., 2006). It is need to note that there is some discrepancy in approaching the original data. The series of Wang consisted of seasonal precipitations; Mar to May, Jun to Aug, Sep to Nov, and Dec to Feb, so the annual total precipitation is the sum from Dec to Nov of next year. But, the annual precipitation of CRU is the sum from Jan to Dec. However; the series of CRU shows great similarity of interannual variability to the series of Wang. CC between the two series is 0.88 for the whole 20th century. Two series are nearly identical since 1951, while plenty of observations are available. Some discrepancy is found in the period of first half of 1940s. It can be attributed to the impact of Word War II.



Fig.5. Mean annual precipitation of China in the east of 105°E. Red line: Dec-Nov of next year from Wang, blue line: Jan.-Dec. from CRU (Wen et al., 2006).



Fig.6. Mean annual precipitation of China. red line: NCC 160 stations, blue line: CRU.

Fig.6 gives the precipitation anomalies referred to the normal of 1971-2000. Red line represents the mean based on the data of 160 stations of NCC. Of course, the station data firstly transformed into the grid point data at 1°×1° lat × long grid, then the latter is averaged with weighting of area size of the grid. The accordance of two series is quite high; the CC between them is 0.93 for the second half of the 20th century. CRU series provides the unique information of precipitation over whole China in the first half of the 20th century. The famous droughts in 1920s and 1940s widely outlined in the literatures and magazines of China manifested well in

* the result of the KeyProject of National Science Foundation: 《Study of Climate Variability over the Globe and in China during the 20th Century》, which were implemented during 1996-1999 by Wang Shaowu and Zhao Zhenguo et al. during 1996-1999.

decadal precipitation anomaly maps (Wang et al., 2002b) and in the blue line in Fig.6. Plentiful precipitation was found roughly in 1910s, 1930s, 1950s, 1970s and 1990s. It infers that bi-decadal oscillation of precipitation is predominated over China during the 20th Century.

4. Conclusions and Discussions

The Holocene climate change research in China has come a very long way and indeed make a big progress in the recent decades. Some consistent results have been archived: The climate of the Holocene was unstable, generally warm is the main characteristics, and the Megathermal was the warmest period of the Holocene in China, but a series of cold events occurred in 8.7-8.5 kaBP, 7.3 kaBP, 5.5kaBP and 4.0 kaBP during the Holocene period; A warming trend in the 20th century was clearly detected, but from the several reconstructed series, the warming magnitude was less than the maximum level, which occurred in the last 2000 years; The notable Medieval Warm Period showed inconsistent change trends and fluctuations between eastern and western China; The dry/wet spatial pattern has significant regional difference in Eastern China, which not only caused that the dry/wet trend in the Yangze and Huaihe valley is opposite with that in the North China, but also changed the dry/wet difference spatial pattern during the last 2000 years; The modern warm period lasted till now only about twenty years from 1987 to 2006 at the centennial time scale; Bi-decadal oscillation for the precipitation was dominated over China during the 20th Century.

However, we should adjust our research focuses and improve our research methods and ways, in order to adapt to the shifting requirements of international research on past global change, so the new questions should be addressed. For example, how and why has climate varied naturally on different time-scales (annual, centennial and millennial) over the Holocene period? How can an understanding of past variability improve the performance of climate models, leading to an improved prediction of future climate change? How can climate models help to explain past climate change? In conclusion, a lot of research works are still conducting and the new achievements are making, the research results are undoubtedly updating. There are many challenges but much more will be achieved in the coming decades.

References

- Academy of Meteorological Science of China Central Meteorological Administration, 1981: *Yearly Charts of Dryness/Wetness in China for the Last 500-year Period*. Cartographic Publishing House, 332pp. (in Chinese)
- An Zhisheng, 2000: The history and variability of the East Asian paleomonsoon climate. *Quater Sci. Rev.*, **19**, 171-187.
- An Zhisheng, Stephen C. Porter, John E. Kutzbach, Wu Xihao, Wang Suming, Liu Xiaodong, Li Xiaoqiang, and Zhou Weijian, 2000: Asynchronous Holocene optimum of the East Asian monsoon. *Quarter Sci. Rev.*, **19**, 743-764.
- Bond, G., and Coauthors, 1997: A pervasive millennial-scale cycle in North Atlantic Holocene and glacial climates. *Science*, **278**, 1257-1266.
- Chen Chen-Tung A., Lan Hsin-Chi, Lou Jiann-Yuh, and Chen Yan-Cheng, 2003: The dry Holocene Megathermal in Inner Mongolia. *Palaeogeogr Palaeoclimatol Palaeoecol*, **193**, 181-200.
- Chen Fahu, Wu Wei, J. A. Holmes, Zhu Yan, Jin Min, and C. G. Oviatt, 2003: A mid-Holocene drought interval as evidenced by lake desiccation in the Alashan Plateau, Inner Mongolia, China. *Chinese Sci. Bull.*, **48** (14): 1401-1410.
- Chu Kechen, 1973: A preliminary study on the climatic fluctuations during the last 5000 years in China. *Scientia Sinica*, **16**, 226-256.
- Cook, E.R., D.M. Meko, and C.W. Stockton, 1997: A new assessment of possible solar and lunar forcing of the bi-decadal drought rhythm in the western United States. *J. Climate*, **10**:1343-1356.
- Cook, E.R., D.M. Meko, D.W. Stahle, and M.K. Cleaveland, 1999: Drought reconstructions for the continental United States. *J. Climate*, **12**:1145-1162.
- Duan Keqin, Yao Tandong, and Pu Jianchen, 2002: Monsoon rainfall variability in central Himalaya Mountains over the past 300 years. *Quaternary Sciences*, **22**, 236-242. (in Chinese)
- Eddy, J.A., 1992: Past global changes project: Proposed implementation plans for research activities. Global Change Report No. 19, Sweden, Stockholm: IGBP, 112pp.
- Fleitmann, D., S. J. Burns, M. Mudelsee, U. Neff, Jan Kramers, A. Mangini, and A. Matter, 2003: Holocene Forcing of the Indian Monsoon Recorded in a Stalagmite from Southern Oman. *Science*, **300**, 1737-1739.
- Ge Qusheng, Zheng Jingyun, Fang Xiuqi, Man Zhimin, Zhang Xueqin, and Wang Wei-Chyung, 2003: Temperature changes of Winter-Half-Year in Eastern China during the Past 2000 Years. *The Holocene*, **13**, 933-940.
- Ge Quansheng, Zheng Jingyun, Hao Zhixin, Zhang Piyuan, and Wang Wei-Chuyung, 2005: Reconstruction of historical climate in China: High-resolution precipitation data from Qing Dynasty archives. *Bull. Am.*

Meteorol. Soc, **86**, 671–679.

Guo Zhengtang, P.M. Nicole, and K. Stefan, 2000: Holocene non-orbital climatic events in present-day arid areas of northern Africa and China. *Global Planet Change*, **26**, 97-103.

Hong Yetang, Hong Bin, Lin Qinghua, Yasuyuki Shibata, Masashi Hirota, and X.T. Leng, 2005: Inverse phase oscillations between the East Asian and Indian Ocean summer monsoon during the last 12000 years and palaeo-El Nino. *Earth Planet Sci. Lett.* **231**, 337-346.

Huang Chunchang, Zhou Jie, Pang Jiangli, Han Yuping, and Hou Chunhong, 2000: a regional aridity phase and its possible cultural impact during the Holocene Megathermal in the Guanzhong Basin, China. *The Holocene*, **10**, 135-142.

IPCC, 1990: *Climate Change: The IPCC Scientific Assessment*. J.T. Houghton, G.J. Jenkins, and J.J. Ephraums, Eds., Cambridge University Press, 365pp.

IPCC, 1992: *Climate Change 1992: The Supplementary Report to the IPCC Scientific Assessment*. J.T.Houghton et al., Eds., Cambridge University Press, 198pp.

IPCC, 1996: *Climate Change 1995: The Science of Climate Change. Contribution of Working Group I to the Second Assessment Report of the Intergovernmental Panel on Climate Change*. J. T. Houghton et al., Eds., Cambridge University Press, 572pp.

IPCC, 2001: *Climate Change 2001: The Scientific Basis. Contribution of Working Group I to the Third Assessment Report of the Intergovernmental Panel on Climate Change*. J .T. Houghton et al., Eds., Cambridge University Press, 881pp.

Liu Jian, Chen Xing, Wang Suming, and Zheng Yiqun, 2004: Palaeoclimate simulation of Little Ice Age. *Progress in Natural Science*, **14**, 716-724.

Liu Xiaodong, Li Xiaoqiang, and Zhou Weijian, 2000: Asynchronous Holocene optimum of the East Asian monsoon. *Quater Sci. Rev.*, **19**, 743-762.

Liu Yu, and Coauthors, 2004: Reconstruction of May-July precipitation in the north Helan Mountain, Inner Mongolia since A.D. 1726 from tree-ring late-wood width. *Chinese Sci. Bull.*, **49**, 405-409.

Man Zhimin and Zhang Xiugui, 1996: Research on the documental evidence and the characteristics of MWP in the east part of China. *Research on the past life-supporting environment change of China (I)*, Zhang Lansheng, Ed., Ocean Press, 95-103. (in Chinese)

Mann, M.E., 2002: Medieval climate optimum. *Encyclopedia of global environment (Vol.1), The earth system*, M. C. MacCracken, and J.S. Perry, Eds., John Wiley & Sons Ltd., 514-516.

- Shao Xuemei, Huang Lei, Liu Hongbin, Liang Eryuan, Fang Xiuqi, and Wang Lili, 2004: Reconstruction of precipitation variation from tree rings in recent 1000 years in Delingha, Qinghai. *Science in China (Ser. D)*, **34**, 145-153.
- Shao Xuemei, Liang Eryuan, Huang Lei, and Wang Lili, 2006: A reconstructed precipitation series over past Millennium in the Northeastern Qaidam Basin. *Advances in Climate Change Research*, **2**(3),122-126. (in Chinese)
- Shi Yafeng, and Coauthors, 1992: Basic characteristics of climate and environment of China in the Megathermal of the Holocene. *The Climate and Environment of China in the Megathermal of the Holocene*, Shi Yafeng, Ed., Ocean Press, 212pp. (in Chinese)
- Shi Yafeng, Shen Yongping, Li Dongliang, Zhang Guowei, Ding Yongjian, and Kang Ersi, 2003: Discussion on the present climate change from warm-dry to warm-wet in Northwest China. *Quaternary Sciences*, **23**,152-164. (in Chinese)
- Tan Ming, Liu Tungsheng, Hou Juzhi, Qin Xiaoguang, Zhang Hucui, and Li Tieying, 2003: Cyclic rapid warming on centennial-scale revealed by a 2650-year stalagmite record of warm season temperature. *Geophy. Res. Lett.*, **30**, doi: 10.1029/2003GL017352.
- Tan Ming, Hou Juzhi, and Liu Tungsheng, 2004: Sun-coupled climate connection between eastern Asia and northern Atlantic. *Geophy. Res. Lett.*, **31**, doi: 10.1029/2003GL019085.
- Tang Guoli and Ren Guoyu, 2005: Reanalysis of surface air temperature change of the last 100 years over China. *Climate Environment Research*, **10** (4), 791-798. (in Chinese)
- Thomson, L., and Coauthors, 1997: Tropical climate instability: the last glacial cycle from a Qinghai-Tibetan ice core. *Science*, **276**, 1821-1825.
- Wang Hongya, Liu Hongyan, Cui Haiting, and Niels Abrahamsen, 2001: Terminal Pleistocene/Holocene palaeoenvironmental changes revealed by mineral-magnetism measurements of lake sediments for Dali Nor area, southeastern Inner Mongolia Plateau, China. *Palaeogeogr. Palaeoclimatol. Palaeoecol.*, **170**, 115-132.
- Wang Luejiang, M. Sarnthein, H. Erlenkeuser, P. M. Grootes, J. O. Grimalt, C. Pelejero, and G. Linck, 1999: Holocene variations in Asian monsoon moisture: A bidecadal sediment record from the South China Sea. *Geophy. Res. Lett.*, **26**, 2889-2892.
- Wang Pinxian, Bian Yunhua, Li Baohua and Huang Chi-yu, 1996: The Younger Dryas in the West Pacific marginal seas. *Science in China (Ser. D)*, **26**, 522-532.
- Wang Shaowu and Wang Risheng, 1990: Variations of seasonal and annual temperatures during 1470–1978AD in

- eastern China. *Acta Meteorologica Sinica*, **48**(1), 26-35. (in Chinese)
- Wang Shaowu, 1991: Reconstruction of temperature series of North China from 1380s to 1980s. *Scientia Sinica (Ser. B)*, **6**, 751-759.
- Wang Shaowu, Zhao Zongci, and Chen Zhenhua, 1993: Drought/flood type in China for 950-1991AD. *Drought/flood disasters in Changjiang and Huanghe River region and its impact on the economy*, Wang Shaowu et al., Eds., China Meteorological Press, 55-66. (in Chinese)
- Wang Shaowu, Ye Jinlin, and Gong Daoyi, 1998a: Climate in China during Little Ice Age. *Quaternary Sciences*, **18**, 54-64. (in Chinese)
- Wang Shaowu, Ye Jinlin, Gong Daoyi, Zhu Jinhong, and Yao Tandong, 1998b: Reconstruction of the temperature series in China for the last one hundred years. *Quart. J. Appl. Meteor.*, **9**(4), 392-401. (in Chinese)
- Wang Shaowu and Gong Daoyi, 2000a: Climate in China during the four special periods in Holocene. *Progress in Natural Sciences*, **10**, 379-386.
- Wang Shaowu, Gong Daoyi, and Ye Jinlin, 2000b: Seasonal precipitation series over China since 1880. *Acta Geograph Sin.*, **55**(3), 281-293. (in Chinese)
- Wang Shaowu, Gong Daoyi, and Zhu Jinhong, 2001: Twentieth-century climatic warming in China in the context of the Holocene. *The Holocene*, **11**(3), 313-321.
- Wang Shaowu, Cai Jingning, Mu Qiaozhen, Xie Zhihui, and Dong Wenjie, 2002a: Climate change of annual precipitations in western China. *Journal of Natural Resources*, **17**, 415-422. (in Chinese)
- Wang Shaowu, Cai Jingning, and Zhu Jinhong, 2002b: The interdecadal variations of annual precipitation in China during 1880s-1990s. *Acta Meteor. Sin.*, **60**(5), 637-639. (in Chinese)
- Wang Sumin, Ji Lei, Yang Xiangdong, Xue Bin, Ma Yan, and Hu Shouyun, 1994: The record of Younger Dryas event in lake sediment from Jalai Nur, Inner Mongolia. *Chinese Sci. Bull.*, **39**, 831-835.
- Wei Jiangfeng and Wang Huijun, 2004: A Possible Role of Solar Radiation and Ocean in the Mid-Holocene East Asian Monsoon Climate. *Adv. Atmos. Sci.*, **21**(1), 1-12.
- Wen Xinyu, Wang Shaowu, Zhu Jinhong, and D. Viner, 2006: An overview of China climate change over the 20th century using UK UEA/CRU high resolution grid data. *Chinese J. Atmos. Sci.*, **30**, 894-904. (in Chinese)
- Xu Ruizhen and Zhou Lusheng, 2000: Reconstruction of summer precipitation in Southeastern Qinghai Plateau using spruce chronology at Banma. *Meteorological monthly*, **26**(1), 3-8, 34. (in Chinese)
- Yang Bao, A. Braeuning, and K. R. Johnson, 2002: General characteristics of temperature variation in China during the last two millennia. *Geophys. Res. Lett.*, **29**(9), 381-384.

- Yang Bao, B. Braeuning, and Shi Yafeng, 2003: Late Holocene temperature fluctuations on the Tibetan Plateau. *Quater Sci. Rev.*, **22**, 2335-2344.
- Yang Zhihong, Yao Tandong, Huang Cuilan and Sun Weizhen, 1997: Record of Younger Dryas event in ice core of Gulia. *Chinese Sci. Bull.*, **42**, 1975-1978.
- Yao Tandong, and Shi Yafeng, 1992: Climate change of the Holocene recorded in ice core of Dunde, Qilian Mountain. *The Climate and Environment of China in the Megathermal of the Holocene*, Shi Yafeng, Ed., Ocean Press, 206-211. (in Chinese)
- Yu Shulong, Yuan Yujiang, Jin Hailong, Cui Yu, Liu Bin, and Lin Chunliang, 2005: A 379-Year July-August Precipitation Series Reconstructed from Tree-Ring on the Midwestern Part of the Northern Slopes of Tianshan Mountains. *Journal of Glaciology and Geocryology*, **27**,404-410. (in Chinese)
- Zhang De'er, 1980: Winter temperature changes during the last 500 years in South China. *Kexue Tongbao (Chinese Science Bulletin)*, **25**(6), 497-500.
- Zhang De'er and P.-K. Wang, 1991: A study on Meiyu activity of eighteenth century in the lower Yangtze Region, *Science in China (Ser. B)*, **34**, 1237-1245.
- Zhang De'er and Liu Yuewei, 2002: A new approach to the reconstruction of temporal rainfall sequences from 1724-1904 Qing Dynasty weather records from Beijing. *Quaternary Sciences*, **22**, 199-208. (in Chinese)
- Zhang De'er, Liu Chuanzhi, and Jiang Jianmin, 1997: Reconstruction of six regional dry/wet series and their abrupt changes during the last 1000 years in east China. *Quaternary Sciences*, **17**(1), 1-11. (in Chinese)
- Zhang De'er, Liu Yuewei, Liang Youye, and Li Jing, 2005: Reconstruction of annual and seasonal precipitation series of Nanjing, Suzhou and Hangzhou during the 18th century. *Quaternary Sciences*, **25**, 121-128. (in Chinese)
- Zhang Jiacheng, 1988: *Reconstruction of Climate in China for Historical Times*. Science Press, 174pp. (in Chinese)
- Zhang Piyuan, 1996: *Climate Change in China during Historical Times*. Shandong Science and Technology Press, 195-440. (in Chinese)
- Zhang Piyuan and Wang Zheng, 1994: The stages of climate change in recent 2000 years. *Science in China (Ser. D)*, **24**, 998-1008.
- Zhang Zhihua and Wu Xiangding, 1992: Utilizing two Qinghai tree-ring chronologies to reconstruct and analyze local historical precipitation. *Quarterly Journal of Applied Meteorology*, **3**, 61-69. (in Chinese)
- Zheng Jingyun and Zheng Sizhong, 1993: An analysis on cold/warm and dry/wet in Shandong Province during

historical times. *Acta geographica Sinica*, **48**(4), 348-357. (in Chinese)

Zheng Jingyun, Zhang Piyuan, and Ge Quansheng, 1999: Abrupt climatic change: Evidence and implication.

Advance in earth sciences, **14**, 177-182. (in Chinese)

Zheng Jingyun, Zhang Piyuan, Ge Quansheng, and Man Zhimin, 2001: Centennial changes of drought/flood spatial pattern in eastern China for the last 2000 years. *Progress in Natural Science*, **11**,280-287.

Zheng Jingyun, Hao Zhixin, and Ge Quansheng, 2005: Variation of precipitation for the last 300 years over the middle and lower reaches of the Yellow River. *Science in China (Ser. D)*, **48**, 2182-2193.

Zheng Jingyun, Wang Wei-Chyung, Ge Quansheng, Man Zhimin, and Zhang Piyuan, 2006: Precipitation variability and extreme events in eastern China during the past 1500 years. *TAO*, **17**,579-592.

Zhou Weijian, Li Xiaoqiang, Dong Guangrong, S. C. Porter, M. Stuiver, D. Donahue, and A. J. T. Jull, 1996: High-resolution peat record in desert/loess transition zone during the period of Younger Dryas -- An example of climatic oscillation of East Asian monsoon. *Science in China (Ser. D)*, **26**,118-124.

Zhou Weijian, Lu Xuefeng, Wu Zhengkun, Deng Lin, A.J.T. Jull, D. Donahue, and W. Beck, 2002: Peat record reflecting Holocene climatic change in zoige plateau and AMS radiocarbon dating. *Chinese Sci. Bull.*, **47**(1), 66-70.

Figure Captions

Fig.1. $\delta^{18}\text{O}$ in Guliya (1), simple pollen diversity (2), total pollen concentration (3) and upland pollen concentration (4), in Zhuyeze Lake, after Chen Fahu et al., 2003

Fig. 2. The reconstructed temperature series during the last 2000 years in China derived from various historical climate proxy data. (a) summer temperature (May-Aug.) in Beijing by Tan et al.(2003), line: annual temperature, bar: temperature change with 30-year resolution; (b) Winter half year temperature in Eastern China at 30-year time resolution by Ge et al.(2003); (c) temperature change at 50-year resolution in whole Tibet Plateau by Yang et al.(2003); (d) Weighted temperature reconstruction over China by Yang et al(2002), line: 10-year resolution, bar: 30-year resolution.

Fig. 3. The reconstructed precipitation (dry/wet) series from the tree ring in western China during the last 1000 years (a, Shao et al., 2004), and historical document in eastern China during the last 1500 years (b, Zheng et al., 2006). The consistent increasing or decreasing change trend is marked with shaded area, The heavy line is 31-year running average smoothing.

Fig.4. Temperature series of China. Red: Wang et al. 1998, blue: Tang and Ren (2005), black: CRU, average of 1971-2000 as referenced value.

Fig.5. Mean annual precipitation of China in the east of 105°E. Red line: Dec-Nov of next year from Wang, blue line: Jan-Dec from CRU (Wen et al., 2006).

Fig.6. Mean annual precipitation of China. Red line: NCC 160 stations, blue line: CRU.

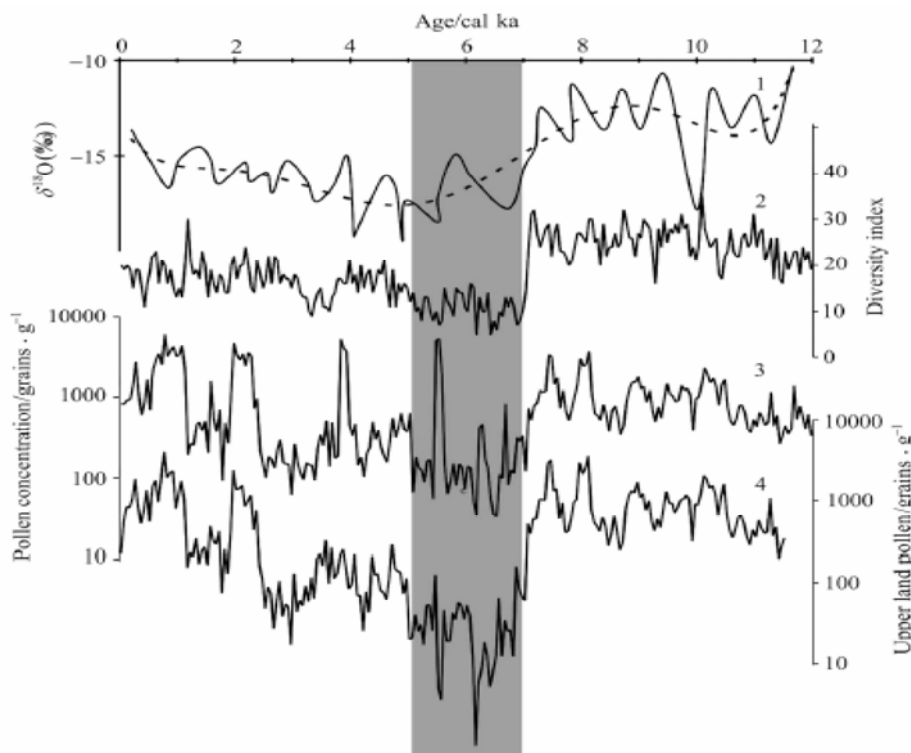


Fig.1. $\delta^{18}\text{O}$ in Guliya (1), simple pollen diversity (2), total pollen concentration (3) and upland pollen concentration (4), in Zhuyeze Lake, referenced from Chen Fahu et al., 2003.

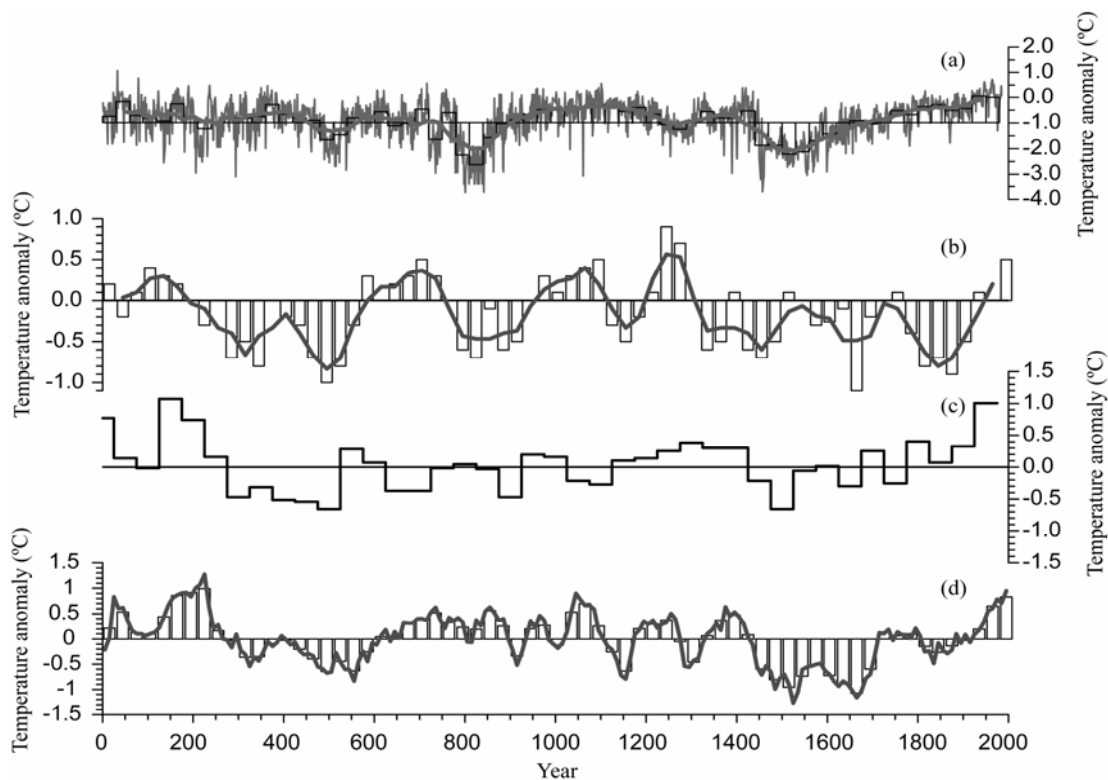


Fig. 2. The reconstructed temperature series during the last 2000 years in China derived from various historical climate proxy data. (a) summer temperature (May-Aug.) in Beijing by Tan et al.(2003), line: annual temperature, bar: temperature change with 30-year resolution; (b) Winter half year temperature in Eastern China at 30-year time resolution by Ge et al.(2003); (c) temperature change at 50-year resolution in whole Tibet Plateau by Yang et al.(2003); (d) Weighted temperature reconstruction over China by Yang et al(2002), line: 10-year resolution, bar: 30-year resolution.

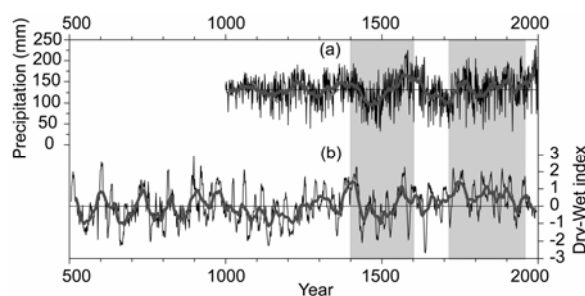


Fig. 3. The reconstructed precipitation (dry/wet) series from the tree ring in western China during the last 1000 years (a, Shao et al., 2004), and historical document in eastern China during the last 1500 years (b, Zheng et al., 2006). The consistent increasing or decreasing change trend is marked with shaded area, The heavy line is 31-year running average smoothing.

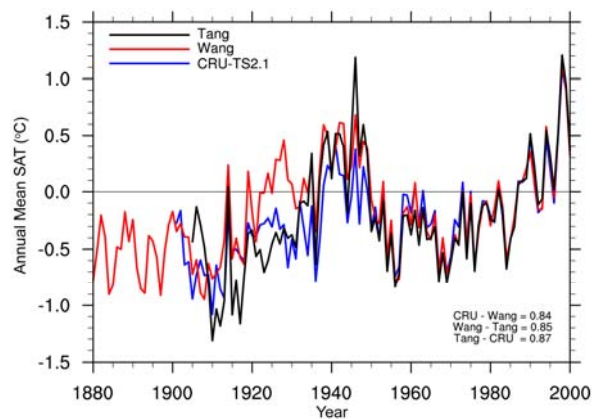


Fig.4. Temperature series of China. Red: Wang et al. 1998, blue: Tang and Ren (2005), black: CRU, average of 1971-2000 as referenced value.

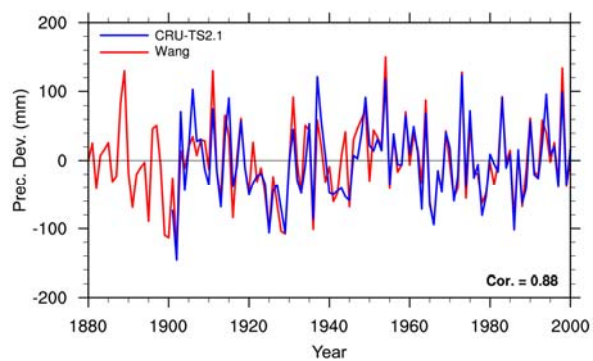


Fig.5. Mean annual precipitation of China in the east of 105°E. Red line: Dec-Nov of next year from Wang, blue line: Jan-Dec from CRU (Wen et al., 2006).

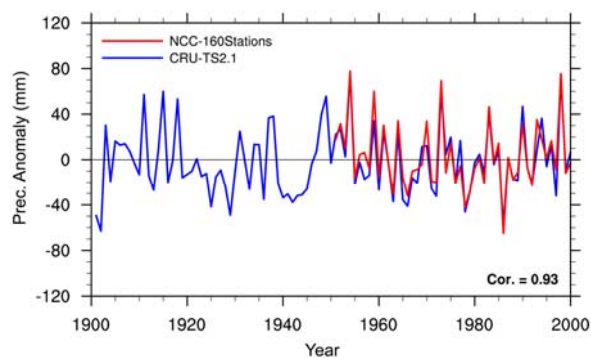


Fig.6. Mean annual precipitation of China. Red line: NCC 160 stations, blue line: CRU.

DETECTION, ATTRIBUTION AND PROJECTION OF CLIMATE CHANGE OVER CHINA: AN OVERVIEW OF THE RECENT PROGRESS

*Ding Yihui*¹ (丁一汇) *Ren Guoyu* (任国玉) *Zhao Zongci* (赵宗慈) *Xu Ying* (徐影)

Luo Yong (罗勇) *Li Qiaoping* (李巧萍) *Zhang Jin* (张锦)

National Climate Center, China Meteorological Administration

Abstract

This article summarizes the main results and findings of the studies conducted by Chinese scientists in the past five years. It is shown that observed climate change in China bears a large similarity with that of global average. The country-averaged annual mean surface air temperature has increased by 1.1°C for the past 50 years and 0.5~0.8°C for the past 100 years, slightly larger than the global temperature increase in the same periods. Northern China and wintertime witness the largest increase in surface air temperature. Although no significant trend has been found in country-averaged annual precipitation, inter-decadal variability and obvious trends on regional scales are detectable, with northwestern China and the mid-and lower Yangtze River basin undergoing an obvious increase and North China a severe drought. Some analyses show that frequency and magnitude of extreme weather and climate events also undergoes significant changes in the past 50 years or so.

Studies of attribution of regional climate change, by using climate models and taking consideration of various forcings, show that the warming of the last 50 years may have been

¹ Email: dingyh@cma.gov.cn

mainly caused by increased atmospheric concentration of greenhouse gases, while the temperature change of the first half of 20th century may have been dominantly induced by solar activities, volcano's eruptions and sea surface temperature change. Significant decline of sunshine duration and solar radiation at the surface in eastern China has been attributed to the increased emission of pollutants.

Projections of future climate by models of the NCC (National Climate Center, China Meteorological Administration) and IAP (Institute of Atmospheric Physics, Chinese Academy of Sciences) as well as 40 abroad models indicate a significant warming in 21st century in the country, with the largest warming occurring in winter and northern China. Under varied emission scenarios, the country-averaged annual mean temperature is projected to increase by 1.5~2.1°C by 2020, 2.3~3.3°C by 2050, and 3.9~6.0°C by 2100, in comparison to the 30 year average of 1961~1990. Most models project a 10-12% increase in annual precipitation in China by 2100. The wet trend will be particularly evident in Northeast and Northwest China, but part of the central China will probably undergo a drying trend. Large uncertainty exists in projection of precipitation, and further study is needed. Besides, anthropogenic climate change will probably lead to a weaker winter monsoon and a stronger summer monsoon in eastern Asia.

Key words: Observed climate change in China, detection and attribution, climate models, projection

1. Introduction

Studies on climate change have been intensively conducted by Chinese scientists in recent

two decades. In this time period, the Chinese government sponsored a series of State Key Research Programs related to basic science and the impact of climate change, such as the Projects “Projection, impact and response policy of global climate change”, “Study on global climate change and environmental policy”, “Study on response policy and supporting technologies to global environmental change”, “Trend of life-supporting environment in 20-50 years to come in China”, “Study on mechanism and prediction theories of major weather and climate disasters in China”, “Study on life-supporting environment change and trend of northern China aridification”, “Changes in climate and sea level in China and the future trend and impact”, “Response of China terrestrial ecosystems to global change” and “Interaction between China agricultural ecosystem and global change”. And Chinese Academy of Sciences also launched some Key Projects such as “Study on carbon budget in land and the costal zones” and “Western ecosystem and environment and the sustainable exploration of natural resources”. Due to the supports from the state-funded projects and other research projects, great progresses have been achieved in the field of climate change, which has also significantly contributed to the development of earth system science and the formulation of response policies of the country to global climate change.

Under the State Key Project of the Tenth Five-Year Plan “Study on response policy and supporting technologies to global environmental change”, a sub-project related to regional climate change detection and attribution, and projection was established, with a goal to further understand the observed climate change and the possible causes, and to project the future trend of climate probably induced by anthropogenic increase of atmospheric CO₂ concentration. (Ding et al., 2006). Scientists involved in the sub-project have updated historical climate series including those of the last 1000 years, 100 years and 50 years in the country(Wang and Gong, 2000; Ren et al., 2005,

2006; Tang and Ren, 2005; Ding et al., 2006), and have made an effort to attribute the observed change to anthropogenic and natural factors(Zhao et al., 2005a,b). They have done a series of simulations using global climate models and regional climate models to obtain the possible climate change scenarios for the 50 years and 100 years to come in East Asia and China(Zhao et al., 2003; Xu et al., 2005; Luo et al., 2005; Ding et al., 2006). The other two sub-projects have also assessed the impacts of projected climate change on agriculture, water resource, terrestrial ecosystems and coastal zones of the country, and put forward the measures and policies for adaptation and mitigation to the climate change. However, their achievements will not be reported in this paper.

Large uncertainty still exists in the studies of climate change, especially in the projection of future climate trend on regional scale. Major uncertainties have been identified by the scientists involved in the sub-projects, and they need surely to be tackled in the near future.

This paper presents a brief summary of the research results of the sub-project of the climate change science under the State Key Project of the Tenth Five-Year Plan “Study on response policy and supporting technologies to global environmental change”. More details are included in the National Assessment Report on Climate Change, which has been available from China Science Press in Beijing. After the introduction, the second section of the paper gives the major results of surface climate changes as observed in the past, followed by the third section briefing the research results of attribution of regional climate change. The fourth section presents a few modeling results of the future climate trend in China, followed by conclusions given in the last section of the present paper.

2. Change in surface climate

2.1 Surface air temperature

Analysis of surface air temperature is based on a data set of 726 stations across the country. Nationwide average temperature anomalies and temperature trends for the time periods of 1951-2001 and 1905-2001 are calculated, taking 1971-2000 as the base period. The method of Jones et al. (1996, 2003) for constructing the nationwide average surface air temperature anomaly series is adopted. Trends of temperature are obtained using the least square method. Different from the previous analyses which showed major differences mainly in 1910s-1930s (Ding et al., 1994; Lin et al., 1995; Chen et al., 1998; Wang et al., 1998, 2002; Zeng et al., 2001; Hu et al., 2003), the inhomogeneity induced by shift of stations and change of instruments has been checked and adjusted in the present work. The inhomogeneity of the monthly mean temperature data has been proved to be mainly caused by relocation of stations and daily observation times. Inhomogeneities of monthly temperature data of prior to 1950 has been also checked, and those caused by different daily observation time and the changed time systems have been minimized by re-calculating the monthly mean temperature using the maximum and minimum temperatures (Ren et al., 2005; Tang and Ren, 2005).

Annual mean surface air temperature in China increases significantly, and the trends of change reaches $0.22^{\circ}\text{C}/10\text{yr}$ for the time period of 1951-2001 and $0.08^{\circ}\text{C}/10\text{yr}$ for the time period of 1905-2001, respectively. Annual mean temperature has risen by about 1.1°C during the past half a century, and 0.8°C during the past a century (Figure 1) (Ren et al., 2005). It is obvious that the warming dominantly occurred in two time periods of 1920s-1940s and 1980s-2001. Annual mean

temperature anomalies in the 1990s and the 1940s were 0.37°C and 0.36°C , respectively. The highest temperature record occurred in 1998, and the second highest temperature occurred in 1946. The warming period in the period of 1920s-1940s in China was much higher than the global warming in the same period. It is not clear yet why this warming period occurred in the first half of the 20th century when the anthropogenic effect was not intensive as the present time.

Figure 1 Change in country-averaged annual mean surface air temperature anomalies in China during 1905-2001 (a: temperature anomalies; b: number of observations. Unit: $^{\circ}\text{C}$) (Tang and Ren, 2005)

The warming in the last half century (1951-2001) is very significant, and it is more rapid than the world average. The warming mainly started in the early to mid-1980s. Before that time, temperatures in China only fluctuated within a small range, and no significant trend can be detected; but starting from early the 1980s, the temperature has kept rising steadily. 1998 was the warmest year in the past 50 years or so, with the annual mean surface air temperature anomaly reaching 1.13°C . The 1990s was the warmest decade in the latter half of the 20th century.

Seasonal mean temperature for almost all seasons in 1951-2001 has been in an upward trend, with the warming in winter being the most obvious. Warming is also significant in spring and autumn, but it is very weak in summer. Temperature change in spring and summer is also comparatively similar, with the warming dominantly starting after mid-1990. On the other hand, temperature change in autumn and winter is more similar, with an obvious warming trend starting

after early 1980s and an accelerating warming after 1987.

The warming in terms of annual mean surface air temperature dominantly occurred in Northeast, North and Northwest China, while most southern parts of the country did not see significant warming. Rising of temperature in winter and spring most significantly contributed to the warming in northern China. However, a cooling trend reported in earlier studies is still continuing in southwestern part of China, with the Sichuan Basin and northern Yunnan-Guizhou Plateau experiencing the most remarkable cooling. Analysis for different seasons shows that the cooling was mainly caused by the obvious drop in seasonal mean temperature in spring and summer. The middle and lower reaches of the Yangtze River also witnessed a cooling trend in summer in the last 50 years. The phenomenon of temperature decrease in Southwest China might have been caused by increased emission of pollutants such as SO₂ and the resulting acid rain (Li et al., 1995; Hu et al., 2003).

The above-mentioned results were all based on a dataset of surface air temperature without any correction for urbanization bias. This might be a problem for most of the meteorological stations located in growing big cities. In Beijing region, for example, temperature records from two national basic/reference stations used in constructing temperature series of the past 50 years were significantly impacted by urban warming, especially for the last 20 years. Warming induced by urbanization or enhanced heat-island effect in two stations of this city accounts for about 70% of the total increase in annual mean temperature for period from 1961 to 2000 (Chu et al., 2005). Effect of urbanization on records of nationwide climate stations in other regions such as North China and a few provinces is also significant (Ren et al., 2005). These cases indicate the importance to pay more attention to the effect of urban heat island effect on long-term mean

temperature series in the country.

Besides, a 1000-year annual mean temperature series has been reconstructed preliminarily (Chu et al., 2005). The reconstruction used twenty seven tree-ring chronologies from 7 individual sites in western and northeastern China, and the winter-half-year temperature series in eastern China as reconstructed by Ge et al. (2003). Variability in temperature in China over the past 1000 years is evident. Annual mean temperature of China is generally warmer from A.D.1000 to A.D. 1310 with a relatively cool episode in 13th century, and it is significantly colder from A.D.1310 to 1910 with minimum anomalies occurring in 15th, 17th and 19th century, respectively. Modern warm period beginning from the end of 19th century looks unusual in terms of the 1000-year variation of annual mean temperature, but it is not significantly warmer than the earlier warm period or Medieval Warm Period (MWP). The “Medieval Warm Period” approximately came to an end at the end of the 13th century, and the “Little Ice Age” may have lasted for a comparatively longer period of time, from the early 14th century to the end of the 19th century. The coldest climate occurred in the mid-and late periods of the 17th century and in the 19th century when temperature anomalies dropped to less than -0.4°C . It was also colder in the mid-and late period of the 15th century. Some differences between the series of western and eastern China have been detected, and there seems to be no significant warming during the MWP in the temperature series. But, Wang (2002) pointed out that the anomalous warming in the mid-13th century in eastern China was also evident in western China.

2.2 Precipitation

Less confidence could be lent to the precipitation data prior to 1950 period. Data quality for

1951-2001 is good, however, though no adjustment has been made for the bias probably induced by wind and solid precipitation measurement. In spite of the problems with data, it is still interesting to note that no significant long-term trend in the country-averaged annual precipitation can be detected for the past 100 years. Changing trend in annual precipitation in the country is also difficult to detect for the time period of 1951-2001. If the beginning year is set at 1956, however, a slight increase in the average annual precipitation could be seen, with 1998 being the wettest year in the country (Ren et al., 2005).

Large regional difference is notable in precipitation trend in 1956-2002 (Figure 2). An obviously dropping trend in annual precipitation occurred in the Yellow River Basin and the North China Plain, and the largest drop occurred in Shandong Province and southern Liaoning Province. Annual precipitation in the Yellow, Haihe and Liaohe River basins decreased by about 50-120mm during the time period analyzed. Meanwhile, an insignificant wetting trend in the Yangtze Basin, southeast coastal region and most parts of western China could be detectable, though some sites underwent a more significant increase in annual precipitation. The Yangtze River Basin and southeast coastal region as a whole witnessed an increase in annual precipitation of about 60-130mm for the time period of 1956-2002. The increase mainly resulted from the significant rising of summer rainfall, though winter precipitation also tended to rise. Decrease in annual precipitation in the Yellow River Basin and the North China Plain is mostly caused by the less rainfall in summer and autumn. The obvious regional difference in annual precipitation change, in particular the contrast between the south and the north, has generally been attributed to a weaker summer monsoon in East Asian region since late 1970s (Ding et al., 2005).

A few sites of tree-ring data are available, and they provide a historical perspective of

summer or annual precipitation change on local scale. For example, annual precipitation of the past 1000 years as reconstructed from tree-rings on eastern rim of the Caidamu Basin in the Tibetan Plateau indicates a wetter climate in 20th century than any centuries in history, and much more severe droughts in mid-to late 15th century and in late 17th century and early 18th century than in 20th century occurred (Shao et al., 2004). Historical documental records also show much more severe droughts in North China during some decades of the time period corresponding to the Little Ice Age.

Figure 2 Tendency of precipitation over China (1956-2002). Blue color: positive trend; Red color: negative trend. (Ren et al., 2005)

2.3 Other climate elements

Change in sunshine duration, pan-evaporation and wind speed for the last 50 years has been also analyzed. Fig. 3 shows the change in nationwide average sunshine duration during 1956-2002. A significant decreasing trend can be seen, especially for the time period from mid-1960s to early 1990s. For the whole period analyzed, the decreasing trend is -38 hrs/10yr, but it can reach about -50 hrs/10yr for the period of 1966-1993. Sunshine duration began to stop dropping or to go up slightly from mid-1990s. Spatial feature is characterized by the largest decrease in North China Plain including Hebei, Henan and Shandong Provinces, and an insignificant increase in a few places of the eastern Tibetan Plateau, Gansu Province, western Inner Mongolia and northern

Northeast China (Ren et al., 2005).

Figure 3 Change in national average sunshine duration during 1956-2002 (Unit: hours) (Ren et al., 2005)

Since 1956, the country-averaged pan evaporation has had a significant tendency to decrease, with a changing rate of -35mm/10yr. The most significant decrease occurred in spring and summer in the North China Plain and the lower reach of the Yangtze River. The largest decrease in pan evaporation in terms of absolute values is in northwestern China (Ren et al., 2005). From early 1990s on, however, pan evaporation in China has stopped to decrease and begun to rise a little. It is noticed that the temporal and spatial pattern of change of pan evaporation is very similar to that of sunshine duration in the country, implying a dominant influence of solar radiation on observed pan evaporation (Guo et al., 2005; Ren and Guo, 2006).

Country-averaged annual mean wind speed is also experiencing a tremendous drop during the past 50 years. However, the obvious decrease in wind speed began from mid-1970s, and it has not stopped as sunshine duration and pan evaporation in the early 1990s. The largest decrease in wind speed occurs in Northwest China, while Southwest China and northern Northeast China only witness a smaller drop.

2.4 Extreme climate events

A mixed picture could be seen for changes in extreme weather and climate events for the past

50 years. As expected, country-averaged daily minimum temperature and days with minimum temperature below 0°C have been significantly decreasing since 1950. Due to the fact that minimum temperature above 0°C are generally seen as frost-free period, and the decrease in days with minimum temperature below 0°C implies the lengthening of frost-free period. At the same time, country-averaged daily maximum temperature and days with maximum temperature above 35°C have not tended to significantly increase, though some places of North China have a rising of the hot wave frequency. Days with cold wave in wintertime in northern and eastern China have undergone a significant decrease for the last 50 years, especially for the period beginning from 1970 (Zhai et al., 1997; 2003).

Although obvious increase in days with heavy rain in the Yangtze River Basin and in area suffering serious drought in North China Plain and southern Northeast China has been detected for the recent 50 years, no significant change in the extreme precipitation events can be seen for the country as a whole. Stronger rainfall is more frequently recorded in western China including Xinjiang Autonomous Region and most areas of the Tibetan Plateau (Zhai et al., 1999; Gong and wang, 2000), but it has been less frequently observed in North China and southern Northeast China where annual total precipitation has undergone large decrease (Figure 4). The pattern of drier North China and wetter South China has resulted in more difficult situation for water management in the country.

Figure 4 Trends of days with extreme strong rainfall ($\geq 25 \text{ mm day}^{-1}$) for 1951-2000 in China.

Solid and open circles indicate increase and decrease respectively, and sizes of the circles are scaled to strength of the trends. (Ding et al., 2006)

Annual total volume of precipitation induced by tropical cyclones equivalent to areal rainfall amount and the total days with torrential precipitation of $\geq 50 \text{ mm day}^{-1}$ due to tropical cyclones all tend to decrease since 1957, though the two years with the largest typhoon-induced rainfall occurred after 1980 (Fig. 5). Frequency of landing typhoons in southeastern coastal areas also tends to decrease after early 1980s (Ren et al., 2006). Dust storm, a disastrous weather phenomenon in northern China, has experienced a significant decreasing trend in number of days over the last 50 years, and the last two decades have witnessed a much lower frequency of dust storms, in spite of the fact that it appears a little more frequently after 1997.

Fig. 5 Variations of tropical cyclone induced precipitation in China. **a.** Variations of total annual volume of precipitation (equivalent to areal rainfall amount); **b.** Variations of accumulated number of days with torrential precipitation due to tropical cyclone ($\geq 50 \text{ mm day}^{-1}$) (Unit: mm day^{-1}) (Ren, et al., 2006).

3 Understanding and attributing climate change in China

Understanding and attributing climate change is a key issue in the international climate research (IPCC, 2001). There are further advances in China for this field since the recent decade.

Similar to the international studies, most Chinese research also concentrates on the detection and attribution of climate warming in China for the 20th century. Some other studies focus on the understanding to the dimming of surface solar radiation in China and the pattern with wetter/cooler condition in South China and drier/warmer condition in North China for the last three decades than the averages of 1961~1990. In the attribution analysis, both natural and anthropogenic forcing is considered. The major methods of detection and attribution of climate change in China are both multiple climate models and the numerical-statistic methods based on the observed data (Wang et al., 2001; Zhao et al., 2005a,b; Luo et al., 2005; Ding et al., 2006).

3.1 Detection and attribution of annual mean temperature in China for the 20th century

According to the analyses of four sets of the observed data in China collected from both domestic and overseas studies (Lin et al., 1995; IPCC, 2001; Wang et al., 2001; Tang and Ren, 2005), similar to the global warming, it is concluded that warmer condition occurred certainly in China for the 20th century, especially for the last 50 years. The large differences among four observed datasets have been noticed before 1950 due to insufficient observed data in China. But four data have a high agreement with the correlation coefficients 0.76~0.90. The linear trends of temperature in China for four data from 1900 to 1999 are 0.35°C/100yr, 0.39°C/100yr, 0.72°C/100yr and 0.19°C/100yr, respectively. During the latter half of the 20th century (1950~1999), the linear trends are 0.73°C/50yr, 0.77°C/50yr, 0.92°C/50yr, and 0.64°C/50yr, respectively (Zhao et al., 2005a). All evidences point out the warming evidence in China, especially obvious warming for the last 50 years.

Paleoclimate studies of detection in China for the last 1000 years indicate the consistent

characteristics with the temperature change in the Northern Hemisphere. The 20th century might be a warmest century in China during the last 1000 years. But some research argued that Medieval-Warm Period might be much warmer than the 20th century. As we know, due to the limited proxy data in China for the last 1000 years, one only can say that the 20th century is a warm century for the last 1000 years (Zhao et al., 2005a). Whether or not it was the warmest century during the last millennium still needs to be further examined. It does also require more evidences to detect the warming status of the 20th century during the last 1000 years.

Figure 6 Evolutions of both observed and simulated annual mean temperature anomalies in China for the 20th century relative to 1961~1990, (a) About 40 human emission simulations (thick red - GCM7-GG, thick apricot - GCM7-GS, thick claret - GCM7-SRESA2, thick lilac - GCM7—SRESB2, thick black – observation, thick blue – GCM7 control run mean) (Zhao et al., 2005a), (b) 19 models with all forcing (thick black – observation, thick red – 19 models ensemble mean. Unit:°C) (Zhou and Yu, 2006b; Zhou and Zhao, 2006a)

Figure 6a provides the evolutions of the annual mean temperature anomalies in China for the 20th century as simulated by about 40 climate models, of which nine models are from China, with the various human emissions scenarios such as a doubled CO₂, 1% increasing greenhouse gases, increasing greenhouse gases, both greenhouse gases and sulfate aerosols increasing, IS92 scenarios, SRES scenarios (Zhao et al., 2005a). Figure 6a also gives the observation and the model control run for comparisons to the simulations of the various scenarios. First of all, it is found that

the model control run is not able to simulate the warming trend in China for the 20th century. The correlation coefficient between the observation and control run is -0.02. It means that there is not a significant relationship between the observation and model control run. Secondly, almost all models with the various human emission scenarios simulate the warming trends in China for the 20th century reasonably, especially the obvious warming trends for the last 50 years. The correlation coefficients between the observation and the multi-model ensemble mean is 0.47, the linear trends are 0.71°C/100yr and 0.90°C/50yr, respectively, which are similar to the observations (see Table 1) (Zhou and Zhao, 2006a). Therefore, the human emissions very likely explain the warming in China for the 20th century, especially for the last 50 years. The conclusion is in agreement with that of IPCC (2001).

Another research considers all radiative forcing by 19 global climate system models, of which two models are from China, to simulate the annual mean temperature anomalies changes in China for the 20th century. All radiative forcing included the changes of the solar radiation, volcanic activity, greenhouse gases, sulfate aerosols, black carbon, ozone, land-use/vegetation changes and others (see Figure 6b) (Zhou and Yu, 2006; Zhou and Zhao, 2006). The correlation coefficient of the annual mean temperature anomalies between the observation and multi-models ensemble for the 20th century is 0.55 which is better than that by only using the human emissions (see Table 1) (Zhou and Zhao, 2006a). It implies that the solar activity and volcanic activity, as well as the interactions between the air and sea might be the reasons of the temperature change in China for the first half of the 20th century.

Third numerical experiment (E3 in Table 1) uses the NCAR CAM2 driven by the observed sea surface temperature and sea ice provided by Hadley Center. The model simulates the annual

mean temperature in China for the 20th century with 12-member ensembles (Zhou and Yu, 2006b; Zhou and Zhao, 2006a). The model has a certain capability to reproduce the colder periods of 1900~1915 and 1970s and a warmer period of 1940s than the means of 1961~1990. But the model does not reproduce the obvious warming trends in China during the second half of the 20th century (see Table 1).

Table 1 Anomaly correlation coefficients (ACC) and linear trends of annual mean temperature in China for the 20th century between the observations and the numerical simulations (developed from Zhou and Zhao, 2006)

Numerical Experiments (E)	ACC	Linear trends (20 th century)	Trends (past 50 years)	Trends for 1960-1970	Trends for 1980-1999
CT (control run)	-0.02	0.11 °C/100yr	0.11 °C/50yr	0.10 °C/10yr	-0.02 °C/10yr
E1 (about 40 models with human emission)	0.47	0.71 °C/100yr	0.90 °C/50yr	-0.07 °C/10yr	0.38 °C/10yr
E2 (19 models with both natural and human forcing)	0.55	0.70 °C/100yr	0.85 °C/50yr	-0.06 °C/10yr	0.24 °C/10yr
E3 (12-member ensembles with observed SST and sea ice as input)	0.50	0.33 °C/100yr	0.01 °C/50yr	-0.12 °C/10yr	0.21 °C/10yr
Observed mean (4 data)		0.4~0.8 °C/100yr	0.5~0.9 °C/50yr	-0.55 °C/10yr	0.53 °C/10yr

The ensemble means of the human emissions experiments or all radiative forcing experiments are not able to simulate the warming range in China for the last decades of the 20th

century well. It implies that the simulated ensembles underestimate the real warming extents in China. It is also noticed that the models do not simulate the warm period of 1920~1940 in China reasonably (see Figure 6). Most of models and their ensemble average considerably underestimate this warming period, with 0.5-1°C lower than observed temperature.

3.2 Possible anthropogenic signals of climate changes in China for the last 50 years

There are the complete and accurate observed data in China for the last 50 years. It is possible to understand and detect the anthropogenic signals on the climate change in China (Zhai and Eskridge, 1997; Wang and Shi, 2001; Wu et al., 2004; Ren et al., 2005; Zhao et al., 2005b; Che et al., 2005; Shi et al., 2006). Based on the observed data of the annual mean surface solar radiation that have had the control of the quality at 122 stations of China for 1957~2000 (Che et al., 2005; Shi et al., 2006), and of the annual mean sunshine at 574 stations in China (Ren et al., 2005), it is found that the surface solar radiation and sunshine decreased (dimming) from 1961 to 1990, then increased (brightening) after 1990, but it was still lower than 1960's (see Fig.7a, b) (Zhao et al., 2005b; Ren et al., 2005; Che et al., 2005; Shi et al., 2006). Those phenomena were also found in the other countries of the world (IPCC, 2001).

Several attribution analyses explore the changes of the clouds, atmospheric water vapor and dust that had the physical feedback processes with the surface solar radiation. At first, according to the observed annual mean total cloud amounts at 466 stations of China from 1961 to 2000, it is found that the total cloud amounts have a reducing trend for the last 40 years. The total cloud amount was reduced by about 0.4 part of the total from 1977 to 1995 (see Fig.7c) (Ren et al., 2005). It implies that the reducing total cloud amount cannot explain the dimming surface solar

radiation. Secondly, based on the observed data of the annual mean dust-storm days in about 600 stations of China for the last 50 years, the annual mean dust-storm days were reduced by about -13 days /52a (Climatic Assessment Division of National Climate Center, personal communication, 2006). Therefore, the dimming surface solar radiation does not depend on the dust-storm days as well. Thirdly, the atmospheric water vapor in China is paid more attention. Calculating the annual and seasonal atmospheric water vapor in China from both surface and sounding observation at 378 stations of China from 1970 to 1990, it is found that the atmospheric water vapor in China increased obviously for the last several decades (see Figure 7d). The linear trend is 1.2%/10yr. The correlation coefficient between the atmospheric water vapor and surface air temperature in China is 0.61 which reached 99% confidence level (Zhai and Eskridge, 1997). It means that the warming climate in China caused the increasing atmospheric water vapor, therefore, it might be a reason of the dimming surface solar radiation in China.

Figure7 (a) Surface solar radiation change in China for 1957~2000 (Unit: MJ m⁻²) (Che et al., 2005; Shi et al., 2006) (b) Change of annual mean sunshine time for 1956~2002 (Unit: hours) (Ren et al., 2005), (c) Total cloud amount change for 1961~2000 (Unit: 0.1 part) (Ren et al., 2005). (d) Annual mean atmospheric water vapor change for 1970~1990 (Unit: mm) (Zhai and Eskridge, 1997)

With the developing economics and increasing industrial emissions in China, the air pollution becomes a serious problem. The sulfate and black carbon aerosols increase with time significantly.

The atmospheric aerosol optical depth increases obviously (Wang and Shi, 2001; Zhao et al., 2005a,b; Che et al., 2005; Shi et al., 2006). Those phenomena were more serious before 1990. Since 1990, the policy-makers and public have paid more attention to improve the air pollution, the atmospheric pollutants decreased with time. It implies that the change in anthropogenic aerosols in the atmosphere might be a reason of the dimming surface solar radiation before 1990 and brightening after 1990.

The further studies of the dimming surface solar radiation in China used the global and regional climate models nested to the atmospheric chemical models for providing the additional evidences. Most studies used the global or regional climate models to consider the effects of sulfate aerosols or black carbon, or greenhouse gases plus sulfate aerosols, black carbon and organic carbon on the climate change in China (Wang and Shi, 2001; Zhao et al., 2004; Wu et al., 2004; Zhao et al., 2005b). As some examples, three numerical simulations are shown in Figure 8. As simulated by the models, the increasing anthropogenic aerosols bring the increasing atmospheric aerosol optical depth and the reducing (dimming) surface solar radiation. It is estimated that the atmospheric aerosol optical depth is about 0.6~0.8 in the Sichuan basin and along the Yangtze River Valley, the surface air temperature is cooler by about -0.2~ -0.5°C for two simulations or slightly warmer for one simulation (Figure not shown) than the control runs or present time. But two models do not simulate the significant warming over North China (see Figure 8a.). Only one model with both increasing greenhouse gases and anthropogenic aerosols simulates the warming in North China reasonably (Figure not shown). For the rainfall simulations, two models with the anthropogenic aerosols do not reproduce the floods along the Yangtze River Valley and droughts in North China (see Figure 8b.). One model with both greenhouse gases and anthropogenic aerosols reproduces

the rainfall pattern in China, but it does not simulate the severe droughts over Shandong Province well and underestimates the wet range along the Yangtze River Valley (Figure not shown).

The climate characteristics of the more frequent floods with the cooler weather along the Yangtze River Valley and the sustaining droughts with the warmer weather in North China for the last 25 years than the period of 1961~1990 have been noticed. Plentiful evidences have revealed the role of the natural climate variabilities, such as decadal and interdecadal variabilities of East Asian summer monsoon, the periodicities and transitions of rainfall and temperature changes in China, abrupt (fast) climate change, the impacts of NAO(North Atlantic Oscillation), AO(Arctic Oscillation), AAO(Antarctic Oscillation), PDO (Pacific Decadal Oscillation), ENSO (El Niño-Southern Oscillation), and snow cover on the climate pattern in China. Upper part of Table 2 summarizes those studies (Wang, 2001; Zhao et al., 2005b), while the possible anthropogenic signals are given in bottom part of Table 2. It can be seen from Table 2 that the increasing greenhouse gases contribute to enhance the East Asian summer monsoon and to warm and wet climate in China. The black carbon and land-use changes might produce the weakening of the East Asian summer monsoon with the pattern of floods in South and droughts in North China. The sulfate aerosols might bring the lower temperature and floods along the Yangtze River Valley. The attribution analyses of the anthropogenic factors such as greenhouse gases emitted into the atmosphere of the globe and the sulfate aerosols and black carbon, as well as “Atmospheric brown clouds” produced by local areas is even contradictory. Therefore, there does not still exist a consensus on the possible mechanisms that caused the patterns of the climate change in China for the last 25 years. More research should be carried out in future.

Table2 Effects of both natural climate variability and anthropogenic factors on floods/cool over the Yangtze River Valley and droughts/warm over North China for the last 25 years relative to 1961~1990 (Zhao et al., 2005b)

Natural climate variability	Contribution to Asian summer monsoon	Climate consequence in China
PDO+ENSO	weaker	North China drought/South China floods
AO in spring	weaker	Strong rainfall over Yangtze river valley and southern Japan
Periodicity and transition of T/Pr	weaker	Wetter/cooler over Yangtze River valley, droughts in North China
Abrupt climate change	weaker	Floods over Yangtze River valley
IOD	Significant	Insignificant
Eurasian snow cover	stronger	Inconsistent
Tibetan Plateau snow cover	weaker	North China drought/South China flood
Anthropogenic factors	Contribution to Asian summer monsoon	Climate consequence in China
Greenhouse gases increasing (global warming)	stronger	Warmer and wetter
Sulfate aerosols increasing	weaker	Lower temperature and floods in

		Yangtze River Basin
Black carbon aerosol increasing	weaker	Droughts in North China/floods in South China
Greenhouse effects + aerosols (brown clouds) increasing	likely weaker in the last 25 years	Warmer/drier in North China, floods along Yangtze River Valley
Land use change (vegetation degeneration)	weaker	Droughts in North China, floods in South China

Figure 8 Geographical distributions of annual mean temperature (left, unit: °C) and precipitation (right, unit: mm),(a) and (b) as simulated by the TEACOM regional climate model with the black carbon (sensitivity minus control) (Wu et al., 2004).

3.3 Understanding anthropogenic effects on climate change in China

Attribution analyses of climate change is based on demonstration that the detected observed change is consistent with model estimated responses to both natural and anthropogenic forcing as well as demonstration that the detected observed change is not consistent with alternative, physically plausible explanations that exclude these forcing.

As proposed above, a broad range of climate variables indicates the evidences of the possible anthropogenic signals in China. As summarized in Table 3 in Conclusions, the observed and simulated evidences of climate change in China for the 20th century have shown the significant contribution of anthropogenic activities. It is very likely that greenhouse gas forcing has been the dominant cause of the observed warming in China over the last 50 years. Both climate warming which brings the increasing atmospheric water vapor and the increasing anthropogenic aerosols might be a reason of the dimming surface solar radiation in China. But we cannot definitely answer whether the anthropogenic forcing has caused the changes of patterns of rainfall, floods/droughts in China, and East Asian monsoon, as well as typhoons/tropical cyclones. It needs the further studies.

4. Projections of climate change over China in the future

4.1 Surface air temperature change in the future

For recent years, a number of the new atmosphere-ocean general circulation models (AOGCMs) with including effect of only greenhouse gases (GG), greenhouse gases plus aerosol (GS), SRES A2 and B2 scenarios have made the projections of the climate change for the 21st century. Using these AOGCM simulations, we analyzed climate change over China in the future (Hu et al., 2000; Zhao and Xu, 2002; Xu, 2002; Bueh et al., 2003; Zhao, 2003; Ding and Xu, 2003; Xu et al., 2003a,b,c; Xu et al., 2005; Kimoto, 2005). In recent years, Chinese scientists have also developed an atmosphere-ocean-land general circulation model with a high resolution of T63 (named NCC/IAP T63) to simulate climate change in the past 100 years and to project future climate change (Xu, 2002; Ding and Xu, 2003).

Figure 9 shows the time evolution of the annual average temperature anomaly for the 20th and 21st century relative to the years of 1961~1990 as projected by 40 AOGCMs. It indicates that the models with the greenhouse gases (GG, GS, A2, B2) simulated the warming trend which is very similar between the observation and simulations. It means that the one of the warming reasons for the 20th century over China is likely the increasing greenhouse gases made by the anthropogenic emissions, especially for the last 50 years. The results indicate that the temperature will further increase by 1.5~2.1°C in the 2020 year and 2.3~3.3°C in the 2050 year, warming of 3.9~6.0°C by 2100. The linear trends of the Chinese mean temperature in the 21st century will be larger than global and lower than the East Asia region.

For the different season over China, under SRES scenarios A2 and B2, the temperature will increase for four season, most obvious in the winter and spring and smaller in the summer and autumn; the temperature will increase by 5.6°C and 4.0°C over whole China by the end of 21st, respectively.

For the geographical distributions of annual average temperature for 2020 year, 2050 year and 2070 year, the results show that warming is 1.2~1.8°C in the 2020 year with GG scenario, especially in Northeast and western area of China; the warming is smaller in GS scenario which is from 1.0°C to 1.5°C, warming is largest in North China, Northwest and the northern part of Northeast China; the warming is 0.6~1.8°C and 0.9~2.1°C A2 and B2 scenarios, respectively. The warming will be larger in 2050 year and it will be 2.4~3.9°C for GG, 1.5~3.0°C for GS, 1.8~3.9°C for A2 and 1.8~3.3°C for B2. The temperature increasing is double compared to 2020 year. The warming is most obvious over North China, Northwest China and Northeast China.

Figure 9 Simulated and projected temperature change of China (1900-2100) by multi-models with various human emission scenarios. (CCC-GG, CCSR/NIES-GG, CSIRO-GG, DKRZ-GG, GCM7-GG, GFDL-GG, HADL-GG, LASG/IAP2-GG, NCC/IAP T63-GG, NCAR-GG, CCC-GS, CCSR/NIES-GS, CSIRO-GS, DKRZ-GS, GCM7-GS, GFDL-GS, HADL-GS, LASG/IAP2-GS, LASG/IAP2-GSS, NCC/IAP T63-GS, NCAR-GS, RegCM/CN-GG, RegCM/CN-GS, CCSR/NIES2-A1, CCSR/NIES2-A2, CCSR/NIES2-B1, CCSR/NIES2-B2, CCSR/NIES2-SRES4, CCC-A2, CSIRO-A2, ECHAM4/OPYC-A2, GFDL-A2, HADL3-A2, NCAR-A2, CCC-B2, CSIRO-B2, ECHAM4/OPYC-B2, GFDL-B2, HADL3-B2, NCAR-B2, GCM-SRES, NCC/IAP T63-A2, NCC/IAP T63-B2).(Black-thick curve: observation, provided by Wang Shaowu and Gong Daoyi; Red-thick curve: average in GG scenario; Orange-thick curve: average in GS

scenario; Brown-thick curve: average in A2 and B2 scenarios; Yellow-thick curve: simulated result by NCC/IAPT63)

There are different warming condition from south to north over whole China. The warming is obviously larger in North than South China. In the same latitude, the temperature increasing is smaller in the eastern coastal areas than inland area.

4.2 Precipitation change in the future

The reasons of the precipitation change are more complicated than the temperature by the effect of human activities. There are different future trends depending on different models and scenarios, especially for greenhouse gases plus aerosol scenarios (GS). But, in summary, the precipitation will increase for the most models simulations by GG, A2 and B2 scenario, the increasing of precipitation will be 20% over China by GG and A2 in the end of 21st, and 10% by B2. Figure 10 shows the change of annual average precipitation anomalies from 1900 to 2100 year for seven models by different scenarios. The results indicate that the precipitation will increase for most models and scenarios, especially for GG and A2, but precipitation will decrease for some models, especially for the first 50 year of 21st century.

Figure 10 Change of precipitation for different models and emission scenarios of greenhouse gases and aerosols from 1900~2100 year (Unit: %, Ding et al., 2007)

5 Conclusions

Following conclusions can be drawn from above discussions:

(1) Main feature of the climate change in China during last 100 years is characterized by the climate warming which is consistent with the global warming trend. Based on the analysis of observed maximum and minimum temperature during the period of 1905-2001 mostly in East China, the mean temperature increase rate was $0.81^{\circ}\text{C}/100\text{yr}$. But, if daily mean temperature at the stations in western China and some proxy data are included, the mean temperature increase rate for 1880-2002 was $0.58/100\text{yr}$. Therefore, the warming rates are different due to different data sources and analysis methods. Overall, the warming range in China for the last 100 years is taken as $0.5\text{-}0.8^{\circ}\text{C}$, slightly higher than the global warming range ($0.6\pm 0.2^{\circ}\text{C}$). During this period, there occurred two warming episodes: 1920's-1940's and 1980's-present.

There has been no long-term trend for precipitation for last 100 years in East China. However, since mid-1950's, the precipitation in China has shown a slight increase, consistent with the global trend. The inter-decadal change in precipitation amount in China has two dominant modes of 20-and 80-years. The North China had much precipitation in the period from 1950's to the late 1970's and then shifted to reverse precipitation condition in the period from 1980's to 1990's. In Northwest China the precipitation has started increasing significantly since mid-1980's, with Xinjiang Autonomous Region being most significant (the precipitation increase rate of $10\text{-}15\%/10\text{yr}$).

(2) As the climate warms up, the intensity and frequency of occurrence of the extreme weather and climate events have increased, including rise of extreme minimum temperature, decrease in temperature diurnal variation, and increase and intensification in extreme precipitation events. Especially, in 1990's, the total precipitation amount, extreme precipitation amount and

intensity of precipitation events tended to increase. The area and intensity of drought events has also increased. In addition, the frequency of occurrence of heat waves in summer has increased, the day number of frost has decreased, the frequency of cold waves has decreased, the probability of occurrence of snow disasters has increased and dust-storms tend to decrease.

(3) Based on detections and projections by using climate models developed by international communities and China, China will continue to warm, especially in winter and North China, and will have a wetter condition, especially in Northeast and Northwest China in the 21st century, due to increase in emission of greenhouse gases. The future climate condition in China will be considerably different from that in the 20th century.

Warming will continue over China in the 21st century by 3~5°C, and warming is more obvious than 20th century, especially for North China and Northwest China. Annual mean temperature warming will be 1.5~2.1°C in the 2020 year, 2.3~3.3°C in 2050 year, and 3.9~6.0°C in 2100 year. Synthesizing all scenarios, the results show that it will possibly become wet over most part of China, especially in Northeast and Northwest China, it will possibly become dry over central part area of China. For example, the precipitation increase is most obvious in western China. Especially for GS scenarios, the precipitation will increase 20% in Northwest China, but the precipitation will decrease in south of Yangtze River; In 2050 year, the precipitation increase will become more obviously with greenhouse gases increasing, it will increase by 15~40%. With human emission increasing, the winter monsoon will weak over East Asia, while the summer monsoon will intensify (Table 3)

Table 3 Detection of climate change in China for the 20th century and projection in the 21st century due to the human emissions (based on this paper and Zhao et al., 2005a, b; Ding et al., 2006)

Climate phenomena	Observed evidences in 20th century	Simulated evidences with anthropogenic emissions in 20th century	Projected climate change due to human emissions in 21st century
Increase of surface air temperature	Trends: 0.5~0.8°C/100y 0.6~0.9°C/50y Distributions: obvious warming of 0.8°C/100y in North China	Trends: 0.3~1.6°C/100yr 0.6~1.6°C/50yr Distributions: obvious warming of 0.5~1.8°C/100yr in North China (about 40 simulations)	3. 0~5.0°C/100yr, Distributions: obvious warming of 4.5~7.5°C/100yr in North China (about 40 projections)
Increase of Tmax	Trends: 0.5°C/49y	Trends: 0.5~0.8°C/50yr (about 12 simulations)	Trends: 4.1~5.0°C/50yr (about 12 projections)
Increase of Tmin	Trends: 1.4°C/49y	Trends: 0.7~1.0°C/50yr (about 12 simulations)	Trends: 4.1~4.9°C/50yr (about 12 projections)
Other warming Evidences	17 warm winters since 1986 longer hot summer spells in some parts of China	12 warm winter since 1986 nine warmer summers for 1993~2002 (about 40 simulations)	98~99 warmer winter and 100 warmer summer in 21 st century than averages of 1961~1990
Precipitation change	Trends: 3%/99yr 2%/49yr	-14 ~ 21%/100yr -6 ~ 29%/50yr (about 40 simulations)	11 ~17%/100yr (about 40 projections)
Patterns of floods/droughts	More floods over Yangtze river valley, and more droughts in Huabei for the last 25 years	Wetter/cooler over Yangtze river valley, and Drier/warmer over North China for 1976-2000 minus 1961-1990 (about 5~6 simulations)	Wetter by 10~20% in Northwest, wetter by 15~25% in Northeast, wetter by 10~15% in Huanan, drier by 0~2% in Yangtze delta and Bohai coasts (about 10 and more projections)
Heavy rain and rainstorm	Increasing along Yangtze river and parts of South China, decreasing over Huaihe river and middle and lower branches of Yellow river	No obvious change	Increasing along Yangtze river, parts of South China and NW, NE, decreasing over parts of Liaoning (about 2~3 projections)
East-Asian Winter monsoon	Weakened	Weakened (one AOGCM with SRES)	Weakening (one model with SRES)
East-Asian Summer monsoon	Weakened obviously	weakened (one AOGCM with SRES)	Enhancing (one model with SRES)

Typhoons/tropical cyclones influence on China	Decreasing by linear trend: -3.9times /50yr (1951-2000)	Decreasing by linear trend: -3.0times /50yr (1951-2000) (one AOGCM with SRES)	Annual total typhoon numbers decreasing by -5 ~ -10 times/100yr (one AOGCM with SRES), annual total typhoon numbers landing China increasing (one regional model with CO ₂ increasing)
SST over ENSO regions	Nino3.4: 0.33°C/53yr	0.83°C/53yr (one AOGCM with SRES)	More warm anomalies than warm pool (one AOGCM with SRES)
SST over warm pool	warming	Warming (one AOGCM with SRES)	Warming (one AOGCM with SRES)
Surface solar radiation	dimming by 3.1W/m ² /10yr	Weakening effects (2~3 simulations with black carbons)	No calculations
Atmospheric water vapor	Increasing by 1.2%/10yr	No simulations	No calculations

Acknowledgments: This study was funded by the Ministry of Science and Technology of China (2001BA611B-01), SCSMEX Project (1996-2003) and the Ministry of Water Resource of China. A number of investigators have contributed to the results summarized in this paper. They include Guoyu Ren, Panmao Zhai, Guoli Tang, Li Zhang, Hongbin Liu, Fumin Ren, Xukai Zou, Ziyang Chu and so on. Authors also thank Ms. Zhang Jin and Ms. Song Yafang for their much assistance in preparation of this paper.

(Lab for Climate Studies, National Climate Center, CMA, 46 South Zhongguancun Dajie, Beijing 100081, China)

Caption of Figure

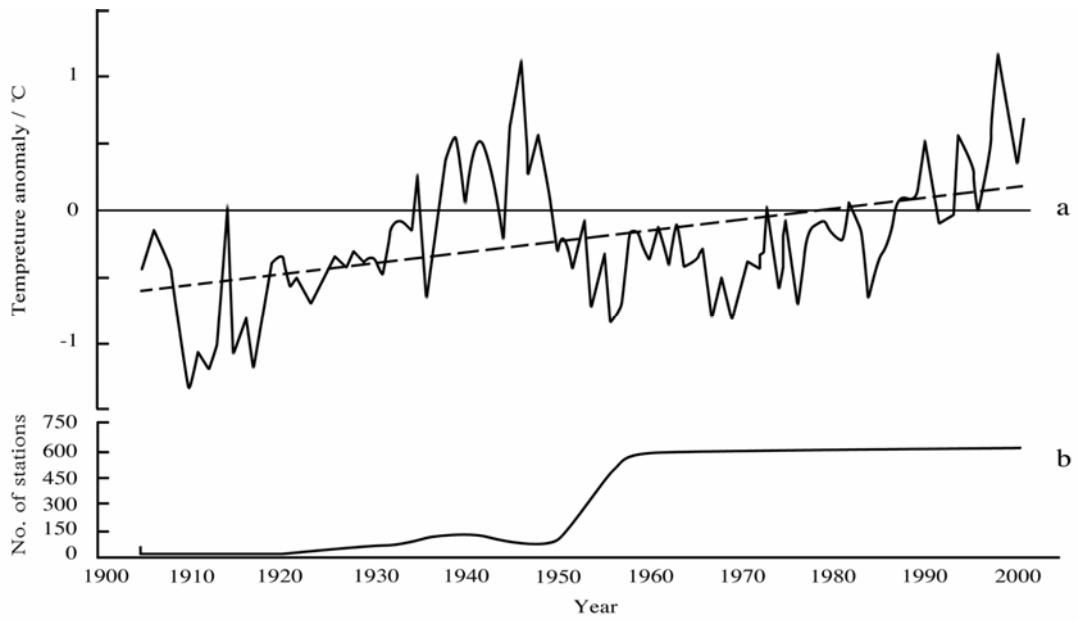


Figure 1 Change in country-averaged annual mean surface air temperature anomalies in China during 1905-2001 (a: temperature anomalies; b: number of observations. Unit: °C) (Tang and Ren, 2005)

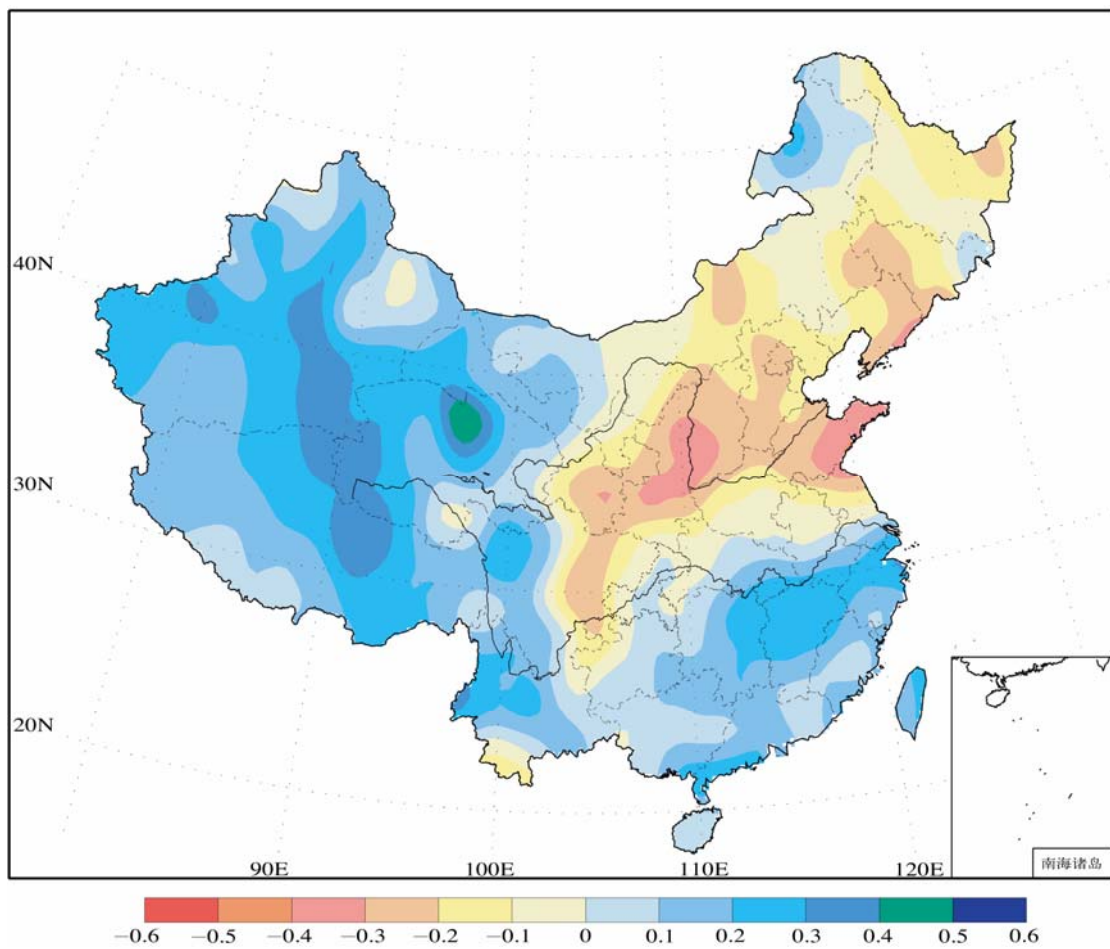


Figure 2 Tendency of precipitation over China (1956-2002). Blue color: positive trend; Red color: negative

trend. (Ren et al., 2005)

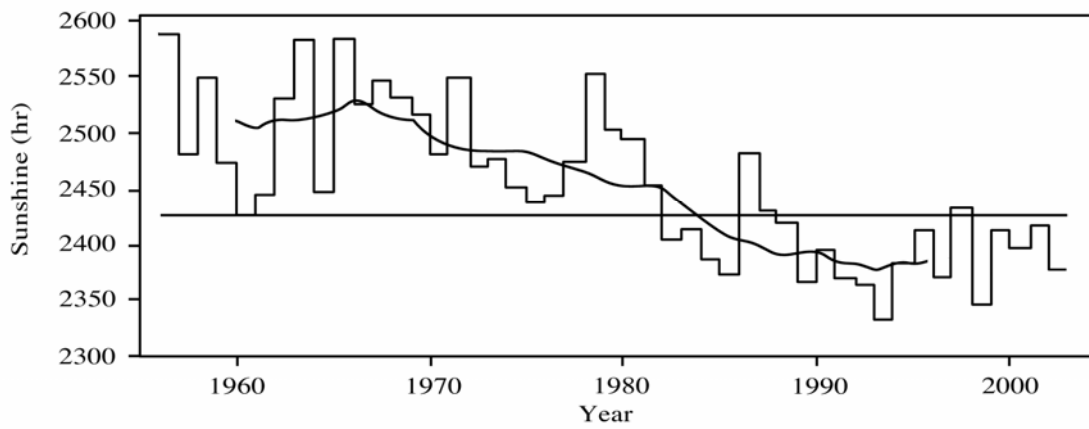


Figure 3 Change in national average sunshine duration during 1956-2002 (Unit: hours) (Ren et al., 2005)

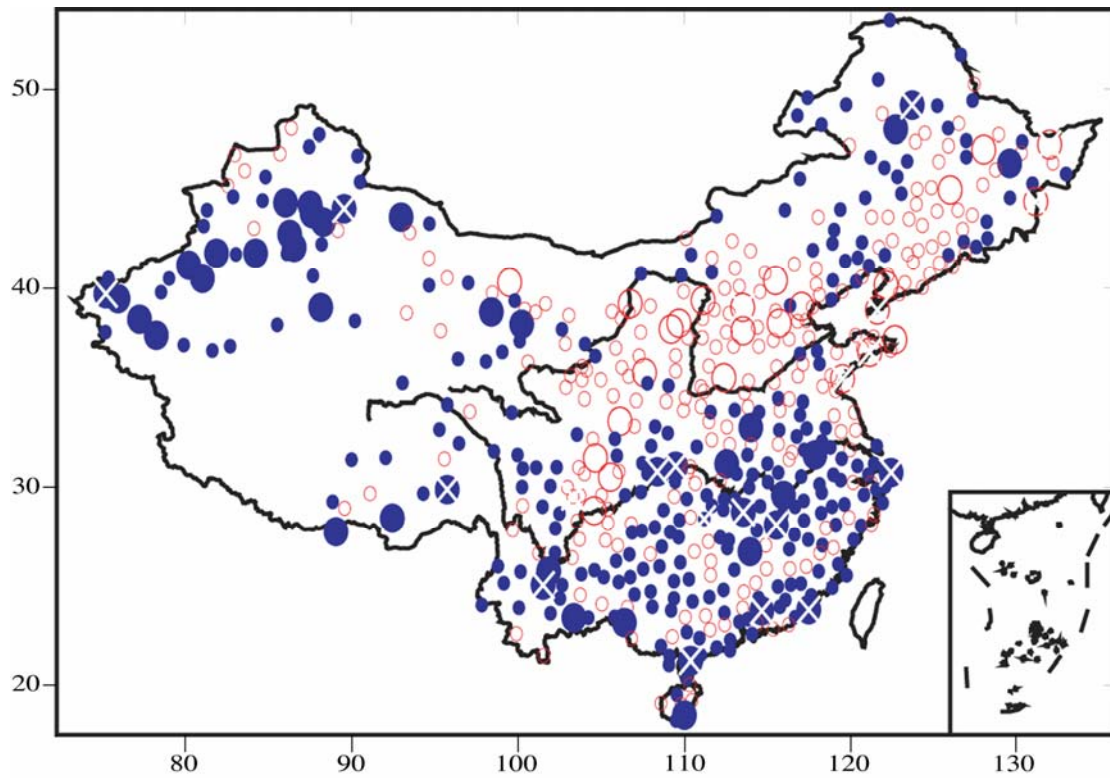


Figure 4 Trends of days with extreme strong rainfall for 1951-2000 in China. Solid and open circles indicate increase and decrease respectively, and sizes of the circles are scaled to strength of the trends. (Ding et al., 2006)

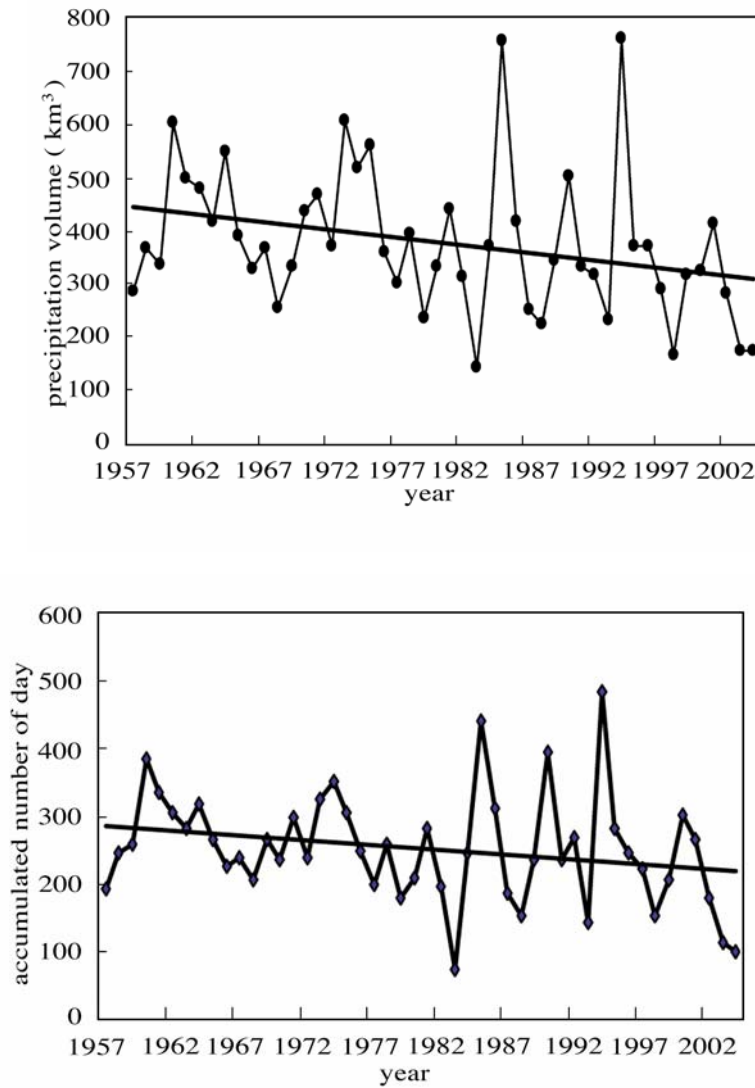


Figure 5 Variations of tropical cyclone induced precipitation in China. **a.** Variations of total annual volume of precipitation (equivalent to areal rainfall amount) ; **b.** Variations of accumulated number of days with torrential precipitation due to tropical cyclone ($\geq 50\text{mm/day}$) (Unit: mm day^{-1}) (Ren, et al., 2006).

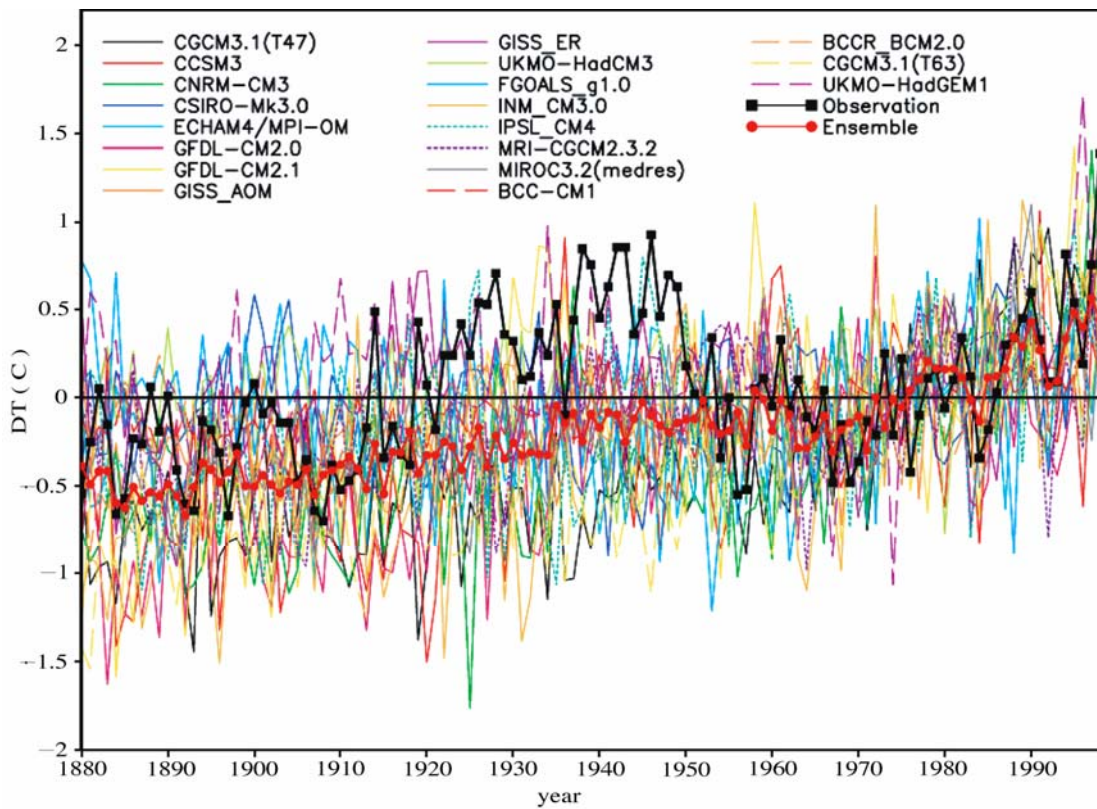
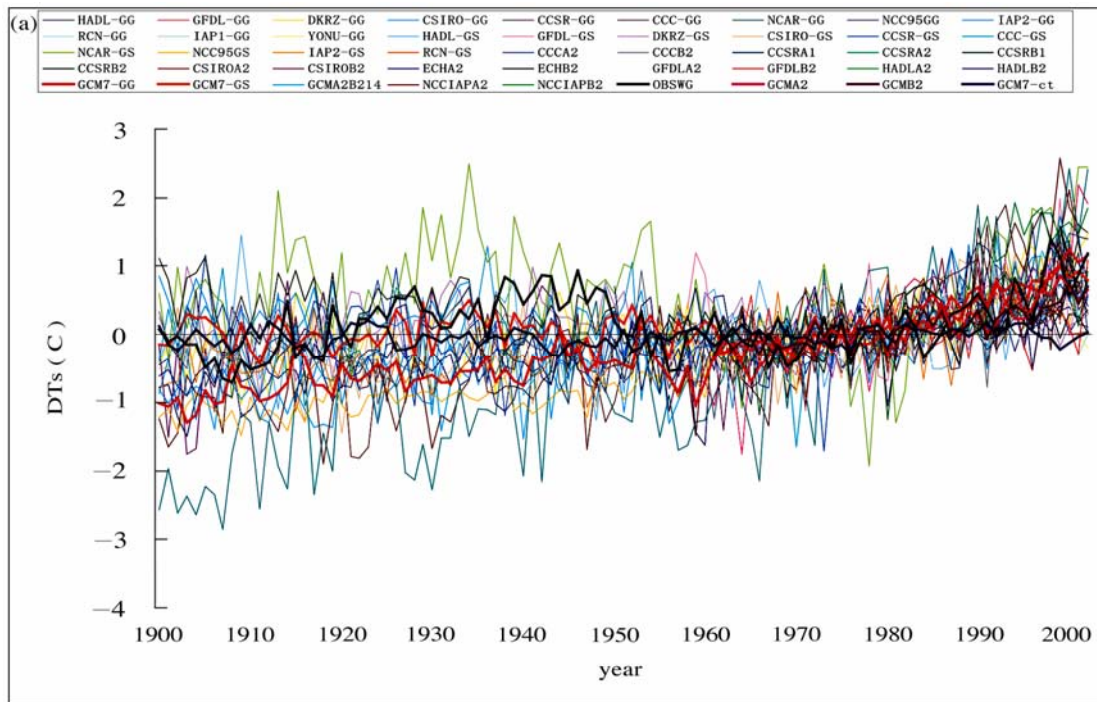


Figure 6 Evolutions of both observed and simulated annual mean temperature anomalies in China for the 20th century relative to 1961~1990, (a) About 40 human emission simulations (thick red - GCM7-GG, thick apricot - GCM7-GS, thick claret - GCM7-SRESA2, thick lilac - GCM7—SRESB2, thick black – observation, thick blue –

GCM7 control run mean) (Zhao et al., 2005a), (b) 19 models with all forcing (thick black – observation, thick red – 19 models ensemble mean. Unit: °C) (Zhou and Yu, 2006b; Zhou and Zhao, 2006a)

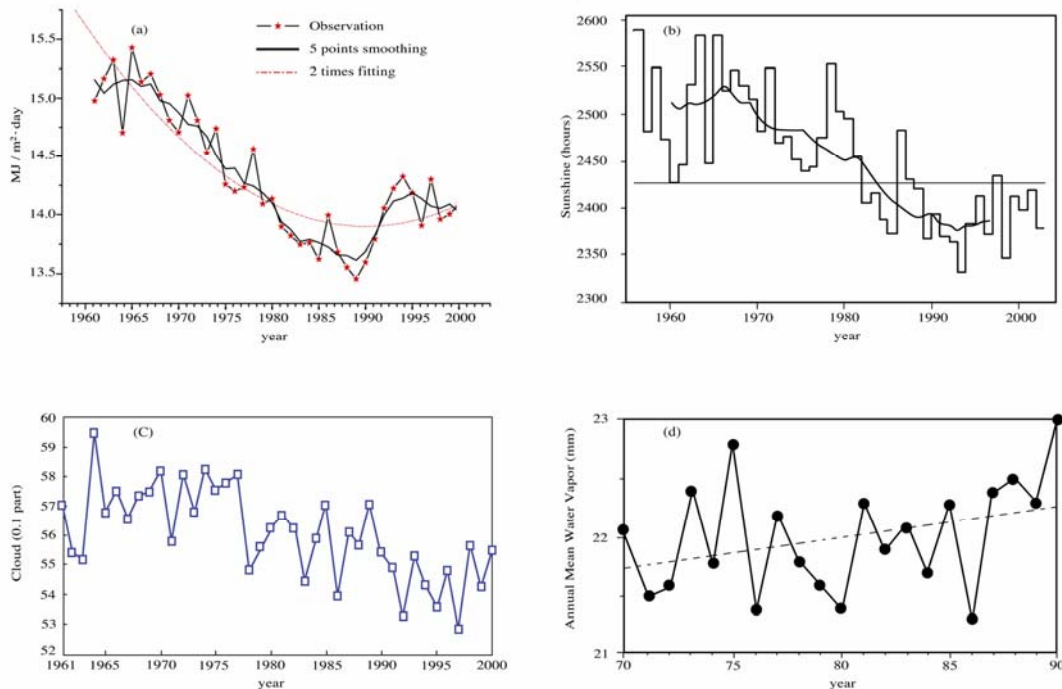


Figure7 (a) Surface solar radiation change in China for 1957~2000 (Unit: MJ/m²) (Che et al., 2005; Shi et al., 2006) (b) Change of annual mean sunshine time for 1956~2002 (Unit: hours) (Ren et al., 2005), (c) Total cloud amount change for 1961~2000 (Unit: 0.1 part) (Ren et al., 2005). (d) Annual mean atmospheric water vapor change for 1970~1990 (Unit: mm) (Zhai and Eskridge, 1997)

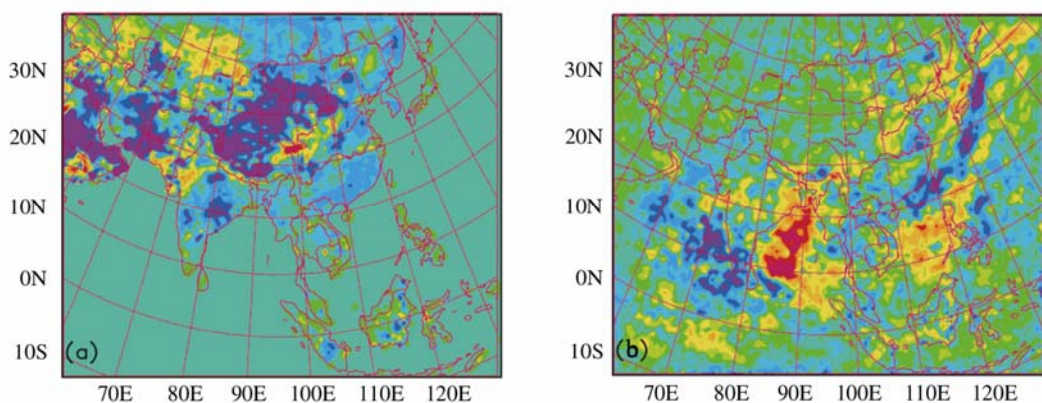


Figure 8 Geographical distributions of annual mean temperature (left, unit: °C) and precipitation (right, unit: mm), (a) and (b) as simulated by the TEACOM regional climate model with the black carbon (sensitivity minus

control) (Wu et al., 2004).

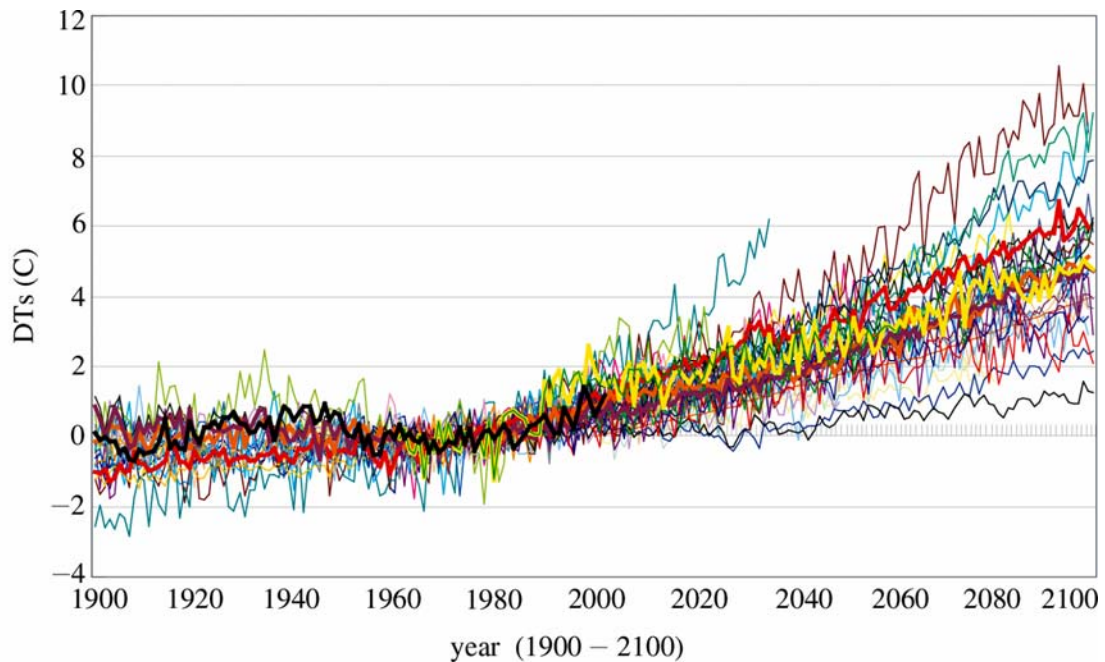
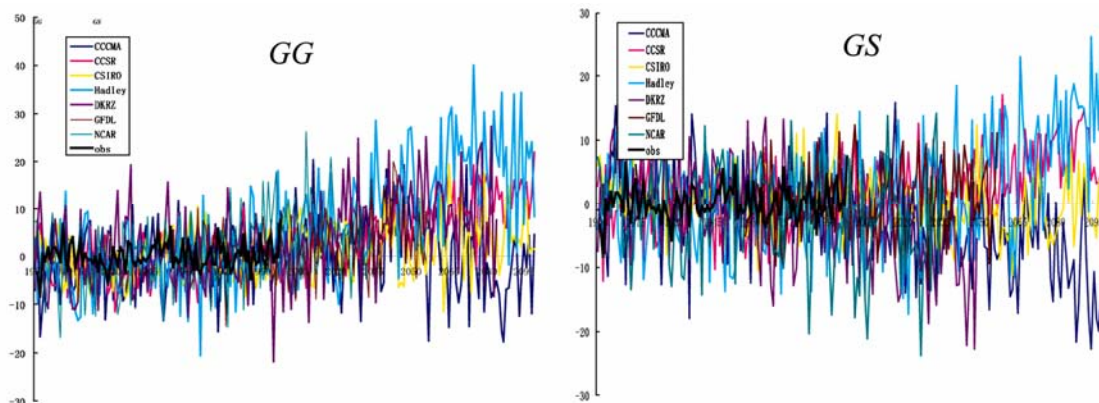


Figure 9 Simulated and projected temperature change of China (1900-2100) by multi-models with various human emission scenarios. (CCC-GG, CCSR/NIES-GG, CSIRO-GG, DKRZ-GG, GCM7-GG, GFDL-GG, HADL-GG, LASG/IAP2-GG, NCC/IAP T63-GG, NCAR-GG, CCC-GS, CCSR/NIES-GS, CSIRO-GS, DKRZ-GS, GCM7-GS, GFDL-GS, HADL-GS, LASG/IAP2-GS, LASG/IAP2-GSS, NCC/IAP T63-GS, NCAR-GS, RegCM/CN-GG, RegCM/CN-GS, CCSR/NIES2-A1, CCSR/NIES2-A2, CCSR/NIES2-B1, CCSR/NIES2-B2, CCSR/NIES2-SRES4, CCC-A2, CSIRO-A2, ECHAM4/OPYC-A2, GFDL-A2, HADL3-A2, NCAR-A2, CCC-B2, CSIRO-B2, ECHAM4/OPYC-B2, GFDL-B2, HADL3-B2, NCAR-B2, GCM-SRES, NCC/IAP T63-A2, NCC/IAP T63-B2). (Black-thick curve: observation, provided by Wang Shaowu and Gong Daoyi; Red-thick curve: average in GG scenario; Orange-thick curve: average in GS scenario; Brown-thick curve: average in A2 and B2 scenarios; Yellow-thick curve: simulated result by NCC/IAPT63)



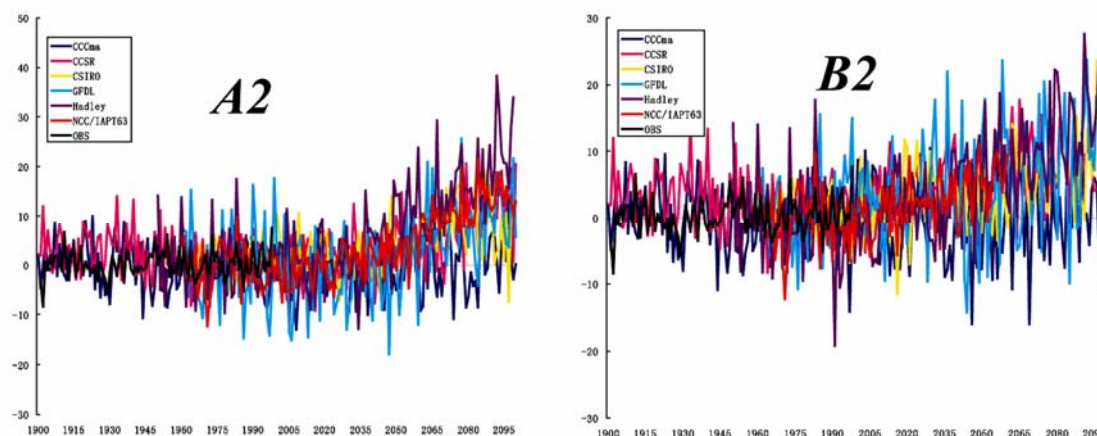


Figure 10 Change of precipitation for different models and emission scenarios of greenhouse gases and aerosols from 1900~2100 year (Unit: %, Ding et al., 2007)

References

- Bueh, C., U. Cubasch, Lin Yonghui, and Ji Liren, 2003: The change of North China climate in transient simulations using the IPCC SRES A2 and B2 scenarios with a coupled atmosphere-ocean general circulation model. *Adv. Atmos. Sci.*, **20(5)**, 755-766.
- Che, H.Z., G.Y. Shi, X.Y. Zhang, R. Arimoto, J.Q. Zhao, L. Xu, B. Wang and Z.H. Chen, 2005: Analysis of 40 years of solar radiation data from China, 1961~2000. *Geophys. Res. Lett.*, **32**, L06803, doi: 10.2929/2004GL022322.
- Chen Longxun and Zhu Wenqing, 1998: Study on climate change of China over the past 45 years. *Acta Meteorologica Sinica*, **56 (3)**: 257-271. (in Chinese)
- Chu Ziyong, Ren Guoyu, Shao Xuemei and Liu Hongbin, 2005: A preliminary reconstruction of mean surface air temperature over the last 1000 years in China. *Climatic and Environmental Research*, **10(4)**, 826-836. (in Chinese)
- Chu Ziyong, and Ren Guoyu, 2005: Effect of enhanced urban heat island magnitude on average surface air temperature series in Beijing region. *Acta Meteorologica Sinica*, **63 (4)**, 534-540.
- Ding Yihui, and Dai Xiaosu, 1994: Temperature change during the recent 100 years over China. *Meteorology*

Monthly, **20 (12)**: 19-26.(in Chinese)

Ding Yihui, and Xu Ying, 2003: The project of Climate Change in the futury. Research Report of the Thenth Five Plan Project , Beijing

Ding Yihui, and Dong Wenjie, 2005: Asian monsoon and its effect on China climate and environmental changes.

Changes of Climate and Environment in China (Vol. 1), Qin, Dahe, Ding, Yihui and Su, Jilan eds, Science Press, 398-454.

Ding Yihui, and Coauthors, 2006: National Assessment Report of Climate Change (I): Climate change in China and its future trend. *Advances in Climate Change Research*, **2 (1)**, 3—8. (in Chinese)

Ding, Yihui, and Coauthors, 2007: History and future trend of climate change in China. *National Assessment Report on Climate Change, Vol. 1*, Beijing: Science Press,3-176. (in Chinese)

Ge, Quansheng, Zheng Jingyun, Fang Xiuqi, Man Zhimin, Zhang Xueqin, Zhang Piyuan and Wang Wei-Chyung, 2003: Winter half-year temperature reconstruction for the middle and lower reaches of the Yellow River and Yangtze River, China, during the past 2000 years. *The Holocene*, **13**, 995-1002.

Gong D. and S.Wang, 2000: Severe summer rainfall in China associated with the enhanced global warming. *Climate Res.*, **16(1)**,51-59.

Guo, Jun. and Ren, Guoyu, 2005: Characteristics and possible causes of pan-evaporation change of the Huang-Huai-Hai Plain, China. *Advance in Water Sciences*, **16(5)**, 666-672. (in Chinese).

Hu, Z.-Z., L. Bengtsson and K. Arpe, 2000: Impact of global warming on the Asian winter monsoon in a coupled GCM. *J. Geophys. Res. (Atmosphere)*, **105(D4)**, 4607-4624.

Hu, Z.-Z., S. Yang, R.R. Wu, 2003: Long-term climate variations in China and global warming signals, *Journal of Geophysical Research*, **108(D19)**, 4614-4626.

IPCC2001. Climate Change 2001: The Scientific Basis. Contribution of Working Group I to the Third Assessment Report of the Intergovernmental Panel on Climate Change. J.T.Houghton and Ding Yihui, et al., eds.

Cambridge University Press, Cambridge, 881pp

Jones, P. D. and Moberg, 2003: A. Hemispheric and large-scale surface air temperature variations: An extensive revision and an update to 2001. *J. Climate*, **16**, 206-223.

Jones, P. D., and M. Hulme, 1996: Calculating regional climatic time series for temperature and precipitation: methods and illustrations. *International Journal of Climatology*, **16**, 361-377.

Kimoto, M., 2005: Simulated change of the East Asian circulation under the global warming scenario. *Geophys. Res. Lett.*, **32**, L16701, doi:10.1029/2005GL023383.

Li Xiaowen, Zhou Xiuji, Li Weiliang, and Chen Longxun, 1995: The cooling of Sichuan Province in recent 40 years and its probable mechanisms. *Acta Meteorologica Sinica*, **9(1)**, 57-68.

Lin Xuechun, Yu Shuqiu, and Tang Guoli, 1995: Temperature series in China for the last 100 years. *Scientia Atmospherica Sinica*, **15(5)**, 525-534. (in Chinese)

Luo Yong, Ding Yihui, Zhao Zongci, Gao Xuejie, Xu Ying, and Xie Zhiren, 2005: Chapter 10 Projection of the future anthropogenic climate change in China. *Assessment of Climate and Environment Changes in China (I): Climate and environment changes in China and their projection*, Qin Dahe, Ding Yihui, Su Jilan and Wang Sumin, eds. China Science Press, 507—555. (in Chinese)

Ren Guoyu, Guo Jun, Xu Mingzhi, Chu Ziyang, Zhang Li, Zou Xugai, Li Qingxiang, and Liu Xiaoning, 2005: Climate changes of Mainland China over the past half century. *Acta Meteorologica Sinica*, **63 (6)**, 942-956. (in Chinese)

Ren Guoyu, and Guo Jun, 2006: Change in pan evaporation and the influential factors over China: 1956~2000. *Journal of Natural Resources*, 21(1),31-44. (in Chinese)

Ren Fumin, Wu Guoxiong, Dong Wenjie, Wang Xiaoling, Wang Yongmei, Ai Wanxiu, and Li Wijing,2006: Change in tropical cyclone precipitation over China, *Geophy. Research Letters*, **33**, L20702,

doi:10.1029/2006GL027951.

Shao Xuemei, Huang Lei, Liu Hongbin, Liang Eryuan, Fang Xiuqi, and Wang Lili, 2004: Annual precipitation change of the past 1000 years as reconstructed from tree-rings on eastern rim of the Caidamu Basin.

Sciences in China (D), **34 (2)**, 145-153. (in Chinese)

Shi Guangyu, Tadahiro Hayasaka, Chen Zhihua, Wang Biao, Zhao Jianqi, Che Huizheng, and Xu Li, 2006: Quality detection of surface solar radiation data and its impacts on the long-term change trends. *Journal of Geophysics*, (submitted)

Tang Guoli and Ren Guoyu, 2005: Reanalysis of surface air temperature change of the past 100 years over China.

Climate and Environmental Research, **10 (4)**, 791-798. (in Chinese)

Wang Shaowu, Ye, Jinling, and Gong Daoyi, 1998: Construction of annual mean temperature series of the last 100 years over China, *Journal of Applied Meteorological Science*, **9(4)**, 392-401.

Wang S., and D. Gong, 2000: Enhancement of the warming trend in China. *Geophys. Res. Lett.*, **27(16)**: 2581-2584.

Wang Shaowu, 2001: *Advances on Modern Climatic Research*, China Meteorological Press, Beijing, 458 pp (in Chinese)

Wang Xihong, and Shi Guangyu, 2001: Numerical investigation on the climate effects of anthropogenic sulfate aerosols. *Plateau Meteorology*, **20(3)**, 258-263. (in Chinese)

Wu Jian, Jiang Weimei, Fu Congbin, Su Bingkai, Liu Hongnian, and Tang Jianping, 2004: Simulation of the radiative effect of black carbon aerosols and the regional climate responses over China. *Adv. Atmos. Sci.*, **21**, 637-649.

Xu Ying, 2002: A study of numerical simulation of impact of human activities on climate change. Ph.D. dissertation. Beijing: Chinese Academy of Meteorological Sciences.

Xu Ying, Ding Yihui, Zhao Zongci, and Zhangjin, 2003a: A Scenario of Seasonal Climate Change of the 21st

- Century in Northwest China. *Climatic and Environmental Research*, **8**,19~25. (in Chinese)
- Xu Ying, Ding Yihui, and Zhao Zongci, 2003b: Scenario of Temperature and Precipitation Change in Northwest Chinaduo to Human Activity in the 21st Century. *Journal of Glaciology and Geocryology*, **25**, 327-330. (in Chinese)
- Xu Ying, Ding Yihui, and Zhao Zongci, 2003c: Prediction of climate change in middle and lower reaches of the Yangtze River in the 21st century, *Journal of Natural Disasters*, **13**, 25-31. (in Chinese)
- Xu Ying, Luo Yong, Zhao Zongci, Gao Xuejie, Liu Yanju, Wang Lanning, and Wei Min, 2005: Detection of climate change in the 20th century by the BCC-AGCM1.0 model. *Special Report on Climate Change*, **6**, 1-7.
- Zeng Zhaomei, Yan Zhongwei, and Ye Duzheng, 2001: Regions of most significant temperature trend during the last century. *Adv. Atmos. Sci.*, **18 (4)**, 481-496.
- Zhai Panmao, and R.E.Eskridge, 1997: Atmospheric water vapor over China. *J. Climate*, **10**, 2643-2652.
- Zhai Panmao, and Ren Fumin, 1997: Changes in maximum and minimum temperatures of the past 40 years over China. *Acta Meteorologica Sinica*, **55 (4)**, 418-429. (in Chinese)
- Zhai Panmao, Sun Anjian, Ren Fumin, Liu Xiaonin, Go bo, and Zhang Qiang, 1999: Changes of climatic extremes in China. *Climatic Change*, **42(1)**, 203-219.
- Zhai, P., X. Pan, 2003: Trends in temperature extremes during 1951~1999 in China. *Geophys. Res. Lett.*, **30(17)**, CLM 9(1~4).
- Zhao Zongci, and Ying Xu, 2002: Detection and projection of temperature change in East Asia for the 20th and 21st centuries. *Review of World Resources (USA)*, **9**, 223-234.
- Zhao Zongci, Akimasa Sumi, Chikako Harada, and Toru Nozawa, 2003: Projections of extreme temperature over East Asia for the 21st century as simulated by the CCSR/NIES2 coupled model, WMO and CMA eds, Proceedings of International Symposium on Climate Change, China Meteorological Press, 158-164.
- Zhao Zongci, Akimasa Sumi, Chikako Harada, and Toru Nozawa, 2004: Detection and projections of floods/droughts over East Asia for the 20th and 21st centuries due to human emission. *World Resource Review*

(USA), **16(3)**, 312-329.

Zhao Zongci, Wang Shaowu, Xu Ying, Ren Guoyu, Luo Yong, and Gao Xuejie, 2005a: Attribution of the 20th century climate warming in China. *Climatic and Environmental Research*, **10 (4)**, 808—817. (in Chinese)

Zhao Zongci, Ding Yihui, Luo Yong, and Wang Shaowu, 2005b: Recent studies on attributions of climate change in China. *Acta Meteorologica Sinica*, **19**, 389-400.

Zhou Tianjun, and Zhao Zongci, 2006a: Attribution of the climate warming in China for the 20th century. *Advances in Climate Change Research*, **2 (1)**, 28-31. (in Chinese)

Zhou Tianjun, and Yu Rucong, 2006b: 20th century surface air temperature over China and the globe simulated by coupled climate models. *J.Climate*, **19(22)**, 5843-5858.

BRIEF REVIEW ON SOME OF THE CLIVAR-RELATED STUDIES IN CHINA

Wang Huijun, Han Jinping, Zhang Qingyun, Sun Jianqi, and Jiang Dabang

(Institute of Atmospheric Physics, Chinese Academy of Sciences, Beijing, 100029, China)

Abstract

Climate Variability and Predictability (CLIVAR) program is one of the sub-programs of the World Climate Research Program (WCRP). In this paper, the CLIVAR related researches in China (2003-2006) was briefly reviewed, including four major parts, namely the low frequency oscillation, the interannual variability, the decadal variation in East Asia, and the global warming simulations.

1. Low frequency oscillation

The intraseasonal oscillation (ISO) is a strong signal of the tropical atmospheric activities and also a common phenomenon in the tropical ocean. The Madden-Julian Oscillation (MJO) represents the most significant form of atmospheric variability in the tropics on intraseasonal timescales.

1.1 ISO in East Asia

Many studies indicated that the anomalous summer rainfall in East China is closely associated with the strengthened or weakened East Asian summer monsoon circulation. Strengthened (weakened) atmospheric ISO at 850 hPa near the South China Sea (SCS) region results in the strong (weak) SCS summer monsoon (Ding et al., 2004). The study also revealed that the variability of atmospheric ISO in the SCS region is usually in opposite phase with that in the Jiang-Huai River basin. The strong (weak) atmospheric ISO in the SCS region is associated with the weak (strong) atmospheric ISO in the Jiang-Huai River basin. The low frequency oscillation (LFO) of 30~60d is quite remarkable in the strong summer monsoon surge years in the South China Sea and easily causes the flooding in the middle and lower reaches of the Yangtze River

valley. In the weak summer monsoon surge years, the LFO of 10~20d is more active than that of 30~60d and likely causes the drought. The propagation of monsoon surge LFO is important to medium and long-range prediction of rainfall in Yangtze River valley. (Ju and Zhao, 2005).

ISO of convection intensity during summer half year relates to sea surface temperature (SST) of South China Sea in the following winter. When intensity of ISO convection is strong (weak), SST of South China Sea in the following winter is negative (positive) (Lin et al., 2005). The analyses also suggest that the interannual variability of the winter monsoon over East Asia is responsible for the interannual variability of tropical atmospheric 30~60 day oscillation. Corresponding to the strong (weak) winter monsoon over East Asia, the cumulus convection in the tropical western Pacific is strengthened (weakened) and the atmospheric 30~60 day oscillation is active (inactive) (Long and Li, 2001). A meridional wave train along the East Asian coast is discovered that a 30 – 60 day oscillation propagates northward. It was revealed that the northward propagation of the ISO wave in the east coast of China is the main cause for the activities of the East Asian summer monsoon (EASM) in tropical and subtropical areas respectively (Ju et al., 2005b). The characteristics of zonal and meridional propagations of ISO in tropical atmosphere and kinetic energy transportation were revealed by Yang and Li (2005). The climatic characteristics of tropical intraseasonal oscillation (TIO) can be presented by using the spectral analysis and wavelet analysis. It was found that there are three regions where TIO are active, namely, the West Pacific region, the tropical Indian Ocean, and the region north to the equator in East Pacific. TIO has obvious seasonal transition. Two centers with maximal values, locating in western Pacific and Indian ocean respectively, moves southward to 10°S in winter and northward to 10°N in summer. They are inactive during spring and autumn. The TIO in the eastern Pacific north to the equator is active only in summer. It is very weak during winter and it does not shift to southern hemisphere at any time.

1.2 The relationships between ISO and climate over East Asia - Pacific region

The ISO was studied during the severe flood and drought years of the Changjiang-Huaihe River basin with the NCEP/NCAR reanalysis data and precipitation data in China. The results show that the upper-level (200 hPa) ISO pattern in severe flood (drought) years is characterized by an anticyclone (cyclone) over the south of Tibetan Plateau and a cyclone (anticyclone) over the

north of Tibetan Plateau. The lower-level (850 hPa) ISO pattern is presented by an anticyclone (cyclone) over south of the Yangtze River, the South China Sea, and the western Pacific, and a cyclone (anticyclone) from north of the Changjiang River to Japan. According to the vector EOF expansion, the low-level ISO circulation pattern is the first mode of the ISO wind field with relative large value in time coefficient during severe flood years. The analyses also revealed that the atmospheric ISO in middle and high troposphere over the Changjiang-Huaihe River basin, North China, and the middle-high latitudes in North China are more active in flood years than those in drought years. The meridional winds of ISO over the middle-high latitudes propagates southward and meet with those northward propagating from low latitudes over the Changjiang-Huaihe River basin during severe flood years (Yang and Li, 2003).

The extremely hot weather with daily highest temperature over 35°C in 2003 happened mainly from early July to August. The number of hot day was increased by 100 %~200 % in most regions except for the Leizhou Peninsula. The high temperature weather took place during the positive phase of 60~80 days seasonal oscillation (Ji et al., 2005).

The modulation of tropical depression/ cyclone (TD/TC) over the Indian - western Pacific Oceans by MJO was addressed for the period of September 1996 to June 1997 on the basis of daily wind vector in NCAR/ NCEP Reanalysis and outgoing long wave radiation (OLR) data sets. Results suggested that there are more (less) TD/TCs, which formed in the wet (dry) phase of MJO convection, except those in the western North Pacific sectors, where the TD/TC can be alternatively affected by the eastward or westward propagating MJO. Along with the eastward propagation of MJO convection, the region-averaged position of TD/TC occurrence also appears an eastward shift (Zhu et al., 2004).

1.3. Simulation of ISO

Jia et al. (2004) studied the ability of atmospheric general circulation model to simulate the tropical intraseasonal oscillation by comparing with NCEP/ NCAR Reanalyses during 1978-1989. The model displays an evident periodic signal of intraseasonal oscillation in tropical area. The basic moving character of tropical ISO is prominent, and the change in phase speed between eastern and western hemispheres is also well present. The simulated eastward propagation is better than that of the westward propagation. Reproduction in winter and spring is better than its summer

and autumn. The model can simulate the strength of the tropical intraseasonal oscillation well, especially a marked strong kinetic energy of ISO at 200 hPa. The model can simulate horizontal structure of the wind of ISO with convergence in lower air and divergence in upper air as well as vertical structure of the zonal wind. However, there were discrepancies between simulation and observation. The simulated ISO is strong in winter and summer and weak in spring and autumn, while there is preference to winter and spring in observation. The structure of some physical elements such as vertical velocity, divergence and specific humidity and the special distribution of ISO are also different with these from reanalysis data.

2. Interannual variability of the East Asian climate

2.1 The East Asian summer climate interannual variability

East Asia is a typical region that is mainly influenced by the summer monsoon (Ding and Chan, 2005). In recent four years, the major progresses in the East Asian summer monsoon are focused on the exploration of the causes of the monsoon anomaly. Xu et al. (2004) and Zhou and Yu (2005) analyzed the atmospheric water vapor transports associated with typical anomalous summer rainfall patterns in China, finding that the variability of the long-distant transportation of moisture from the tropical ocean (the tropical western pacific, the tropical Indian Ocean, and the South China Sea) provides water vapor conditions responsible for the occurrence of the floods / droughts in China. Thus, the tropical ocean is important for the East Asian summer climate because of its role acting as the main source of the water vapor for the monsoon rainfall. Besides, the tropical ocean can change the East Asian monsoon circulations via the teleconnection process (Zhang et al., 2003; Huang et al., 2005). Above influence of the tropical ocean on the East Asian summer monsoon is investigated via models as well. (Gao et al., 2004)

The atmospheric teleconnections are very important for the East Asian climate variability. Many components are documented to have close links with the East Asian climate, like the boreal winter sea level pressure anomaly over the tropical western Pacific (Wu et al., 2003), the May Arctic Oscillation (Gong and Ho, 2003), the ridge-line of subtropical anticyclone over the western Pacific (Zhang and Tao, 2003), the boreal spring Hadley circulation (Zhou and Wang, 2006a), the

East Asia—North Pacific zonal dipolar of the sea level pressure (Zhao and Zhang, 2006), etc. These tropical and Northern Hemisphere atmospheric circulation systems have strong influences on the East Asian summer climate.

In addition, it is documented recently that the climate systems in the Southern Hemisphere (SH) is closely related to the EASM and climate as well (Xue et al. 2003; Gao et al. 2003; Wang and Fan 2005; Wang and Fan 2006; Fan 2006; Nan and Li, 2003, Xue et al., 2004) investigated the relationships between the AAO and summer rainfall in the Yangtze River valley. Fan and Wang (2004) found the relationship between the AAO and the dust weather frequency in North China. In this influence process, the cross-flow, especially the Somali jet, plays an important role bridging the SH circulations and the EASM (Wang and Xue, 2003).

These above variability of the ocean and atmospheric circulations, in particular the preceding signals, can provide valuable signal for the prediction of the East Asian summer climate.

2.2 East Asian winter climate interannual variability

IPCC reported the substantial warming trend since the 1980s. Under this background, East Asia exhibits strong climate variability on both interannual and decadal time scales. In the last 54 years, the winter of 2002 is of the warmest in North Asia (Wang 2003). Analysis on the atmospheric circulation shows that the interannual variability is proved to be as the main cause for the event, and it is related to the global scale atmospheric circulation anomalies, with substantial components in the Eastern Hemisphere and in the middle and high latitude region of the Southern Hemisphere.

Later, some studies were carried out to investigate the causes responsible for the atmospheric circulation variability. Chen and Sun (2003) suggested that the ground snow over the Eurasian continent has influence on the boreal winter atmospheric circulations, for example, the Eurasian teleconnection pattern and East Asian winter monsoon. Chen et al. (2004) addressed that the tropical Quasi-Biennial Oscillation has an important role in the general circulation evolution in the Northern Hemisphere winter. Zhao and Zhang (2006) found that the sea level pressure over the Eurasian continent is related out-of-phase to that over the North Pacific. This zonal dipole can change the East Asian winter monsoon. Gong and Wang (2003) suggested that, in a strong (weak) AO year, the air temperature and precipitation increase (decrease) over most of China in winter.

Fan and Wang (2006) addressed that the AAO is closely associated with the Eurasian zonal wind and the Pacific-North American teleconnection pattern via the meridional teleconnection pattern from the Antarctic to the Arctic.

2.3 The East Asian dust events

The dust events acting as the most frequent occurrence of weather over East Asia in the boreal spring have strong interannual variability and significant impacts on the air quality, weather, and climate of East Asia (Shi and Zhao, 2003; Zhou and Zhang, 2003; Wang and Fang, 2004; Qian et al., 2006). Recently, Yuan and Zhang (2006) found that the East Asian dust events are closely related to the primary productivity of the North Pacific. Much frequent dust events transport more nutrients from the land to the ocean, which favors the abundant oceanic plankton.

Zhai and Li (2003) pointed out that the dust events in the North China are attributed to many weather elements, in which the rainfall has more importance in the interannual variability of the dust events. Thus the previous boreal summer rainfall can be regarded as a predictor for the following spring dust events of the North China. Fan and Wang (2004) revealed the relationship between the AAO and the dust weather activities of the North China. They addressed that these two climate phenomena are significantly negatively correlated each other. The meridional teleconnection pattern for the Antarctic to the Arctic and the circle teleconnection around the Pacific mainly are responsible for the linkage of the AAO and dust events. Zhao et al. (2004) investigated the relationship between climatic factors and dust storm frequency in Inner Mongolia of China, and found that the main climatic factors controlling dust storm frequency in this region are number of days with gale, intensity index of Asian polar vortex, and area index of the northern hemispheric polar vortex which are good representatives for large-scale cold air activities. In addition, Xu and Chen (2006) indicated that the vegetation and snow cover over the western China are important terrestrial conditions for the dust events frequency. Based on these observational findings, Wang et al. (2003) started the seasonal prediction of the winter and spring dust weather frequency, and the successful seasonal forecast for the year of 2003 has been demonstrated.

2.4 The relationship between the East Asian monsoon and ENSO

Lu (2005) suggested that the SST in the tropical eastern Pacific could affect the summer

rainfall in the North China via modulating the East Asian jet. Li et al. (2005) explored the mechanism for the impact of the East Asian winter monsoon on the ENSO evolution. They found that the East Asian winter monsoon could change the meridional gradient of pressure over the tropical western Pacific, which in turn stimulate anomalous zonal wind and anomalous cyclone/anticyclone circulation of the region. These changes of atmospheric circulation favor the occurrence of the ENSO events. The strong EAWM is associated with a La Niña pattern of SST anomaly in the tropical region in winter and even to the following summer. However it would gradually change to an El Niño pattern from the following autumn resulting from the forcing of west wind stress connected with the strong EAWM in the western tropical Pacific. The warm SSTA center in the western Pacific shifts eastward. For the weak EAWM situation, the process is reversed. Thus both the observation and model simulation indicate that the anomalous East Asian winter monsoon plays important role in the evolution of the ENSO.

3. Decadal variation of the East Asian climate

As for its complicity and short length of the instrumental record, decadal variation of climate system became a hotspot only after the 1990s. Many studies suggest that interdecadal climate change taking place in the 1970s is a wide-existing phenomenon, which is represented in various elements in atmosphere and sea surface temperature (SST) (Hurrell, 1995; Zhang et al., 1997; Wang, 1995; Wang, 2001).

3.1 Precipitation and temperature

The precipitation changes in East China have multi-timescale variations and are area-dependent (Dai et al., 2003; Gu et al., 2005; Qin and Wang, 2005). Spatial distribution of summer precipitation in China has abrupt change since the late 1970s (Zhai et al., 2005). The significant patterns in precipitation change that cause huge loss and attract much effort to study are the extremely decreasing rainfall in North and the strongly increasing rainfall in the Yangtze River valley. Background for interdecadal variation in precipitation is quite different from that for interannual variation (Lu, 2003). Spectral structure of precipitation varies in historical record, especially in recent decades. Those temporal scales of 5-year and 2-year are weakening and

decadal time scale is very remarkable (Dai et al., 2003). As for persistent drought in North China in the late 20th century, Yang et al. (2005) indicates that it is decadal variation superimposed on long-term decreasing trend that strengthens drought phase and makes the situation worse. Generally, it is out of phase relationship in total rainfall over North China with Yangtze River valley and in phase with those in South China. Precipitation increases strongly, even causing devastating flood over Yangtze River valley, and decreases over South China (Xin et al., 2006). Additionally, decadal timescale changes occur over India and Africa (Wu, 2005).

The surface air temperature increases over northern China, northeastern China and northwestern China (Su and Wang, 2006), but decreases over the downstream of the Tibetan Plateau (Yu and Zhou, 2004; Li et al., 2005). Temperature at high level of troposphere increased at the same time (Zhou and Zhang, 2005; Duan et al., 2006).

3.2 Monsoon circulation systems

Monsoon over East Asia, combination of tropical and subtropical monsoon, has a set of components, including airflows from tropical oceans, ITCZ in South China Sea, subtropical high over the northwestern Pacific, Meiyu front and westerlies over middle latitudes. Complicated interactions between these components are responsible for multi-timescale monsoon variations. South wind flows, picking up moisture from oceans, encounter with cold and dry air coming down from mid-high latitudes to form a front and zonal oriented rain belts moving northward and southward with summer monsoon going forward and backward.

Studies reveal that anomalies in the Northern Hemisphere and weakening of summer monsoon are the main causes for decreased precipitation in North China (Xu et al., 2005; Dai et al., 2003). Strengthened westerlies, positive geopotential height anomalies at 500 hPa and EU teleconnection make North China under the control of warm ridge (Wei et al., 2003; Zhang et al., 2003) and being influenced by northern wind diverging from high pressure system. The subtropical high in the western Pacific becomes strong and shifts southwest after the 1970s, blocking moisture entering into relative high latitudes and leading to their piling up over the Yangtze River valley, then associated with anomalies in mid-high latitudes, brings much precipitation there (Ping et al., 2006; Zhou and Wang, 2006b).

Additionally, systems far from the monsoon region also present decadal changes. The

Antarctic Oscillation (AAO) keeping in large variation after the 1970s has influenced precipitation over the Yangtze River valley (Nan and Li, 2003). Staying in positive phase after the 1970s, Arctic Oscillation (AO) also impacts on rainfall over the Yangtze River valley (Ju et al., 2005a). Kang and Wang (2005) and Fan and Wang (2004) documented the decreasing dust weather frequency but decreasing strength of AAO and AO. Li et al. (2005) and Xin et al. (2006) found that anomalies in surface temperature and precipitation are connected with eastern propagating signal of North Atlantic Oscillation (NAO) that enters in positive phase in recent years. Relationship between NAO and precipitation in China is unstable and exhibits large variability (Fu and Zeng, 2005).

3.3 Sea surface temperature and ocean-atmosphere interaction

Oceans, covering 2/3 global area and providing basic energy and moisture for atmosphere movement, is an important factor in decadal climate variability. Circulation and climate features corresponding to 2 decadal variations in North Pacific Ocean are distinctly different (Li and Xian, 2003). Pacific decadal oscillation (PDO), a strong signal in climate change that revealed recently (Yang and Zhang, 2003), has lead-lag relationship with AO and lagging correlation is maximal when AO leads PDO by 7~8 years (Sun and Wang, 2006). Yang et al. (2005) indicates that decadal change of precipitation over North China is related with warm phase of PDO, represented as warming in mid-east tropical Pacific and cooling in North Pacific causing North China under the control of anomalous westerlies and keeping moisture flows from the region. Although spatial pattern is similar, temporal scale of PDO is much longer than ENSO cycle so that the former modulates the latter. The phase of PDO cycles is associated with rainfall anomalies in North China (Yang et al., 2005). As strong anomalous signals in climate system, El Niño and La Niña (ENSO), extreme events happening in tropical Pacific, have great influence on China climate, especially the SST anomalies over the western Pacific warm pool (Zhou and Huang, 2003). Su and Wang (2006) found that the relationship between ENSO and drought-wet index in China is unstable. Warm phase of ENSO favors dry condition in North China and wet in South, and vice versa. Zhao et al. (2004) suggested that anomalies of sea ice extent over Bering Sea and the Sea of Okhotsk is closely related to the summer monsoon.

4. Simulation on the global warming

Chinese scientist has paid considerable effort to address global and East Asian climate changes related to human activities in recent several years. Ma et al. (2004) employed the IAP/LASG GOALS coupled model, created and developed by the Institute of Atmospheric Physics under the Chinese Academy of Sciences (IAP/CAS) (Zhang et al., 2000; Yu et al., 2004), to simulate climate changes forced by atmospheric greenhouse gasses, sulfate aerosols, and solar variability during the 20th century. Zhou et al. (2005) examined the response of the Atlantic thermohaline circulation (THC) to global warming as reproduced by the model. The evidence indicates that the gradually warming climate associated with the increased atmospheric CO₂ concentration leads to a warmer and fresher sea surface water at high latitudes of the North Atlantic Ocean, which prevents the down-welling of the surface water. The reduction of the pole-to-equator meridional potential density gradient finally results in the decrease of the THC in intensity. When atmospheric CO₂ concentration is doubled, the maximum value of the Atlantic THC decreases approximately by 8%.

At the same time, the NCC/IAP T63 coupled model, developed jointly by the National Climate Center under the China Meteorological Administration and the IAP/CAS (Climate System Modeling Division, 2005), was used to project the global and East Asian climate changes under the SRES A2 and A1B scenarios (Xu Ying et al., 2005). The model computed a global warming of 3.6°C/100 yr and 2.5°C/100 yr under the SRES A2 and A1B scenarios over the 21st century, respectively.

Besides the above simulations based on Chinese CGCMs, the oversea CGCMs' outputs have also been analyzed widely to further explore near-future climate changes in China. Jiang et al. (2005b) used observation and reanalysis data throughout 1961–1990 to evaluate East Asian surface temperature, precipitation and sea level pressure climatology as generated by seven CGCMs, namely CCSR/NIES, CGCM2, CSIRO-Mk2, ECHAM4/OPYC3, GFDL-R30, HadCM3, and NCARPCM. On the whole, the above models can successfully reproduce annual and seasonal surface temperature and precipitation climatology in East Asia. The models' ability to simulate surface temperature is relatively reliable compared with precipitation. It is revealed that the simulation errors for surface temperature, precipitation and sea level pressure are generally large over and around the Tibetan Plateau.

Based on the above seven CGCMs' outputs, climate changes in Northwest China due to both increasing of greenhouse gasses and increasing of greenhouse gasses plus sulfate aerosol over the 21st century were investigated, respectively (Xu et al., 2003; Zhao et al., 2003). Moreover, Jiang et al. (2004) employed the above seven CGCMs' outputs under the SRES A2 and B2 scenarios to address East Asian climate changes through the 21st century. During the former half of the 21st century, the concentration increase of atmospheric greenhouse gasses slightly impacts annual and seasonal precipitation in China except for the Tibetan Plateau, where summer precipitation rises significantly. However, both annual and seasonal precipitation will increase notably in China during the latter half of the 21st century (Jiang et al., 2005a).

Recently, the multi-model ensemble mean under about 40 emission scenarios for atmospheric greenhouse gasses and aerosols was also used to analyze future climate changes in China (Luo et al., 2005). As the global warming of the 21st century, surface temperature in China rises on average by 4.5°C, with a large range from 1.2°C to 9.2°C by the end of the 21st century. Changes of precipitation in the future are more complicated than that of surface temperature. In general, most models project wetter conditions in China over the 21st century.

Gao et al. (2003d) simulated climate changes under the doubled atmospheric CO₂ concentration by the regional climate model RegCM2 nested in one-way mode within a globally coupled atmosphere-ocean model. The model computes a remarkable warming over China due to greenhouse effect, with a range from 2.2°C in southern China to 2.8°C in northern China. Annual surface temperature increases by an average of 2.5°C. The largest warming occurs in winter season. Daily maximum and minimum surface temperature also increase over China, giving rise to much more hot spell days in summer and less cold spell days in winter. Precipitation increases in all seasons of the year, with the highest value in summer. Annual precipitation increases significantly in western China, parts of the area in south of the Yangtze River, and northern parts of Northeast China, while decreases in the area from southern part of Northeast China to North China. Meantime, the RegCM2 was used to investigate the impacts of greenhouse effect upon the typhoons affecting inland China (Gao et al., 2003b). It is indicated that the number of the typhoons affecting China increases on average by 26% under the doubled atmospheric CO₂ concentration. In addition, greenhouse effect also causes the changes of typhoon route, and there is a substantial increase of landing typhoons over Mainland China.

Furthermore, the RegCM2 was used to investigate the direct climate effect of anthropogenic sulfate aerosol under the doubled atmospheric CO₂ concentration (Gao et al., 2003a). Preliminary analysis shows that the direct climate effect of aerosol causes a decrease of surface temperature. The decrease tends to be larger in winter and in South China. The area-averaged monthly precipitation also decreases at most of the months due to the effect. Annual precipitation decreases in East China and increases in West China. But the simulated changes of both surface temperature and precipitation are much weaker as compared to the greenhouse effect.

Gao et al. (2003c) simulated climate effects of land use changes over inland China by the RegCM2. It follows that the land use changes give rise to a decrease of annual precipitation in Northwest China, an arid and semi-arid region, an increase of annual surface temperature in the southern portions of Northeast China and the Sichuan Basin as well as the parts of Northwest China, and a decrease of surface temperature along coastal areas. Additionally, summer daily maximum surface temperature increases in many locations, while winter daily minimum surface temperature decreases in East China and increases in Northwest China. The upper soil moisture decreases significantly across China. The results indicate that the same land use change can cause different climate effects in different regions, depending on the surrounding environment and climate characteristics.

It should be reminded here that there are large uncertainties in the prediction of future regional climate changes by numerical models. These mainly come from the inadequacies in the climate model's formulation and physical processes as well as parameterization, in the specification of future emission estimation of atmospheric greenhouse gasses and aerosols, or in the length limitation of the observation-based data. Nevertheless, scientist have confidence in the ability of the complex physically-based climate models to provide useful projection of near-future climate due to their demonstrated performances on a range of space and time-scales.

References

- Chen Haishan, and Sun Zhaobo, 2003: The effects of Eurasian snow cover anomaly on winter atmospheric general circulation: Part I. Observational studies. *Chinese J. Atmos. Sci.*, **27**(3), 304~316. (in Chinese)
- Chen Wen, Yang Lei, Huang Ronghui, and Qiu Qihong, 2004: Diagnostic analysis of the impact of tropical QBO on the general circulation in the Northern Hemisphere winter. *Chinese J. Atmos. Sci.*, **28**(2), 161~173. (in

Chinese)

Climate System Modeling Division, 2005: An introduction to the first-generation operational climate model at National Climate Center. *Advances in Climate System Modeling*, **1**, 14pp.

Dai Xingang, Wang Ping, and Chou Jifan, 2003: Multiscale characteristics of the rainy season rainfall and interdecadal decaying of summer monsoon in North China. *Chinese Science Bulletin*, **48**(24), 2730~2734.

Ding, Y.H., and J.C.L. Chan, 2005: The East Asian summer monsoon: an overview. *Meteoro. Atmos. Phys.*, **89**, 117~142.

Ding Yihui, and Coauthors, 2004: South China Sea Monsoon Experiment(SCSMEX) and the East-Asian Monsoon. *Acta Meteorologica Sinica*, **62**(5), 561~586. (in Chinese)

Duan Anmin, Wu Guoxiong, Zhang Qiong, and Liu Yimin, 2006: New proofs of the recent climate warming over the Tibetan Plateau as a result of the increasing greenhouse gases emissions. *Chinese Science Bulletin*, **51**(11), 1369~1400.

Fan, Ke, and Huijun Wang, 2004: Antarctic oscillation and the dust weather frequency in North China. *Geophys. Res. Lett.*, **31**, L10201, doi: 10.1029/2004GL019465.

Fan Ke, 2006: Atmospheric circulation in southern Hemisphere and summer rainfall over Yangtze River valley. *Chineses J. Geophys.*, **49**(3), 672~679.

Fan Ke, and Wang Huijun, 2006: Interannual variability of Antarctic Oscillation and its influence on East Asian climate during boreal winter and spring. *Science in China (Series D)*, **49**(5), 554~560.

Fu Congbin, and Zeng Zhaomei, 2005: Correlations between North Atlantic oscillation index in winter and eastern China flood/drought index in summer in the last 530 years. *Chinese Science Bulletin*, **21**, 2505~2516.

Gao Xuejie, Lin Wantao, Fred Kucharsky, and Zhao Zongci, 2004: A simulation of regional climate in China by using CCM3 and observed SST. *Chinese J. Atmos. Sci.*, **28**(1), 78~90. (in Chinese)

Gao Xuejie, Lin Yihua, and Zhao Zongci, 2003a: Modelling the effects of anthropogenic sulfate in climate change by using a regional climate model. *Journal of Tropical Meteorology*, **19**, 169~176. (in Chinese)

Gao Xuejie, Lin Yihua, Zhao Zongci, and F. Giorgi, 2003b: Impacts of greenhouse effect on typhoon over China as simulated by a regional climate model. *Journal of Tropical Oceanography*, **22**, 77~83. (in Chinese)

Gao Xuejie, Luo Yong, Lin Wantao, Zhao Zongci, and F. Giorgi, 2003c: Simulation of effects of land use change on climate in China by a regional climate model. *Adv. Atmos. Sci.*, **20**, 583~592.

Gao Xuejie, Zhao Zongci, Ding Yihui, Huang Ronghui, and F. Giorgi, 2003d: Climate change due to greenhouse effects in China as simulated by a regional climate model, Part II: Climate change. *Acta Meteorologica Sinica*,

- 61, 29~38. (in Chinese)
- Gao Hui, Xue Feng, and Wang Huijun, 2003: Influence of interannual variability of Antarctic oscillation on Mei-yu along the Yangtze and Huaihe River valley and its importance to prediction. *Chinese Science Bulletin*, **48**, 61~67.
- Gong, D. Y., and C. H. Ho, 2003: Arctic Oscillation signals in East Asian summer monsoon. *J. Geophys Res.*, **108**(D2), 4066, doi: 10.1029/2002JD002193.
- Gong Daoyi, and Wang Shaowu, 2003: Influence of Arctic Oscillation on winter climate over China. *Journal of Geophysical Sciences*, **13**(2), 208~216.
- Gu Wei, Li Chongyin, and Yang Hui, 2005: Analysis on interdecadal variation of summer rainfall and its trend in East Chin. *Acta Meteorologica Sinica*, **63**(5), 728~739. (in Chinese)
- Huang Ronghui, Gu Lei, Xu Yuhong, Zhang Qilong, Wu Shangsen, and Cao Jie, 2005: Characteristics of the interannual variations of onset and advance of the East Asian summer monsoon and their associations with thermal states of the tropical western Pacific. *Chinese J. Atmos. Sci.*, **29**(1), 20~36. (in Chinese)
- Hurrell, J. W., 1995: Decadal trends in the North Atlantic Oscillation: Regional temperatures and precipitation. *Science*, **269**, 676~679.
- Ji Zhong-ping, Lin Gang, Li Xiao-juan, and Xiong Ya-li, 2005: High temperature anomalies in guangdong in summer 2003 and its climatic background. *Journal of Tropical Meteorology*, **21**(2), 207~216. (in Chinese)
- Jia XiaoLong, Li Chongyin, and Zhou Ningfang, 2004: A GCM study on tropical intraseasonal oscillation (in Chinese), *Acta Meteorologica Sinica*, **62**(6), 725~739. (in Chinese)
- Jiang Dabang, Wang Huijun, and Lang Xianmei, 2004: East Asian climate change trend under global warming background. *Chinese J. Geophys*, **47**, 675~681.
- Jiang Dabang, and Wang Huijun, 2005a: Natural interdecadal weakening of East Asian summer monsoon in the late 20th century. *Chinese Science Bulletin*, **50**, 1923~1929.
- Jiang Dabang, Wang Huijun, and Lang Xianmei, 2005b: Evaluation of East Asian climatology as simulated by seven coupled models. *Adv. Atmos. Sci.*, **22**, 479~495.
- Ju Jianhua, Lu Junmei, Cao jie et al., 2005a: Possible impacts of the Arctic Oscillation on the interdecadal variation of summer monsoon rainfall in East Asia. *Adv. Atmos. Sci.*, **22**(1), 39~48.
- Ju Jian-Hua, Qian Cheng, and Cao Jie, 2005b: The intraseasonal oscillation of East Asian Summer Monsoon. *Chinese J. Atmos. Sci.*, **29**(2), 187~194. (in Chinese)
- Ju Jian-hua, and Zhao Er-xu, 2005: Impacts of the low frequency oscillation in East Asian summer monsoon on the

- drought and flooding in the middle and lower valley of the Yangtze River. *Journal of Tropical Meteorology*, **21**(2), 163~171. (in Chinese)
- Kang Dujuan, and Wang Huijun, 2005: Analysis on the decadal scale variation of the dust storm in North China. *Science in China (Series D)*, **12**, 2260~2266
- Li Chongyin, Long Zhenxia, and Mu Mingquan, 2003: Atmospheric intraseasonal oscillation and its important effect. *Chinese J. Atmos. Sci.*, **27**(4), 518~535. (in Chinese)
- Li Chongyin, Pei Shunqiang, and Pu Ye, 2005: Dynamical impact of anomalous East-Asian winter monsoon on zonal wind over the equatorial western Pacific. *Chinese Science Bulletin*, **50**(14), 1520~1526.
- Li Chongyin, and Xian Peng, 2003: Atmospheric anomalies related to interdecadal variability of SST in the North Pacific. *Adv. Atmos. Sci.*, **20**(6), 859~874.
- Li, Jian, Rucong Yu, Tianjun Zhou, and Bin Wang, 2005: Why is there an early spring cooling shift downstream of the Tibetan Plateau? *J. Clim.*, **18**, 4660~4668.
- Lin Ailan, Liang Jianyin, and Li Chunhui, 2005: Spectral variation characteristics of South China Sea summer monsoon convection intraseasonal oscillation. *Journal Of Tropical Meteorology*, **21**(5), 542~548. (in Chinese)
- Long Zhenxia, and Li Chongyin, 2001: Interannual variability in the of 30-60 day low-frequency kinetic energy lower tropical atmosphere. *Chinese J. Atmos. Sci.*, **25**(6), 798~808. (in Chinese)
- Lu Riyu, 2003: Linear relationship between the interdecadal and interannual variabilities of North China rainfall in rainy season. *Chinese Science Bulletin*, **48**(10), 1040~1044.
- Lu Riyu, 2005: Interannual variation of North China rainfall in rainy season and SSTs in the equatorial eastern Pacific. *Chinese Science Bulletin*, **50**(18), 2069~2073.
- Luo Yong, Zhao Zongci, Xu Ying, Gao Xuejie, and Ding Yihui, 2005: Projections of climate change over China for the 21st century. *Acta Meteorologica Sinica*, **19**, 401~406.
- Ma Xiaoyan, Guo Yufu, Shi Guangyu, and Yu Yongqiang, 2004: Numerical simulation of global temperature change during the 20th century with the IAP/LASG GOALS model. *Adv. Atmos. Sci.*, **21**, 227~235.
- Nan, S., and J. Li, 2003: The relationship between summer precipitation in the Yangtze River valley and the boreal spring Southern Hemisphere Annular Mode. *Geophys. Res. Lett.*, **30**(24), 2266, doi: 10.1029/2003GL018381.
- Ping Fan, Luo Zhexian, and Ju Jianhua, 2006: Differences between dynamics factors for interannual and decadal variations of rainfall over the Yangtze River valley during flood seasons. *Chinese Science Bulletin*, **51**(8), 994~999.
- Qian Zheng'an , Cai Ying , Liu Jingtao , Liu Chungming , Li Dongliang , and Song Minhong, 2006: Some

- advances in dust storm research over China-Mongolia areas. *Chinese J. Geophys.*, **49**(1), 83~92. (in Chinese)
- Qin Jun, Wang Panxing, 2005: Interdecadal variations of monsoon rainbands over China and their relationships with ocean-atmospheric systems in mid-high latitudes. *Journal of Tropical Meteorology*, **21**(1), 63~71. (in Chinese)
- Shi Guangyu, and Zhao Sixiong, 2003: Several scientific issues of studies on the dust storms. *Chinese J. Atmos. Sci.*, **27**(4), 591~606. (in Chinese)
- Su Mingfeng, and Wang Huijun, 2006: Relationship and its instability of ENSO-Chinese variations in droughts and wet spells. *Science in China (Series D)*, in press.
- Sun Jianqi, and Wang Huijun, 2006: Relationship between Arctic oscillation and Pacific decadal oscillation on decadal timescale. *Chinese Science Bulletin*, **51**, 75~79.
- Wang B., 1995: Interdecadal changes in El Niño onset in the last four decades. *J. Clim.*, **8**, 267~285.
- Wang Huijun, 2001: The Weakening of the Asian Monsoon Circulation after the End of 1970's. *Adv. Atmos. Sci.*, **18**, 376~386.
- Wang Huijun, 2003: 2002: The extra-strong warm winter event in North Asia and its accompanying anomalous atmospheric circulation. *Chinese Science Bulletin*, **48**(10), 1031~1033.
- Wang Huijun, and Fan Ke, 2006: Southern Hemisphere mean zonal wind in upper troposphere and East Asian summer monsoon circulation. *Chinese Science Bulletin*, **51**(12), 1508~1514.
- Wang, Huijun, and Ke Fan, 2005: Central-north China precipitation as reconstructed from the Qing dynasty: Signal of the Antarctic atmospheric oscillation. *Geophys. Res. Lett.*, **32**, L24705, doi: 10.1029/2005GL024562.
- Wang Huijun, Lang Xianmei, Zhou Guangqing, and Kang Dujuan, 2003: A preliminary report of the model prediction on the forthcoming winter and spring dust climate over China. *Chinese J. Atmos. Sci.*, **27**(1), 136~140. (in Chinese)
- Wang Huijun, and Xue Feng, 2003: Interannual variability of Somali jet and its influences on the inter-hemispheric water vapor transport and on the East Asian summer rainfall. *Chinese J. Geophys.*, **46**(1), 18~25. (in Chinese)
- Wang Wei, and Fang Zongyi, 2004: Review of dust storm weather and research progress. *Quarterly Journal of Applied Meteorology*, **15**(3), 366~381. (in Chinese)
- Wei Jie, Zhang Qingyun, and Tao Shiyan, 2003: Characteristics of atmospheric circulation anomalies during persistent drought in North China for last two decades. *Journal of Applied Meteorological Science*, **14**(2), 140~151. (in Chinese)
- Wu Bingyi, 2005: Weakening of Indian summer monsoon in recent decades. *Adv. Atmos. Sci.*, **22**(1), 21~29.

- Wu Bingyi, Wang Dongxiao, and Huang Ronghui, 2003: Relationship between sea level pressure of the winter tropical western Pacific and the subsequent Asian summer monsoon. *Adv. Atmos. Sci.*, **20**(4), 496~510.
- Xin Xiaoge, Yu Rucong, Zhou Tianjun, and Bin Wang. 2006: Droughty late spring of South China in recent decades. *J. Clim.*, **19**(13), 3197~3206.
- Xu Guiyu, Yang Xiuqun, and Sun Xuguang, 2005: Interdecadal and interannual variation characteristics of rainfall in North China and its relation with the northern hemisphere atmospheric circulation. *Chinese J. Geophys.*, **48**(3), 511~519. (in Chinese)
- Xu Xiangde, Chen Lianshou, Wang Xiurong, Miao Qiuju, and Tao Shiyan, 2004: Moisture transport source / sink structure of the Meiyu rain belt along the Yangtze River valley. *Chinese Science Bulletin*, **49**(2), 181~188.
- Xu Xingkui, and Chen Hong, 2006: Influence of vegetations and snow cover on sand-dust events in the west of China. *Chinese Science Bulletin*, **51**(3), 331~340.
- Xu Ying, Ding Yihui, and Zhao Zongci, 2003: Scenario of temperature and precipitation changes in Northwest China due to human activity in the 21st century. *Journal of Glaciology and Geocryosphere*, **25**, 327~330. (in Chinese)
- Xu Ying, Zhao Zongci, Luo Yong, and Gao Xuejie, 2005: Climate change projections for the 21st century by the NCC/IAPT63 Model with SRES scenarios. *Acta Meteorologica Sinica*, **19**, 407~417.
- Xue, F., H. J. Wang, and J. H. He, 2004: Interannual variability of Mascarene high and Australian high and their influences on East Asian summer monsoon. *J. Meteorol. Soc. Japan*, **82**(4), 1173~1186.
- Xue Feng, Wang Huijun, and He Jinhai, 2003: Interannual variability of Mascarene high and Australian high and their influences on summer rainfall over East Asia. *Chinese Science Bulletin*, **48**, 492~497.
- Yang Haijun, and Zhang Qiong, 2003: On the decadal and interdecadal variability in the Pacific Ocean. *Adv. Atmos. Sci.*, **20**(2), 173~184.
- Yang Hui, and Li Chongyin, 2003: The relation between atmospheric intraseasonal oscillation and summer severe flood and drought in the Changjiang-Huaihe River Basin, *Adv. Atmos. Sci.*, **20**(4), 540~553.
- Yang Hui, and Li Chongyin, 2005: A study of propagation of tropical intraseasonal oscillation and its influence mechanism. *Climatic and Environmental Research*, **10**(2), 145~156. (in Chinese)
- Yang Xiuqun, Xie Qian, Zhu Yimin et al., 2005: Decadal-to-interdecadal variability of precipitation in North China and associated atmospheric and oceanic anomaly patterns. *Chinese J. Geophys.*, **48**(4), 789~797. (in Chinese)
- Yu, Rucong, and Tianjun Zhou, 2004: Impacts of winter-NAO on March cooling trends over subtropical Eurasia

- continent in the recent half century. *Geophys. Res. Lett.*, **31**, L12204, doi: 10.1029/2004GL019814.
- Yu Yongqiang, Zhang Xuehong, and Guo Yufu, 2004: Global coupled ocean- atmosphere general circulation models in LASG/IAP. *Adv. Atmos. Sci.*, **21**, 444~455.
- Yuan, W., and J. Zhang, 2006: High correlations between Asian dust events and biological productivity in the western North Pacific. *Geophys. Res. Lett.*, **33**, L07603, doi: 10.1029/2005GL025174.
- Zhai Panmao, and Li Xiaoyan, 2003: On the climate background of dust storms over northern China. *Acta Geographica Sinica*, **58**(suppl), 125~131. (in Chinese)
- Zhai, Panmao, Xuebin Zhang, Hui Wan, and Xiaohua Pan, 2005: Trends in total precipitation and frequency of daily precipitation extremes over China. *J. Clim.*, **18**, 1096~1108.
- Zhang Qingyun, and Tao Shiyan, 2003: The anomalous subtropical anticyclone in western Pacific and their association with circulation over East Asia during summer. *Chinese J. Atmos. Sci.*, **27**(3), 369~380. (in Chinese)
- Zhang Qingyun, Wei Jie, and Tao Shiyan, 2003: The decadal and interannual variations of drought in the Northern China and Association with the circulation. *Climatic and Environmental Research*, **8**(3), 307~318. (in Chinese)
- Zhang Qiong, Liu Ping, and Wu Guoxiong, 2003: The relationship between the flood and drought over the lower reach of the Yangtze River Valley and the SST over the Indian Ocean and the South China Sea. *Chinese J. Atmos. Sci.*, **27**(6), 992~1006. (in Chinese)
- Zhang Xuehong, Shi Guangyu, Liu Hui, and Yu Yongqiang, 2000: *IAP Global Ocean-Atmosphere-Land System Model*. Science Press, Beijing, 252pp.
- Zhang, Y., J. M. Wallace, and D. S. Battisti, 1997: ENSO-like interdecadal variability: 1900-93. *J. Clim.*, **10**, 1004~1020.
- Zhao, C., X. Dabu, and Y. Li, 2004: Relationship between climatic factors and dust storm frequency in Inner Mongolia of China. *Geophys. Res. Lett.*, **31**, L01103, doi: 10.1029/2003GL018351.
- Zhao Ping, and Zhang Renhe, 2006: Relationship of interannual variation between an eastern Asia- Pacific dipole pressure pattern and East Asian monsoon. *Chinese J. Atmos. Sci.*, **30**(2), 307~316. (in Chinese)
- Zhao, Ping, Xiangdong Zhang, Xiuji Zhou, Moto Ikeda, and Yonghong Yin, 2004: The sea ice extent anomaly in the North Pacific and its impacts on the East Asian summer monsoon rainfall. *J. Clim.*, **17**, 3434~3447.
- Zhao Zongci, Ding Yihui, Xu Ying, and Zhang Jin, 2003: Detection and prediction of climate change for the 20th and 21st century due to human activity in Northwest China. *Climatic and Environmental Research*, **8**, 26-34.

(in Chinese)

Zhou, B. T., and H. J. Wang, 2006a: Relationship between the boreal spring Hadley circulation and the summer precipitation in the Yangtze River valley. *J. Geophys. Res.*, **111**, D16109, doi: 10.1029/2005JD007006.

Zhou Botao, and Wang Huijun, 2006b: Interannual and interdecadal variations of the Hadley circulation and its connection with tropical sea surface temperature. *Chinese J. Geophys.*, **49**(5), 1271~1278. (in Chinese)

Zhou Liantong, and Huang Ronghui, 2003: Research on the characteristics of interdecadal variability of summer climate in China and its possible cause. *Climatic and Environmental Research*, **8**(3), 274~290. (in Chinese)

Zhou Shunwu, and Zhang Renhe, 2005: Decadal variations of temperature and geopotential height over the Tibetan Plateau and their relations with Tibet ozone depletion. *Geophys. Res. Lett.*, **33**, L18705, doi: 10.1029/GL023496.

Zhou, T. J., and R. C. Yu, 2005: Atmospheric water vapor transport associated with typical anomalous summer rainfall patterns in China. *J. Geophys. Res.*, **110**, D08104, doi: 10.1029/2004JD005413.

Zhou Tianjun, Yu Rucong, Liu Xiyang, Guo Yufu, Yu Yongqiang, and Zhang Xuehong, 2005: Weak response of the Atlantic thermohaline circulation to an increase of atmospheric carbon dioxide in IAP/LASG Climate System Model. *Chinese Science Bulletin*, **50**, 592-598.

Zhou Zijiang, and Zhang Guocai, 2003: Typical severe dust storms in northern China during 1954—2002. *Chinese Science Bulletin*, **48**(21), 2366~2370.

Zhu Congwen, Tetsuo Nakazawa, and Li Jianping, 2004: Modulation of tropical depression/cyclone over the Indian-Western Pacific Oceans by Madden-Julian Oscillation. *Acta Meteorologica Sinica*, **62**(1), 42~50. (in Chinese)

RECENT PROGRESS IN CLOUD PHYSICS

RESEARCH IN CHINA

MA Jianzhong^{1*} (马建中), *GUO Xueliang*² (郭学良), *ZHAO Chunsheng*³ (赵春生), *ZHANG Yijun*¹ (张义军) and *HU Zhijin*¹ (胡志晋)

¹ Chinese Academy of Meteorological Sciences, Beijing 100081

² Institute of Atmospheric Physics, Chinese Academy of Sciences, Beijing 100029

³ Department of Atmospheric Sciences, School of Physics, Peking University, Beijing 100871

* E-mail: mjz@cams.cma.gov.cn * Phone: 010-58995270; Mobile: 13911511326

Abstract

A review of China cloud physics research during 2003-2006 is made in this paper. The studies on cloud field experiments and observation, cloud physics and precipitation, including its theoretical applications in hail suppression and artificial rain enhancement, cloud physics and lightning, and clouds and climate change are included. Due primarily to the demand from weather modification activities, the issue of cloud physics and weather modification has been addressed in China with many field experiments and model studies. While cloud physics and weather modification is still an important research field, the interaction between aerosol, cloud and radiation processes, which is the key issue of current climate change research, has been becoming a new research direction in China over the past four years.

Key words: cloud, precipitation, weather modification, aerosols, climate change, China

1. Introduction

Clouds cover approximately 60% of the Earth's surface. Average global coverage over the oceans is estimated at 65% and over land at 52% (Warren et al. 1986, 1988). Clouds affect the atmosphere by absorbing and reflecting radiation, modifying local air temperature, pressures, and winds, producing precipitation, and mixing and removing gases and particles. In addition to various natural processes, it has been well recognized that human activities may change physical characteristics of clouds, in the way other than the traditional method used in weather modification (Twomey, 1974, 1977; Albrecht, 1989; Houghton et al., 1995; Ramanathan et al., 2001). Recent study has shown that the precipitation in eastern central China is significantly reduced during the last 40 years and this reduction of precipitation is strongly correlated to the high concentrations of

aerosols (Zhao et al, 2006a). However, our understanding of detailed processes involved in the aerosol's effects on the formation of clouds and precipitation is still limited, and much research in multi-disciplines is being done around the world to improve this situation.

The rapid progress in studies on cloud physics has been made in recent years in China due primarily to the demand from weather modification operation. The more sophisticated cloud models with two-momentum, bin-microphysics and aerosol processes and advanced observational instrumentation like Doppler radar, polarized radar and airborne microwave radiometer, particle measuring system (PMS) and GPS mesonet have been used in cloud physics studies. These studies focused on cloud physical processes ranging from convective cloud scale to mesoscale cloud systems. Several projects directed towards cloud physics and weather modification, and air quality pollution, clouds and climate change have been conducted with funds from the Ministry of Science and Technology (MOST) and the Natural Science Foundation of China (NSFC). The threats from long-term drought, severe weather and air pollution pose new challenges in cloud physics research.

Huang et al. (2003) reviewed the advance of research on cloud, fog, precipitation and weather modification at the Institute of Atmospheric Physics, Chinese Academy of Sciences (IAP/CAS) in the latest half century before 2003. Fang et al. (2003) and Guo et al. (2003) gave overviews of hail suppression projects and hail-cloud modeling activities in China, respectively. An introduction of progresses in precipitation enhancement in China was made by Wu (2005), with a focus on operational conditions, efficiency evaluation and practical management. Yao (2006) reviewed weather modification research at the Chinese Academy of Meteorological Sciences (CAMS) over the last 40 years. In this paper, we give an overview of the studies on cloud physics in China over the last four years, from 2003 to 2006. Some previous studies, especially in 2002, are also cited for the continuity. The contents include cloud field experiments and observation (Section 2), cloud physics and precipitation (Section 3), cloud physics and hail suppression (Section 4), cloud physics and artificial rain enhancement (Section 5), cloud physics and lightning (Section 6), and clouds and climate change (Section 7). Conclusions and remarks are presented in Section 8.

2. Cloud field experiments and observation

2.1. Aircraft measurements

The airborne PMS (Particle Measuring System) is a set of microphysical instruments that have been widely used in the world since the late 1970s. IAP/CAS and CAMS introduced and implemented the new-generation PMS (Liu et al., 2003f; Liu et al., 2005b), respectively, which have been used for the weather modification field experiments in several provinces of China. Although the PMS is used primarily in the studies of weather modification, it provides invaluable data for the theory studies of cloud microphysics, and in particular, for comparisons with cloud model simulations.

The measurements on cloud microphysical properties with airborne PMS were generally made in the north parts of China during springtime, and the results have been reported in several papers (Liu et al., 2003f; Su et al., 2003a, 2003b; Li et al., 2003c; Wang and Lei, 2003; Yang et al., 2005; Huang et al., 2005; Liu et al., 2005b; Wang et al., 2005; Jin et al., 2006; Li, 2006). According to the measurements made in the Qinghai Province of northwest China by Su et al. (2003a, 2003b), liquid water content is low at the stage of cloud development, and high at the stage of precipitating cloud mature. As summarized in Huang et al. (2005), droplet number concentration, liquid water content and mean diameter of stratiform clouds in the northern parts of China range $10\text{-}200\text{ cm}^{-3}$, $0.01\text{-}0.1\text{ g m}^{-3}$, and $7\text{-}15\text{ }\mu\text{m}$, respectively.

The evolution of cloud hydrometeor spectrum and the precipitation is the most important processes in cloud physics. Understanding and adequate modeling such processes are essential for cloud researches on scales ranging from micro-meter to thousands kilometer. The observed cloud particle spectra were fitted using a N -order Γ -type function for Sc and As clouds by Li et al. (2003c) and a distribution function for warm St clouds, $N(r) = m r^f \exp(-ar + br^2 - cr^3)$, developed by Wang et al. (2005), respectively. On the other hand, the case study of Su et al. (2003a, 2003b) showed that the cloud droplet spectra is discontinuous at the stage of cloud development, and becomes wider with an order increase of number concentration at the stage of cloud mature. Yang et al., (2005) found the inhomogeneity of stratiform clouds in returning processes based on the analysis of PMS data. They showed that when the aircraft flies into stronger precipitating cloud bands, the mean diameter and the particle concentration leap up and spectrum width becomes wider. However, microphysical mechanisms behind these variations in cloud drop spectrum were not addressed, and aerosol spectrum observed by PCASP, which plays an important role in the activation of aerosol particles into clouds, was rarely reported.

In addition to PMS probes, other instruments were installed in the airplane for different studies. An Airborne Upward-Looking Microwave Radiometer was developed and used for the measurement of vertical-integrated cloud liquid water content during the operation of precipitation-enhancement in the Jilin Province of northeast China (Lei et al., 2003; Jin et al,

2004). The integrated supercooled cloud liquid water content was found to be great for convection cells inlaid in sheet clouds, with magnitude levels up to $10^3 \text{ g}\cdot\text{m}^{-2}$.

2.2. Retrieval from Radar reflectivity

The total amount of water in the atmosphere, in particular liquid water content in clouds, is one of important factors that determine precipitation process and need considering in the artificial rain enhancement. In addition to aircraft measurements, remote sensing on the ground base appears to be more economic and efficient for the long-term observations. The radar echo has been used in many studies (e.g., Zhao et al., 2003; Fang, 2004; Li et al., 2003a; Xiao et al., 2004; Tian et al., 2005) for cloud microphysical structure analysis and model evaluation. Lu et al. (2003) reviewed the progress in atmospheric remote sensing and satellite meteorology in China, in particular within the Institute of Atmospheric Physics. Liu and Ge (2006) gave an overview on radar meteorology research at the Chinese Academy of Meteorological Sciences for a half century, and especially the application of the advanced dual linear polarization radar they developed in watching, warning and microphysical structures retrieval of heavy rain fall (Liu et al., 2002; Liu et al., 2005c; Cao and Liu, 2006; Cao et al., 2006). Chen (2002) proposed a concept that can determine cloud liquid water path from cloud microwave attenuation along the satellite-earth path. Li et al. (2004b, 2004c) developed a method of retrieving cloud water mixing ratio (q_c), rainwater mixing ratio (q_r) and water vapor mixing ratio (q_v) from Doppler weather radar's reflectivity. They showed that the initial fields of mesoscale numerical model including these retrieved cloud microphysical messages would be helpful for numerical nowcasting of the precipitation. Wang and Chu (2002) made an introduction of the successful application of polarization weather radar abroad, and discussed the application problem of polarization weather radar in weather modification. Liu et al. (2003e) reported their progress in developing a polarization lidar for measuring profiles of depolarization ratio of cirrus clouds and Asian dust aerosols. The primary observational results over Hefei, in the Anhui Province of central east China, show that the depolarization ratio for cirrus clouds varies from 0.4 to 0.5. Liu et al. (2006) introduced a method of ground-based microwave radiometer remote sensing retrieval of integrated water vapor and cloud liquid water in the atmosphere. However, bias of the retrieved results is still large, and more work on comparisons between radar retrieval and aircraft measurements should be done.

2.3. Satellite observation

There have been increasing studies and usage of satellite data focusing on both macro- and micro- physical characteristics of clouds during the last four years in China. Images of satellite, such as National Oceanic and Atmospheric Administration (NOAA) Advanced Very High Resolution Radiometer (AVHRR), were used to analyze the cloud features of regional hail processes, and water content, cloud top temperature and cloud cover were obtained and used to

discriminate hail clouds and choose best time and area for precipitation enhancement (Zhang and Jin, 2003; Zhang et al., 2004a; Zhang et al., 2004b; Zhang et al., 2004c). The effect of a precipitation enhancement operation with AgI using an aircraft over the Shangxi Province of west China was viewed by NOAA-14 satellite (Yu et al., 2005). A vivid zigzag cloud track was demonstrated on the satellite image and it also was well simulated with a three-dimensional numerical model of transport and diffusion of seeding material (Yu et al., 2005; Dai et al., 2006).

The passive remote sensing data from the TRMM Microwave Imager (TMI) were applied to retrieve cloud liquid water by Yao et al. (2003). Since the vertical polarization channel of TMI 85.5 GHz they applied is very sensitive to precipitation as well, the method Yao et al. (2003) have developed cannot be used for retrieving cloud water of precipitating clouds. Liu et al. (2003d) indicated that the channel of 6.9 GHz on satellite-borne radiometer can be used to estimate column liquid water content of precipitating clouds. Wang et al. (2006a) developed a joint retrieval algorithm for retrieving cloud water of non-precipitating clouds by using the microwave brightness temperature measured at the horizontal polarization channels of TMI 37.0 GHz and 85.5 GHz. They showed that their algorithm can be applied to the precipitating clouds in a qualitative sense as well. TRMM remote sensing data were also used to study the three-dimensional structure of rainfall rates and hydrometeors in Typhoon precipitation cloud systems (Zhong et al., 2006; He et al., 2006).

Using the reflection measured by the MODerate Resolution Imaging Spectroradiometer (MODIS) on Terra and Aqua satellites at the channels of 0.65 μm and 2.1 μm , Zhang et al. (2006c) retrieved cloud optical thickness, efficient radius and liquid water content over the Qilian Mountains of the Tibetan Plateau for the period between 2002 and 2005. They also did correlation analysis between these three parameters and 6 hr precipitation over the Qilian Mountains. Their analytical results provide important information for further research on the water resource usage in wet China.

Chinese meteorological satellite FY-1C was successfully launched on May 10, 1999. There are ten spectral channels in FY-1C, some of which such as channel 1 (0.58 - 0.68 μm), channel 4 (10.3- 11.3 μm) and channel 6 (1.58-1.64 μm), can be used for cloud particles phase detection. A case study by Liu et al. (2003a) showed that 1.6 μm channel could be used to analyze the thermodynamic phase of cloud particles. Much more work is needed for the retrieval of cloud microphysical parameters with Chinese satellites data.

2.4. Video images

The Precipitation Particle Image Sensor (PPIS) was used to directly observe the cloud microphysical structures vertically from the base to the top of the cloud during the heaviest rainfall

of the Meiyu front in June 1999 (Wang and Yang, 2003). PPIS is a balloon-borne video-sounder developed by Takahashi et al. (1995), from which images of precipitation particles larger than 0.5 mm are recorded by a camera. In addition to the particle images, the PPIS records the electric charge on the particles and the ambient temperature, humidity and pressure. The vertical distributions of various cloud particle sizes, number density and mass density were retrieved from the observations by Wang and Yang (2003). Their analyses showed that icecrystals, graupels, snowflakes and frozen droplets often coexist with the liquid phase in the convective cloud clusters inbanded in Meiyu front rainband. The interactions of these particles play important roles in the formation and evolution of rainfall.

3. Cloud physics and precipitation

3.1. Model development and application

Cloud microphysical models. Numerical simulations have been playing a more important role in the studies of cloud microphysical process, precipitation mechanism and weather modification evaluation. Although a great amount of model studies have been reported in China during the last four years, most of these were merely of models' application without fundamental changes in cloud microphysical processes in the model itself. The models used include:

- 1) CAMS (Chinese Academy of Meteorological Sciences) models: the 1-D stratiform cloud model (Liu et al., 2005a), which was originally developed by Hu and Yan (1986), and the 1-D time-dependant convective cloud model (Zhao et al., 2003) and the 3-D convective cloud model (Li et al., 2003a; Fang, 2004; Fang et al., 2005a, 2005b; Liu et al., 2005a; Li et al., 2006c), which was originally developed from the microphysical cloud model of Hu and He (1987);
- 2) SGBH model of Beijing Institute of Applied Meteorology: the 2-D cloud model with a microphysical scheme of size categories of hydrometeor particles (Zhao et al., 2004), which was originally developed by Xu and Wang (1990) and Xu and Duan (1999);
- 3) IAP (Institute of Atmospheric Physics, Chinese Academy of Sciences) models: the 1-D stratus cloud model (Hong and Zhou, 2005; Wang et al., 2006b), which was simplified from the 2-D microphysical cloud model of Hong (1996), and the 3-D hailstorm model (Xiao et al., 2002; Zhou et al., 2003; Li et al., 2003b; Hu et al., 2003; Kang et al., 2004a, 2004b; Zhou et al., 2005a; Li and

Hong, 2005; Chen et al., 2005; Guo et al., 2006b; Xiao et al., 2006; Yu et al., 2006) and rainstorm model (Xiao et al., 2004), which was improved from a 3-D convective cloud model developed by Kong et al. (1990), Hong (1998) and Guo and Huang (2002). Both two-momentum and bin cloud microphysics were used in these models.

Cloud schemes in the mesoscale model. The moisture processes are very important for precipitation, atmospheric general circulation, atmospheric chemistry and climate, and they cannot be ignored in a mesoscale model. Lou et al. (2003) presented a review of the convective parameterization and explicit cloud schemes used in mesoscale models such HLAFS and MM5. Ping et al. (2003) developed and improved the features of Gregory cumulus parameterization scheme used in British Weather Office according to the characteristics of area precipitation over China. They showed that the model with improved Gregory scheme can well simulate the precipitation over China.

Liu et al. (2003b, 2003c) implemented three sets of explicit prognostic cloud schemes (two-moment warm cloud, simple mixed-phased cloud and two-moment complicate mixed-phased cloud schemes) into the dynamic framework of the limited-area numerical weather prediction model HLAFS of the National Meteorological Center. According to their simulation results, the mesoscale model including explicit schemes is able to reveal the cloud field evolution and cloud physical characteristics during heavy rainfall development. Zhao et al. (2005b) developed a double-moment microphysical scheme based on the Reisner explicit cloud scheme in MM5. In their new scheme, the number concentration of activated cloud condensation nuclei (CCN) is described with the hypergeometric function and the more reasonable gamma law is used as basic function for the hydrometeor drop-size distribution. The numerical simulations suggested that the new scheme could provide some valuable information on macro- and micro- structure characteristic of stratus cloud, physical process of precipitation and weather modification research.

Aerosol-cloud-radiation coupled model. The first known work on the development and application of size-resolved aerosol model in China had been carried out by Zhao et al. (1998). This mutli-component size-resolving aerosol model was used to investigate the impacts of nss-sulfate and sea-salt on marine clouds microphysical properties (Zhao et al. 2005a). According to the numerical results of Zhao et al. (2005c), soluble organic components will decrease maximum supersaturation, leading to a decrease of cloud drops activated at the case of a high nss-sulfate and a high updraft velocity. Sea-salt will increase cloud optical depth (COD) in case of

low nss-sulfate but decrease COD when nss-sulfate concentration is high.

3.2. Cloud microphysics and precipitation mechanism

Stratiform cloud. The comprehensive field experiments showed that the precipitation microphysical process of stratiform clouds in North China observes basically to the “seeder - feeder” mechanism (You et al., 2002a). Su et al. (2003a) found the layer-separating phenomena in the development stage of precipitating clouds by aircraft measurements in the Qinghai Province of west China. The frontal precipitation cloud system is an important seeding object for artificial precipitation, and generally has the typical structure of “seeder - feeder” cloud.

Using the same 1-D stratiform cloud model of IAP, Hong and Zhou (2005) and Wang et al. (2006b) studied independently the microphysical structure and processes of precipitation formation in cold frontal precipitation stratus cloud system occurring on 4-5 April 2002 in the Henan Province of central east China. Both studies showed that the cold cloud processes play an important role in rainfall, and the growth of ice particles in the mixed ice water layer and melting of graupels into rain water when falling to the warm zone are very important for precipitation formation. Wang et al. (2006b) showed that ice-phase particles are the main components in the cold clouds both before and after the front. According to Hong and Zhou (2005), the ice cloud (seeder cloud), mixed ice water layer and liquid water layer made a contribution to rainfall by 25.5 %, 31.3 % and 43.1 %, respectively, and the contribution of the last two (feeder cloud) is about 74.4 %. Wang et al. (2006b) argued that almost all of rainwater may come from graupel melting, and the mechanism of cold front precipitation could mainly be described as “vapor-snow-graupel-rain water”.

Li et al (2006a) further studied the macro- and micro- structures and precipitation mechanism of the cold-frontal cloud of 4-5 April 2002 in the Henan Province of central east China using the MM5 with the combined Reisner cloud scheme included. For the same case, the different precipitation mechanism was proposed by Li et al. (2006a). They argued that the cold- and warm-cloud processes coexist in the area and the plentiful cloud water is initially produced by warm-cloud process at both the low and middle levels. Their analyses showed that after being generated at the upper level, ice crystals are most converted into snowflakes and less graupel, and the melting of these ice particles, especially mass snowflakes, contributes to the most of surface

precipitation.

Convective cloud. The upper reach of the Yellow River is located in the east of Tibetan Plateau with much water vapor resource and frequent rainfall. Zhao et al. (2003, 2004) studied the precipitation mechanism of shallow convective clouds in the upper reach of the Yellow River. They analyzed radar echo data, surface observation data and rain particle spectrums data over the upper reach area of the Yellow River from June to September 1997–2000, and found that in summer all kinds of clouds belong to mixed-phase cloud with a thick layer of warm cloud inside below. Through the case study of rain particle spectrum evolution, Zhao et al. (2003) preliminarily inferred that both warm rain and cold rain formation mechanisms exist in the microphysical processes of rainfall, but the warm rain mechanism plays an important part in the precipitation development of cloud. Zhao et al. (2004) further simulated microphysical character of convective cloud precipitation using a 2-D size-resolved cloud model - SGBH, and argued that the formation mechanism of warm rain in the shallow convective cloud may play a very important role in the development of convective precipitation.

The results of Zhao et al. (2003, 2004) seemed to be in disagreement with the pervious study of Wang et al. (2002). Through numerical simulation of the characteristics of convective cloud with a 3-D fully elastic cloud model of IAP, the latter indicated that the main process of convective cloud in the upper reach of the Yellow River is cold, and most of the precipitation are graupel and frozen droplets. But it should be noted that the conclusion given by Zhao et al (2004) are for shallow convective cloud. On the basis of observational data and the CAMS 3-D convective cloud model simulations, Fang (2004) showed that the precipitation of convective cloud in the Qinghai Province of west China is mainly determined by cold cloud raining processes. She also demonstrated that graupels play an important role in precipitation and their formation is closely related to ice crystals. Li et al. (2006b) analyzed the raindrop-size distribution in the Maqu region of Gansu Province of west China. They argued that the warm rain process can make a contribution to precipitation although cold rain process is the main precipitation mechanism over the Tibetan Plateau.

It is noted that, although those models used could reproduce convective cloud structure, only radar echo and rain droplet spectrum data, instead of observational cloud microphysical parameters, were used for model comparisons in these studies.

3.3. Cloud physical processes and heavy rainfall

The mesoscale models with explicit cloud schemes have been used to study the effects of

cloud physical processes on heavy rainfall, in particular Meiyu front rainfall (Sun and Wang, 2003; Kang et al., 2003; Yang et al., 2003; Liu et al., 2003c; Wang and Yang, 2003, Zhou et al., 2005b; Zhou et al., 2006). The cloud-top temperature of black body (TBB) observed from the satellite was generally used to compare with the cloud-top temperature simulated by the model. The outline, location, strength, scale, formation and dissipation, and moving direction of a cloud system were generally simulated better with the explicit cloud microphysical schemes, such as the Reisner scheme. It was concluded that ice-phase cloud microphysics processes have significant effects on mesoscale processes and their thermal and dynamical structure, especially for precipitate production and maintenance of heavy rainfall during its early developing stage.

Wang and Yang (2003) investigated the cloud microphysical structures for the heaviest rainfall during the Meiyu front in June 1999 by analyzing both the observational data obtained using the balloon-borne Precipitation Particle Image Sensor and the model results simulated using the MM5 with the Reisner graupel explicit moisture scheme. According to their analysis, the mixed-phase cloud process, in which ice phase coexists and interacts with cloud and liquid phase (cloud and rain drops), plays the most important role in the formation and development of heavy convective rainfall in the Meiyu front system.

Using a 3-D severe convective rainstorm model of IAP Xiao et al. (2004) studied the torrential rainstorm occurring in Wuhan of Hubei Province of south China, on July 21, 1998. They showed that the warm-cloud process was the main developing process in the rain formation of this event. But they also pointed out that the ice-phase microphysical processes can greatly speed the rain formation with the graupel particles contributing the highest to the melting ice-phase particles.

The change of cloud droplet spectra can modify the microphysics and radiative processes of the atmosphere, which in turn affects surface precipitation. Zhou et al. (2005b, 2005c) studied the impact of cloud droplet spectral change (CDSC) on mesoscale precipitation for the two cases, a South China Storm on June 8, 1998 and a Yangtze River Storm on July 22, 2002 by employing the MM5v3 with newly developed, dual-parameterized CAMS explicit moisture scheme coupled. According to their results, CDSC has a slight influence on the rainfall distribution pattern, but can significantly change the precipitation intensity, especially the position and intensity of the precipitation centers.

3.4. Effect of the urbanization on mesoscale convective system

Rapid development of urbanization in China poses a new challenge in forecasting severe mesoscale convective system in the urban regions. Guo et al. (2003, 2006a) studied the effect of urbanization on mesoscale convective system in the Beijing region by using MM5 model. They found that the upper convection weakens and the lower convection strengthens, due primarily to the increase of surface roughness over land that enhances the lower convergence. They also showed that the total accumulated precipitation in the whole domain decreases, especially in the urbanized region, and its distribution tends to become concentrated and also intensified along the borderline between urban and non-urban region. The simulated precipitation intensity and distribution with the urbanization effect included are more consistent with those observed in this region.

4. Cloud physics and hail suppression

4.1. Formation mechanism of hail clouds

With a 3-D parameterized hail cloud model of IAP, Hu et al. (2003) demonstrated that most of the hailstorms in the Xunyi County of Shanxi Province of west China have an accumulation zone for supercooled raindrops, which is the area where most of hail embryos form mainly from frozen drops. Kang et al. (2004b) simulated the formation and growth of hail storm over the central part of Gansu Province of west China, which is located in the northeast of the Tibetan Plateau, using the hail cloud model with hail-bin microphysics. They showed that the mesoscale humidity and dynamics are one of important factors that determine the hailstorm intensity and hails size. By adding snow as a new kind of hydrometeor, Li et al. (2003a) improved the CAMS 3-D convective cloud model. The structure of hail clouds during a hailstone case in Beijing, 1996 was well simulated with the improved model.

The mechanism of cave channels (CC) had been proposed by Xu and Duan (2001, 2002). With the numerical simulation of hailstorm and hailstone growth, they found that there exist a core of main-updraft (MUD) and a zero-area for the horizontal wind speed in relative to hailstorm. They also showed that in the vertical section there is a zero-line from the edge to the core of MUD, below which the wind blows towards the core and upon which the wind blows away. The cave channel with a volume of about 6% or smaller of the total of hailstorm, is just located close to the core of MUD and below the zero area. Once the particles enter CC, they cannot escape its attraction, just like a trap, until they become large stones and fall down from the exit-end. Kang

et al. (2004a) showed that the formation and growth of hails on the northern border of Qinghai-Xizang Plateau observed the CC mechanism. In addition to the zero-line region, they found another high water content region for small ice particles ($D < 1$ mm), graupel and hail embryos ($1 \text{ mm} < D < 5$ mm) and small hailstones ($5 \text{ mm} < D < 10$ mm) over $-30 \sim -50^\circ\text{C}$ altitude at the initial stage of hail formation. It was revealed that the CC is the effective region for the formation and growth of hail. Tian et al. (2005) further verified the CC mechanism by the Doppler radar observations and the analysis of some reliable previous work. They showed that the existing of cave channels (CC) in hail clouds depends on the interaction between the stream and hydrometeor field. One end of the CC connects with embryo formation area, and the other with large stone formation area. While moving around the zero line of horizontal wind, particles concentrate to the CC and, as a result, the accumulation of particles can be found in a whole. Zhu et al. (2004) analyzed the structure of three hailstorms based on a series of the radar scan data. They pointed out that the “cave channel” might exist at the middle-up level of the “S” shape intense reflectivity area that had formed within the anticyclone in the storms.

The heat and mass transfers play a critical role during the hail growth. Zheng (1994) had proposed a parameterization of measured heat transfer coefficients under Reynolds numbers that are related to actual hail scales more closely. Fang et al. (2005b) applied this parameterization to the CAMS 1-D and 3-D hail cloud models. It was indicated that the simulated melting rate, evaporation rate and dry-wet growth rate of a hailstone increase by 12%-50%, 10%-200% and 10%-40%, respectively, with the improved models with respect to the prototype models.

4.2. Hail suppression

Seeding tools of AgI - containing artillery shells and rockets are widely used in hail suppression at present in China, but systematic studies on their efficiency are lacking. On the basis of the theory of liquid water accumulation for hail - formation and growth, Zhou et al (2003) and Li et al (2003b) studied the effects of AgI seeding in the Henan Province and the Shanxi Province, respectively, using the IAP 3-D hail cloud model. The influences of seeding time, height and other conditions were investigated through numerical experiments. These results are expected to give some guidance for the improvement of the seeding efficiencies in practice.

The mechanism of cave channels (CC) provides one of the scientific bases for hail suppression. Kang et al. (2004b) pointed out that the region of formation and growth of hail in hail cloud is in agreement with the intersection of upwards air flow and downwards air flow, where is the main region to put hail embryo for hail suppression. Tian et al. (2005) further suggested that

the target area should include the CC, which locates at the flank of the main updraft and closely below the zero line of horizontal wind.

The dynamical effects on precipitation formation of hailstorm were studied by Zhou et al. (2005a) by means of introducing artificial updraft restraint in the IAP 3-D convective storm numerical model. The results indicated that at the earlier stage of the development of a hailstorm, an artificial restraint with a common intensity (4 m s^{-1} reduction of vertical velocity in 5 min) can highly influence the development and precipitation of the hailstorm, increasing its surface precipitation, especially the hail fall amount, but in the later stage of the hailstorm development, the restraint has small influence on the precipitation.

Li and Hong (2005) improved the IAP 3D hail cloud numerical seeding model by treating the seeding ice crystal as a separate predicted parameter in the equations. The mechanism of hail suppression they proposed is that a number of seeding ice crystal are produced by seeding, so that graupel and frozen drops increase quantitatively, and so do the amount of hailstone from converting of graupel and frozen drop. Thus, the size of hailstone size decreases and, as a result, the intensity of hail fall and the kinetic energy flux of hailstone decrease.

5. Cloud physics and artificial rain enhancement

Studies on cloud microphysics and precipitation, which are closely related to artificial precipitation, have been introduced in Section 3 and will not repeated in this section.

5.1. Theory and model simulations

During the dry seasons of spring and autumn in the northern China, cold stratus clouds are the main precipitation cloud and thus the object of artificial rain enhancement. It had been suggested that supersaturated water vapor with respect to ice would be converted into precipitation after ice seeding besides supercooled water, and the release of sublimation latent heat leads to the increase of temperature and updraft in the seeded cloud regions, promoting to the development of cloud precipitation (Hu, 2001). Hong and Zhou (2005, 2006) argued that the “seeder - feeder” cloud system is an important structure for artificial precipitation and, in addition to cloud structure in the cloud system, the precipitation mechanism, amount of supersaturated water vapor with respect to ice, thickness of cloud water, supercooled water content, ice concentration and precipitation efficiency (precipitation efficiency of condensation water and sublimation water) are also import conditions for artificial precipitation, which should be considered in an integrated way for qualitative assessment of seeding potential. Mao and Zheng (2006) emphasized the importance

of the lifting movement, which induces cloud formation, and the water vapor content in the lifting air mass for the choice of the cloud seeding location and time in weather modification. They argued that in addition to the microphysical conditions, measurements of the lifting movement and the water vapor in the lifting air mass should be greatly strengthened as well.

The natural cloud development processes in the Qinghai Province of west China were studied with the CAMS 3-D cloud model (Fang, 2004; Fang et al., 2005a; Li et al., 2006c). Li et al. (2006c) indicated that convective precipitation is almost all transformed by melting of graupels, but in unseeded clouds, the ice crystals amount is such rare that it contributes little to graupel formation. After seeding, the transformation from ice crystals to graupel is enhanced. Fang (2004) and Fang et al. (2005a) suggested that AgI seeding should be done before ice nucleus largely activate, so that rain enhancement could be improved by increasing ice crystals and decreasing supercooled water. Chen et al. (2005) simulated an event of cold vortex precipitation and hails in the Liaoning Province of northeast China with the IAP 3-D convective cloud model and showed that the ice particles melting, especially graupels melting, play a main role in cloud and precipitation formation. They argued that the optimal time of AgI-seeding should be at the cloud mature stage and the convective-stratiform mixed clouds have a considerably seeding potential to enhance precipitation.

In 1995, De Mott (1995) published their dynamic chamber experiment results, in which they identified and quantified the effect of the four ice-forming mechanisms by AgI, i.e., deposition, contact freezing, condensation and immersion freezing. Liu et al. (2005a) applied the experiment results of De Mott (1995) to the box model, the 1-D stratiform cloud model and 3-D convective model of CAMS. They showed that humidity, temperature, cloud droplet concentration and the cloud holding time are the main influence factors in AgI nucleating process.

The quasi-precipitation efficiency is defined as the ratio of precipitation water to the total water resource in the atmosphere over the region (Li et al., 2006a). Li et al. (2006a) studied a cold-frontal cloud in the Henan Province of central east China during 4-5 April 2002 and showed that most of the precipitation is yielded along the cold-frontal line. They estimated that only 23.1 % of the total water vapor in the simulated area is converted into surface precipitation, which means that most water vapor entering the studied region is not effectively converted into the surface precipitation. Thus, the cold-frontal clouds imply a very high seeding potential for

precipitation enhancement.

Guo et al. (2006b) compared dynamic and microphysical effects of cloud seeding by silver iodide (AgI) and liquid carbon dioxide (liquid CO₂) using the IAP 3-D cloud model initialized with the rawinsonde sounding taken from the Pinliang station located in the western China. The model results showed that the seeding by liquid CO₂ and AgI at -15 to -20 °C levels of cloud has almost the same dynamic effect on the simulated clouds. However, the initial seeding conducted by liquid CO₂ in the region of maximum supercooled water with temperature of 0 to -5°C enable to produce much stronger dynamic effect and precipitation by forming many convective new cells at low levels in the later stage of seeded clouds. Using the same model, but for a case in Beijing, Xiao et al. (2006) showed that the seeding effect in the region of maximum supercooled water (temperature range: 0 to -10 °C) by AgI is better than that by liquid CO₂. In the region of maximum updraft (temperature range: 8 to -7 °C), liquid CO₂ is better than AgI for rain enhancement, and vice versa for hail suppression.

5.2. Field experiments

Zhou et al. (2004) studied the difference in microphysical characteristics between the seeded and unseeded stratiform clouds by analyzing the PMS data obtained during an artificial precipitation in the Liaoning Province of northeast China. They found that the effect of seeding AgI on the microphysical structure of stratiform cloud is obvious. After seeding the concentration of the ice (or snow) crystals increased from 618 m⁻³ to 2267 m⁻³, water content increased from 0.10 g·m⁻³ to 0.17 g·m⁻³, the concentration of the cloud droplet decreased from 34.38 cm⁻³ to 8.97 cm⁻³, and supercooled liquid water content decreased from 0.015 g·m⁻³ to 0.005 g·m⁻³.

Liu et al. (2005b) analyzed the observational data obtained with PMS during rain enhancement operation in precipitating stratus in the Jilin Province of northeast China. They showed that different cloud types have different supercooled water content and cloud droplet number concentration. The estimated rainfall enhancement potential of the three types of clouds they observed were up to 41.3% for Ns, about 28.4% for Sc op, 26.6 % for As tra.

Based on the PMS data obtained during a returning weather process, Yang et al. (2005) found that the stronger precipitating cloud bands have abundant liquid water content and ice crystals, indicating better natural seeding potential. The cold cloud seeding was tested with the PMS by

aircraft measurement in the Shandong Province of central east China in spring of 2000 by Wang and Lei (2003). They reported that liquid water content was decreased, the ice crystal concentration increased, and the particle size distribution widened in the diffuse zone in the five minutes after seeding.

6. Cloud physics and lightning

Lightning is produced by severe thunderstorm and related tightly to other weather disasters such as heavy rain, downburst, hail and tornado. In addition, lightning activity may be a sensitive indicator of global or local climatic variation. The lightning characteristics and their relationship with the microphysical, dynamic features and electric structure of thundercloud in different geographic and climatic zones have been one of the important issues receiving great attention in China.

6.1. The spatial and temporal variations of lightning characteristics in China

With the grounded lightning detecting and locating technology as well as OTD (Optical Transient Detector)/LIS (Lightning Imaging Sensor) database, the characteristics and parameters of the lightning discharges in different areas were obtained (Qie et al., 2003; Ma et al., 2005a, b). Their analysis showed that (1) the Lightning Density (LD) of China's continent regularly varies with latitude and distance off coast, with 2.5 times greater over the eastern than the western area of China, which is consistent with the varying trend of annual mean precipitation. (2) The regional differences in LD distribution are closely related to the mesoscale orographic forcing. On the coastal land, the high LD centers appear in regions where mountain and hill and large cities are located. This seems to be related to the interaction between the sea-land breeze and mountain-valley wind or city heat island effect. (3) Lightning activities on the Tibetan Plateau are found to be a continental-type behavior, which exhibits the diurnal variation with a single peak at 16:00 LT and the annual variation with a single peak in June. China are found to exhibit a double-peak-type diurnal and annual variation.

6.2. Lightning discharges and electric charge structure of thundercloud

The three-dimensional spatial and temporal development of impulsive VHF radiation events

during lightning discharges in two supercell thunderstorms was analyzed based on the data measured by the lightning mapping array (LMA) system with high space and time resolution (Zhang et al., 2006a, b). The results indicated that the charge structures in main part (convective region) of the thunderstorms are inverted tripole while a number of positive cloud-to-ground (CG) lightning discharges occur in the two thunderstorms. The positive CG lightning discharges occurred in main part of the thunderstorms and originated from the positive charge region are located at the middle part of the thunderstorms. The negative charge region located at the upper part of anvil produces a lot of negative CG lightning discharges. The charge region in lower part of the thunderstorm plays an important role for the occurrence of CG lightning from charge region above it.

The analysis of Zhang et al. (2002) revealed that intracloud (IC) discharges occur not only between the upper positive and middle main negative charge region, but also within the inverted polarity between the lower positive and middle main negative charge regions. Their results further confirmed the existence of the lower positive charge region involved in the lightning discharge. They also found that the inverted charge structure opposite to the normal polarity appears in some storms or at a certain stage of the storm development.

Qie et al. (2005) studied the characteristics of lightning discharge and charge structure in the northeastern verge of Tibetan Plateau on the basis of surface electric field measurements in 6 sites and a high-speed digital camera records. It was estimated that a sequence of 30 flashes are produced from a storm with a tripole structure in the mature stage. Most of the intracloud (IC) flashes occur in the lower part and only a few occur in the upper part of the thunderstorm.

Tan et al. (2006a, b) integrated inductive and non-inductive electrification as well an improved Stochastic Lightning Model into 2-D and 3-D cumulus model in CAMS, and reproduced the fine channel structure of IC and CG lightning flashes in different electric structures of thunderstorm. Their results indicated that there appear both types of positive and negative polarity IC flashes and their channels exhibit the bi-level branched structure, whenever the positive (or negative) potential well is collocated with an upper negative (or positive) well and its size extending along horizontal direction is greater than that along vertical direction.

6.3. Relationship of lightning activity with the climatic changes

On the basis of the 5-year or 8-year OTD/LIS satellite-based lightning detecting data and the NCEP reanalysis data, Ma et al. (2005c) did a reanalysis of the response of the global and regional lightning activities to temperature variations. The results showed that on the interannual time scale the global total flash rate has positive response to the variation in global surface air temperature, with the sensitivity of $17 \pm 7\% \text{ K}^{-1}$. In addition, Ma et al. (2005b) found the LD positive anomalies in the southeastern China and adjacent coastal areas associated with the 1997/98 El Niño event.

7. Clouds and climate change

7.1. Cloud climatology

The International Satellite Cloud Climatology Project (ISCCP) D2 dataset have been used in a few studies to analyze the global and regional cloud amount variation over the past 20 years. Ding et al. (2004, 2005) showed that the global cloud amount distribution is mainly affected by atmospheric circulation and has remarkable regional features. Liu et al. (2003g) studied the climatic characteristics of cloud over China observed by the ISCCP with comparison to the routine surface observation. According to their analysis, there were a decrease of $5\% \text{ yr}^{-1}$ in the total cloud amount over the North-China Plain during the period 1984-1994 and a decrease of $10\% \text{ yr}^{-1}$ in the low-cloud amount over the Sichuan Basin of northwest China during the period 1975-1994. The most manifest decrease ($40\% \text{ yr}^{-1}$) in the low-cloud amount was found over Chengdu, the center of the Sichuan Basin, for the period 1975-1985. Liu et al. (2004) studied the spatial distribution and temporal variation of cloud amount over China with the ISCCP data. It was concluded that the cloud amount increased in the northeastern China, and decreased in the western and northern China during the period 1983-2001. ISCCP data were also used for the comparison and evaluation of a regional numerical model by Li and Yu (2006).

7.2. Clouds and radiation

Almost no cloud field on Earth is horizontally and vertically uniform, but most studies on cloud radiation are based on the assumption of plane - parallel radiative transfer. Hu and Liu (2004) gave an overview of the theory of 3D multimode radiative transfer, and developed a code based on this theory and the radiative transfer model - DISORT to investigate the influence of the sides of

the finite clouds on cloud shortwave absorption. Zhang et al. (2005) computed the cloud shortwave radiative forcing in southeast China using the cloud radiative parameters retrieved from the GMS satellite data.

The impacts of cloud radiative transfer processes on precipitation were studied using a two-dimensional cumulus model (Zhao et al., 2003). Numerical results showed that cloud top cooling radiation and heating at the cloud base due to longwave could enhance convective processes within cloud by modifying the vertical temperature structure in the cloud. Further, Zhou et al., (2006) proposed a method to quantitatively estimate the effects of radiative transfer process on precipitation by defining equivalent radiative cooling/heating which is combined by radiative cooling/heating and the vertical velocity variation ascribed to radiative transfer process. This algorithm was verified by modeling a long period rainfall case in June 2002. The results showed that radiative transfer process enhances diurnal precipitation variation by increasing the nocturnal rainfall and suppressing the daytime's as well as the total rainfall. The effects of radiation on a mesoscale precipitating system was investigated during a sever storm in South China on June 8, 1998 (Zhou et al., 2005c). The results suggested that the rainfall patterns do not differ too much for the various radiation schemes used in the numerical calculations, but rather influence the rainfall intensity in the central areas. As mentioned in Section 3.3, the impact of cloud droplet spectral on the microphysics and radiative processes was studied by Zhou et al. (2005b, 2005c).

7.3. Atmospheric aerosols and clouds

Huang et al. (2005) analyzed the PMS data on stratus cloud microphysical properties in the Hebei Province of central east China during October 1990 and April 1991. They found that there is a positive correlation between aerosol number concentrations below the cloud base and cloud droplet number concentrations. Using a mutli-component size-resolving aerosol model, Zhao et al. (2005a, 2005c) investigated the role of sea-salt in marine cloud microphysical processes. They showed that sea-salt particles are activated into cloud drops in the initial cloud development, and sea-salt activation decreases supersaturation by consuming water vapor and suppresses nss-sulfate activation. Nss-sulfate indirect forcing may be overestimated in some conditions (such as updraft is low) because of the presence of sea-salt particles.

Ice nuclei (IN) are very important in many weather events for the reason that IN can affect

the initial concentrations of ice particles in cold cloud and then change the physical characteristics of cold cloud. Observations in Beijing showed that the concentrations of IN, which could be activated at $-20\text{ }^{\circ}\text{C}$, increased about 15 times from 1963 to 1995 (You et al., 2002b). Using the CAMS 3-D convective cloud model, Li et al. (2004a) studied the 18-days precipitation processes over the Beijing area for the period between June and September 1996. They conducted the numerical experiments by supposing that the concentration of IN had increased 5 times. The model results indicated that for the most precipitation processes, the height of cloud top, the area of cloud top and the quantity of ice crystals increase, and the size of ice crystals decreases, leading to the change in the radiant properties of cloud. Li and Mao (2006) analyzed the cold cloud reflectivity in China during the period 1982-1999 using the PAL (NOAA/NASA Pathfinder AVHRR Tiled Land Data). They found that the cold cloud reflectivity had changed over some areas for this period. For the case of the Beijing area, the cold cloud reflectivity changed nonlinearly, with an increase over the first 10-years and a decrease over the last 10-years. They inferred that the ice nuclei may have an effect on the cold cloud reflectivity.

Zhao et al., (2006b) studied the relationship between cloud spectral relative dispersion (ϵ) and cloud droplet number concentration (N_c) using a large amount of aircraft measurements of cloud droplet size distributions. The results indicated that the value of ϵ varies between 0.2 and 0.8 when the cloud droplet number concentration is low (about 50 cm^{-3}), and converges towards a narrow range of 0.4 to 0.5 when the cloud number concentration is higher. Because the distribution of the cloud droplet size is an important parameter in estimating the first indirect radiative effect of aerosols on the climate system, the uncertainty in the corresponding radiative forcing can be reduced by 10-40% (depending on cloud droplet number density) under high aerosol loading. This finding is important for improving climate change projections, especially for the regions where aerosol loading is high and continues to increase.

Huang et al. (2006b) studied the effects of dust storms on cloud properties and Radiative Forcing (RF) over Northwestern China using the data collected by MODIS and the Earth's Radiant Energy System (CERES) scanning radiometer on the Aqua and Terra satellites. They demonstrated that on average, ice cloud effective particle diameter, optical depth and ice water path of cirrus clouds under dust polluted conditions are 11%, 32.8%, and 42% less, respectively, than those derived from ice clouds in dust-free atmospheric environments. Due to changes in cloud microphysics, the instantaneous net RF is increased from $-161.6\text{ W}\cdot\text{m}^{-2}$ for dust-free clouds to $-118.6\text{ W}\cdot\text{m}^{-2}$ for dust-contaminated clouds. By analyzing the satellite data from ISCCP, MODIS and CERES, Huang et al. (2006a) showed that the water path of dust-contaminated clouds is considerably smaller than that of dust-free clouds, and there is significant negative correlation

between dust storm index and ISCCP cloud water path. They inferred that the semi-direct effect may play a role in cloud development over arid and semi-arid areas of East Asia and contribute to the reduction of precipitation.

8. Conclusion and remarks

In our review of China cloud physics research from 2003 to 2006, we see increasing interest in studying cloud physics from a wide variety of topics covering cloud field experiments and planned weather modification, relationships between cloud physics and precipitation, hails, lightnings, and aerosols-cloud-radiation interactions. This is derived by an interest in solving the complex problems of climate change, weather forecasting, the growing demand for fresh water and agriculture purposes. We believe that cloud physics and planned weather modification is still an important direction and active research field both in theoretical and measurements in future years.

Aircraft measurements have provided important physical evidence about in-cloud conditions in China. New onboard instrumentations for aerosol and cloud observations have widely been used in the most parts of North China during 2003-2006. But we should realize that there are still large uncertainties existing in quantifying the spatial and temporal character of cloud and precipitation. Much work will be needed for a comprehensive evaluation of the quality of these data. A systematic analysis of the data with comparisons of model simulations should also be performed for the understanding of the microphysical mechanisms behind the variations in cloud properties.

Planned weather modification in China attracts more attention from public and the local governments in many provinces due to fresh water and agriculture purposes. Although the development of a scientifically accepted cloud seeding technology is probably several years away due to relative poor understanding of purely statistical evaluations for seeding effects, planned weather modification in China offers the unique opportunity to actively experiment with clouds. We believe that more physical oriented measurements would not only improve knowledge about natural cloud and precipitation processes, but also help us to better understand how anthropogenic activities affect cloud microphysical properties. This requires us to do more work on interpreting aircraft observations of rapidly evolving, small-scale convection events into appropriate spatial and temporal quantities useful for model evaluation.

The comprehensive field experiments have shown that the precipitation microphysical process of stratiform clouds in North China observes basically to the “seeder - feeder” mechanism. The frontal precipitation cloud system is an important seeding object for artificial precipitation, and generally has the typical structure of “seeder - feeder” cloud. While most studies have indicated the importance of cold cloud process in rainfall, some have argued that the warm rain mechanism plays an important part in the precipitation development of cloud.

In addition to the microphysical conditions, the importance of the lifting movement, which

induces cloud formation, and the water vapor content in the lifting air mass for the choice of the cloud seeding location and time in weather modification has been emphasized. Concurrent measurements of cloud microphysical parameters as well as the vertical speed and water vapor in the lifting air mass need to be strengthened in the future intensive field experiment. More conditions than cloud structure should be considered for the assessment of seeding potential in artificial precipitation.

The mechanism of cave channels (CC) has been proposed, and would provide one of the scientific bases for hail suppression. Although there are a few reports on the verification of the CC mechanism by the model simulations and Doppler radar observations, more work is needed to confirm the CC phenomenon and reveal the mechanisms associated with the accumulation of particles.

There have been increasing studies and usage of satellite data focusing on both macro- and micro- physical characteristics of clouds during the last four years in China. Many cloud parameters imaged from satellites, such as liquid and ice water content, cloud top temperature, cloud cover, cloud optical thickness, cloud drop effective radius, and 3D structure of rainfall rates have been used for various research from cloud microphysics, to mesoscale precipitation, and to climate change. The effect of the precipitation enhancement operation with an aircraft has been viewed by the satellite, which highlights the potential application of satellite images in the operation of weather modification. Much more work is needed for the retrieval of cloud microphysical parameters with Chinese satellites data.

Due the limitation of aircraft measurements in deep convective clouds, other measuring methods such as microwave radiometer remote sensing and video images are also useful, in particular for the study of cloud microphysical processes in heavy rainfall. This may be an important and challenge work in the field experiment of thunderstorms over China. It has been found that ice-phase microphysical processes of clouds may have significant effects on precipitation formation and heavy rainfall. Measurements of ice-phase particles should be strengthened in the future field experiments.

Various cloud models, which were originally developed in 1980s and 1990s by different Chinese groups/institutes, have been used in the studies over the last four years. These include 0-D, 1-D, 2-D or 3-D cloud model, stratiform or convective model, and size-resolved or bulk cloud model with various cloud microphysical processes included. Model results have generally been compared with cloud macro- structure retrieved from radar echoes and satellite data. Much work on the comparison between model simulations and microphysical parameters obtained, e.g., with the PMS, needs to be done in the future study. This will be the most important for the

understanding of microphysical processes occurring in the clouds.

The interactions between aerosol, cloud and radiation processes are one of the front research fields both in global climate changes and short-term weather forecasting. Measurements and theoretical studies in this field have been carried out in China during the past four years. A significant challenge is to study the role of atmospheric chemistry in cloud physics and precipitation. Correlations between aerosol pollution and cloud microphysical properties have been found through the analysis of historical data. While the research on weather modification pays more attention to large particles, the research on aerosols, clouds and radiation interaction should focus more on fine and ultra fine particles. Integrated space-, air- and ground- born observations of aerosol, cloud and radiation parameters are suggested to get invaluable information on the issues. Coupled models that include aerosol and cloud chemical/physical processes and radiative transfer need to be developed and applied in the studies related to climate changes. The urbanization effects including urban aerosol emissions and land surface change on cloud and precipitation processes pose a new challenge in both regional weather forecasting and climate change.

Acknowledgments.

References

- Albrecht, B. A., 1989: Aerosols, cloud microphysics, and fractional cloudiness. *Science*, **245**, 1227-1230.
- Cao Junwu and Liu Liping, 2006: Hail identification with dual-linear polarimetric radar observations. *Meteor. Mon.*, **32**, 13-19.
- Cao Junwu, Liu Liping, Chen Xiaohui, and Chen Gang, 2006: Data quality analysis of 3836 C-band dual-linear polarimetric weather radar and its observation of a rainfall process. *J. Appl. Meteor. Sci.*, **17**, 192-200.
- Chen Hongbin, 2002: A concept for measuring liquid water path from microwave attenuation along satellite-earth path. *Chinese J. Atmos. Sci.*, **26**, 695-701. (in Chinese)
- Chen Baojun, Zhou Deping, Gong Fujiu, Wang Jihong, and Geng Sujiang, 2005: AgI-Seeding modeling study on the 12 July 2002 cold vortex precipitation in Shenyang. *J. Nanjing Inst. Meteor.*, **28**, 483-491. (in Chinese)
- Dai Jin, Yu Xing, D. Rosenfeld, and Xu Xiaohong, 2006: Analysis of satellite observed microphysical signatures of cloud seeding tracks in supercooled layer clouds. *Acta Meteor. Sinica*, **64**, 622-629.
- De Mott, P.J., 1995: Quantitative descriptions of ice formation mechanism of silver iodide-type aerosols. *Atmos. Res.*, **38**, 63-99.
- Ding Shouguo, Shi Guangyu, and Zhao Chunsheng, 2004: Analyzing global trends of different cloud types and their potential impacts on climate by using the ISCCP D2 dataset. *Chinese Science Bulletin*, **49**, 1301-1306.

- Ding Shouguo, Zhao Chunsheng, Shi Guangyu, and Wu Chun'ai, 2005: Analysis of global total cloud amount variation over the past 20 years. *Quarterly J. Appl. Meteor.*, **16**, 670-677. (in Chinese)
- Fang Wen, 2004: Study of convective clouds in Qinghai Province. *Meteor. Sci. Tech.*, **32**, 343-347. (in Chinese)
- Fang Wen, Guoguang Zheng, Xueliang Guo, and Huanbin Xu, 2003: Overview of hail suppression projects in China. WMO/WHP report No. 41, 165-173.
- Fang Wen, Zheng Guoguang, and He Guanfang, 2005a: Simulation study on the precipitation and seeding process of convective-cloud in Qinghai with a 3D cloud model. *J. Nanjing Inst. Meteor.*, **28**, 763-769. (in Chinese)
- Fang Wen, Zheng Guoguang, and Hu Zhijin, 2005b: Numerical simulations of the physical process for hailstone growth. *Acta Meteor. Sinica*, **19**, 93-101.
- Guo, X. L., and M. Y. Huang, 2002: Hail formation and growth in a 3D cloud model with hail-bin microphysics. *Atmos. Res.*, **63**, 59-99.
- Guo Xueliang and Fu Danhong, 2003: The formation process and cloud physical characteristics for a typical disastrous wind-producing hailstorm in Beijing. *Chinese Science Bulletin*, **48**, Suppl ii, 77-82.
- Guo Xueliang, Meiyuan Huang, Danhong Fu, Guoguang Zheng and Wen Fang, 2003: Hail-cloud modeling activities in China. WMO/WHP report No. 41, 143-148.
- Guo X. L., D. H., Fu and J. Wang, 2006a: Mesoscale convective precipitation system modified by urbanization in Beijing City. *Atmos. Res.*, **82**, 112-116.
- Guo, X. L., G. G. Zheng, and D. Z. Jin, 2006b: A numerical comparison study of cloud seeding by silver iodide and liquid carbon dioxide. *Atmos. Res.*, **79**, 183-226.
- He Huizhong, Cheng Minghu, and Zhou Fengxian, 2006: 3D structure of rain and cloud hydrometeors for Typhoon Kujira (0302). *Chinese J. Atmos. Sci.*, **30**, 491-503.
- Hong Yanchao, 1996: The numerical simulation study of convective-stratiform mixed cloud, part (I) — The model and parameterization of microphysical processes. *Acta meteor. Sinica*, **54**, 557. (in Chinese)
- Hong Yanchao, 1998: A 3-D hail cloud numerical seeding model. *Acta Meteor. Sinica*, **56**, 641-653. (in Chinese)
- Hong Yanchao and Zhou Feifei, 2005: A numerical simulation study of precipitation formation mechanism of "seeding-feeding" cloud system. *Chinese J. Atmos. Sci.*, **29**, 885-896. (in Chinese)
- Hong Yanchao and Zhou Feifei, 2006: The study of evaluation of potential of artificial precipitation enhancement in stratiform cloud system. *Chinese J. Atmos. Sci.*, **30**, 913-926. (in Chinese)
- Houghton, J. T., L. G. Meira Filho, B. A. Callander, N. Harris, A. Kattenberg, and K. Maskell (Eds), 1995: Climate Change 1995, The Science of Climate Change, Contribution of the Scientific Assessment Working Group (WGI) to the Second Assessment Report of the Intergovernmental Panel on Climate Change, 572 pp. Cambridge Univ. Press, New York.
- Hu Zhijin, 2001: Discussion on mechanisms, conditions and methods of precipitation enhancement in stratiform clouds. *Quart. J. Appl. Meteor.*, **12**, Suppl. 10-13. (in Chinese)
- Hu Zhijin and Yan Caifan, 1986: Numerical simulation of microphysical processes of stratiform clouds (I) — microphysical cloud model. *J. Academy Meteor. Sci.*, **1986**, 37-52. (in Chinese)
- Hu Zhijin and He Guanfang, 1987: Numerical simulation of microphysical processes of convective clouds (I) — microphysical cloud model. *Acta Meteor. Sinica*, **45**, 467-484. (in Chinese)
- Hu Liqin and Liu Changsheng, 2004: An attempt to study the three-dimensional radiative properties of cloud using the theory of multimode transfer. *Chinese J. Atmos. Sci.*, **28**, 91-100. (in Chinese)
- Hu Zhaoxia, Li Hongyu, Xiao Hui, Hong Yanchao, Huang Meiyuan, and Wu Yuxia, 2003: Numerical simulation of hailstorms and the characteristics of accumulation zone of supercooled raindrops in Xunyi County. *Clim. Environ. Res.*, **8**, 196-208. (in Chinese)
- Huang Meiyuan, Shen Zhilai, and Hong Yanchao, 2003: Advance of research on cloud and precipitation and

- weather modification in the latest half century. *Chinese J. Atmos. Sci.*, **27**, 536-551. (in Chinese)
- Huang Mengyu, Zhao Chunsheng, Zhou Guangqiang, Duan Ying, Shi Lixin, and Wu Zhihui, 2005: Stratus cloud microphysical characters over North China region and the relationship between aerosols and clouds. *J. Nanjing Inst. Meteor.*, **28**, 360-368. (in Chinese)
- Huang, J., B. Lin, P. Minnis, T. Wang, X. Wang, Y. Hu, Y. Yi, and J. K. Ayers, 2006a: Satellite-based assessment of possible dust aerosols semi-direct effect on cloud water path over East Asia. *Geophys. Res. Lett.*, **33**, L19802, doi:10.1029/2006GL026561.
- Huang, J., P. Minnis, B. Lin, T. Wang, Y. Yi, Y. Hu, S. Sun-Mack, and K. Ayers, 2006b: Possible influences of Asian dust aerosols on cloud properties and radiative forcing observed from MODIS and CERES. *Geophys. Res. Lett.*, **33**, L06824, doi:10.1029/2005GL024724.
- Jin Dezhen, Gu Shufang, Zheng Jiaoheng, Zhang Jinghong, Li Maolun, and Chen Zhixin, 2004: Measurement of column cloud liquid water content by airborne upward-looking microwave radiometer. *Acta Meteor. Sinica*, **62**, 868-874. (in Chinese)
- Jin Hua, Wang Guanghe, You Laiguang, and Feng Daxiong, 2006: On physical structure of stratiform cloud during a precipitation process in Henan Province. *Meteor. Mon.*, **32**, 3-10. (in Chinese)
- Kang Lili, Lei Hengchi, and Xiao Wenan, 2003: Simulation of various moist physical processes in mesoscale model. *J. Nanjing Inst. Meteor.*, **26**, 76-83. (in Chinese)
- Kang Fengqin, Zhang Qiang, Ma Shengping, Qiao Yanjun, and Guo Xueliang, 2004a: Mechanism of hail formation on the northeast border of Qinghai-Xizang Plateau and its neighbourhood. *Plateau Meteor.*, **23**, 749-757. (in Chinese)
- Kang Fengqin, Zhang Qiang, Qu Yongxing, Ji Lanzhi1, and Guo Xueliang, 2004b: Simulating study on hail microphysical process on the northeastern side of Qinghai-Xizang Plateau and its neighbourhood. *Plateau Meteor.*, **23**, 735-742. (in Chinese)
- Kong Fanyou, Huang Meiyuan, and Xu Huaying, 1990: A three-dimensional numerical model of ice-phase convective cloud. *Chinese J. Atmos. Sci.*, **14**, 441-453. (in Chinese)
- Lei Hengchi, Wei Chong, Shen Zhilai, Zhang Xiaoqing, Jin Dezhen, Gu Shufang, Li Maolun, and Zhang Jinghong, 2003: Measurement of column cloud liquid water content by airborne upward-looking microwave radiometer (I): Instrument and its calibration. *Plateau Meteor.*, **22**, 551-557. (in Chinese)
- Li Shuri, 2006: Case study of cloud and precipitation micro-physics structure over North West China. *Meteor. Mon.*, **32**, 59-63. (in Chinese)
- Li Xingyu and Hong Yanchao, 2005: The improvement of 3D hail cloud model and case simulation. *Acta Meteor. Sinica*, **63**, 874-888. (in Chinese)
- Li Juan and Mao Jietai, 2006: Influence of atmospheric ice nucleus concentrations on cold cloud radiant properties and cold cloud reflectivity changes in past years. *Chinese Science Bulletin*, **51**, 480-489.
- Li Yunying and Yu Rucong, 2006: Comparison of cloud parameters between AREM simulation and satellite retrieval. *Chinese J. Atmos. Sci.*, **30**, 1198-1205. (in Chinese)
- Li Shuri, Hu Zhijin, and Wang Guanghe, 2003a: Improvement and simulation of three-dimension convective cloud seeding model of CAMS. *J. Appl. Meteor. Sci.*, **14**, Supp. 78-91. (in Chinese)
- Li Hongyu, Hu Zhaoxia, Xiao Hui, and Hong Yanchao, 2003b: Numerical studies of the practical seeding methods in hail suppression. *Chinese J. Atmos. Sci.*, **27**, 212-222. (in Chinese)
- Li Zhaorong, Li Rongqing, and Li Baozi, 2003c: Analyses on vertical microphysical characteristics of autumn stratiform cloud in Lanzhou region. *Plateau Meteor.*, **22**, 583-589. (in Chinese)
- Li Juan, Mao Jietai, Hu Zhijin, You Laiguang, and Zhang Qiang, 2004a: Numerical simulation experiments for the effect of changes of atmospheric nuclei concentrations on radiant properties of cloud. *Acta Meteor. Sinica*, **62**, 77-86. (in Chinese)

- Li Yongping, Yuan Zhaohong, and Wang Xiaofeng, 2004b: Microphysical adjustments using reflectivity of Doppler radar for meso-scale model. *Quarterly J. Appl. Meteor.*, **15**, 658-664. (in Chinese)
- Li Yongping, Zhu Guofu, and Xue Jishan, 2004c: Microphysical retrieval from Doppler radar reflectivity using variational data assimilation. *Acta Meteor. Sinica*, **62**, 814-820. (in Chinese)
- Li Hongyu, Wang Hua, and Hong Yanchao, 2006a: A numerical study of precipitation enhancement potential in frontal cloud system. *Chinese J. Atmos. Sci.*, **30**, 341-350. (in Chinese)
- Li Juan, You Laiguang, Hu Zhijin, Tu Duobin, and Li Lunge, 2006b: Analysis on raindrop-size distribution characteristics of Maqu region in upper reach of Yellow River. *Plateau Meteor.*, **25**, 942-949.
- Li Yanwei, Zheng Guoguang, Du Bingyu, and Guo Xueliang, 2006c: Numerical simulation of a convective cloud precipitation enhancement in Qinghai in autumn. *J. Nanjing Inst. Meteor.*, **29**, 328-325.
- Liu Liping and Ge Runsheng, 2006: An overview on radar meteorology research in Chinese Academy of Meteorological Sciences for a half century. *J. Appl. Meteor. Sci.*, **17**, 682-689. (in Chinese)
- Liu Liping, Ge Runsheng, and Zhang Peiyuan, 2002: A study of method and accuracy of rainfall and liquid water content measurements by dual linear polarization Doppler radar. *J. Atmos. Sci.*, **26**, 709-720. (in Chinese)
- Liu Jian, Dong Chaohua, Zhu Yuanjing, Zhu Xiaoxiang, and Zhang Wenjian, 2003a: Thermodynamic phase analysis of cloud particles with FY21C data. *Chinese J. Atmos. Sci.*, **27**, 901-908. (in Chinese)
- Liu Qijun, Hu Zhijin and Zhou Xiuji, 2003b: Explicit cloud schemes of HALFS and simulation of heavy rainfall and cloud, Part I: explicit cloud schemes. *J. Appl. Meteor. Sci.*, **14**, Suppl., 60-67. (in Chinese)
- Liu Qijun, Hu Zhijin and Zhou Xiuji, 2003c: Explicit cloud schemes of HALFS and simulation of heavy rainfall and cloud, Part II: simulation of heavy rainfall and clouds. *J. Appl. Meteor. Sci.*, **14**, Suppl., 68-77. (in Chinese)
- Liu Jin-li, Lv Da-ren, Zhang Ling, and Duan Shu, 2003d: Space-borne remote sensing on liquid water content of precipitating cloud. *J. Remote Sensing*, **7**, 227-232. (in Chinese)
- Liu Dong, Qi Fudi, Jin Chuanjia, Yue Guming, and Zhou Jun, 2003e: Polarization lidar observations of cirrus clouds and Asian dust aerosols over Hefei. *Chinese J. Atmos. Sci.*, **27**, 1093-1100. (in Chinese)
- Liu Weiguo, Su Zhengjun, Wang Guanghe, and Li Shuri, 2003f: Development and application of new-generation airborne particle measuring system. *J. Appl. Meteor. Sci.*, **14**, Suppl. 11-18. (in Chinese)
- Liu Hongli, Zhu Wenqin, Yi Shuhua, Li Weiliang, Chen Longxun, and Bai Lijie, 2003g: Climatic analysis of the cloud over China. *Acta Meteor. Sinica*, **61**, 466-473. (in Chinese)
- Liu Ruixia, Liu Yujie, and Du Bingyu, 2004: Cloud climatology characteristics of China. *Quarterly J. Appl. Meteor.*, **15**, 468-476. (in Chinese)
- Liu Shijun, Hu Zhijin, and You Laiguang, 2005a: The numerical simulation of AgI nucleation in cloud. *Acta Meteor. Sinica*, **63**, 30-40. (in Chinese)
- Liu Jian, Li Maolun, Jiang Tong, Mi Changshu, and Chen Zhixin, 2005b: The preliminary study of the basic structure of precipitating stratus and precipitation potential in spring in Jilin Province. *Scientia Meteor. Sinica*, **25**, 609-616. (in Chinese)
- Liu Liping, Ruan Zheng, Qin Danyu, 2005c: Case studies on mesoscale structures of heavy rainfall system in the Yangtze River generated by Meiyu front. *Science in China: Ser. D - Earth Sciences*, **48**, 1303-1311.
- Liu Chaoshun, Lü Daren, and Du Bingyu, 2006: A study on ground-based remote sensing of atmospheric integrated water vapor and cloud liquid water. *J. Nanjing Inst. Meteor.*, **29**, 606-612. (in Chinese)
- Lou Xiaofeng, Hu Zhijin, Wang Penyun, and Zhou Xiuji, 2003: Introduction to microphysical scheme of mesoscale atmospheric models and cloud models. *J. Appl. Meteor. Sci.*, **14**, Suppl. 50-59. (in Chinese)
- Lu Daren, Wang Pucai, Qiu Jinhuan, and Tao Shiyuan, 2003: An overview on the research progress of atmospheric remote sensing and satellite meteorology in China. *Chinese J. Atmos. Sci.*, **27**, 552-566. (in Chinese)
- Ma Ming, Tao Shanchang, Zhu Baoyou, and LÜ Weitao, 2005a: Climatological distribution of lightning density

- observed by satellites in China and its circumjacent regions. *Science in China: Ser. D - Earth Sciences*, **48**, 219-229.
- Ma Ming, Tao Shanchang, Zhu Baoyou, and LÜ Weitao, 2005b: The anomalous variation of the lightning activity in southern China during the 1997/98 El Niño event. *Science in China: Ser. D - Earth Sciences*, **48**, 1537~1547.
- Ma Ming, Tao Shanchang, Zhu Baoyou, LÜ Weitao, and Tan Yongbo, 2005c: Response of global lightning activity to air temperature variation. *Chinese Science Bulletin*, **50**, 2640~2644.
- Mao Jietai and Zheng Guoguang, 2006: Discussions on some weather modification issues. *J. Appl. Meteor. Sci.*, **17**, 643-646. (in Chinese)
- Ping Fan, Gao Shouting, and Wang Huijun, 2003: Development and improvement of mass flux convection parameterization scheme and its applications in the seasonal climate prediction model. *Chinese Science Bulletin*, **48**, 1006-1015.
- Qie X., R. Toumi, T. Yuan, 2003: Lightning activities on the Tibetan Plateau as observed by the lightning imaging sensor. *J. Geophys. Res.*, **108** (D17), 4551, doi:10.1029/2002JD003304.
- Qie, X., X. Kong, G. Zhang, T. Zhang, T. Yuan, Y. Zhou, Y. Zhang, H. Wang and A. Sun, 2005: The possible charge structure of thunderstorm and lightning discharges in northeastern verge of Qinghai-Tibetan Plateau. *Atmospheric Research*, **76**, 231-246.
- Ramanathan, V., P. J. Crutzen, J. T. Kiehl, and D. Rosenfeld, 2001: Aerosols, climate, and the hydrological cycle. *Science*, **294**, 2119-2124.
- Su Zhengjun, Liu weiguo, Wang Guanghe, and Xu Chenhai, 2003a: Microphysical characteristics of a precipitation process in Qinghai Province. *J. Appl. Meteor. Sci.*, **14**, Suppl. 27-35. (in Chinese)
- Su Zhengjun, Wang Guanghe, Liu weiguo, and Li Lunge, 2003b: Micro-structure analysis of spring precipitable clouds in Qinghai Province. *J. Appl. Meteor. Sci.*, **14**, Suppl. 36-40. (in Chinese)
- Sun Jing and Wang Pengyun, 2003: Numerical study of heavy rainfall in south China with Reisner graupel scheme. *Meteor. Mon.*, **29**, 10-14. (in Chinese)
- Takahashi, T., K. Suzuki, and M. Orita, 1995: Videosonde observation of precipitation processes in equatorial cloud clusters. *J. Meteor. Soc. Japan*, **73**, 509-534. (in Chinese)
- Tan Yongbo, Shanchang Tao, and Baoyou Zhu, 2006a: Fine-resolution simulation of the channel structures and propagation features of intracloud lightning. *Geophys. Res. Lett.*, **33**, L09809, doi:10.1029/2005GL025523.
- Tan Yongbo, Shanchang Tao, Baoyou Zhu, Ming Ma, and Weitao LÜ, 2006b: Numerical simulations of the bi-level and branched structure of intracloud lightning flashes. *Science in China: Ser. D - Earth Sciences*, **49**, 661-672.
- Tian Liqing, Xu Huanbin, and Wang Angsheng, 2005: Verification and reproduction of the new understanding for mechanism of hail cloud. *Plateau Meteor.*, **1**, 78-83. (in Chinese)
- Twomey, S. J., 1974: Pollution and the planetary albedo. *Atmos. Environ.*, **8**, 1251-1256.
- Twomey, S. J., 1977: The influence of pollution on the shortwave albedo of clouds. *J. Atmos. Sci.*, **34**, 1149-1152.
- Wang Zhijun and Chu Rongzhong, 2002: Application potential of polarization radar in weather modification. *Plateau Meteor.*, **21**, 591-598. (in Chinese)
- Wang Yilin and Lei Hengch, 2003: Test of cold cloud seeding. *Chinese J. Atmos. Sci.*, **27**, 929-938. (in Chinese)
- Wang Pengyun and Yang Jing, 2003: Observation and numerical simulation of cloud physical processes associated with torrential rain of the Meiyu front. *Adv. Atmos. Sci.*, **20**, 77-96.
- Wang Hong, Lei Hengchi, Deligeri, Li Lunge, Xiao Wenan, Hong Yanchao, and Huang Meiyuan, 2002: A numerical simulation of characteristics of convective cloud at the upper reaches of the Yellow River. *Clim. Environ. Res.*, **7**, 397-408. (in Chinese)
- Wang Yangfeng, Lei Hengchi, Wu Yuxia, Xiao Wenan, and Zhang Xiaoqing, 2005: Size distributions of the water

- drops in the warm layer of stratiform clouds in Yan' an. *J. Nanjing Inst. Meteor.*, **28**, 787-793. (in Chinese)
- Wang Yu, Fu Yunfei, and Liu Guosheng, 2006a: Retrieval of liquid water path in nonprecipitating clouds using TNI measurements. *Acta Meteor. Sinica*, **64**, 443-452. (in Chinese)
- Wang Baizhong, Liao Fei, and Hu Yamin, 2006b: Microphysical mechanisms of regional cold-front precipitation. *Meteor. Sci. Tech.*, **34**, 35-40. (in Chinese)
- Warren, S.G., C.J. Hahn, J. London, R.M. Chervin, and R.L. Jenne, 1986: Global distribution of total cloud cover and cloud type amounts over land. NCAR Technical note TN-273+STR. National Center for Atmospheric Research, Boulder, CO.
- Warren, S.G., C.J. Hahn, J. London, R.M. Chervin, and R.L. Jenne, 1988: Global distribution of total cloud cover and cloud type amounts over land. NCAR Technical note TN-317+STR. National Center for Atmospheric Research, Boulder, CO.
- Wu Dui, 2005: A general perspective of precipitation enhancement in China and abroad. *Guangdong Meteor.*, **1**, 25-29. (in Chinese)
- Xiao Hui, and coauthors, 2002: Earlier identification and numerical simulation of hail storms occurring in Xunyi region. *Plateau Meteor.*, **21**, 159-166. (in Chinese)
- Xiao Hui, Wang Xiaobo, Zhou Feifei, Hong Yanchao, and Huang Meiyuan, 2004: A three-dimensional numerical simulation on microphysical process of torrential rainstorm. *Chinese J. Atmos. Sci.*, **28**, 385-404. (in Chinese)
- Xiao Mingjing, Guo Xueliang, and Xiao Wen, 2006: Numerical modeling study on hail suppression and rain enhancement by seeding convective clouds with silver iodide and liquid carbon dioxide. *J. Nanjing Inst. Meteor.*, **29**, 48-55.
- Xu Huanbin and Wang Siwei, 1990: A three-dimensional cloud-scale model suitable for compressible atmosphere. *Acta Meteor. Sinica*, **48**, 80-90. (in Chinese)
- Xu Huanbin and Duan Ying, 1999: Some questions in studying the evolution of size-distribution spectrum of hydrometeor particles. *Acta Meteor. Sinica*, **57**, 450-560. (in Chinese)
- Xu Huanbin and Duan Ying, 2001: The mechanism of hailstone's formation and the hail-suppression hypothesis: "beneficial competition". *Chinese J. Atmos. Sci.*, **25**, 277-288. (in Chinese)
- Xu Huanbin and Duan Ying, 2002: The accumulation of hydrometeor and depletion of cloud water in strongly convective cloud (hailstorm). *Acta Meteor. Sinica*, **60**, 575-584. (in Chinese)
- Yang Jing, Wang Pengyun, and Li Xingong, 2003: Meso-scale simulation of cloud and precipitation physical processes in Mei-yu front system in June 1999. *J. Tropical Meteor.*, **19**, 203-212. (in Chinese)
- Yang Wenxia, Niu Shengjie, Wei Junguo, and Sun Yuwen, 2005: Inhomogeneity of stratiform clouds in returning weather processes. *Meteor. Sci. Tech.*, **33**, 256-259. (in Chinese)
- Yao Zhanyu, 2006: Review of weather modification research in Chinese Academy of Meteorological Sciences. *J. Appl. Meteor. Sci.*, **17**, 786-795. (in Chinese)
- Yao Zhanyu, Li Wanbiao, Zhu Yuanjing, and Zhao Bolin, 2003: Remote sensing of cloud liquid water using TRMM microwave imager. *J. Appl. Meteor. Sci.*, **14**, Suppl. 19-26. (in Chinese)
- You Laiguang, Ma Peiming, and Hu Zhijin, 2002a: A study on experiment of artificial precipitation in North China. *Meteor. Sci. Tech.*, **30**, Suppl. 19-56. (in Chinese)
- You Laiguang, Yang Shaozhong, Wang Xiangguo, and Pi Jiexiong, 2002b: Study of ice nuclei concentration at Beijing in spring of 1995 and 1996. *Acta Meteor. Sinica*, **60**, 101-109. (in Chinese)
- Yu Xing, Dai Jin, Lei Hengchi, Xu Xiaohong, Fan Peng, Chen Zhengqi, Duan Changhui, and Wang Yong, 2005: Physical effect of AgI cloud seeding revealed by NOAA satellite imagery. *Chinese Science Bulletin*, **50**, 44-51.
- Yu Huaying, Gu Songshan, Liu Peng, Chen Zhangfa, and Huang Xiaoyu, 2006: Three-dimensional numerical simulation of a strong convective storm. *Nanjing J. Meteor. Sci.*, **29**, 303-313.

- Zhang Xiyong and Jin Fengling, 2003: The application of satellite images and radar echo to the choice of precipitation enhancement. *Meteor. Mon.*, **29**, 52-54. (in Chinese)
- Zhang Yijun, P. R. Krehbiel and Liu Xinsheng, 2002: Polarity inverted intracloud discharges and electric charge structure of thunderstorm. *Chinese Sci. Bulletin*, **47**, 1725-1729.
- Zhang Xiyong, Fang Lijuan, Jing Xueyi, and Xu Xiuhong, 2004a: Characteristics of satellite images of hail clouds in Heilongjiang Province. *J. Nanjing Inst. Meteor.*, **27**, 106-112. (in Chinese)
- Zhang Jie, Li Wenli, Kang Fengqin, Qu Yongxing, and Song Xuying, 2004b: Analysis and satellite monitor of a developing process of hail cloud. *Plateau Meteor.*, **23**, 758-763. (in Chinese)
- Zhang Jie, Zhang Qiang, Kang Fengqin, and He Jinmei, 2004c: Satellite spectrum character of hail cloud and pattern of remote sensing monitor in east of Northwest China. *Plateau Meteor.*, **23**, 743-748. (in Chinese)
- Zhang Jianping, Chen Weimin, Sun Fan, and Du Jianfei, 2005: Estimation of summer cloud short-wave radiative forcing in southeast China using GMS satellite data. *J. Nanjing Inst. Meteor.*, **28**, 499-506. (in Chinese)
- Zhang Yijun, Meng Qing, Krehbiel Paul, Liu Xinsheng, Yan Muhong, Zhou Xiuji, 2006a: Spatiotemporal characteristics of positive cloud-to-ground lightning discharges and bidirectional leader of the lightning. *Science in China: Ser. D - Earth Sciences*. **49**, 212-224.
- Zhang Yijun, Meng Qing, Lu Weitao, Paul Krehbiel, Liu Xinsheng, and Zhou Xiuji, 2006b: Charge structures and cloud-to-ground lightning discharges characteristics in two supercell thunderstorms. *Chinese Science Bulletin*, **51**, 198-212.
- Zhang Jie, Zhang Qiang, Tian Wenshou, and He Jinmei, 2006c: Remote sensing retrieval and analysis of optical character of cloud in Qilian Mountains. *J. Glacio. Geocryo.*, **28**, 722-727.
- Zhao Chunsheng, Zhang Daizhou and Qin Yu, 1998: Simulation of the formation and development of aerosol in marine boundary layer. *Progress in Natural Science*, **8**, 440-448. (in Chinese)
- Zhao, Chunsheng., Y. Ishizaka, and D. Y. Peng, 2005a: Numerical study on impacts of multi-component aerosols on marine cloud microphysical properties, *J. Meteor. Soc. Japan*, **83**, 977-986.
- Zhao Chunsheng, Peng Dayong, and Duan Ying, 2005b: The impacts of sea-salt and nss-sulfate aerosols on cloud microproperties. *J. Appl. Meteor. Sci.*, **16**, 417-425. (in Chinese)
- Zhao, Chunsheng, X. Tie, and Y. Lin, 2006a: A possible positive feedback of reduction of precipitation and increase in aerosols over eastern central China. *Geophys. Res. Lett.*, **33**, L11814, doi:10.1029/2006GL025959.
- Zhao, Chunsheng, and coauthors, 2006b: Aircraft measurements of cloud droplet spectral dispersion and implications for indirect aerosol radiative forcing. *Geophys. Res. Lett.*, **33**, L16809, doi:10.1029/2006GL026653.
- Zhao Shixiong, Deli Geer, and Tu Duobin, 2003: A study on convective characteristics and formation mechanism of precipitation over upper reaches of Yellow River. *Plateau Meteor.*, **22**, 385-392. (in Chinese)
- Zhao Shixiong, Xu Huanbin, and Deli Geer, 2004: Numerical simulation of microphysical character of convective cloud precipitation in upper reach of Yellow River. *Plateau Meteor.*, **23**, 495-500. (in Chinese)
- Zhao Zhen, Lei Hengchi, and Wu Yuxia, 2005: A new explicit microphysical scheme in MM5 and numerical simulation. *Chinese J. Atmos. Sci.*, **29**, 609-619. (in Chinese)
- Zheng Guoguang, 1994: An experimental investigation of convective heat transfer of rotating and gyrating hailstone models. Ph. D. dissertation, Dept of Physics, University of Toronto, Canada, 121 pp.
- Zhong Min, Lü Daren, and Du Bingyu, 2006: A primary study on three dimensional structure of rainfall rates of Typhoon Dan's precipitation cloud systems. *J. Nanjing Inst. Meteor.*, **29**, 41-47.
- Zhou Yuquan, Chen Baojun, Xiao Hui, Huang Yimei, and Li Zihua 2003: A case study of hail suppression by AgI seeding using 3D hailstorm model. *Chinese J. Atmos. Sci.*, **27**, 8-12. (in Chinese)
- Zhou Deping, Gong Fujiu, Wang Jihong, Li Zihua, and Gao Jianchun, 2004: The studies of the microphysical characteristics of an aircraft cloud seeding. *Scientia Meteor. Sinica*, **24**, 405-412. (in Chinese)

- Zhou Feifei, Xiao Hui, Huang Meiyuan, and Li Zihua, 2005a: Modeling evaluation of effects of artificial updraft restraints in a strong hailstorm on its precipitation. *J. Nanjing Inst. Meteor.*, **28**, 153-162. (in Chinese)
- Zhou. G. Q., C. S. Zhao, and Y. Qin, 2005b: Numerical study of the impact of cloud droplet spectral change on mesoscale precipitation. *Atmospheric Research*, **78**, 166-181.
- Zhou Guangqiang, Zhao Chunsheng, and Qin Yu, 2005c: Impact of cloud droplets spectral uncertainty on the mesoscale precipitation. *J. Tropical Meteor.*, **21**, 605-614. (in Chinese)
- Zhou, G. Q., C. S. Zhao and M. Y. Huang, 2006: A method for estimating the effects of radiative transfer process on precipitation. *Tellus*, **58B**, 187-195.
- Zhu Junjian, Zheng Guoguang, Wang Ling, Fang Wen, and Diao Xiuguang, 2004: The air flow and the large-hail generation area in hailstorms. *J. Nanjing Inst. Meteor.*, **27**, 732-742. (in Chinese)

RECENT ADVANCES IN STUDY OF PARAMETERIZATION AND CHARACTERISTIC ANALYSES ON URBAN LAND SURFACE IN CHINA

JIANG Weimei (蒋维楣) LIU Gang (刘罡) LIU Hongnian (刘红年)

(Nanjing University, Nanjing 210093, China)

Email: wmjiang06@jsoil.com.cn

Abstract

The progresses in understanding urban land surface process characteristics, urban sub-layer parameterization scheme for urban area land surface process analysis, building urban canopy layer model through urban boundary layer observation, satellite remote sensing and retrieval and urban boundary layer numerical simulation in the urban land surface process researches in China are reviewed.

1. Background

The main meanings of land surface processes research are as follows: fine understanding the physical, chemical, biological and hydrological processes taking place between the land surface and atmosphere and their interactions, identifying their characteristics and introducing them into various kinds of numerical models through the approaches of parameterization or building model, to improve the ability, correctness and scientificism of numerical simulation. Since 1960's, significant progresses in the relationship between land surface processes and climate system and the parameterizations of land surface processes have been made. Deardorff (1978) began to consider the effect and impact of vegetations, adding vegetations into land surface processes research. Then, Dickinson (1993) and Bonan (1996) furthered to take the handling of land surface changes into account in climate system simulation. Later, many authors furthered to build many complex and effective land surface process models considering biological and physical effects. In recent years, researchers have studied on coupled atmosphere, biosphere and hydrosphere environment models and ocean, sea water and land climate forecast models in climate and meteorological models, carried out amounts of deep and detailed works on transportation and exchange of material and energy in the soil, vegetation and atmosphere system. For example, Dai et al. (2003), Sun et al. (1997), Niu et al. (1997), Zuo (2004) and Sun (2005) carried out land surface process researches in a few aspects, building and developing some land surface process models for the purpose of weather prediction and climate change researches.

At present, the study on special and complex underlying surface, such as urban area underlying surface composed of various land use types (land surfaces) and meso and small scale circulations induced by the land surface inhomogeneous characteristics, has been paid more and more attention. So far, the research field has still scarcely been probed.

Niu et al. (1997) proposed in their paper that the systematic areas of the land surface process research related to the boundary layer research should include: (1) the parameterization of the surface turbulent fluxes in the mesoscale fluxes on homogeneous underlying surface; (2) the impact of sub-grid complex terrain on flux transportation; (3) canopy layer and ground surface hydrological model treating; (4) parameterization of the atmospheric boundary layer. The United Nations (UNPD, 2001) pointed out that urban areas only occupy 0.2% of the total land area of the earth, but they are populated more than 50% of the total population on the earth. The simulation on urban weather and climate is closely related to anthropogenic activities and has important meaning. The urban scheme in the land surface model (LSM) is being built and developed. In the 6th International Conference on Urban Climate held at Goteborg in 2006, in addition to amounts of papers paying attention to urban environment and the relationship between urban land surface and urban climate, there was a round table conference on the topic of urban sub-layer parameterization scheme (ICUC-6, 2006).

In this paper, the progresses in understanding urban land surface process characteristics, urban sub-layer parameterization scheme for urban area land surface process analysis, building urban canopy layer model through urban boundary layer observation, satellite remote sensing and retrieval and urban boundary layer numerical simulation in the urban land surface process researches in China are reviewed.

2. Study on the Parameterization Scheme of Urban Sub-Layer (USL) and Surface Energy Balance (SEB)

The impact of material and energy transportation between the surface of the earth and the atmosphere and their interactions on the development of the boundary layer is very important. Specially, the exchanges of radiation fluxes, momentum fluxes, sensible heat fluxes and latent heat fluxes directly influenced atmospheric dynamical, thermodynamical and moisture fields. Thus, it is also important to the descriptions of the interactions between the land and atmosphere (i.e. the land surface processes) and improvement of modeling performance of the atmospheric models. So it is necessary for all the climate, weather and atmospheric environment models to introduce relatively perfect land surface process parameterization schemes.

At present, besides the relatively simple grassland, forest and oasis underlying surfaces, the people have already begun to pay attention to the more complex underlying surfaces like urban areas, so as to carry out the simulation researches introducing the urban area meteorological environment issues into various kinds of meteorological numerical models. For this purpose, it is necessary to first build and develop the land surface process parameterization schemes suitable to urban underlying surface, which should take into account the exchange processes of heat, momentum and moisture between the urban underlying surface and atmosphere.

2.1 Study on Surface Energy Balance (SEB)

Contemporary observation experiments and analysis researches show that the atmospheric boundary layer structures and surface energy balance equation in urban area can be depicted in the Fig. 1.

Due to the strong inhomogeneous characteristics of the urban canopy three-dimensional structures, the terms in the urban area surface energy balance are influenced by the following factors: (1) the trap and capture of net radiation R_n ; (2) ΔQ_s occupying large proportion of net radiation flux due to large heat storage on urban surface in daylight; (3) urban turbulent heat fluxes going upwards in nighttime; (4) urban sensible heat far larger than urban latent heat; (5) anthropogenic heat fluxes too large to be ignored.

2.2 Parameterization Scheme of Anthropogenic Heat in SEB of Urban Area

In order to take into account the impact of urban underlying surface on surface energy balance, the two types of surface energy balance parameterization schemes are obtained as the following:

The first type is the empirical models. With the surface energy balance data from field observations, the statistical relationships between the terms of the surface energy balance equation and the short wave radiation are obtained, which are then substituted into the atmospheric models to compute the ground surface fluxes. The advantage of the method is that the short wave radiation can be calculated with the underlying surface types known and there are no too many driving quantities needed and many equations solved.

The second type is the soil vegetation adjustment transportation (SVAT) models. This is presently the ordinary method to study on urban SEB. In particular, it needs to modify the radiation, latent heat flux and heat storage. The modification of the radiation is realized through diminishing the albedo in the urban area (Arnfield and Grimond, 1998; Taha, 1999; Kondo, 1990, 1995; Atkinson, 2003). Since the conclusion 'urban latent heat is very little compared to urban

sensible heat' has been generally accepted by the community, the modification of the latent heat is usually realized through assigning a large Bowen ratio. Brown et al. (1998), Ca et al. (1999) assigned a Bowen ratio in the urban canopy layer in order to directly compute the latent heat fluxes by the sensible heat fluxes. The modification of the heat storage is realized through the following two approaches: the first, taking the underlying surface as the characteristics of the cement and assigning fixed values for the heat roughness and momentum roughness on the surface (Voogt and Grimmond, 2000); the second, introducing the so-called Object Hysteresis Model (OHM) (Grimmond and Oke, 1991), in which the heat storage term is defined as a function of the net radiation flux obtained from observation, into the mesoscale models.

In the second type of method, a new challenge is to fine take into account the contribution and impact of anthropogenic heat source of modern city on surface energy balance. In a monographical study, Jiang et al. (2006), He (2006) introduced the impacts of the anthropogenic heat sources into the Nanjing University Regional Boundary Layer Model (NJU-RBLM) and made significant progresses in the simulation performances of many cities.

The anthropogenic heat sources include the industrial heat sources, transportation heat sources and civil heat sources. The industrial heat sources are estimated with the urban-related data, such as the GDP, population, energy consumption amount per ten-thousand-Yuan GDP, energy transformation efficiency and heat emission rate per unit standard coal. The civil heat sources include the amount of gas and power consumed in a total year, which can be transformed into the heat emission according to the transformation efficiency. The transportation heat sources are calculated with Tong et al.'s method (2004). Fig. 2 is the diurnal variations of the anthropogenic heat fluxes in Nanjing and Hangzhou.

Through the tests on the introduction schemes of the anthropogenic heat sources with the NJU-RBLM numerical model, it is concluded that the anthropogenic heat sources are an important factor that cannot be ignored in the numerical simulation on the urban meteorological environment. Introducing the anthropogenic heat sources into the surface energy balance equation and the atmospheric heat conservation equation respectively according to some certain proportions is the optimal scheme in the simulations.

The boundary layer structures vary with the anthropogenic heat fluxes. For example, the anthropogenic heat sources have impact on the outgrowth and range of the urban heat island circulation and the urban heat island intensity. Larger the anthropogenic heat fluxes are, larger the vertical and horizontal ranges of the impact are. The contribution of the anthropogenic heat sources to the urban heat island intensity is strongest in the night and noon. The mean contribution in a total day is 29.6%. If the current anthropogenic heat fluxes are doubled, the

contribution reaches 42.9%. The contribution in Hangzhou is similar to the case in Nanjing. The anthropogenic heat sources have impact on the variation of the boundary layer structures in the morning. It destroys the inversion in the surface layer and makes the stratification become unstable earlier. The anthropogenic heat sources make the air temperature in the surface layer increase significantly, which increases by 0.5—1.0°C in the center of the urban area. The anthropogenic heat sources have little impact on the variation of the turbulent kinetic energy in the upper level, but the case is on the contrary in the daylight.

The introduction of the anthropogenic heat sources has impact on the simulation of the components in the surface energy balance. It changes the computations of the water vapor, substance and energy fluxes, thus influences the simulations on the boundary layer structures and air pollution in the surface layer. Therefore it is necessary to control the total amount of the anthropogenic heat sources, especially, to improve the transportation heat emission and energy transformation efficiency.

3. Building the Urban Canopy Model (UCM)

The above-mentioned two types of parameterization schemes have their limits on handling surface energy balance. The approach of the empirical models faces the problem that the determination of a certain parameter depends on the field observation data, but the field observation experiments are always limited. The method of depicting the urban surface energy balance by the modification of the soil vegetation transportation parameterizations is simple although, its physical foundation is still the M-O similarity theory, the validity of which is questionable within the urban canopy layer and rough sublayer. Thus, a new method is developed in recent years to parameterize the urban surface energy by building the so-called urban canopy model (UCM). The following is the description of a UCM built by He (2006).

Firstly, the UCM has some basic characteristics to be particularly treated. The street canyon is thought to be the basic element of the city. The physical process of the UCM is based on the consideration of a typical street canyon. According to the geometrical properties of the urban surface, various kinds of radiation effects in the street canyon are fine taken into account and the energy balance relationships are built on various kinds of surfaces respectively. The UCM is built based on the following hypotheses:

- (1) All the buildings within a grid have the same height and width. The top of the UCM is located at the first layer of the atmospheric model;
- (2) The two rows of buildings opposite to each other stretch along a street. The length of

the building is the same as the street and far larger than the height of the building;

(3) If the proportions of the street canyons with various directions within the grid cannot be resolved by the available data, the hypothesis is simplified as follows: within a grid, there is the same probability for any street canyon with any direction. If the data on the proportions of the directions of the street canyons can be provided, the UCM can handle the surface energy balance in any street canyon with any direction.

(4) The surface energy balances on different urban surfaces such as roof, road surface and wall surface etc. are handled respectively. However the two buildings opposite to each other are not handled separately, because the physical mechanisms for most of the physical processes on the wall surfaces of the two buildings are similar to each other, such as the sky view factor, thermodynamical structures of the wall surface, indoor temperature in the building, and absorption of the scattering radiation. The main difference is the solar radiation received. The direct solar radiation received by the wall surfaces is different, which can make difference on the surface temperatures on the two walls, but the difference does not have significant impact on the heat fluxes transferring from the top of the street canyon to the upper atmosphere.

The basic characteristic of the UCM is that the surface energy balance relationships are built on the three kinds of surfaces separately in the urban area. The temperatures are solved in accordance with the balance relationships, and then the heat transferring from the surfaces to the atmosphere are solved with the separate surface temperatures. Additionally, the method of Masson (2000) is referred in order to handle the heat transportation between the building and the atmosphere and the heat transfer upward and downward in the road surface layer. All the interfacial surfaces are classified into the three kinds of surfaces as roof, wall and road, whose temperatures are computed separately.

Amounts of observation data indicate that latent heat flux in urban area is little and close to zero, hence for simple processing we do not consider computing the latent heat flux when introducing the parameterization scheme.

Through computing the shading lengths and sky view factors between the surfaces, the impacts of the geometrical shape of the block on the shortwave radiation can be considered in relative completion. For the roof, the directly downward solar shortwave radiation is not multiply reflected and shaded, so the net shortwave radiation can be directly computed according

to the albedo of a flat surface. After reaching the top of the canopy layer, the shortwave radiation can be directly reflected, shaded, and absorbed after multiple reflections in the street canyon, due to the impacts of the geometrical shapes of the buildings. So as to depict the above-mentioned processes, the method of Kusaka et al. (2001) is referred to handle the net shortwave radiation on the wall, road and roof separately. The parameters characterizing the turbulent exchange ability must be firstly computed before the UCM is run.

According to the above approach, we build a UCM. Its structure and computation flowchart are as the Fig. 3.

3.1 Verification and application of the built UCM

The UCM is built as the Fig. 3. Further, the coupling of the UCM and the NJU-RBLM (Xu et al., 2002) is realized and the offline and online verifications are carried out.

Firstly, the offline verification of the UCM is carried out with the Nanjing Urban Field Observation Experiment data. Then, the two online simulations for real cases on the region of 80km×80km in Nanjing are carried out by the NJU-RBLM model, with the UCM coupled and without the UCM coupled respectively. The figures 4, 5, 6, 7 and 8 show the verification results of the simulation performances on the meteorological field, flux field, albedo and urban heat island phenomenon.

In the Fig. 4, the marked line is the observation data; the unmarked line is the offline simulation results of the UCM. Both in the winter and summer, the values of the simulated sensible heat fluxes by the UCM are close to the observed values; the simulated variation trends also match the observed ones well.

The comparisons of the ground temperature, wind speed and air temperature diurnal variations between the simulations and observations are respectively shown in the figure 5 (a), (b) and (c), indicating the improvement of the simulation performances with the UCM introduced. In the plots, the curves marked with the hollow circles represent the observation data; the simulation results by the land surface process model with the 'two-layer soil vegetation model' introduced are shown as the broken curves, which is named the 'traditional scheme' and marked as the 'old-scheme'; the solid curves represent the simulation results by the land surface process model with the urban canopy parameterization scheme introduced, which is named the 'new

scheme' and marked as the 'new-scheme'.

It is indicated in the figure 5 (a) that the simulation performances on the air temperature are improved significantly after the urban canopy parameterization scheme is introduced into the NJU-RBLM. Especially, the diurnal variation trend of the air temperature is simulated very well; and the improvement of the simulation performances on the thermodynamical field by the new scheme also makes the simulation performances on the dynamical field more reasonable, which is shown in the figure 5 (b), the simulated wind speeds by the new scheme are closer to the observed wind speeds in terms of value. The figure 5 (c) shows the comparisons between the air temperature diurnal variation curves in the urban area simulated by the two schemes and the air temperatures observed at five stations in the modeling area. In the plot, the solid curve marked with the hollow circles is the average of the five observation curves; the curve marked with the hollow squares is the simulation results of the air temperature diurnal variation at the center point by the traditional scheme; the curve marked with the triangles is the simulation results of the air temperature diurnal variation at the center point by the new scheme. It is revealed in the plot that the new scheme significantly improves the simulation performances on the air temperature for the winter case.

The comparisons between the surface fluxes simulated with the two schemes and the simultaneous results retrieved from the satellite observation data show that the simulation performances are significantly improved with the new scheme introduced. The figure 6 is the comparison between the surface sensible heat fluxes simulated with the two parameterization schemes and the MODIS satellite retrieval results.

The simulation of the albedo by the new scheme is precise in terms of value, showing that the upward shortwave radiation in the urban area and the physical processes of the shortwave radiation shading, multiple reflection and absorption in the daylight in the urban canopy are precisely simulated.

The figure 7 (a) and (b) show the surface albedo retrieved from the Landsat satellite data and the surface albedo simulated with the UCM introduced, which is indirectly computed by the ratio of the upward shortwave radiation to the downward shortwave radiation. Because the UCM is run only on the grid points in the urban area, the upward shortwave radiation can be computed only in the urban area. So in the plot the albedo is shown only in the urban area. In order to highlight the contrast, the albedo is set to be zero in the grid points out of the urban area in the

plot.

Compared to the traditional scheme, the UCM can simulate the urban heat island phenomenon more precisely and clearly. The figure 8 shows the urban heat island distributions in the night in the winter and summer simulated by the two land surface process schemes.

Based on the verification and analysis of the offline and online simulations by the UCM, the newly-built UCM simulates the heat fluxes very well. The simulation performances on the surface dynamical and thermodynamical fields are significantly improved by the NJU-RBLM with the urban land surface process parameterization scheme introduced. With the scheme, the urban heat island phenomenon is clearly depicted. In short, the UCM is a new kind of land surface process parameterization scheme applicable to urban underlying surface.

4. Building morphological characteristics and its effect on the wind

Miao et al. (2006) of Beijing Urban Meteorological Institute, China Meteorological Administration presented the paper on their parameterization scheme of the impacts of the buildings in the urban canopy in the ICUC6 conference. They introduced the scheme into the NJU-RBLM. With the fine buildings data of Beijing used, they simulated the impacts of the urban buildings on the wind fields and obtained good results, which is a successful attempt. The description of the paper is as follows:

Numerical simulation is a significant approach on this study. In the face of multi-scale heterogeneous urban boundary layer (UBL), urban canopy model (UCM) (to parameterize the effect of sub-grid urban building on UBL) is usually used in numerical models. Urban building morphological characteristics/parameters are essential to UCM. These researches are especially urgent for city.

Firstly, building morphological characteristics are determined from detailed building height and land use/land cover data of a city. Then, urban canopy parameters are derived which can be used directly in urban canopy model. The effect of buildings on the wind field is investigated with the aid of a regional scale PBL model with urban canopy parameterization.

In order to simulate the effect of buildings, the building canopy parameterization (Coceal et al., 2004, 2005) is introduced into a regional scale PBL model RBLM (Xu et al., 2002; Jiang et al., 2002). A new term representing the building canopy element drag is added to the momentum equations, which can be expressed as

$$D_i = -\frac{|U|U_i}{L_c}$$

Where the canopy drag length scale, L_c , is defined by

$$L_c = \frac{2h}{c_d(z)} \frac{(1-\beta)}{\lambda_f}$$

Where h is the plan-area-weighted average building height, $1-\beta$ is the fractional volume occupied by air in the canopy, $C_d(z)$ is the sectional drag coefficient (Macdonald, 2000), and λ_f is the total frontal area per unit ground area.

Building morphological characteristics for Beijing are determined from detailed building height data of Beijing, including plan-area-weighted average building height (h), plan area fraction, frontal area index, et al.

Further, urban canopy parameters are derived which can be used directly in urban canopy model, including canopy drag length scale (L_c), wind adjustment length scale (x_0), building canopy 'density' (h/L_c) etc. It can be seen that due to the special urban layout of Beijing (old town is surrounded by new town) the above parameters for Beijing have special distribution. The maximum of building plan area fraction appears in the range of the Second Circle, while the 'densest' building canopy is between the Second Circle and the Forth Circle.

Fig. 9 shows the simulation results with uniform initial field ($u_g=12\text{m/s}$ under adiabatic conditions). We can see from the figures that due to the building element drag, the wind in urban area is less than that in suburb and rural area at the height of 2.5 m, 10 m and 50 m, and the distribution is consistent with the urban layout. Further analysis indicate that, at the height of 2.5 m, there are some regions with negative wind speed (u), which is corresponding to the sharp variation of the building canopy 'density'.

Based on the building morphological parameters and urban canopy parameters, the building canopy parameterization is introduced into a regional scale PBL model RBLM, and the effect of buildings on the wind in Beijing is simulated. The analysis shows that,

(1) Due to the special urban layout of Beijing (old town is surrounded by new town), the building morphological and urban canopy parameters for Beijing have special distribution. The maximum of building plan area fraction appears in the range of the Second Circle, while the 'densest' building canopy is between the Second Circle and the Forth Circle.

(2) The regional scale PBL model RBLM with the building canopy parameterization can simulate the effect of buildings on the wind field. For example, there is a negative wind speed (u) region corresponding to the sharp variation of the building canopy 'density'.

5. Summary

At the beginning, the UCM is built for mesoscale meteorological models. For example, the parameterization scheme of the effects of the urban canopy layer was introduced into the MM5 model, such as the works of Li et al. (2003). Tong et al. (2004) introduced the parameterization scheme of the contributions and impacts of the anthropogenic heat on the urban surface energy balance. Wang et al. (2003) studied the winds around the high buildings in the urban canopy layer by numerical modeling. Zhang et al. (2004) investigated how the urban canopy layer buildings affect the airflow properties by large eddy simulation approach. The works are innovative research on urban canopy layer parameterization and urbanization the Chinese researchers did in recent years. In the works, He (2006) of Nanjing University built the UCM, pioneering the early study on urban canopy model, especially on the thermodynamical properties of the urban canopy. Through the application and verification of the simulation on the urban heat island circulation, it is proved that the simulation on the urban heat island phenomenon by the urban boundary layer model is significantly improved. However some deficiencies still exist in the explicit modeling on the impacts of the urban buildings. Miao et al. (2006) of Beijing Urban Meteorological Institute of China Meteorological Administration improved the modeling of the drag forces in the UCM, doing a meaningful work on the modeling of the impacts of the morphological properties of the urban buildings on the urban winds by the urban boundary layer model. As an example, the work of modeling on the Chinese megacity, Beijing with the urban building morphological parameterization scheme and fine buildings data (the least grid space is 10m) is proved to be so effective and meaningful.

So far, on the thermodynamical and dynamical aspects in urban canopy model, the present works have been carried out by the single-layer or multi-layer approaches. The work of He et al. (2006) is a single-layer canopy thermodynamical model, i.e. taking the urban canopy as a whole layer and considering its impacts on the radiation and humidity. The work of Miao et al. (2006) is a multi-layer canopy dynamical model, i.e. explicitly considering the vertical distributions of the urban buildings and obtaining the vertical distributions of the wind speeds in the building canopy. The former has the ability to simulate the urban thermodynamical effects, such as the heat island phenomenon and anthropogenic heat. The latter has the ability to simulate the urban dynamical effects, such as the impacts of the buildings on the wind. Evidently the two kinds of built canopy model have the two different canopy parameterization approaches with different coverage, different emphasis and different handling, being able to satisfy the two needs of fine simulation and short-cut application both.

The next work is how to blend the two different approaches into a new and more perfect urban canopy model adaptive to the urban canopy parameterization scheme of a city having very complex underlying surface for various purposes, needs and coverage. To better build, develop and perfect fine urban canopy model adaptive to various needs and applications, the fine electronic information data of urban energy flow, heat flow (including anthropogenic heat) and social economical development need to be indexed, and the corresponding database should be built with the GIS system technique. Eventually, we will introduce the impacts of the canopy layer into the regional boundary layer model by the urban canopy model or appropriate parameterization scheme and take into account and introduce the multiple factors induced by the inhomogeneous characteristics of the urban underlying surface to carry out finer diagnosis and modeling of the urban boundary layer structures.

6. Exploring and Study on Characteristics of the Urban Land Surface

Investigating the impacts of the surface energy balance and its distribution (i.e. the information of the momentum fluxes, heat fluxes, energy and material exchange properties in the urban area) induced by the interactions between the land and atmosphere with various approaches is the key issue important to the urban land surface process analysis, since they are caused by the complex urban underlying surface. At present, it is paid more and more attention. The major approaches are as follows: observation experiment, satellite remote sensing and urban boundary layer numerical simulation etc.

6.1 Exploring and Measurements in Urban Area

In Beijing, for the need of air pollution investigation and comprehensive control strategy in the capital, Professor Xiangde Xu of the Chinese academy of meteorological sciences, the principle investigator of the project ‘the Study of Mechanism on Atmospheric Environment Pollution in Capital Beijing’, led to carry out the urban environment scientific experiment. The synchronous observation system of urban scale boundary layer meteorological structure and atmospheric chemical composition was designed in the experiment. Meantime, by satellite remote sensing and ground three-dimensional observation comprehensive analysis technique, the polluted air dome structure over the city and its impacts in the surrounding areas and the relative atmospheric dynamical and thermodynamical structures and impacting mechanism in the boundary layer are revealed (website: <http://www.wmo.ch/web/arep/gaw/urban.html>; Xu et al.,

2003).

In the research project of Beijing Urban Meteorological Institute of China Meteorological Administration for the 2008 Beijing Olympic Games, urban boundary layer observation experiments (2004~2008) are planned every year, probing the momentum and heat fluxes and meteorological element distributions in the boundary layer (Li et al., 2004).

In the workshop hosted jointly by the Urban Meteorological Institute of China Meteorological Administration and National Center for Atmospheric Research of USA, the institute reported their initiated Beijing Urban Boundary Layer Experiment-BUBLEX 2004 (Li et al., 2004). The following is the major observation items: ground temperature distribution; wind field distribution; urban underlying surface roughness; diurnal variation of urban boundary layer (UBL); wind, temperature and humidity profiles in the UBL. The experiment spanned from July 31 through September 2, 2004, with 24-hour continuous measurements. The major instruments include: 1 lidar; 1 iron meteorological tower (325m, 15 layers); 1 truck-mounted profiler; 3 tethered balloons; 1 radiosonde; 1 flux station (eddy covariance system). Besides, 1 profiler/RASS; 1 troposphere profiler; 8 GPS stations; 1 lightning system; 2 air quality stations; 40 automatic weather stations; 20 weather observation stations; 1 upper-air station; 1 Doppler radar. The observation networks will be kept until the 2008 Beijing Olympic Games. The experiment in summer will be carried out every year.

For the key project of the Natural Science Foundation of China, 'Research on Urban Boundary Layer Three-Dimensional Structures', Nanjing University carried out the urban boundary layer observation experiments from 2004 through 2006. The major items of the observation experiments are as follows:

(1) In the summer of 2004, surface radiation observation and MODIS satellite observation for 30 days, at two stations (urban/rural) synchronously;

(2) In the summer of 2005 and winter of 2006, urban boundary layer observation experiments for a total of 36 days. The layout is:

(a) The measurements on the two iron towers (urban/rural, 50~60 meters high): wind, temperature and humidity gradient; turbulent fluctuating quantities and turbulent fluxes (sensible heat and latent heat);

(b) The meteorological elements at the two surface stations (urban/rural): temperature, pressure, humidity, wind, ground temperature, soil temperature, soil humidity and solar radiation;

(c) The urban boundary layer wind and temperature profiles observation: 2 profilers (urban/rural), boundary layer temperature profile observation;

(d) The ground temperature, humidity and wind: GPS positioning, car-mounted observation (heat island observation);

- (e) The lidar observation of the boundary layer at the two cities (Nanjing/Hefei);
- (f) The satellite observation and retrieval (MODIS/Landsat satellites);
- (g) The Doppler radar observation, retrieval and analysis.

6.2 Remote Sensing and Analysis in Urban Area by Satellite

At present urbanization schemes are being built and developed in land surface models (Jin et al., 2005). The urbanization schemes should include feedbacks of land surface to atmosphere and water cycle. Here 'city' has three special characteristics:

- (1) Impervious surface takes large proportion in the urban area, which affects surface humidity and moisture;
- (2) Plants in the urban area are irrigated;
- (3) Buildings and plants having various heights in the urban area induce urban transportation.

In short, satellite observation information is very useful to modeling urban impacts. Especially, satellite observation data can help us in understanding urban land surface characteristics and their variations. Besides, satellite data can provide various parameters representing land surface characteristics for application and verification of land surface models.

In order to take urban impacts into account in land surface models, the key issue is to build land surface model that can be coupled with urbanization scheme. Here, computation scheme of urban roughness length and building of urban geometry, terrain morphology and land cover database are most important. Jin et al. (2005) gave the urban canopy parameters, which are main references of urban canopy parameters analyzed by satellite remote sensing approach.

In fact, the researches show that ground temperature and albedo can be directly measured by satellite remote sensing approach, and the other surface characteristics quantities, which have important impacts on the atmospheric boundary layer, such as leaf area index, land cover type, surface roughness and vegetation index etc. can be obtained by retrievals. Studying the impacts of the inhomogeneities of the surface characteristics on the boundary layer structure and variation is helpful to understanding the transportation mechanisms of material and energy over the urban/rural inhomogenous surfaces and their impacts on local and regional meteorological environment.

With the Nanjing City and its surrounding area of 83km×83km, the MODIS satellite data and automatic weather station data in January and April of 2004, the two remote sensing models computing surface heat flux (i.e. single source and dual source models), and the remote sensing data and some auxiliary meteorological parameters, the parameterization equations studying the urban/rural surface energy balances and their components are built and some of the surface heat

fluxes in the winter and spring in the urban/rural area are estimated. The study on the remote sensing parameterizations of the surface energy is helpful to understanding the urban/rural nonhomogeneous surface processes and can provide physical references for the urban/rural atmospheric boundary layer numerical simulation (Wang, 2005).

The computations and analyses indicate that the average net radiation over the urban surface is higher than over the cropland but less than over the forestland. However the differences are little. The average net radiation over the urban area is 10 W/m^2 (i.e. 3%) larger than over the cropland but 2.8 W/m^2 (i.e. 1%) less than over the forestland. Due to the differences of the three kinds of surface albedo, the net radiations are different, the all-waveband shortwave albedo in the urban area is less than in the cropland but larger than in the forestland. The average soil heat flux in the urban area is largest, and the average soil heat flux in the cropland is almost the same as in the mixed forestland, which are 66.35 W/m^2 , 60.92 W/m^2 and 59.57 W/m^2 respectively. The value in the urban area is 5.4 W/m^2 (i.e. about 8%) larger than in the cropland. The average sensible heat flux in the urban area is larger than in the other two areas. The value in the urban area is 14 W/m^2 (i.e. about 19%) larger than in the cropland and 27 W/m^2 (i.e. 37%) larger than in the forestland. The average latent heat flux in the urban area is least. The average latent heat flux in the urban area is 9.4 W/m^2 (i.e. about 5%) less than in the cropland and 36.6 W/m^2 (i.e. about 18%) less than in the forestland. In the four components of the surface energy balance, the difference of the sensible heat flux between the urban/rural areas is largest; the second largest is that of the latent heat flux; the third largest is that of the soil heat flux; the least is that of the net radiation.

For the soil heat flux G retrieved from the remote sensing data, its Bowen ratio in the urban area is 1.36. The proportions of the soil heat flux, sensible heat flux and latent heat flux to the net radiation are respectively 28%, 42% and 31%.

In the winter, the soil heat fluxes on the three kinds of underlying surfaces of mixed forest, cropland and urban building are about one third of those in the spring. The net radiations decrease and are about 75% of those in the spring. On the three kinds of underlying surfaces, the urban sensible heat fluxes decrease most, which on the forestland, cropland and urban area are respectively 24%, 43% and 52% of those in the spring. The differences of the latent heat fluxes between the spring and winter are not large; the largest difference is only 10 W/m^2 . All the Bowen ratios on the three kinds of underlying surfaces decrease, which is similar to the variations of the sensible heat fluxes. The decrease on the forestland is relatively little, while the variations on the other two kinds of underlying surfaces are relatively large. The Bowen ratios on the forestland, cropland and urban area are respectively 26%, 40% and 48% of those in the spring.

In the work of Wang (2005), both of the EOS and MODIS satellite remote sensing retrieval data are used to (1) fine analyze and study the ground temperature in the urban area. The results indicate that the satellite data are in good agreement with the automatic weather station (AWS) data in the urban area, and moreover, the ground temperature distributions in the urban area retrieved from the satellite data are finer, which more clearly depicts the heat island phenomenon between the urban and rural area; (2) in particular analyze and study the urban/rural surface albedo to further the understanding of the land surface process below the atmospheric boundary layer, revealing the strong inhomogeneity of the urban landscape and its important impacts on the atmospheric boundary layer structures. Paying special attentions to the differences of the surface albedo between the urban and rural area in the Yangtze River Delta of China needs to analyze and study the seasonal and spatial variations of the surface albedo in various wavebands. Besides, the irrelevancy between the albedo and NDVI is significantly affected by the waveband and land cover.

In the work of Chen (2005), with the urban area as the object of the study, the high-resolution Landsat-5 satellite data is retrieved to obtain the 30m-resolution surface parameters of land use type, surface albedo and leaf area index, and then the impacts of urbanizations of Nanjing and Hangzhou on the atmospheric boundary layer structures are studied. The numerical experiment results of various surface albedo schemes in the urban areas indicate: the surface albedo is the important factor to control the surface net radiation and affect the surface and low-level atmosphere. When the surface albedo is little, the surface net radiation flux and sensible heat flux increase significantly; the turbulent kinetic energy and diffusive coefficient increase; the diurnal amplitudes of the ground temperature and air temperature increase. The impacts of the surface albedo on the urban thermal environment and atmospheric boundary layer structures mainly arise in the daylight. The comparison between the various types of surface albedo is shown in the table 1.

Table 1 The variations of the various meteorological element fields induced by the surface albedo

	net radiation flux (w/m ²)	sensible heat flux (w/m ²)	latent heat flux (w/m ²)	ground temperature (°C)
surface albedo 0.12	640	450	220	41.5
surface albedo 0.18	600	370	220	37.3

	air temperature (°C)	momentum flux (kg/m/s ²)	turbulent kinetic energy (m ² /s ²)	boundary layer height (m)
surface albedo 0.12	36.8	0.58	0.75	580
surface albedo 0.18	35	0.4	0.55	430

In the study, the impacts of the surface albedo on the urban boundary layer structures are presented, the impacts on the surface energy balance, surface fluxes (heat, momentum), turbulent exchange, daytime mixed layer, nighttime inversion temperature and the average meteorological fields are analyzed and studied, and the impacts of the various urbanization factors on the urban boundary layer structures are summarized. The analyses indicate:

With the rapid urbanization, the urban area increases, the buildings increase in number and height, the surface albedo decreases, the vegetation cover and surface humidity decrease. The approach to obtain the land use type, surface albedo and vegetation leaf area index for the regional boundary layer simulation by the high-resolution satellite remote sensing data is an applicable way.

The simulation results of the underlying surfaces in Nanjing area in two different years show:

With the albedo decreasing, the sensible heat fluxes increase; due to the decreased vegetation and surface humidity, the evaporation heat in the latent heat decreases; the surface energy partition is changed, the Bowen ratio in the urban area increases.

Affected by the decreased albedo and vegetation jointly, the turbulent heat fluxes increase; the turbulent exchanges develop strongly; the fully developed mixed layer appears; the boundary layer height increases by 500m at 14:00; the impacts on the nighttime atmospheric stratification is far less than in the daytime.

Influenced by the decreased vegetation and surface humidity, the moisture flux and content decrease both, which causes more heat to heat the surface and atmosphere, and the diurnal amplitudes of the ground temperature and air temperature increase.

The surface parameters in the simulation area of Nanjing in 1993 and 2002 (horizontal 30m-resolution satellite data) are shown in the work of Chen et al. (2007).

6.3 Numerical Modeling on Urban Boundary Layer

It is another active, viable and valid means analyzing and studying the urban land-atmosphere

interaction characteristics induced by many inhomogeneities of the urban underlying surface and investigating the impacts of existence and development of the city on the atmospheric boundary layer structures to obtain the variation laws and further understand the urban land surface process characteristics and build the parameterization schemes that can be introduced into various kinds of numerical models by the numerical simulation approach. Chen (2005) numerically simulated the urban meteorological environment and boundary layer structures with the NJU-RBLM model, obtaining the preliminary results mainly as follows:

(1) The impacts of the urban heat island and anthropogenic heat contribution on the boundary layer structures

Taking the spatial and temporary distribution of the anthropogenic heat and its variation into account, with the scheme of introducing the anthropogenic heat into the surface energy balance and atmospheric heat conservation equations according to the proportions, the simulation results indicate: (A) the anthropogenic heat has important effects. Taking Nanjing as the example, the contribution rate of the urban anthropogenic heat to the urban heat island is about 29.6%. If the anthropogenic heat is double the current value, the contribution rate will be about 42.8%; (B) the lift amplitude of the mixed layer height may attain 400m; (C) the anthropogenic heat in the daylight is about 10~20% of the solar radiation, and can cause the turbulent kinetic energy to increase by 40% in the winter (Jiang et al., 2006).

(2) The impacts of the surface albedo on the boundary layer structures

The impacts of the surface albedo, surface humidity and street-canyon radiation entrapment effect are strongly inhomogeneous, which are the important factors to control and dominate the surface net radiation and put significant influences on the urban boundary layer structures.

When the surface albedo is little, the ground surface absorbs more solar energy. The surface net radiation flux and sensible heat flux significantly increase; the latter can increase by 100 W/m^2 at the maximum. The surface temperature increases, the land-atmosphere heat exchange strengthens, the large heat exchange causes the mixed layer top to lift.

The impacts of the surface albedo on the urban boundary layer structures mainly arise in the daylight; the impacts are largest in the summer, the second in the spring and autumn, the least in the winter.

(3) The impacts of the surface humidity on the boundary layer structures

The surface humidity decreases, the surface net radiation flux decreases slightly, but the sensible heat flux significantly increases and can increase by 170 W/m^2 at the maximum; the latent heat flux significantly decreases and can decrease by 210 W/m^2 at the minimum; the Bowen ratio increases in the urban area. On one hand the ground surface heat capacity changes, on the other

hand the evaporation heat decreases, the diurnal variation amplitudes of the ground temperature and air temperature increase. The impacts are most significant in the daylight and in the summer, second in the spring and autumn, least in the winter.

(4) The impacts of the urban buildings on the boundary layer structures

The numerical experiments on the urban buildings having various heights, densities, distributions and layouts indicate: the buildings cause the wind speeds to decrease, and easily cause the low-level flow fields to converge. The damping effect on the wind fields is particularly significant in the low level. It is significant when the wind speed is large, the wind speed can decrease by 1.6 m/s at the minimum. The forcing uplift effect of the buildings causes the vertical speeds to increase and the heat and moisture in the lower level to transport and exchange towards the upper level. The mechanical effect of the turbulence increases, the exchange strength intensifies, which cause the instability of the atmospheric stratification to increase. The heat exchange is affected jointly by the decrease of wind speed and the intensification of turbulence. The former dominates in the daylight and causes the land-atmosphere exchange to weaken; the latter dominates in the night and meantime the heat exchange strengthens (Chen, 2006).

(5) The impacts of the intensification of urbanization and the variation of land use on the boundary layer structures

The acceleration of urbanization causes the town to develop and the urban area to expand, the anthropogenic heat increases, the buildings increase in number and height both, the surface albedo decreases, the vegetation cover reduces, the surface humidity decreases. The variation of the urban land use causes the surface characteristic parameters to change significantly, various inhomogeneous interactions on the underlying surfaces intensify, which jointly affect the boundary layer structures. The numerical experiments in the Nanjing area indicate: After the buildings increase in number and height, the albedo decreases, the sensible heat flux increases by 140 W/m^2 ; influenced jointly by the decrease of the albedo and the reduction of the vegetation cover, the heat flux increases one time more; the exchange and development of the turbulence intensify; the mixed layer with the height of hundreds of meters appears; the uplift amplitude of the boundary layer height can attain 500 m at 14:00.

The numerical experiments on the variations of the land use types in various years in the metropolitan area indicate: the urban land use types have significant impacts on the thermodynamical and dynamical structures of the urban boundary layer. The impacts are particularly significant in the summer (Chen, 2005).

Due to the variation of the heat storage ability of the buildings and the variation of the surface albedo in the urban area, the urban energy balance is repartitioned: (A) the net radiation flux

increases by 160 W/m^2 on the average in the urban area in the winter; (B) the latent heat flux decreases, and can decrease by 45 W/m^2 at the minimum. The sensible heat flux increases, and can increase by 146 W/m^2 at the maximum; (C) both in the winter and summer, the heat and momentum fluxes increase, the land-atmosphere exchanges intensify, the increasing amplitude of the air temperature in the urban area can attain $2.2 \text{ }^\circ\text{C}$ at the maximum; (D) the height and density of the buildings increase, the turbulent kinetic energy increases, the impacting height also increases, the mixed layer height rises, the material exchanges intensify, the distributions are more homogeneous; (E) the urban dynamical roughness increases, the damping effect is particularly significant when the wind speed is large, the wind speed can decrease by 2.0 m/s at the minimum in the megacity (Wang et al., 2006a).

In short, the urban land use changes induce the significant variation of the urban comprehensive meteorological environment. The comparisons between the urban numerical simulation experiments in various years indicate: in the developing processes of the large city and the town group, various types of urban layouts (scattering, centralization and satellite-town types of layouts) all have great impacts on the meteorological environment. The impacts should be evaluated carefully, and further, the interactions between the towns should be analyzed. In regional climate modeling and weather forecast and prediction, the variation and interaction of the physical environment need to be introduced (Wang et al., 2006b).

7. Discussions and prospect

In short, the inhomogeneity of the urban underlying surface and multi-scale characteristics of the atmospheric boundary layer process and complexity of the turbulence make the material and energy exchanges and transportation characteristics in the urban boundary layer and their variation laws extreme complex, and the wind, temperature and turbulence characteristics in the urban canopy layer are even more complex. In terms of thermodynamics and dynamics, investigating the impacts of the urban underlying surface on the atmospheric boundary layer, analyzing the impacts of the anthropogenic heat sources on the urban temperature structures; studying the impacts of the surface albedo on the surface energy balance; estimating the impacts of the urban buildings on the generation, drag and resistance of turbulence; discussing the impacts of the surface humidity on the urban moisture and heat balance. Studying the material and energy exchange and transportation characteristics in the urban boundary layer and their variation laws in terms of various respects are very necessary and of great importance, and are also valid and viable. However, more researches on the urban boundary layer parameterization need to be carried out:

- To take the heat storage effect of the buildings into account, study the problem of the time-lag

between the anthropogenic heat emission and its effect, parameterize the impacts of the buildings on the heat storage and emission in mesoscale modeling;

- The impacts of the buildings having different shapes on the airflows from the same direction are greatly different, and the impacts of the same building on the airflows from different directions are different too. Hence the relationships between the building shape parameterization and the urban prevailing wind direction need to be built, and the impacting factors need to be parameterized;
- The moisture balance in the urban area has its own characteristics. The precipitation in the urban area and its downwind area is usually larger than in the suburban area, i.e. the urban rain island effect; the anthropogenic activities emit the anthropogenic moisture into the atmosphere, which makes the moisture received in the urban area is more than in the suburban area; most of the urban underlying surfaces are mainly the buildings and the impervious surfaces, which hardly storage the moisture, and the moisture infiltrating into the underground is little. The above factors, together with the urban rain island effect, make the runoff volume in the urban area larger than in the suburban area. The moisture balance on the urban underlying surface necessarily has direct impacts on the moisture exchange in the urban canopy layer. The direct relationships between the anthropogenic moisture and the underlying surface need to be built, taking the spatial distribution, diurnal and seasonal variations of the moisture into account, investigating the impacts of the anthropogenic moisture in the moisture transportation equation;
- To build the relationship between the street-canyon radiation entrapment effect and the building height by the large amounts of observations and experiments, and take the impacts of the relationship into account in mesoscale models;
- How to apply non-conventional observation data such as satellite remote sensing and radar observation data to urban meteorological research is also a hot topic in recent years. To obtain sensible heat and latent heat fluxes by satellite remote sensing data is a new way to study energy exchange between land and atmosphere and can improve urban boundary layer parameterization research too;
- The inhomogeneous level and degree of the inhomogeneous underlying surfaces of the city or city group having different functions and types, structures and layouts, geographical locations are different, which needs large amounts of finer researches, classifying various cities, studying the impacts of the inhomogeneities having various scales and levels induced by the urban land use types and buildings on the urban boundary layer structures and local meteorological environment.

The atmosphere boundary layer is the important passage of momentum, heat and various materials upward and downward transporting between the earth and atmosphere. Hence, the physical processes taking place in the atmospheric boundary layer are the important factors to the formation of large-scale weather and climate. As the urban underlying surface is the important source of energy and sink of momentum in the atmospheric boundary layer, its inhomogeneous characteristics are tightly linked to the physical processes in the atmospheric boundary layer. Studying the impacts of the inhomogeneous characteristics of the urban underlying surface on the three-dimensional structures of the atmospheric boundary layer will necessarily deepen the understanding of the effects and interactions between the urban underlying surface and the weather and climate.

References

- Arnfield, A. J., Grimmond, C. S. B.: An urban energy budget model and its application to urban storage heat flux modeling. *Energy and Building*, 27, 61-68, 1998
- Atkinson, B. W.: Numerical modeling urban heat island intensity. *Boundary Layer Meteorology*, 109, 285-310, 2003
- Bastiaanssen, W. G. M., Menenti, M., Feddes, R. A., Holtslag, A. A. M.: A remote sensing surface energy balance algorithm for land (SEBAL). I. Formulation. *Journal of Hydrology*, 212-213, 198—212, 1998
- Bonan, Gordon B.: A land surface model (LSM version 1.0) for ecological, hydrological, and atmospheric studies: technical description and user's guide. NCAR/TN-417+STR, 1996
- Brown, M. J., Williams, M.: An urban canopy parameterization for mesoscale meteorological models. American Meteorological Society 2nd Urban Environment Symposium, Albuquerque, New Mexico, USA, 1998
- Ca, V., Asaeda, T., Ashie, Y.: Development of a numerical model for the evaluation of the urban thermal environment. *Journal of Wind Engineering and Industrial Aerodynamics*, 81, 181-196, 1999
- Chen Yan: Study of Urban Inhomogeneities' Effect on Atmospheric Boundary Layer. Ph.D. Dissertation, Nanjing University, 2005
- Chen, Yan, Jiang, Weimei: Impact of Nanjing Urban Development on the Boundary Layer. *Chinese Journal of Geophysics*, 50, 67-74, 2007 (in Chinese)
- Coccal, O., Belcher, S. E.: A canopy model of mean winds through urban areas. *Quarterly Journal of the Royal Meteorological Society*, 130, 1349-1372, 2004
- Coccal, O., Belcher, S. E.: Mean wind through an inhomogeneous urban canopy. *Boundary-Layer Meteorology*, 115, 47-68, 2005
- Dai, Yongjiu, Zeng, Xubin, Dickinson, R. E. et al: The Common Land Model. *Bulletin of the American*

- Meteorological Society*, 84, 1013-1023, 2003
- Deardorff, J. W.: Efficient prediction of ground surface temperature and moisture with inclusion of a layer of vegetation. *Journal of Geophysical Research*, 83, 1889-1903, 1978
- Dickinson, R. E., Sellers, A. H., Kennedy, P. J.: Biosphere-Atmosphere Transfer Scheme (BATS) — version as coupled to the NCAR Community Climate Model. NCAR/TN-387+STR, 1993
- Grimmond C. S. B., Oke, T. R.: An evapotranspiration-interception model for urban area. *Water Resource Research*, 27, 1739-1755, 1991
- Grimmond, C. S. B., Oke, T. R.: Turbulent heat fluxes in urban areas: observations and a local-scale urban meteorological parameterization scheme (LUMPS). *Journal of Applied Meteorology*, 41, 792-810, 2002
- He Xiaofeng: Study on Establishment and Application of a Land-Surface Process Parameterization Scheme in Urban Area. Ph.D. Dissertation, Nanjing University, 2006
- Jiang, Weimei, Zhou, Mi, Xu, Min, Wang, Weiguo: Study on development and application of a regional PBL numerical model. *Boundary-Layer Meteorology*, 104, 491-503, 2002
- Jiang, Weimei, Chen, Yan, He, Xiaofeng, Liu, Gang: Study on the impact of anthropogenic heat on urban boundary layer properties. *6th International Conference on Urban Climate Preprints*, 627-630, Goteborg, 2006
- Jin, Menglin, Shepherd, J. Marshall: Inclusion of urban landscape in a climate model—How can satellite data help. *Bulletin of the American Meteorological Society*, 86, 681—689, 2005
- Kondo, H.: A numerical experiment of the extended sea breeze over the Kanto plain. *Journal of the Meteorological Society of Japan*, 68, 419-433, 1990
- Kondo, H.: The thermally induced local wind and surface inversion over the Kanto plain on calm winter nights. *Journal of Applied Meteorology*, 34, 1439-1448, 1995
- Kusaka, H., Kondo, H.: A simple single-layer urban canopy model for atmospheric models: comparison with multi-layer and slab models. *Boundary Layer Meteorology*, 101, 329-358, 2001
- Li, Ju: Introduction of Beijing Urban Boundary Layer Experiment 2004. *US-Sino Joint IUM/NCAR Workshop on Urban Meteorology: Observation and Modeling*, Beijing, October 12-13, 2004
- Li, Xiaoli, He, Jinhai, Bi, Baogui et al.: The design of urban canopy parameterization of MM5 and its numerical simulations. *Acta Meteorologica Sinica*, 61, 526-539, 2003
- Liu, Shuhua, Li, Xinrong, Liu, Lichao, Zhang, Jingguang: Study of land surface processes parameterizations model. *Journal of Desert Research*, 21, 303-311, 2001 (in Chinese)
- Macdonald, R. W.: Modelling the mean velocity profile in the urban canopy layer. *Boundary-Layer Meteorology*, 97, 25-45, 2000
- Masson, V.: A physically based scheme for the urban energy budget in atmospheric models. *Boundary Layer Meteorology*, 94, 357-397, 2000
- Miao Shiguang, Li Pingyang, Wang Xiaoyun: Building morphological characteristics and its effect on the wind in

- Beijing. *6th International Conference on Urban Climate Preprints*, 412-414, Goteborg, 2006
- Niu, Guoyue, Hong, Zhongxiang, Sun, Shufen: Status and developmental trends of land surface processes study. *Advance in Earth Sciences*, 12, 20-25, 1997 (in Chinese)
- Sun, Shufen, Jin, Jiming: Some problems on the study of land surface process model. *Quarterly Journal of Applied Meteorology*, 8 (supplement), 50-57, 1997 (in Chinese)
- Sun, Shufen: The physical, biochemical mechanisms and parameterization models of land surface processes. Meteorological Press, Beijing, 2005 (in Chinese)
- Taha, H.: Modifying a mesoscale meteorological model to better incorporate urban heat storage: A bulk-parameterization approach. *Journal of Applied Meteorology*, 38, 466-473, 1999
- The 6th International Conference on Urban Climate Preprints, International Association for Urban Climate, Goteborg, 2006
- Tong, Hua, Liu, Huizhi, Sang, Jianguo, Hu, Fei: The impact of urban anthropogenic heat on Beijing heat environment. *Climatic and Environmental Research*, 9, 409-421, 2004 (in Chinese)
- UNPD, cited 2001: World Urbanization Prospects: The 2001 Revision. [Available online at www.un.org/esa/population/publications/wup2001.]
- US-Sino Joint IUM/NCAR Workshop on Urban Meteorology: Observation and Modeling. Beijing, October 12-13, 2004
- Voogt, J. A., Grimmond, C. S. B.: Modeling surface sensible heat flux using surface radiative temperatures in a simple urban area. *Journal of Applied Meteorology*, 39, 1679-1699, 2000
- Wang, Baomin, Liu, Huizhi, Sang, Jianguo, Wang, Xiaoyun, Zhang, Qing, Li, Ju: Simulation of flow field in a urban canopy layer during the strong wind. *Chinese Journal of Atmospheric Sciences*, 27, 255-264, 2003 (in Chinese)
- Wang, Guiling: Study on Satellite Remote Sensing Parameterization of Surface Characteristics and Atmospheric Boundary Layer over Urban/Rural Areas. Ph.D. Dissertation, Nanjing University, 2005
- Wang, Yongwei, Jiang, Weimei, Ji, Chongping: Simulation of land use change effect on urban meteorological environment. *Journal of Nanjing University (Natural Science)*, 2006a (in press, in Chinese)
- Wang, Yongwei, Jiang, Weimei, Guo, Wenli: The numerical studying on urban layout and scale effect on atmospheric environment. *Chinese Journal of Geophysics*, 2006b (in press, in Chinese)
- Xu, Min, Jiang, Weimei, Ji, Chongping, Liu, Haitao, Gao, Yanhu, Wang, Xiaoyun: Numerical modeling and verification of structures of the boundary layer over Beijing area. *Journal of Applied Meteorological Science*, 13 (supplement), 61—68, 2002 (in Chinese)
- Xu, Xiangde, Bian, Lingen, Ding, Guoan: Beijing City Air Pollution Observation Field Experiment. Chinese Academy of Meteorological Sciences, 2003
- Zhang, Ning, Jiang, Weimei: Numerical method study of how buildings affect the flow characteristics of an urban

canopy. *Wind & Structures*, 7, 159-172, 2004

Zuo, Hongchao: A Preliminary Study about Boundary Layer Characteristics and Land Surface Parameterization over Heterogeneous Underlying Surfaces. Ph.D. Dissertation, Cold and Arid Regions Environmental and Engineering Research Institute, Chinese Academy of Sciences, 2004

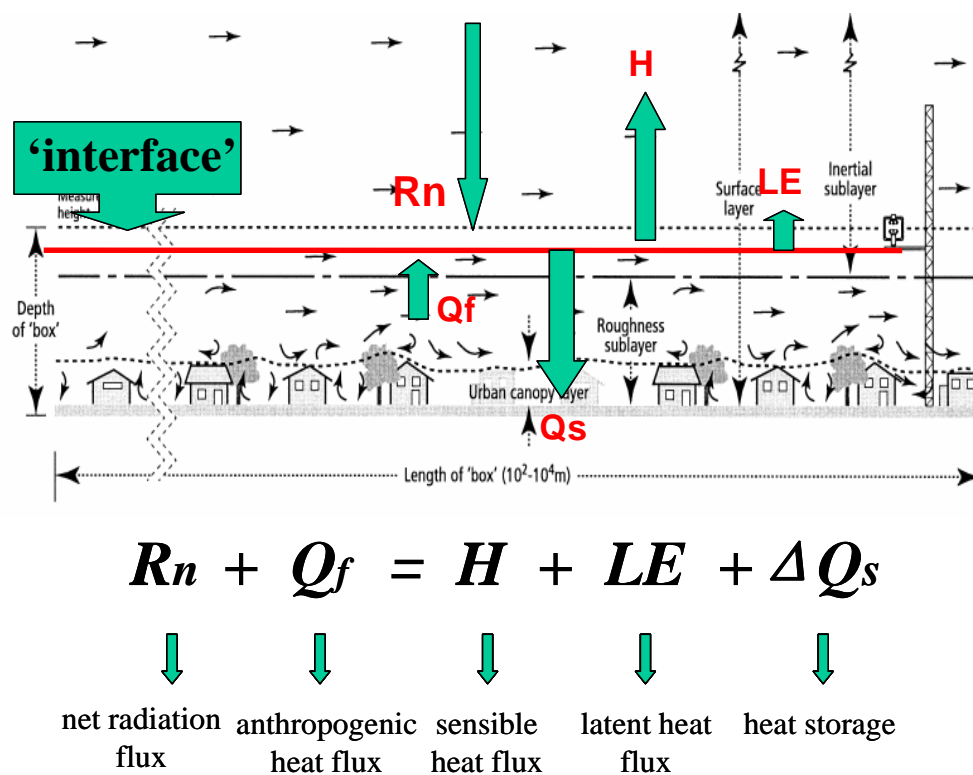


Fig. 1 Urban Surface Energy Balance (from Grimmond and Oke, 2002)

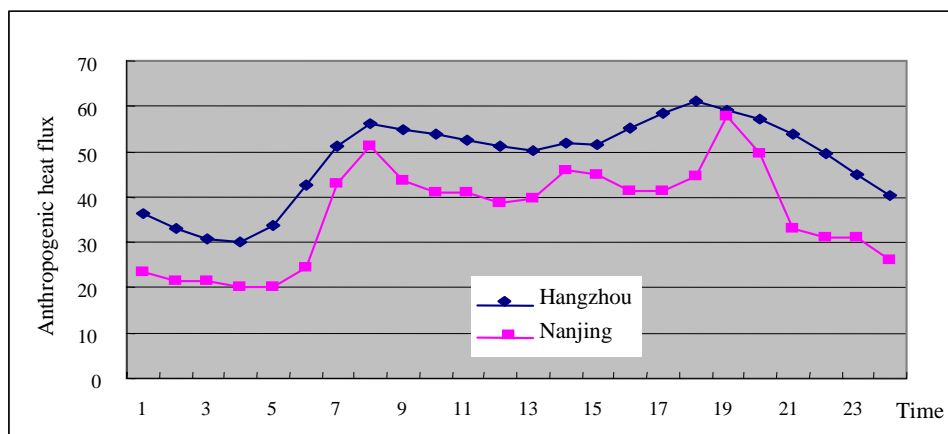


Fig. 2 Diurnal variations of the anthropogenic heat fluxes in Nanjing and Hangzhou (He, 2006). The unit is W/m²; the time is in LST (the same hereinafter)

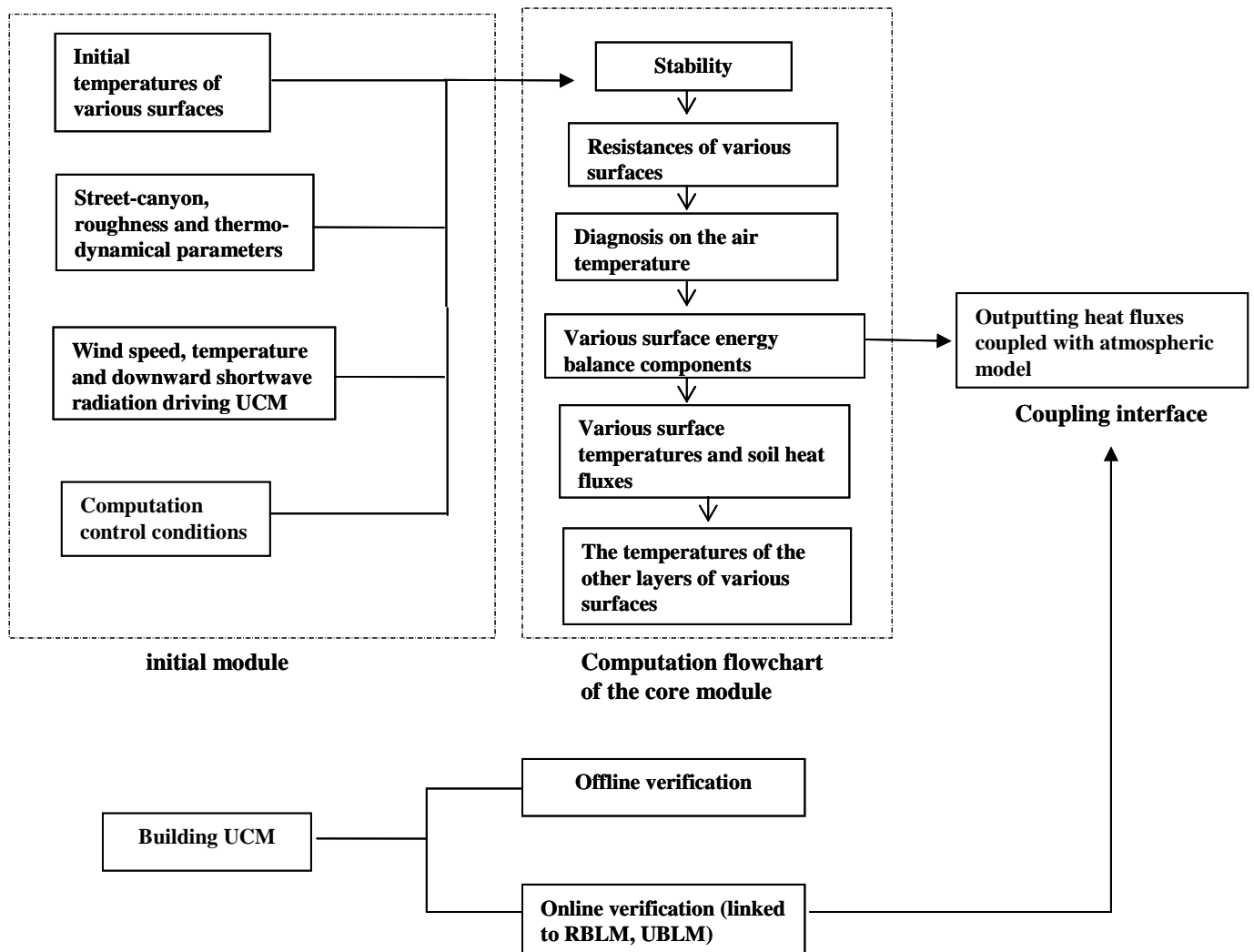
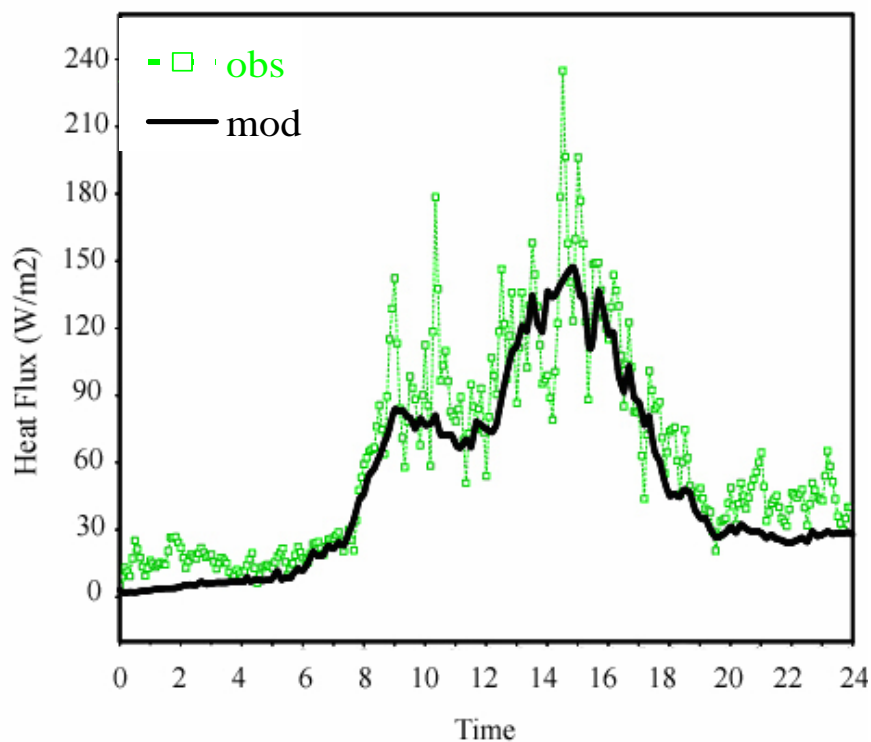
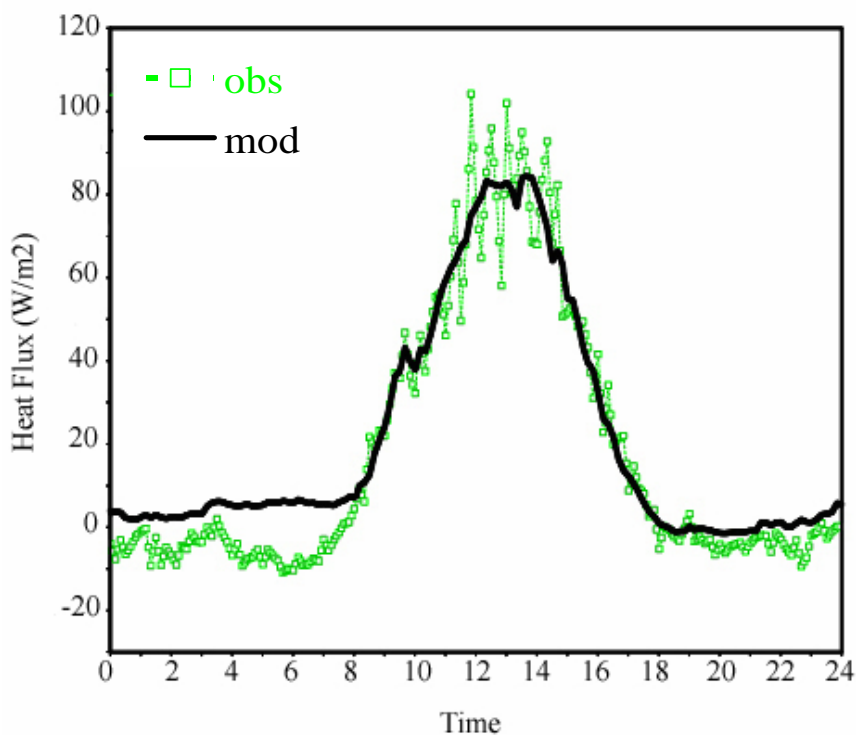


Fig. 3 Structure and flowchart of the UCM (He, 2006)



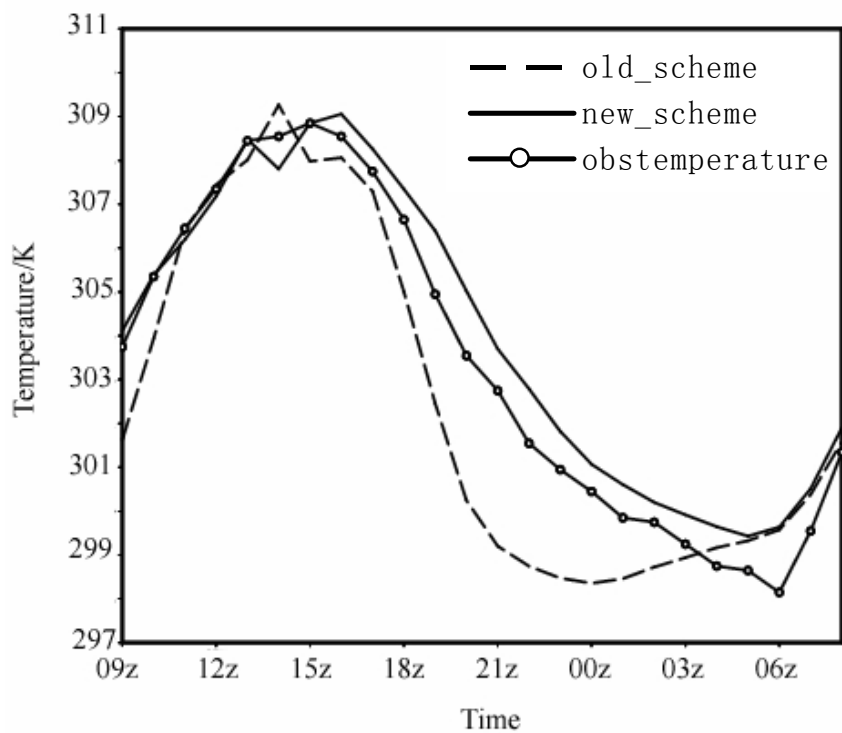
(a)



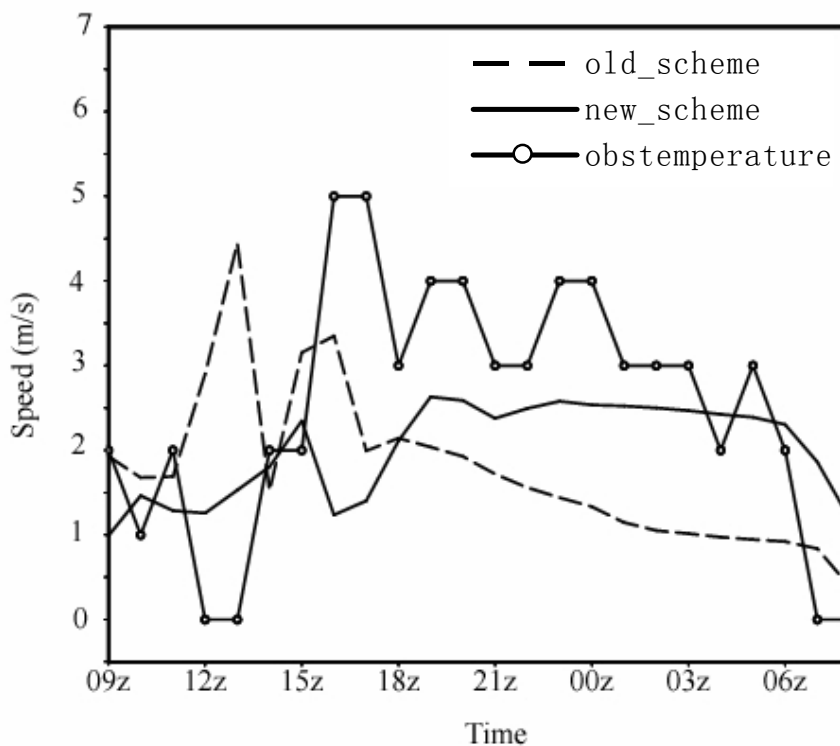
(b)

Fig. 4 Comparison and verification of the offline simulation results of the UCM: the sensible heat fluxes on (a)

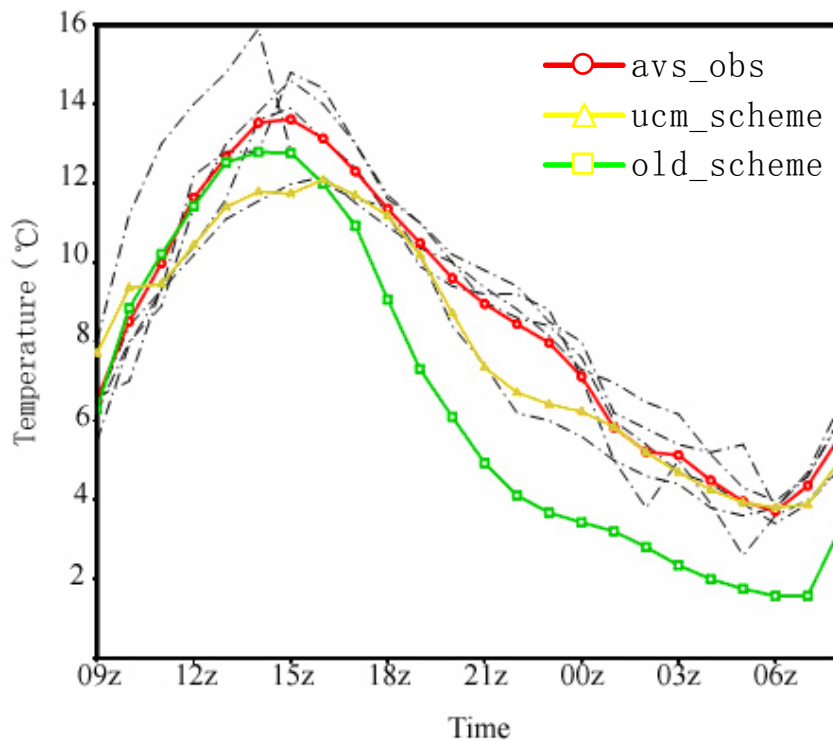
July 17, 2005; (b) March 2, 2006. (He, 2006)



(a)

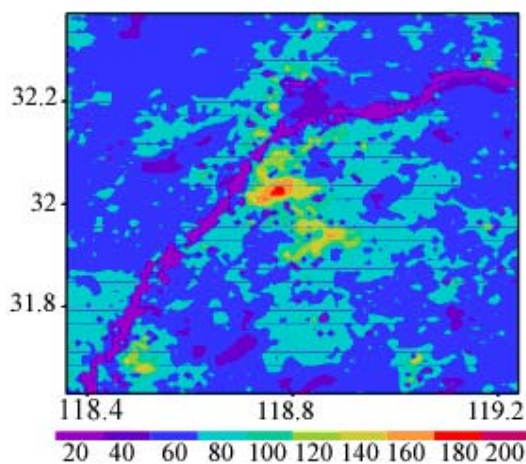


(b)



(c)

Fig. 5 Improvement of the simulation performances on the surface meteorological fields with the UCM introduced: (a) the ground temperatures on July 12, 2002; (b) the surface wind speeds on July12, 2002; (c) the diurnal variation curves of the air temperatures on March 2, 2006. (He, 2006)



(a)

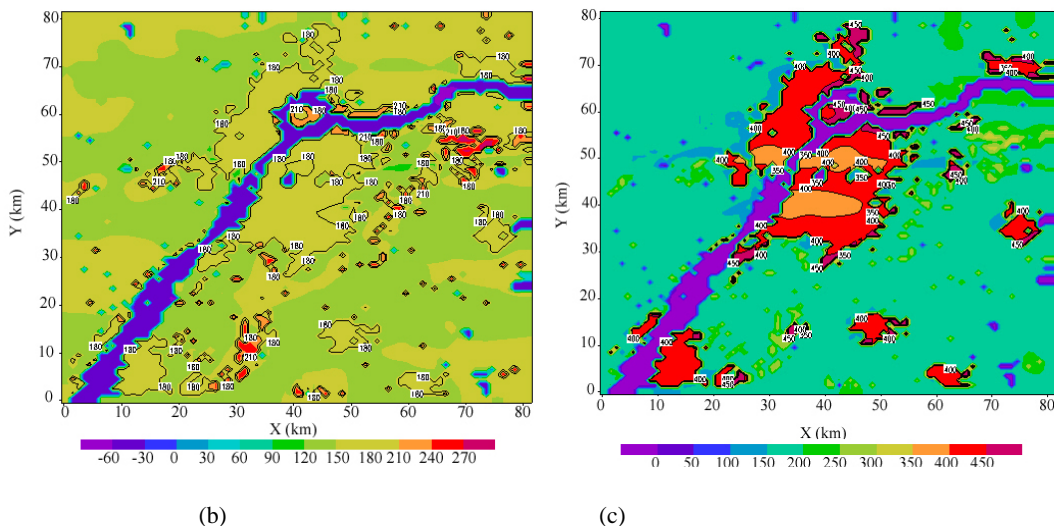


Fig. 6 Improvement of the simulation performances on the surface sensible heat fluxes with the UCM introduced: (a) the average sensible heat fluxes of April retrieved from the MODIS satellite observation data; (b) the sensible heat fluxes simulated with the new scheme; (c) the sensible heat fluxes simulated with the traditional scheme. (He, 2006)

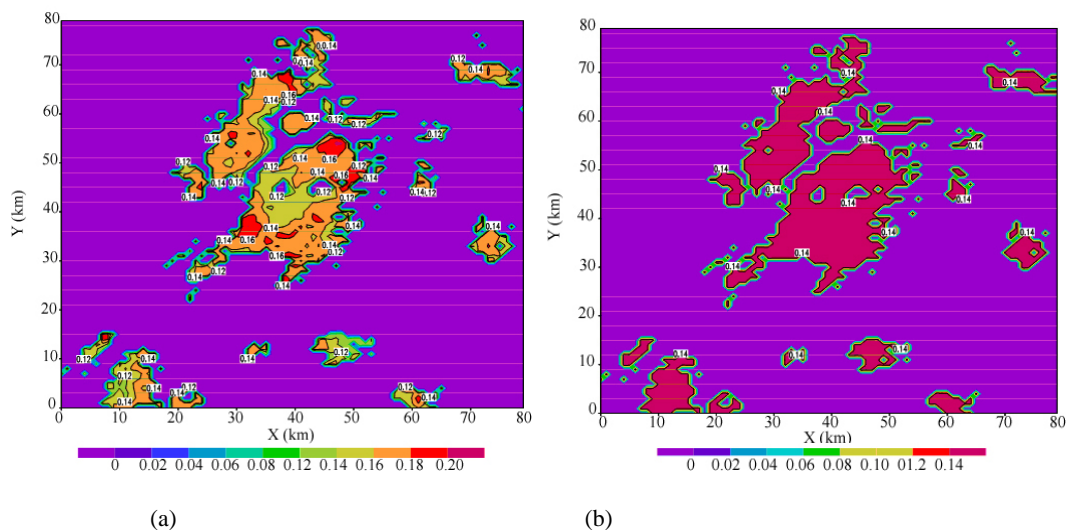


Fig. 7 Simulation of the urban albedo with the UCM introduced: (a) the albedo retrieved from the Landsat data, 10:30, July 12, 2002; (b) the urban albedo simulated with the UCM. (He, 2006)

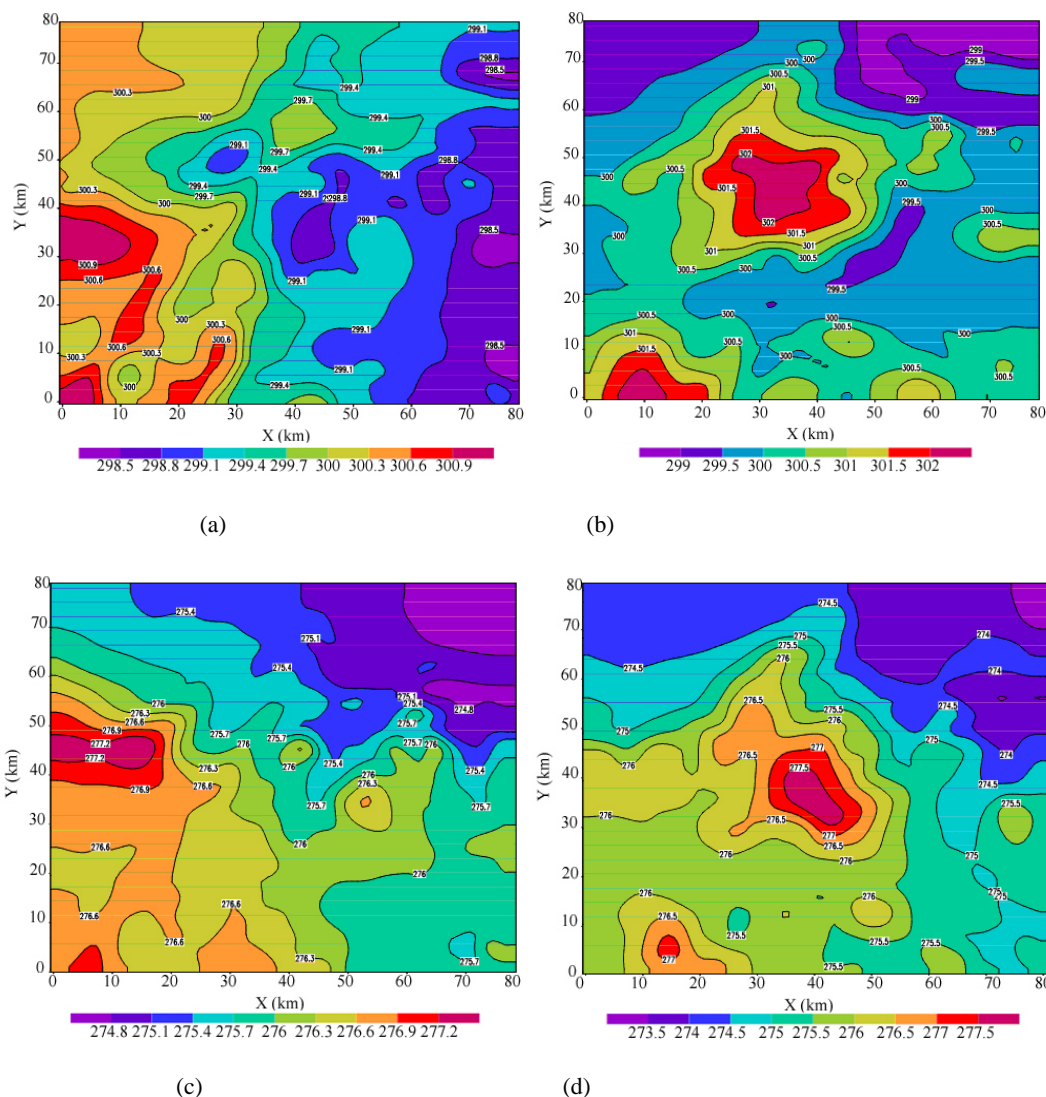


Fig. 8 Simulation of the urban heat island phenomenon in the night in the winter and summer: the simulated air temperature in the night (a) without the UCM introduced, 02:00, July 12, 2002; (b) with the UCM introduced, 02:00, July 12, 2002; (c) without the UCM introduced, 02:00, March 2, 2006; (d) with the UCM introduced, 02:00, March 2, 2006. (He, 2006)

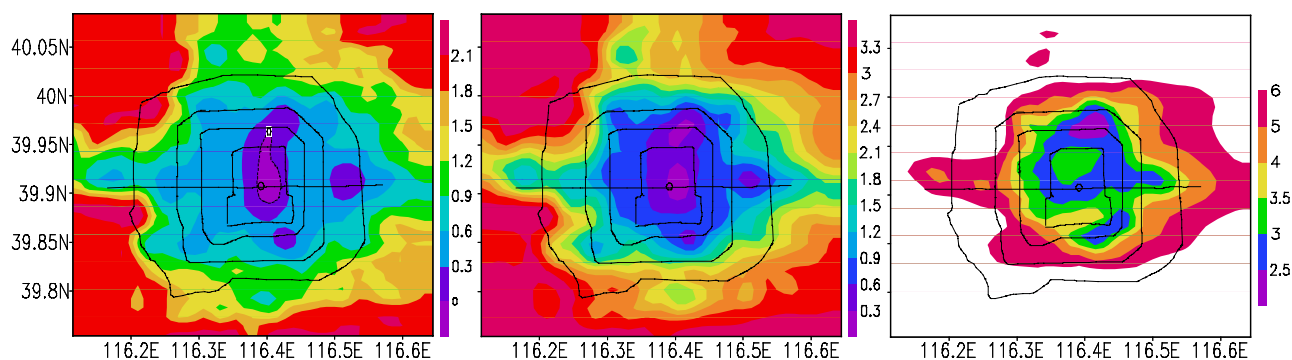


Fig. 9 The distribution of wind speed u from simulation results at different heights: (a) $z=2.5$ m; (b) $z=10$ m; (c) $z=50$ m. (Miao et al., 2006)



Fig. 10 Urban boundary layer observation (iron tower in the urban area)